GEOLOGICA ULTRAIECTINA

Mededelingen van de
Faculteit Geowetenschappen
Universiteit Utrecht

No. 269

Late-orogenic extension and strike-slip deformation in the Neogene of southeastern Spain

Bart Meijninger

Promotor: Prof. R.L.M. Vissers
Faculty of Geosciences
Utrecht University

Members of the dissertation committee:

Prof. Dr. J.P. Platt	Department of Earth Sciences University of Southern California
Prof. Dr. L. Jolivet	Laboratoire de Tectonique Université de Pierre et Marie Curie
Prof. Dr. J.E. Meulenkamp	Faculty of Geosciences Utrecht University
Prof. Dr. S. Cloetingh	Department of Tectonics and Structural Geology, Vrije Universiteit
Prof. Dr. M.J.R. Wortel	Faculty of Geosciences Utrecht University

The research for this thesis was funded by and carried out at:

Department of Earth Sciences
Faculty of Geosciences
Utrecht University
Budapestlaan 4
3584 CD Utrecht
The Netherlands
http://www.geo.uu.nl

The work was conducted under the programme of the Vening Meinesz Research School of Geodynamics (VMSG)

ISBN-10: 90-5744-134-9
ISBN-13: 978-90-5744-134-9

Cover illustration: conjugate normal faults in sediments exposed in the Rambla de Saltador near Huercal Overa, southern Spain. Width of outcrop approximately 2 meters.

Late-orogenic extension and strike-slip deformation in the Neogene of southeastern Spain

Laat-orogene extensie en laterale breuk bewegingen in het Neogeen van zuidoost Spanje

(met een samenvatting in het Nederlands)

PROEFSCHRIFT

TER VERKRIJGING VAN DE GRAAD VAN DOCTOR
AAN DE UNIVERSITEIT UTRECHT
OP GEZAG VAN DE RECTOR MAGNIFICUS, PROF. DR. W.H.GISPEN
INGEVOLGE HET BESLUIT VAN HET COLLEGE VOOR PROMOTIES
IN HET OPENBAAR TE VERDEDIGEN
OP VRIJDAG 17 NOVEMBER 2006 DES MIDDAGS TE 14.30 UUR

DOOR

Bartholomeus Maria Liduina Meijninger

GEBOREN OP 12 JULI 1978 TE BRIELLE

Promotor: Prof. Dr. R.L.M. Vissers

The research for this thesis was funded by financial support of and carried out at the Department of Earth Sciences, Faculty of Geosciences, Utrecht University, The Netherlands.

“One can only see what one observes, and one observes only things which are already in the mind”

“Men kan alleen zien wat men waarneemt, en men neemt alleen die dingen waar die al in de geest aanwezig zijn.”

Alphonse Bertillon

Table of Contents

1

Introduction

General introduction

The western part of the Mediterranean region is dominated by a morphologically distinct mountain belt made up of the Betic Cordillera in southern Spain, the Rif Mountains in northern Morocco, and the Tell - Kabylies Mountains in northern Algeria and Tunisia (Fig. 1.1). Together, they form an arc-shaped orogen, surrounding the Alboran Sea and part of the western Mediterranean. This orogen constitutes the western end of the Alpine chain of southern Europe, developed since the early Tertiary in response to collision of the African and Eurasian plates.

The outer part of the arc consists of the fold and thrust belts of the Betic, Rif and Tell External Zones, whilst the region within the arc is made up of an allochtonous pile of intensely deformed and mostly metamorphic rocks, exposed in the Betic and Rif Internal Zones and in the Kabylies Mountains. Part of the Internal Zone is presently submerged in the Alboran Sea. In essence, the Betic External Zone consists of remnants of the Mesozoic rifted margin of southern Spain (García Hernández *et al.*, 1980; Banks and Warburton, 1991; Peper and Cloetingh, 1992), whilst the metamorphic units of the Internal Zone are considered as the dismembered relics of an early Alpine collisional system (e.g., Platt and Vissers, 1989; Sanz de Galdeano, 1990; Saadallah and Caby, 1996). The geometry of the Betic - Rif - Tell orogenic arc largely developed since the latest Oligocene up to the late Miocene, when a combination of westward motion plus extensional deformation of the Internal Zone and slow but continuous African - European plate convergence resulted in outward thrusting and folding of the Mesozoic - Cenozoic sedimentary cover in front of the migrating Internal Zones (e.g., Sanz de Galdeano, 1990; Sanz de Galdeano and Vera, 1992; Watts *et al.*, 1993; Platt *et al.*, 2003). This Mesozoic - Cenozoic sedimentary cover formed part of the Iberian and African continental margins (the Betic and north African External Zones) and an associated deep, but narrow, marine basin (the North African Flysch Trough).

In this thesis we focus primarily on the Neogene basins in the Betic Cordillera, with emphasis on several of the basins in the Internal Zone. The Internal Zone of the Betic Cordillera, often referred to as the Betic Zone (Egeler and Simon, 1969) or as part of the Sardinian or Alboran Domain (Sanz de Galdeano, 1990; García-Dueñas *et al.*, 1992), is made up of mainly metamorphosed Palaeozoic and Mesozoic rocks (e.g., Egeler and Simon, 1969; Platt and Vissers, 1989), which have been penetratively deformed under a variety of metamorphic conditions and are presently exposed in elongate mountain ranges, typically 15 to 30 km wide, trending parallel to the belt as a whole. The rocks of the Betic Zone are classically grouped into three main tectonic units. These are, in ascending order, the high-greenschist up to amphibolite facies metamorphic rocks of the Nevado-Filabride Complex, the low-grade metamorphic rocks of the Alpujarride Complex, and the anchizone to non-metamorphic rocks of the Malaguide Complex. The occurrence of high pressure - low temperature metamorphic relics in Nevado-Filabride and some Alpujarride rocks as well as repetitions of the inferred stratigraphy point to an early stage of crustal thickening. The initial collisional system, however, became affected by pervasive Neogene extension, and the units of the different complexes now form part of a strongly thinned (Betic-Alboran) continental crust. This is substantiated by the fact that the contacts between the main complexes are crustal-scale extensional detachments, marked by an abrupt upward decrease in metamorphic grade across these structures. The onset of extension was accompanied by the hot emplacement of subcontinental mantle fragments into the crust, now exposed in the Ronda, Alpujata, Caratraca and Beni Bouchera massifs in the western part of the system (e.g., Priem *et al.*, 1979; Platt and Vissers, 1989; van der Wal and Vissers, 1993, and references therein), and by intermediate to low-pressure, high temperature metamorphism of Alpujarride rocks mainly in the western and central part of the Betic Zone but locally also in the eastern Betics (e.g., Monie *et al.*, 1994; Platt and Whitehouse, 1999; Comas et al 1999; Platt *et al.*, 2005).

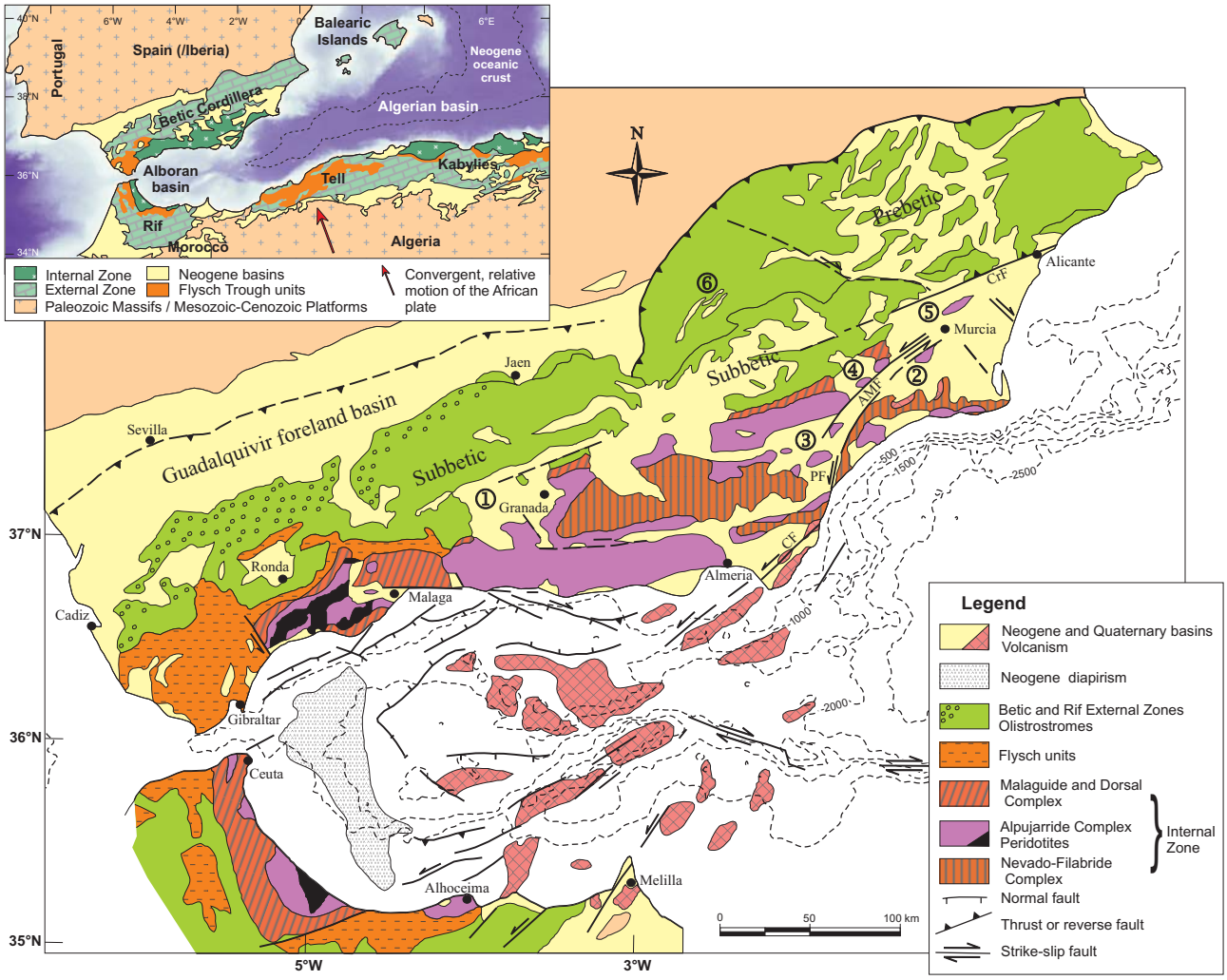

Figure 1.1. Geological map of the Alboran region, modified after Sanz de Galdeano et al. (1995). CrF - Crevillente fault, AMF - Alhama de Murcia fault, PF - Palomares fault, CF - Carboneras fault. (1) Granada basin, (2) Guadalentin-Hinojar basin (3) Huercal Overa basin, (4) Lorca basin, (5) Fortuna basin, (6) Pontones - Santiago de la Espada basin.

The ranges of mostly metamorphic rocks of the Betic Internal Zone are separated by narrow, elongate basins, often referred to as intra- or intermontane basins, filled with Neogene (Miocene-Pliocene) to recent continental siliciclastics and marine mixed siliciclastic / carbonate facies, marls and evaporites (e.g., Montenat and Ott d'Estevou, 1990; Sanz de Galdeano, 1990). These elongate, parallel running basins and ranges form, in fact, a typical "Basin and Range" type morphology. The geology and morphology of the Betic Internal Zone is further complicated by a pronounced NE trending network of faults including the Crevillente fault, the Alhama de Murcia fault, the Palomares fault and the Carboneras fault, that crosses the south-eastern part of the Betic Cordillera (Fig. 1.1). These prominent faults clearly bound several of the Neogene and Quaternary basins. Some segments of these faults, i.e., the Alhama de Murcia, Carboneras and Palomares faults, have been studied in detail and their geometry and kinematics have been documented (e.g., Bousquet and Montenat, 1974; Gauyau *et al.*, 1977; Bousquet, 1979; Martínez-Díaz and Hernández Enrile, 1992a; Keller *et al.*, 1995; Jonk and Biermann (2002), Booth-Rea *et al.*, 2003; Faulkner *et al.*, 2003) but, despite these studies, the timing of the initial movements and amounts of displacement on these faults, as well as their relationship with the Neogene basin development, are still a matter of debate.

Several recent studies of the metamorphic rocks from the Internal Zone have provided evidence for rapid exhumation and associated E-W directed extension of a previously thickened crust (e.g., Platt and Vissers, 1989; García-Dueñas *et al.*, 1992; Jabaloy *et al.*, 1992; Vissers *et al.*, 1995), and a late Oligocene – Miocene age has been assigned to this process (Monie

et al., 1994; Johnson *et al.*, 1997; Lonergan and Johnson, 1998; de Jong, 2003; Platt *et al.*, 2005). Detailed structural and sedimentological studies, e.g., of the Huercal Overa basin (Briend, 1981; Mora-Gluckstadt, 1993), as well as seismic studies of the Granada (Morales *et al.*, 1990; Ruano *et al.*, 2004) and Guadalentin basins (Amores *et al.*, 2001 and 2002) demonstrate the existence of late Miocene half-graben structures. Seismic surveys in the Alboran Sea have revealed similar half graben structures in the Miocene sediments offshore (e.g., Comas *et al.*, 1992; Mauffret *et al.*, 1992; Watts *et al.*, 1993). Moreover, in many of the Miocene basins there is widespread evidence of (syn-sedimentary) extensional faulting, which has led in places to spectacular normal fault geometries (Mora-Gluckstadt, 1993; Vissers *et al.*, 1995; Augier, 2004). The simultaneous exhumation and thinning of the metamorphic middle to upper (Betic – Alboran) crust and the deposition of late Miocene sediments in an extensional setting suggest a dynamic link: the extensional intermontane basins in fact developed on top of a previously thickened, thermally anomalous and locally hot, stretching (collapsing) continental crust.

In essence, two different models have been proposed to explain the Neogene geology and geometry of the Betic – Rif arc and Alboran Sea: (a) removal of a thickened subcontinental lithosphere, either by convection (Platt and Vissers, 1989; Houseman, 1996) or by lithospheric delamination, leading to extensional collapse of previously thickened crust (e.g., García Dueñas *et al.*, 1992; Seber *et al.*, 1996; Calvert *et al.*, 2000; Fig. 1.2a), and (b) subduction roll-back followed by slab detachment (e.g., Morley, 1993; Royden, 1993; Lonergan and White, 1997; Gutscher *et al.*, 2002; Spakman and Wortel, 2004; Fig. 1.2b). These models have been suggested to explain Neogene extension in the Internal Zone and the coeval development of the Miocene basins, including the Alboran basin, largely as either "collapse basins" or back-arc basins, respectively. It is emphasized here that the resultant thinning of the Betic and Alboran crust occurred within an overall setting of continuous slow convergence of the African and Eurasian plates.

Montenat *et al.* (1987), Montentat and Ott d'Estevou (1990, 1996 and 1999) and De Larouzière *et al.* (1988), on the other hand, have suggested that several of the late Miocene intermontane basins, such as the Lorca, Fortuna and Vera basins, are in fact pull-apart basins (wrench furrows or "sillons sur décrochement"), developed as a result of sinistral movements along the NE trending Alhama de Murcia (Bousquet and Montenat, 1974) and the N trending Palomares (Bousquet *et al.*, 1975) faults, respectively (Fig. 1.2c). These faults have been suggested to form part of a crustal-scale transcurrent shear zone (e.g., Leblanc and Olivier, 1984; De Larouziere *et al.*, 1988), referred to as the Eastern Betic shear zone or Trans Alboran shear zone, which continues offshore across the Alboran Sea towards the Rif. In this context, it is noted that seismic refraction studies of the Betic crust show a variation in crustal thickness from up to 38-39 km in the central Betics near Granada, via approximately 22 km in the eastern Betics, to 13-15 km beneath the Alboran basin (Banda and Ansorge, 1980; Banda *et al.*, 1983; Torné and Banda, 1992). The position and trend of the Crevillente, Alhama de Murcia and Palomares faults more or less coincide with the transition from thick crust to the west and northwest to thin crust east and south of the faults (Banda and Ansorge, 1980; De Larouziere *et al.*, 1988). The inferred transcurrent shear zone is thought to have developed since the early Miocene in response to African – European plate convergence, and to have caused a restructuring of the Betic Internal Zone (De Larouziere *et al.*, 1988). Several workers including Bousquet and Montenat (1974), Bousquet *et al.* (1975), Gauyau *et al.* (1977), (2004 and 2005) have provided evidence for intense deformation of Quaternary sediments close to Alhama de Murcia, Palomares and Carboneras faults, which demonstrates recent activity of these faults. According to Bousquet (1979) and Masana *et al.* (2004) such activity may very well be associated with the present-day convergence of the African plate towards Eurasia.

The interpretation of the network of the main faults as a transcurrent shear zone and its role in controlling the development of the Neogene intramontane basins has been questioned in several studies (e.g., Platt & Vissers, 1989; Mora-Gluckstadt, 1993; Vissers *et al.*, 1995). The principal issue concerns the question if strike-slip faulting played a fundamental role in the development, during the Miocene, of the Alboran and Betic basins as pull-apart basins (Bousquet and Montenat, 1974; Bousquet *et al.*, 1975; Montenat *et al.*, 1987; Montenat and Ott d'Estevou, 1990, 1996 and 1999; De Larouzière *et al.*, 1988; Tandon *et al.*, 1998), or if the pertinent main faults are late, possibly reactivated structures that affected and modified the Alboran and Betic basins since the late Miocene but were not fundamental to the initiation of these basins.

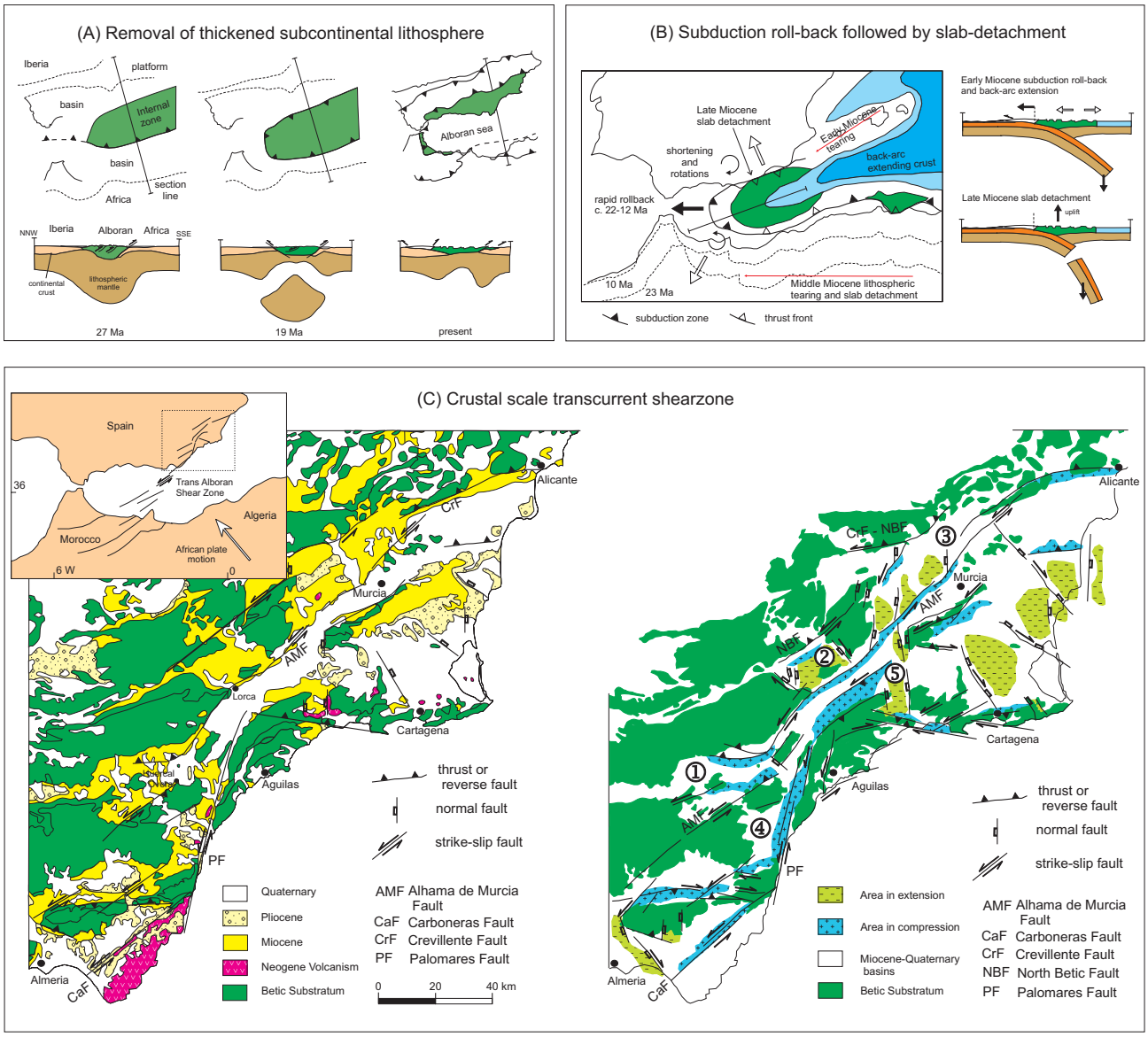

Figure 1.2. Cartoons illustrating current hypotheses regarding the Neogene tectonics of the western Mediterranean. A) Removal of thickened subcontinental lithosphere, either by convection or by delamination (Vissers et al., 1995; Garcia Dueñas et al., 1992). B) Subduction zone roll-back followed by slab-detachment (Lonergan and White, 1997; Spakman and Wortel, 2004). C) Crustal-scale transcurrent shear zone (Leblanc and Olivier, 1984; Montenat et al., 1987). Numbers: (1) Huercal Overa basin, (2) Lorca basin, (3) Fortuna basin, (4) Vera basin, (5) Hinojar basin.

Research objectives

The aim of this study is to test the different hypotheses for Neogene basin development in the Betic - Alboran system as outlined above, mainly via detailed structural studies in few selected Miocene basins in both the Betic Internal and External Zones. We intend to unravel how the Miocene basins developed in a tectonic context of late-orogenic extension and slow plate convergence, and how the basins were modified by large-scale reverse and strike-slip faulting accommodating ongoing convergence between Africa and Iberia. Implicit in the above lithosphere-scale geodynamic models is the possibility that shortening in the external fold and thrust belt was roughly coeval with extensional deformation in the internal part of the system. It is thus of utmost importance to obtain a quantitative estimate of the plate motion history of the surrounding Iberian and African plates, because such estimates may constrain any crustal-scale deformation generated within the system. Our first aim, therefore, is to assess the late Tertiary history of African – Eurasian plate motions, with emphasis on the Alboran Sea and surrounding Alpine belts. A second aim is to

constrain the timing and structure of the Betic fold and thrust belt via study of the Miocene geology of the basins locally developed on top of the fold and thrust belt. These basins, obviously formed in a context of overall shortening during the Neogene, are likely about coeval with the Neogene intermontane basins of the internal zone for which an extensional or strike-slip origin has been proposed as outlined above. Our third aim concerns the origin of the late Miocene basins in the Betic Internal Zone, and any relationship between basin development and either late-orogenic extension in the Betic crust or strike-slip motion within the proposed crustal-scale transcurrent shear zone. This third aim has led us to undertake detailed structural studies of relevant fault systems in selected areas in and adjacent to the Neogene basins. Finally, we wish to obtain as detailed as possible data on the late Miocene basin development in time and space, with the aim to detect lateral variations possibly indicative of lithospheric processes that may have occurred beneath the Betic Cordillera and the Alboran Sea.

Outline of this thesis

In **chapter 2** we focus on the Africa – Iberia plate motion history, with the aim to determine in how far geological data, such as structural trends, thrust directions, sequences of deformational events and amounts of shortening can be understood as a consequence of the amount and direction of plate motion of Africa relative to Iberia with time during the Neogene.

In **chapter 3** we study two Neogene basin remnants in the Betic fold and thrust belt near Pontones and Santiago de la Espada (Fig. 1.1). There are clearly extensional structures developed in the pertinent Miocene basin sediments, which is obviously in contrast with the surrounding compressional setting. The aim of this chapter is to elucidate the development of these extensional structures. It is shown that these structures reflect local extension inherent to the progressive development of a compression-related thrust structure.

Chapter 4 presents an overview of the Miocene stratigraphy of three selected basins in the Betic Internal Zone, i.e., the Huercal Overa, Lorca and Fortuna basins, which incorporates data from earlier studies documented in the literature as well as new litho- and biostratigraphic data. The resulting improved data set allows basin-scale and regional correlations, including hitherto unidentified syn- and diachronic trends in the development of the basins that may be associated with eustatic changes and/or lithospheric processes.

In **chapter 5** we study the geometry and kinematics of the (syn-sedimentary) deformational structures, seen in different levels of the Miocene basin stratigraphy as well as in the basement of the Huercal Overa, Lorca and Fortuna basins, with the aim to investigate the structure of the basins as well as relationships between basin development and extension in the Betic basement and/or any activity of strike-slip faults that belong to the crustal scale transcurrent shear zone. Aside horizontal motions of the basins (stretching or b-factors), we calculate vertical motions via tectonic subsidence curves, to elucidate the development of the basins studied in space and time

Using the stratigraphic and structural data from chapters 4 and 5, we focus in **chapter 6** on the geometry and kinematics of two prominent faults, i.e. the Alhama de Murcia and Crevillente faults, and their effect on the basin fill and basin structure of the Huercal Overa, Lorca, and Fortuna basins, with the aim to elucidate relationships between basin development and the deformation history of the prominent faults.

In **chapter 7** we present a review of currently contending hypotheses regarding the geodynamics of the western Mediterranean and the development of the Alboran arc, and discuss how the development of the late Miocene basins in the Betic Cordillera may be understood in a lithosphere-scale geodynamic context.

2

Late Tertiary relative plate motions of Africa and Iberia

Introduction

During the last two decades several attempts have been made to relate the tectonic history of the European Alps to the relative plate motions of Africa and Europe. Dewey *et al.* (1989) were among the first to present a Cenozoic kinematic model for the western Mediterranean region, integrating relative motions of the African and Eurasian plates inferred from Atlantic paleomagnetic anomalies and fracture zones, and geological observations concerning tectonic structure, sedimentary facies and associated sequences of geological events. The geological evolution of the westernmost part of the Mediterranean between southern Spain and Africa was, however, not included in their analysis. Dewey's model has since been improved and/or applied by others, e.g., by Mazzoli and Helman (1994), Carminati *et al.* (1998a,b), Gueguen *et al.* (1998), Jolivet and Faccenna (2000), Andeweg (2002); Rosenbaum *et al.* (2002a,b), Meulenkamp and Sissingh (2003), but a generally accepted model for the late Tertiary to recent period of the westernmost part of the Mediterranean region has so far not been established.

The Neogene development of the Western Mediterranean basins and surrounding Alpine orogens (e.g., the Alps, Pyrenees, Betic Cordillera, Rif, Atlas, Apennines) has been the subject of ongoing debate (e.g., Cohen, 1980; Dercourt *et al.*, 1986; Sanz de Galdeano, 1990; Brede *et al.*, 1992; Carminati *et al.*, 1998a,b; Guegeun *et al.*, 1998; Frizon de Lamotte *et al.*, 2000; Rosenbaum *et al.*, 2002a; Meulenkamp and Sissingh, 2003), in particular with regard to the evolving position of the plate boundary as well as the direction of relative motion between Africa and Europe through time (e.g., Dewey *et al.*, 1989; Srivastava *et al.*, 1990a,b; Brede *et al.*, 1992; Mazzoli and Helman, 1994). The Neogene, i.e., late-Alpine geology of the region reveals a multiple history resulting in a complex geological structure, and the interpretation of this structure in terms of Neogene African-European plate convergence is not straightforward.

The western part of the Mediterranean region is dominated by a morphologically prominent mountain belt made up of the Betic Cordillera in southern Spain, the Rif Mountains in northern Morocco and the Tell-Kabylies Mountains in northern Algeria and Tunesia, which together form an arc-shaped orogen surrounding the Alboran Sea and part of the western Mediterranean Sea (Fig. 2.1). This Alpine mountain belt consists of an allochthonous Internal Zone in the inner part of the arc, and a broadly autochthonous External Zone forming the outer arc. The allochthonous Internal Zones of the Betics, Rif and Tell Mountains are the dismembered relics of an early Alpine collisional system. The relatively autochthonous External Zones are now deformed into fold and thrust belts, and the morphologically distinct arc shape of the Betic-Rif-Tell range as well as a large part of its fold and thrust structure developed since the latest Oligocene – earliest Miocene (e.g., Sanz de Galdeano, 1990; Platt *et al.*, 2003).

In essence, three different models have been proposed to explain the Neogene geology and geometry of the Betic-Rif arc and Alboran Sea: (1) removal of a thickened subcontinental lithosphere, either by convection (Platt and Vissers, 1989; Houseman, 1996) or by lithospheric delamination (García Dueñas *et al.*, 1992; Seber *et al.*, 1996; Calvert *et al.*, 2000), (2) subduction roll-back followed by slab-detachment (e.g., Royden, 1993; Lonergan and White, 1997; Spakman and Wortel, 2004) and (3) wrench faulting along a NE trending crustal transcurrent shearzone (Leblanc and Olivier, 1984; Montenat *et al.*, 1987; Montenat and Ott d'Estevou, 1990, 1996 and 1999; and De Larouzière *et al.*, 1988). Irrespective of these different scenarios, it is generally believed that the Neogene development of the Betic Cordillera, Rif and the Alboran Sea occurred within an overall setting of continuous slow convergence of the African and Eurasian plates (e.g., Dewey *et al.*, 1989). Consequently, a principal issue in tectonic studies of the westernmost Mediterranean concerns the question in how far the development of the Betic-Rif orogen should be explained in terms of geodynamic processes within the system such as the ones mentioned above, and/or by external boundary conditions imposed by the history of Africa-Iberia plate motions.

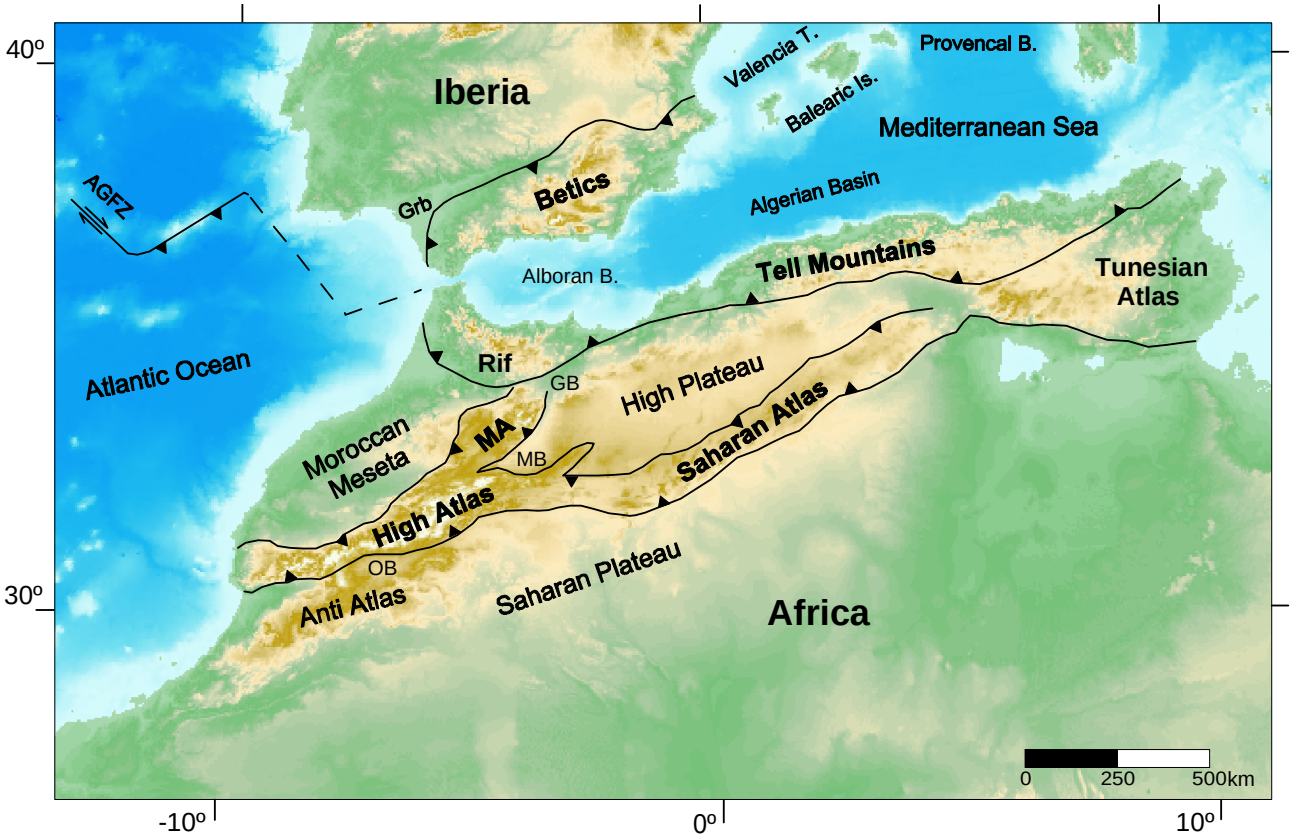

Figure 2.1. Tectonic map of the western Mediterranean region. Grb Guadalquivir basin, MA Middle Atlas, GB Guercif basin, OB Ouarzazate basin, MB Missour basin, AGFZ Azores-Gibraltar Fracture Zone, Alobran B. Alboran basin, Provencal B. Provencal basin, Valencia T. Valencia Trough.

This chapter is focussed on the Africa-Iberia plate motion history, with the ultimate aim to determine in how far geological data such as structural trends, sequences of deformational (compressional) events, directions of relative movements of tectonic units (slip vectors) and amounts of shortening in the Betic-Alboran region can be understood as a consequence of the amount and direction of plate motion of Africa relative to Iberia with time during the Neogene. Dewey *et al.* (1989), Srivastava *et al.* (1990a,b), Roest and Srivastava (1991), Müller and Roest (1992), Mazzoli and Helman (1994), and Rosenbaum *et al.* (2002b) have presented plate motion analyses of the Mesozoic - Cenozoic Africa-Eurasia convergence that differ in their details as reviewed below. Their analyses, however, are not specifically focused on the westernmost part of the Mediterranean region, and therefore the consequences of their models with respect to the Alboran region are not known. In this chapter, we first calculate the amount and the direction of motion of the African plate with respect to Iberia with time, using the Iberian (Eurasian) - African plate motion parameters from these previous studies and adopting the latest geologic time scale (Huestis and Acton, 1997; Cande and Kent, 1995; Gradstein *et al.*, 1994). The azimuths, rates and amounts of convergence calculated from these different model data sets present a range of values. The spreading in results offer an estimate of uncertainty of the plate motion reconstruction in the Alboran region, in the absence of such uncertainty estimates in the published models. Secondly, the results are compared with published structural data (field-observations) from the fold-and-thrust belts of the Betic-Alboran-Rif domain, as well as with the first-order movements in the Atlas ranges further south, and in the Pyrenees, i.e., the boundary between Iberia and Eurasia proper.

Plate motion reconstructions: some background

Plate reconstruction models essentially describe past relative plate motions on the basis of finite rotations around a pole of rotation (or Euler pole). In principle, a pole to a small circle, which defines the average path of a fracture zone, and two great circles, which define the average path of linear paleomagnetic anomalies on both sides of the spreading centre (rift

zone), should meet at a common point on the globe: the rotation pole or Euler pole. In practice, however, there are small deviations, which inevitably lead to the necessity to estimate a best-fit rotation pole, rather than an actual common rotation pole. A finite rotation between, for example, the North American and Eurasian plates is calculated from such a best-fit rotation pole, which is determined from a geometrical best-fit of paleomagnetic anomalies of similar age (ancient plate boundaries) and fracture zones (transform faults) on either side of the Mid-Atlantic ridge (Fig. 2.2).

In the context of this study, the main advantage of this technique is that it relies on datasets that are entirely independent from any geological data, such that plate reconstruction models are principally free of geological subjectivity. On the other hand, this method also carries several deficiencies especially with respect to uncertainties in the data and in the data acquisition, as well as to the assumptions made in the data analysis. Srivastava and Tapscott (1986) emphasize that "most of the plate motion reconstructions are based on a limited amount of geophysical data from one or more regions of the North Atlantic available at the time of publication. Thus different criteria and assumptions had to be made to derive satisfactory configurations between plates for the entire North Atlantic. Consequently these reconstructions differ both in data base and working assumptions… The attempt to find a solution for the entire North Atlantic by combining solutions from different regions is not possible without making further assumptions."

Several papers have addressed the problem of how to handle uncertainties in finite rotations in plate reconstruction models (e.g., Chase, 1978; Hellinger, 1981; Stock and Molnar, 1983; Molnar and Stock, 1985; Chang *et al.*, 1990; Gordon, 1998; Kirkwood *et al.*, 1999). In general, these uncertainties may come from a number of rather obvious sources, such as the navigation record of the research ship involved, the number and the quality of the paleomagnetic anomaly data used in the best-fit model, the length of the linear paleomagnetic anomalies, the distance of the best-fit rotation pole to the centre of the data area (Hellinger, 1981; Stock and Molnar, 1983), and mistakes in the identification of a particular magnetic anomaly (Kirkwood *et al.*, 1999).

One example of a common and important source of uncertainties is in the identification of data points of anomalies along ship tracks and the extrapolation of these anomalies across to adjacent ship tracks: an unmapped (or ignored) transform fault may exist between the ship tracks and across the extrapolated magnetic lineation, which was assumed to connect data points of anomalies of similar age (Hellinger, 1981). Another example of an important source of error in

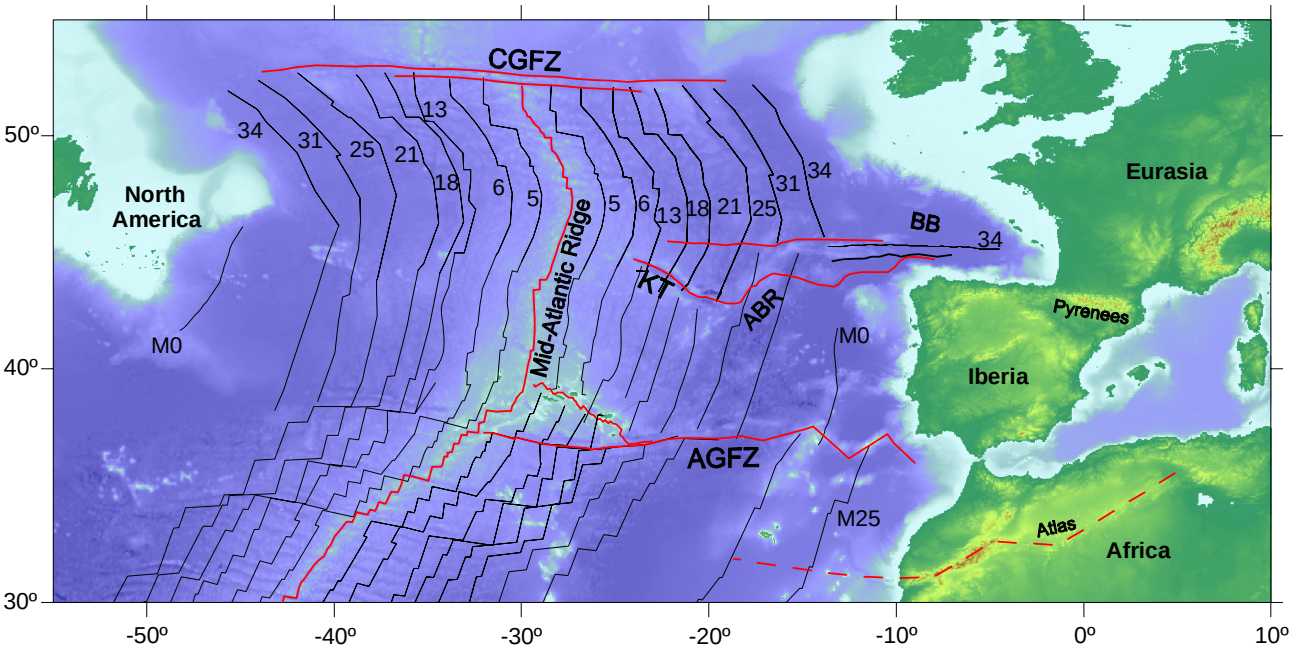

Figure 2.2. Topographic-bathymetric map of the North Atlantic. CFGZ Charlie Gibbs Fracture Zone, KT Kings Trough, ABR Azores-Biscay Rise, BB Bay of Biscay, AGFZ Azores-Gibraltar Fracture Zone. Numbers refer to anomaly numbers. Magnetic lineations after Müller et al. (1997): Digital isochrons of the World's ocean floor (http://www.geosci.usyd.edu.au/research/marinegeophysics/Resprojects/Agegrid/digit_isochrons.html). Fracture zones after Srivastava et al. (1990 a,b).

the position of the pole and angle of rotation is the uncertainty in position and orientation of individual segments of the magnetic anomaly, which are at that moment at or close to the plate boundary (the spreading zone), due to the quality and spacing of observations of magnetic anomalies and fracture zones. The basic assumption generally made is that any systematic error will be small compared with the uncertainty assigned to the position of the magnetic lineation or transform fault.

Two ways have been presented in the literature to quantify uncertainties in the positions of rotation poles and the angles of rotation. One method, introduced by Stock and Molnar (1983), allows to quantify uncertainties on the basis of geometrical relationships between the location and distribution of magnetic anomalies and fracture zones of a given age, and the uncertainty in the corresponding best-fitting rotation. The second method uses statistics to estimate finite rotations and their uncertainties. A number of statistical tools have been proposed in literature (e.g., Chase, 1978; Minster, 1978; Hellinger, 1981; Jurdy and Stefanick, 1987; Kirkwood *et al.*, 1999). A common method to calculate the best-fit rotation pole and its associated uncertainty is to minimize a weighted least squares measure of fit of data points of a magnetic anomaly as a function of rotation parameters. For a given rotation, the sum of squares of the weighted deviations may be taken as a measure of fit of the fixed and rotated data points (e.g., Hellinger, 1981). Other workers have used covariance matrices to describe errors in plate rotations and to combine the contribution of individual plate pairs for plate reconstructions (e.g., Jurdy and Stefanick, 1987; Kirkwood *et al.*, 1999).

These methods in general define the uncertainties within plate rotations via uncertainties of fit, and some methods depend on the sources of error (the quality of the measurement) as well, which, however, require a user's subjective input on the estimation of uncertainty in (or quality of) these data sources (paleomagnetic anomalies, fracture zones, plate boundaries). According to Gordon (1998) it appears that the calculated uncertainties in such a model are in general smaller than expected from their assigned uncertainties. This reveals the weakness of these kinds of datasets: "…the absence of objectively estimated uncertainties that are consistent with the dispersion of the data…" (Gordon, 1998).

The rotation parameters used in this study are taken from Srivastava and Tapscott (1986), Dewey *et al.* (1989), Srivastava *et al.* (1990a,b), Roest and Srivastava (1991), Müller and Roest (1992), Mazzoli and Helman (1994), and Rosenbaum *et al.* (2002b). Unfortunately, these authors do not report any detail on error analysis, nor do they present any errors for each of the rotation parameters. It is, therefore, difficult to quantify uncertainties in their models. We will use and compare all of these models arguing that the spread in results will give at least some idea of the uncertainty involved. Our present aim is to obtain a range of solutions for the late Tertiary relative plate motion between Iberia and Africa using their rotation parameters, not to improve these plate motion models as such.

Proposed African-Eurasian (/Iberian) plate reconstruction models

Dewey *et al.* (1989), Srivastava *et al.* (1990a,b), Müller and Roest (1992), Mazzoli and Helman (1994) and Rosenbaum (2000a,b) have all presented Africa-Eurasia (/Iberia) plate motion reconstructions, but each with a different aim: understanding of Alpine orogenesis, Iberian plate motions, fracture zones, relative plate motions or palinspatic reconstructions. The main differences between these models largely result from re-examination of locations of fracture zones and paleomagnetic anomalies in the Atlantic Ocean as well as from the use of improved ages from the Geomagnetic Polarity Time Scale (GPTS) to the paleomagnetic anomalies in question. Another relevant difference between some of the models is that Iberia sometimes acts as an (independent) plate, but is considered to be part of Eurasia in other studies. An overview of the Cenozoic African-Eurasian (/Iberian) plate motion paths and instantaneous plate motion vectors based on these models is presented in Figures 2.3 and 2.4. The results can be summarized as follows.

Rifting in the southern part of the Atlantic during the late Jurassic and early Cretaceous led to eastward movement of Africa with respect to Eurasia. This resulted first in sinistral motions along the Azores-Gibraltar plate boundary between Africa and Iberia, and later, when rifting began in the central part of the Atlantic, also in sinistral motions along the boundary between Iberia and Eurasia (the North Pyrenean Fault) (Rosenbaum *et al.*, 2002b). From approximately 120 Ma until 83 Ma rifting occurred in the Bay of Biscay. According to both Dewey *et al.* (1989) and Rosenbaum *et al.* (2002b), African-Eurasian convergence commenced in the late Cretaceous between chrons M0 and 34 (120-83 Ma). The generally N to

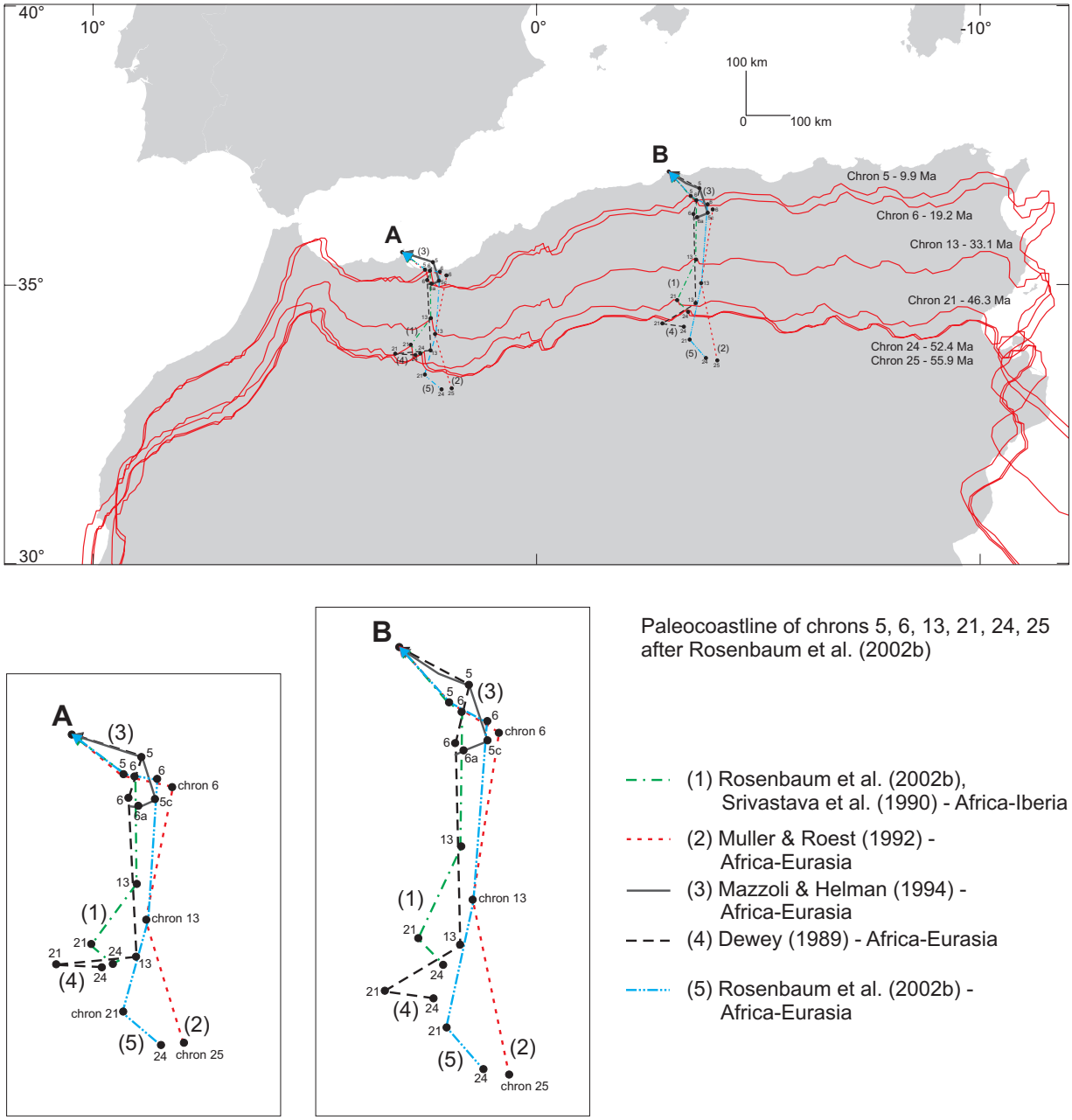

Figure 2.3. Trajectories of two arbitrary chosen points A and B on the African plate relative to Iberia or Eurasia, plotted as a function of time.

NE directed convergent motion was accommodated in periods of rapid convergence (during late Cretaceous and Eocene-Oligocene times) alternating with periods of low convergence rates (during the Paleocene and since the early Miocene). From the middle Cretaceous to the late Eocene, Iberia moved as part of the African plate, and it moved most likely as an independent plate until the late Oligocene. According to Srivastava *et al.* (1990a,b) and Roest and Srivastava (1991), Iberia belongs to the Eurasian plate since the latest Oligocene. The boundary between Eurasia and Africa successively jumped from the Bay of Biscay – Pyrenees (from 118 Ma until 44 Ma) to the King's Trough – Pyrenees lineaments (from 44 Ma to ~25 Ma) to the Azores-Gibraltar fracture zone (at least since 33 Ma and possibly since 40 Ma; see Fig. 2.2).

According to Rosenbaum *et al.* (2002b) convergence in the Pyrenees began at chron 34 to chron 31 (83 to 67.7 Ma), whereas Iberia stopped moving with respect to Eurasia from chron 31 to 25 (67.7 to 55.9 Ma). During the Eocene, Iberia moved towards the west with respect to Eurasia, resulting in a dextral relative motion, followed by a final convergent motion until the Oligocene (Roest and Srivastava, 1991;

Rosenbaum *et al.*, 2002b).

According to both Srivastava *et al.* (1990a,b) and Roest and Srivastva (1991) the Azores-Gibraltar fracture zone acted as the African-Eurasian plate boundary at least since the Oligocene: mainly right-lateral transtension occurred at the western end of the Azores-Gibraltar Fracture Zone near the Azores, and NW to NNW trending compression along the eastern section of the Azores-Gibraltar Fracture Zone. This mode of motion along the Azores-Gibraltar Fracture Zone is similar to the present-day motion (Argus *et al.*, 1989; Roest and Srivastava, 1991; Fernandes, 2004), suggesting kinematic continuity since the Oligocene.

According to both Dewey *et al.* (1989) and Mazzoli and Helman (1994), Africa moved in a generally NNE to NNW direction relative to Europe during the late Oligocene - Burdigalian and Langhian, but suddenly changed to a WNW to NW directed convergent motion during the Tortonian. The late Tortonian to Recent African-European motion vectors seem compatible with a variety of geological phenomena in the Western Mediterranean region as well as with fault plane solutions of recent earthquakes (e.g., Gomez *et al.*, 2000), which is an aspect that will be discussed in more detail later in this chapter.

Africa-Iberia plate motion analysis

The position of Africa relative to either Iberia or Eurasia at a certain time (t) in the geological history has been calculated using a three-plate circuit, consisting of Africa (AF), North America (NAM) and Iberia (IB) or Eurasia (EU), with a fixed Iberian or Eurasian coordinate system. This circuit can be expressed as:

$$_{AF}ROT_{EU}(0;t) = {}_{AF}ROT_{NAM}(0;t) + {}_{NAM}ROT_{EU}(0;t) \quad (1)$$

or

$$_{AF}ROT_{IB}(0;t) = {}_{AF}ROT_{NAM}(0;t) + {}_{NAM}ROT_{IB}(0;t) \quad (2)$$

where ROT (0;t) is the symbolic representation of a total reconstruction pole, comprising the latitude and longitude of the pole and the angle of rotation. A total reconstruction pole fully describes the total rotation, from the present going backward in time, needed to reconstruct the previous position of a plate relative to a given reference frame (Cox and Hart, 2002). For example, $_{AF}ROT_{EU}(0;40)$ describes the finite rotation, about a fixed Euler pole, needed to rotate the African plate from its present position back to its position at 40 Ma ago, with respect to the Eurasian plate. Table 2.1 summarizes the total reconstruction poles of the African-North American and Eurasian-North Ameri-

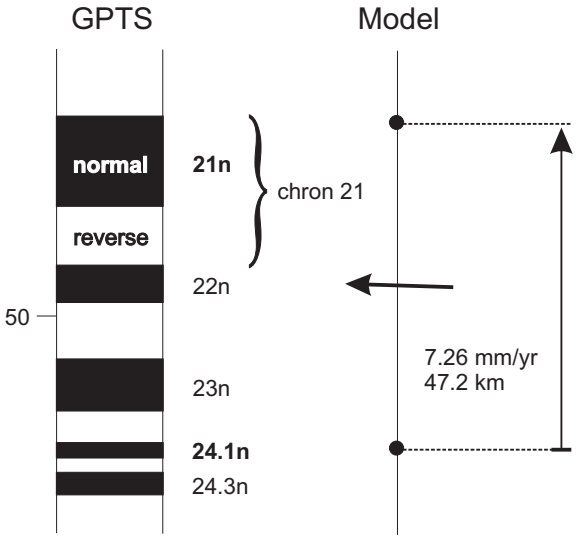

Legend to Fig. 2.4: Plate motion vector (Af-Eu and Af-Ib) is evaluated in point (lat, lon) = (38.75, -2.3) on the northern margin of the Betic Cordillera in Spain.

Plate motion vecor (Ib-Eu) is evaluated in point (lat, lon) = (43.25; 0.75) on the northern side of the Pyrenees in France.

It is assumed that the instantaneous plate velocity vector remains the same from chron 24 to chron 21. Depending on the model the begin and end points of the stage are chosen at the end or the middle of the normal polarity interval of the chron.

Figure 2.4. Instantaneous plate motion vectors calculated after the model data sets from Dewey (1989), Srivastava et al. (1990) etc.,(as shown in table 2.1) shown on a time scale,. The Geomagnetic Polarity Time scale (GPTS) shown is a composite after Kent and Gradstein (1986), Cande and Kent (1995) and Huestis and Acton (1997). Not all known normal and reversed polarity intervals are shown. The number, e.g. 3n, indicates the normal polarity interval of chron 3. A chron consists of a reverse polarity followed by a normal polarity. Overview of the plate boundary positions, estimates of amounts of plate convergence in earlier plate motion studies, as well as geological observations are presented in the three columns to the right.

Late Tertiary relative plate motions of Africa and Iberia

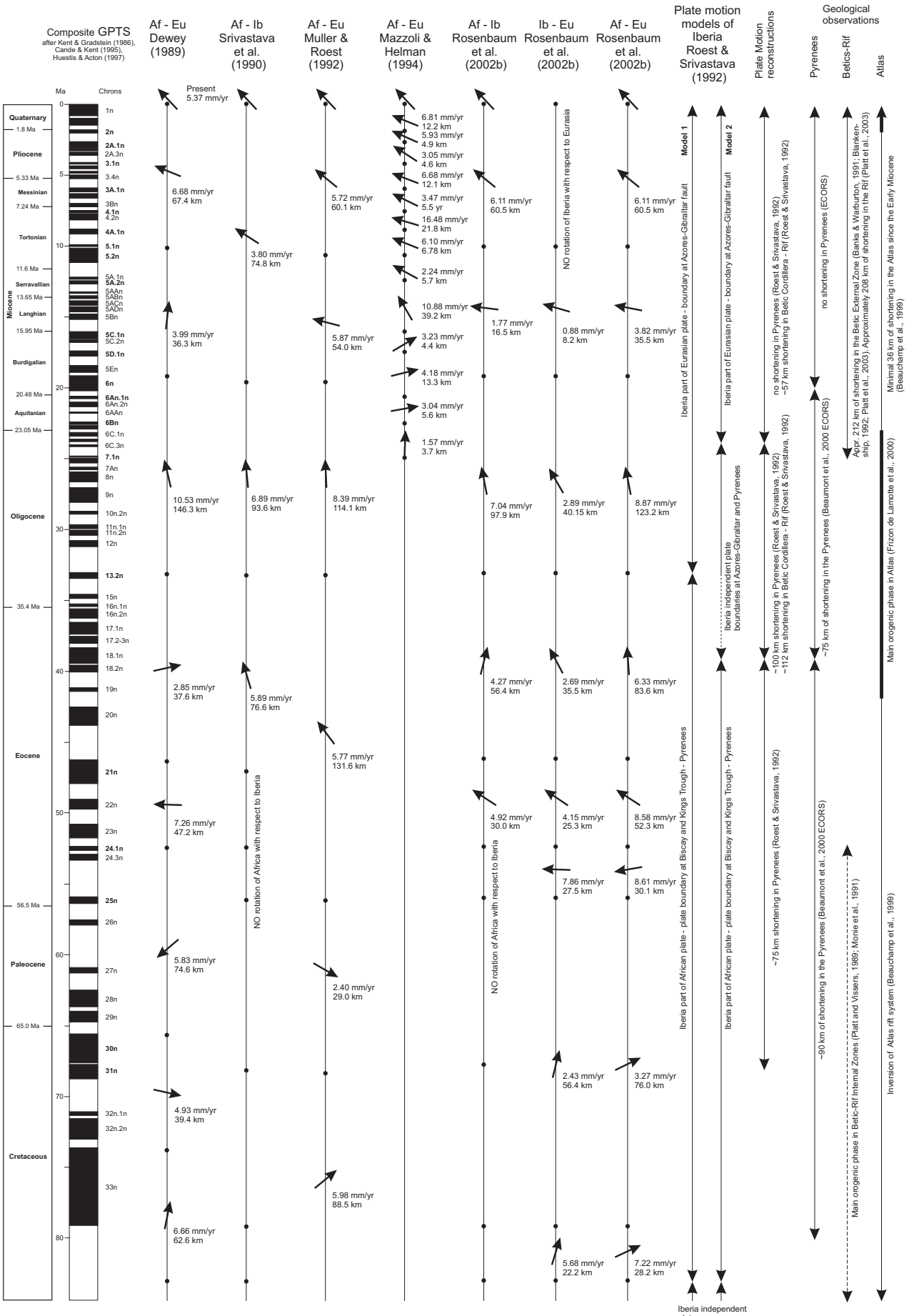

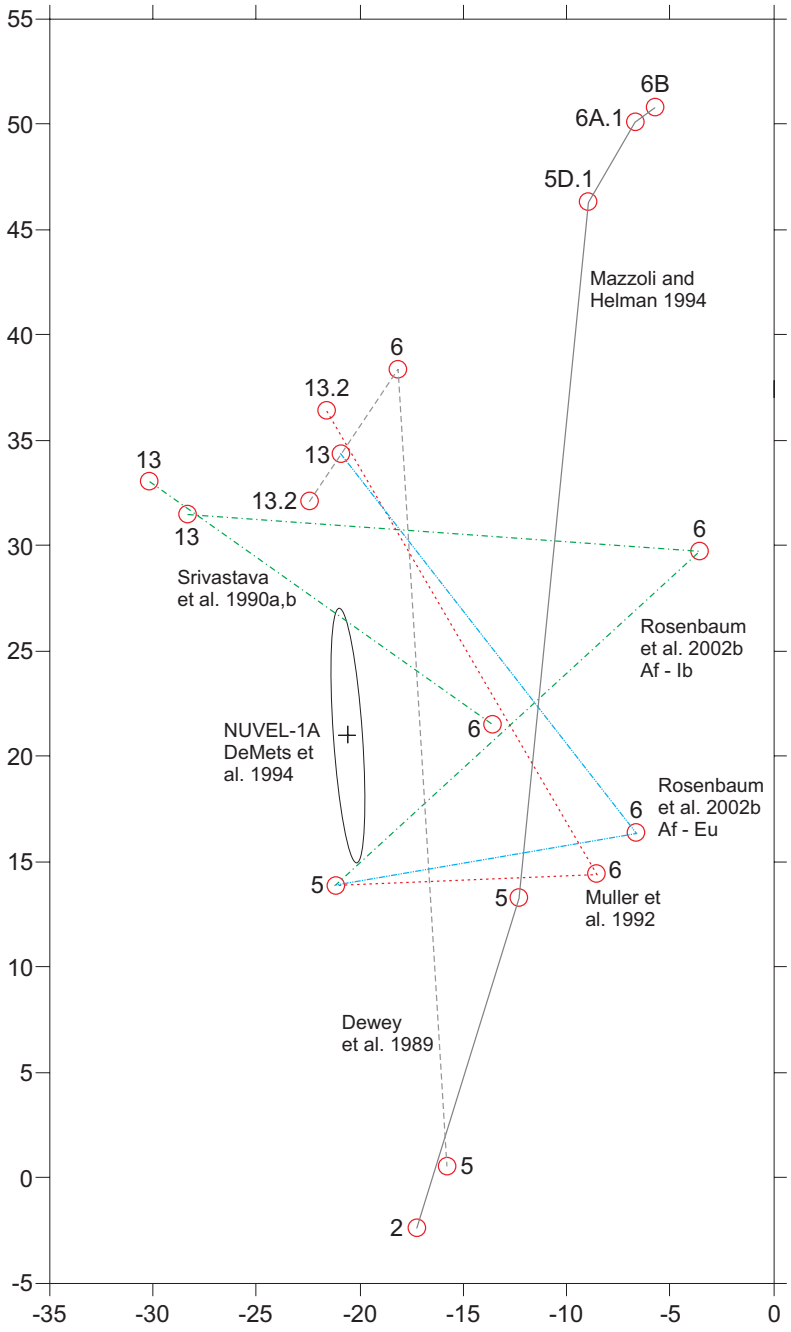

Figure 2.5. Position of Late Oligocene to recent stage poles of the relative motion of Africa with respect to Iberia or Eurasia, based on various plate motion models (Dewey et al., 1989; Srivastava et al., 1990a,b; Muller and Roest, 1991; Mazzoli and Helman, 1994; Rosenbaum et al., 2002b) and NUVEL-1A (DeMets et al., 1994) as shown in Table 2.1. The NUVEL-1A rotation pole is presented with error ellipse.

can or Iberian-North American plates as taken from the above-mentioned studies, as well as the calculated total reconstruction poles for the African-Eurasian and African-Iberian relative plate motions. It should be noted that a total reconstruction pole for the African-North American relative plate motion at anomaly 31 had to be calculated by interpolation from anomalies 30 and 32 in the data set of Müller and Roest (1992).

In order to determine the rate and direction (azimuth) of the velocity of a point on a "rigid" part of the African plate with respect to the fixed Iberian or Eurasian plate, as well as the amount of convergence (shortening) or spreading (extension), a forward stage pole was calculated. A stage pole describes the amount of rotation that occurred during a certain interval of time (a stage) in the history of a pair of plates (Cox and Hart, 2002). This is, for example, for the

African and Iberian or Eurasian plates expressed as: ${}_{AF}ROT_{EU}(t_2;t_1)$ and ${}_{AF}ROT_{IB}(t_2;t_1)$, respectively:

$${}_{AF}ROT_{EU}(t_2;t_1) = {}_{AF}ROT_{EU}(t_2;0) + {}_{AF}ROT_{EU}(0;t_1) = -{}_{AF}ROT_{EU}(0;t_2) + {}_{AF}ROT_{EU}(0;t_1) \quad (3)$$

or

$${}_{AF}ROT_{IB}(t_2;t_1) = {}_{AF}ROT_{IB}(t_2;0) + {}_{AF}ROT_{IB}(0;t_1) = -{}_{AF}ROT_{IB}(0;t_2) + {}_{AF}ROT_{IB}(0;t_1) \quad (4)$$

where –ROT represents either a negative rotation about the Euler pole or a positive rotation about the antipode of that Euler pole, which are equivalent. For example, ${}_{AF}ROT_{EU}(30;20)$ describes the rotation of the African plate from its position at 30 Ma to its position at 20 Ma forwards in time with respect to the Eurasian plate. It is commonly assumed that the Euler pole remains fixed during the stage (time interval) considered, and that it jumps in between successive stages. By dividing the angle of rotation by the duration of a specific stage we obtain the corresponding rate of instantaneous motion (angular rate). From the Euler pole and angular rate, the rate and direction (azimuth) of the relative plate motion of an arbitrarily chosen point on the African plate were calculated. Table 2.1 shows the calculated forward motion stage poles of the African-Eurasian and African-Iberian plates. Figure 2.5 shows the positions of these stage poles on a map, as well as their successive jumps. Instantaneous rotational parameters from DeMets *et al.* (1994) were used to calculate the rate and azimuth at points on the African plate of current relative plate velocities of the African and Eurasian plates (Table 2.1).

The ages of the magnetic anomalies (chrons) have been corrected with up to date ages of magnetic anomalies from Huestis and Acton (1997), Cande and Kent (1995) and Gradstein *et al.* (1994) as shown in Table 2.2. A chron consists of a reversed and a normal magnetic anomaly. The ages used in the plate reconstruction models are either the average age of the normal polarity at the mid-point of the normal anomaly (e.g., Srivastava *et al.*, 1990a,b and Müller and Roest, 1992) or the minimum age at the end of the normal anomaly of that chron (e.g., Dewey *et al.*, 1989 and Rosenbaum *et al.*, 2002b), depending on the source of the rotation parameters.

Results: plate motion reconstructions

Figure 2.3 shows Cenozoic plate motion paths of two arbitrary points A and B on the African plate which move with respect to Iberia and/or Eurasia according to the rotation parameters of Dewey *et al.* (1989), Srivastava *et al.* (1990a,b), Müller and Roest (1992), Mazzoli and Helman (1994) and Rosenbaum *et al.* (2002b). The instantaneous plate velocity vectors shown in Figure 2.4 depict the motion of Africa with respect to a point (38.75N, 2.3W) in the Betic Cordillera in southern Spain. These vectors are calculated from the stage poles listed in Table 2.1 and shown in Figure 2.5. Plate reconstructions for the Alboran region at 33 Ma (chron 13), 19 Ma (chron 6), 10 Ma (chron 5) and the present are illustrated in Figure 2.6, with the present-day shorelines and topography shown for reference. At this stage it is emphasized, that corrections for the ages of the chrons by implementing the newest GPTS as compared with the old GPTS have no effect on the calculated amounts of convergence, but that they result in small differences in calculated plate motion velocities (up to 2.5 mm/yr difference).

The plate motion paths reveal a general NW to WNW-ward convergent motion of the African plate relative to Iberia and Eurasia from chron 25 to 21 (early Eocene). This direction of plate motion changed towards the N to NNE from chron 21 to 6 (late Eocene to early Miocene), after which it switched back to a NW directed convergent path in the middle Miocene (chron 5b to 5a) and this direction of motion has persisted since. Both Dewey *et al.* (1989), Mazzoli and Helman (1994), and Rosenbaum *et al.* (2002b) have made similar observations. In addition, the present-day instantaneous plate motion vector of Africa towards Iberia (Eurasia), based on the rotation parameters of NUVEL-1A (DeMets *et al.*, 1994), has a general direction of 321º, but error values allow a range in azimuth from 312º to 334º.

Below we first compare results calculated for the different sets of rotation parameters, and review differences in trajectory paths, velocity and total convergence obtained for these different sets. We then proceed to compare these results with present-day motions between Africa and Iberia based on the NUVEL-1A model (DeMets *et al.*, 1994).

The trends of the plate motion paths calculated with the different rotation parameter datasets are grossly consistent, but calculated paleo-positions of arbitrary points may differ. As an example, the paleo-positions of points A and B on the African plate shown in Figure 2.3 may vary by tens of kilometers up to an estimated maximum of 100 km. Like the plate motion paths, the azimuths of the instantaneous plate motion vectors (Figure 2.4) calculated with the different datasets for the late Paleogene – Neogene period

(chron 13 to present) are fairly consistent. For periods prior to the Eocene, however, the results show markedly less consistency.

The plate velocities calculated with respect to a point on the Iberian or Eurasian plate as well as the amounts of convergence show relatively large differences up to 3 mm/yr (Figure 2.4: compare Dewey with Müller and Roest, chrons 13 and 6) and more than 30 km, respectively (compare Dewey with Müller and Roest, chron 13). But although velocities may differ for the various models, there is a consistent pattern of changes in convergence rates during the Cenozoic stages. In the Cenozoic, a period of rapid convergence (6 to 10 mm/yr) occurred during the late Eocene and Oligocene, followed by a period of slow convergence (1 to 4 mm/yr) during possibly the latest Oligocene and certainly the early-middle Miocene. Subsequently, the convergence rate has increased since the late Miocene till the present to about 6 mm/yr. These observations are consistent with those of Rosenbaum *et al.* (2002).

The total amount of African-Eurasian convergence calculated for the different sets of rotation parameters appears to be rather consistent, and ranges between ~370 to 380 km since chron 34 (late Cretaceous; 83 Ma) both for the Africa-Eurasia models and for the combined results of the Africa-Iberia and Iberia-Eurasia models. A clear exception is posed by Dewey's model (1989) which indicates a total of 260 km convergence since the late Cretaceous. It is emphasized, however, that a general consistency in the total amount of convergence is implicit in the fact that all models have common starting and end points, i.e., the opening of the Atlantic Ocean and the present-day situation.

The present-day convergence between Africa and Iberia can also be quantified on the basis of the NUVEL-1A model (DeMets *et al.*, 1994). This model is the only model used here in which error values are documented, and it is envisaged that the uncertainties obtained with this model may be indicative for the uncertainties involved in estimates of direction, velocity and total convergence in any of the other models used. The present-day convergence rate of Africa towards Iberia (Eurasia) based on NUVEL-1A suggests a convergence velocity of 5.23 mm/yr, but in view of the error in position and rotation rate this value may vary between 3.68 and 7.21 mm/yr, which gives a variation of 3.53 mm/yr. Note that the rotation parameters of NUVEL-1A (DeMets *et al.*, 1994) are based on Pliocene (chron 2A; ~3 Ma) to present-day relative plate motion reconstructions, as well as inverted present-day plate boundary geometries and fault-plane solutions of recent earthquakes. Assuming that the position of the rotation pole and the rotation rate have not radically changed since 3 Ma, the amount of convergence between the Africa and Iberian plates since 3 Ma is about 15.6 km, and ranges between a minimum of 11 km to a maximum value of 21.6 km, which yields an uncertainty of ±5.3 km.

In view of our aim to place constraints, via plate motion reconstructions, on the role of boundary conditions on the tectonics of the Betic-Rif arc, it is of utmost importance to investigate any motions of Africa with respect to Iberia rather than Eurasia. Table 2.3 summarizes calculated African-Iberian and Iberian-Eurasian stage poles based on rotation parameters from Srivastava et al (1990a,b) and Rosenbaum *et al.* (2002b). These stage poles clearly reveal periods when no or very small rotations occurred between the African and Iberian plates and between the Iberian and Eurasian plates. From chron 34 to 25 (late Cretaceous – Paleocene), and possibly chron 24 (early Eocene), no rotations occurred between Africa and Iberia and both plates have responded as one single entity with respect to the Eurasian plate (see also Figure 2.4). From chron 25 to 21 (Eocene) the Iberian plate has rotated over small angles with respect to Eurasia. A decrease in rotation rate and rotation angle of the Iberian plate with respect to Eurasia since the early Miocene suggests that Iberia effectively becomes part of Eurasia. It is thus important to note that prior to the late Cretaceous (chron M25-M0) and during a period from the late Eocene till the early Miocene (chron 21 to 6) the Iberian plate has rotated with respect to both Eurasia and Africa, which strongly suggests that Iberia acted during those periods as an independent (micro-)plate. These observations are entirely consistent with the results obtained by Srivastava *et al.* (1990a,b) and Roest and Srivastava (1991), who suggest that Iberia acted as an independent plate from chron 18 (39.6 Ma) until chron 6c (24 Ma).

The calculated amount of convergence between Iberia and Eurasia since the late Cretaceous varies between 130 and up to 200 km, from west to east along strike of the Pyrenees, which is consistent with the results of Roest and Srivastava (1992) and Rosenbaum *et al.* (2002b) as shown in Table 2.4 and Figure 2.4. At this stage we note that this calculated total amount of convergence across the Pyrenees is clearly consistent with geological estimates of 165 km shortening since the Cretaceous (Beaumont *et al.*, 2000) based on res-

toration of the balanced ECORS-PYRENEES section across the Central Pyrenees.

Convergence between the Iberian and African plates did not start prior to the middle Eocene (since chron 21: Table 2.3). The calculated amount of convergence since the middle Eocene ranges from 251 to 254 km in the direction of plate motion, with a N-S directed component of 218 to 236 km (Table 2.4: Srivastava *et al.*, 1990a,b and Rosenbaum *et al.*, 2002b). Approximately 83 to 90 km of convergence, with a N-S directed component of 65 to 87 km, occurred during late Eocene until the Oligocene (chron 21 to 13) whilst approximately 100 km of N-S convergence was achieved from the Oligocene to the early Miocene (chron 13 to 6). This was followed by a stage of little convergence till the late Miocene (chron 6 to 5). Since the late Miocene (chron 5), the different datasets yield between 55 and 62 km of convergence, whilst the N-S component of shortening between the African and Iberian-Eurasian plates varies between 30 to 40 km.

Comparison with geological data

As emphasized already, the Iberian-Eurasian plate motion reconstructions are in clear agreement with geological observations in the Pyrenees (e.g., Beaumont *et al.*, 2000), both with respect to the onset of inversion of early Cretaceous rift faults (latest Cretaceous) and the timing of subsequent compressional events from the early Eocene to the Oligocene (from 55 to 25 Ma), and with respect to tectonic transport directions (N-S to NNE-SSW) and associated amounts of shortening (~165 km). The plate motion reconstructions are, however, partly inconsistent with geological observations in the Betic Cordillera of southern Spain, and in the Rif, Tell and Atlas Mountains in northern Africa, which together form an integral part of the African-Eurasian plate boundary zone in the Western Mediterranean region. In this section we therefore summarize the main tectonic characteristics of these different belts, with the aim to evaluate the various plate motion reconstructions against the background of these geological data and vice versa.

Geological data suggest that both the Alboran region and the Atlas have been active convergent zones since the Eocene (e.g., Beauchamp *et al.*, 1999; Frizon de Lamotte *et al.*, 2000; Gomez *et al.*, 2000; Platt *et al.*, 2003; Chalouan *et al.* 2001). According to Monié *et al.* (1991), peak conditions of shortening-related HP/LT metamorphism in the Internal Zone of the Betic – Alboran – Rif system were reached before 48 Ma. Somewhat later during the Eocene, a major uplift and folding phase initiated in the Atlas, involving reactivation and inversion of pre-existing Mesozoic structures of the Atlas rift system. This compressive deformation continued well into the Miocene (e.g., Brede *et al.*, 1992; Beauchamp *et al.*, 1999; Gomez *et al.*, 2000; Frizon de Lamotte *et al.*, 2000; Teixell *et al.*, 2003; Arboleya *et al.*, 2004). As already noted by Gomez *et al.* (2000), the compressional structures in the Atlas are related to NNW to NW directed compression, and these compression directions are consistent with Paleogene and Neogene plate motion vectors.

From the late Oligocene to the early Miocene, the Internal Zone of the Betic-Alboran-Rif system was subjected to E-W directed extension and concomitant migration towards the west. The Mesozoic and Cenozoic cover in front of the migrating Internal Zones were folded and thrusted and became part of the growing Betic – Rif – Tell arc. Tectonic transport in general occurred towards the NW in the eastern Betics, towards the west in the western Betics, towards the WSW and SW in the Rif and towards the S to SSE in the Tell Mountains (e.g., Frizon de Lamotte *et al.*, 2000, Platt *et al.*, 2003 and references therein), i.e., roughly orthogonal to the Betic-Rif-Tell arc geometry.

On the basis of geological maps and field observations, Platt *et al.* (2003) have restored a total of six cross-sections across the external zones of the Betic-Rif arc. The amount of shortening estimated for the eastern Betic External Zone is 212 ± 76 km in a NW direction (300º to 320º), which implies a N-S component of 125 km. In the western part of the Betics, a WNW to NW directed shortening (azimuth 295º to 315º) of 221 ± 61 km is obtained, with a N-S directed component of 127 km. Likewise, they have estimated approximately 210 km (163 to 330 km) of WSW to SW directed shortening (azimuth 235º) in the Rif External Zone, i.e., a N-S directed component of 170 km. Based on restored balanced cross-sections and seismic profiles in central and eastern parts of the Betic External Zone, Banks and Warburton (1991) and Blankenship (1992) have arrived at similar values of about 200 km of shortening in a NW (320º) direction.

Recent studies on the structural development of the Atlas Mountains are somewhat inconsistent. Published estimates of the amounts of shortening in the High Atlas (Morocco) by Brede *et al.* (1992), Beauchamp *et al.* (1999), Gomez *et al.* (2000), Teixell *et al.* (2003) and Arboleya *et al.* (2004) range between

13 and 36 km. According to these authors, shortening occurred during major uplift and convergence in the Oligocene to early Miocene (chron 13 to 6). Frizon de Lamotte *et al.* (2000), on the other hand, suggest that over a hundred kilometer of convergence has occurred in the combined Saharan-Tunesian Atlas-Tell orogenic system since the middle Miocene, when late Eocene compressional structures in the Atlas were reactivated and the Atlas was partially overridden by nappes of the Tell Mountains.

It should be noted that in the External Zones of the Betics - Rif - Tell system and in the Atlas Mountains compressional tectonics have continued till the present (e.g., Sanz de Galdeano, 1990; Frizon de Lamott *et al.*, 2000; Platt *et al.*, 2003, Teixell *et al.*, 2003; Arboleya *et al.*, 2004). This is corroborated by the fact that late Miocene - Pliocene to recent transport directions of faults and shortening directions of folds in the Betics, Alboran and Tell are consistent with late Miocene - Pliocene to recent plate motion vectors and slip vectors determined from fault plane solutions of recent earthquakes (e.g., Buforn *et al.*, 1988; Gomez *et al.*, 2000).

Discussion

The directions and amounts of shortening, estimated on the basis of geological data from the External Betics and the Rif, differ remarkably from those obtained via the various plate motion reconstructions investigated above. The estimated N-S component of shortening in the Betic and Rif profiles ranges between 223 and 455 km. This N-S component of the total shortening accumulated essentially since the latest Oligocene and is considerably larger than the estimated 48 to 72 km N-S component of Iberia-Africa convergence, since the latest Oligocene – early Miocene (since chron 7.1 or 6; Table 2.4), obtained from plate motion reconstructions. It follows that an amount of at least 150 km up to possibly more than 400 km of shortening in the External Betics and Rif is not accounted for in the plate motion reconstruction models. In addition, the trends of the Oligocene - early Miocene tectonic slip vectors and associated fold axes within the External Zones of the Betic and Rif deviate from the calculated plate motion vectors. Note that the relatively small values of shortening in the Atlas Mountains (between 13 and 36 km), which have accumulated since the Oligocene, have not been included in these calculations. Gomez *et al.* (2000) state, however, that the shortening in the Atlas, particularly in the High Atlas, primarily reflects late Tertiary Africa-Europe plate convergence.

The excess amounts of shortening, as stated earlier, can clearly not be accounted for by the inferred motions of the bounding plates. As a matter of fact, the Africa-Eurasia (including Iberia) plate convergence slowed down in the late Oligocene or early Miocene, possibly came temporarily to a halt for about 10 Myrs, and then accelerated to about 6 mm/yr in the late Miocene, to continue at that convergence velocity to the present. It follows, that the excess amount of shortening in the fold and thrust belts of the External Zones must be explained in terms of an internally driven process associated with the simultaneous opening of the Algerian basin and extension in Betic-Alboran-Rif Internal Zone during the early Miocene. These extensional processes, best explained by models such as late-orogenic collapse of an Alpine orogen by removal of a thickened subcontinental lithosphere through convection (Platt and Vissers, 1989) or delamination (García Dueñas *et al.*, 1992), or subduction zone roll-back (e.g., Lonergan and White, 1997; Spakman and Wortel, 2004), likely account for the difference between the calculated total shortening between the bounding plates and the shortening observed in the External Betics and Rif.

Based on a combination of the geological data and plate motion reconstructions presented in this chapter, an improved paleo-geographic and paleo-tectonic reconstruction is proposed for the Alboran region (Figure 2.6) from the early Oligocene onward, i.e. from chron 13 till present:

- During the Oligocene (chron 13 till 6), the convergence direction varies between NNW and NNE (Figure 2.6a); Iberia in that period acts as an independent plate. Alpine folding and thrusting occurs in the Pyrenees, in the Betic-Alboran-Rif Internal Zone, and in the Atlas. The Betic-Alboran-Rif Internal Zone forms part of a domain often referred to as the ALKAPECA (Alboran-Kabylies-Peloritano-Calabria) domain, located most-likely at the present position of the Balearic Islands. In view of the modest shortening in the Atlas Mountains (between 13 and 36 km; see Brede *et al.*, 1992; Beauchamp *et al.*, 1999; Gomez *et al.*, 2000; Teixell *et al.*, 2003; Arboleya *et al.*, 2004), most of the plate convergence of the order of 115 km (Table 2.4) must have been accommodated in the ALKAPECA domain.

- In the early Miocene, Iberia effectively becomes part of the Eurasian plate, and convergence in the Pyrenees comes to an end. In the early - middle Miocene,

Figure 2.6. Palinspatic maps of the Alboran region for the Neogene period till recent.

6a) Chron 13 till chron 6 (33.1 till 19.2 Ma)
Pole at (31.5 N; 28.3 W) and rotation rate at 0.17 deg/Myr, after Rosenbaum et al. (2002)
Note that Iberia is an independent plate.

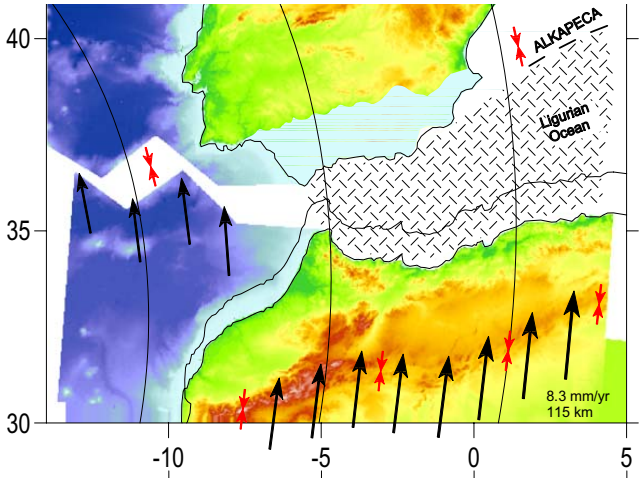

6b) Chron 6 till chron 5 (19.2 till 9.9 Ma)
Pole at (29.7 N; 3.6 W) and rotation rate at 0.10 deg/Myr, after Rosenbaum et al. (2002).
Note that Iberia is part of Eurasia.
(1) Late orogenic extension (Saadallah & Caby, 1996; Comas et al., 1999; Hanne et al., 2003) and rifting in the Alboran domain (Chalouan et al. 2001);
(2) Emplacement Tell nappes at Langhian (Tricart et al., 1994);
(3) Emile Baudot Transform fault (Acosta et al., 2001).

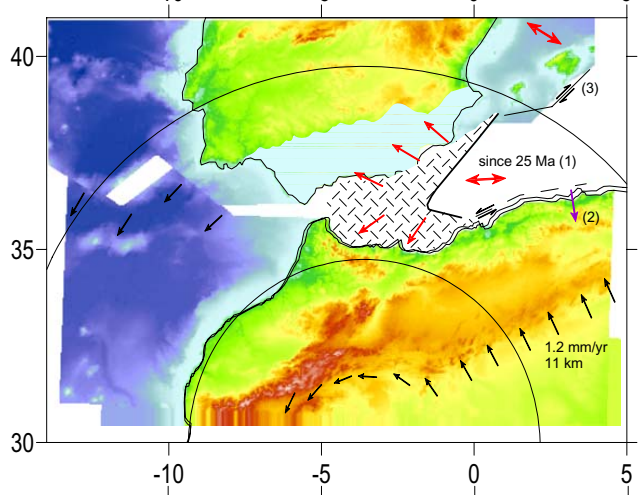

6c) Chron 5 (9.9 Ma) till present
Pole at (13.9 N; 21.2 W) and rotation rate at 0.11 deg/Myr, after Rosenbaum et al. (2002).
Note that Iberia is part of Eurasia.
(4) Refolding during Tortonian (Tricart et al., 1994);
(5) Closure of Taza-Guercif basin begins at 7.2 Ma and emerges at 6 Ma;
(6) Thrusting and folding in Prebetics (Platt et al., 2003; this study: Chapter 3).

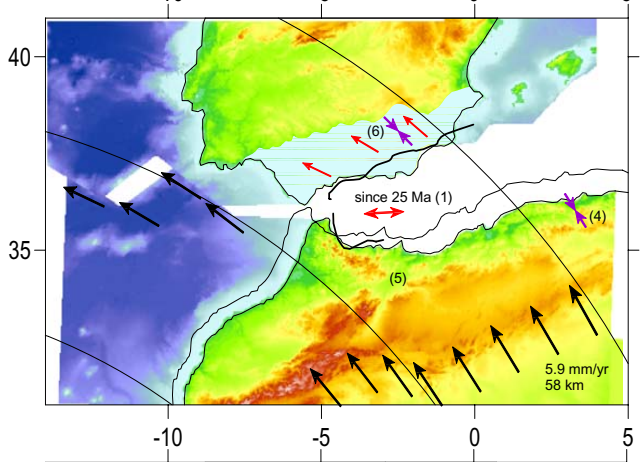

6d) Present-day Africa-Europe relative plate motions
Pole at (21 N; 20.6 W) and rotation rate at 0.12 deg/Myr, after De Metts et al. 1994.

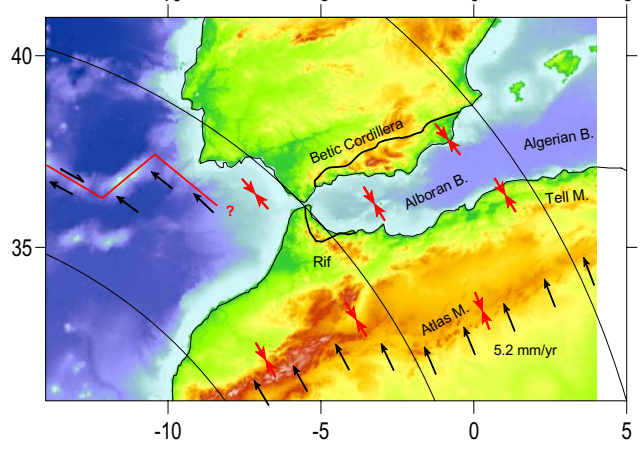

Geological data

- Extension
- Compression
- Thrusting
- Internal-External Zone Boundary

ALKAPECA: Alboran, Kabylies, Peloritan and Calabrian

the African plate motion vector with respect to Eurasia suddenly turns to a WNW direction (Figure 2.6b) and the relative velocity decreases significantly, from 7 - 10.5 mm/yr in the Oligocene down to 1.8 - 5.9 mm/yr in the middle Miocene. The relative motion of Africa and Iberia comes almost to a halt, with the consequence that little convergence occurred between the two plates. During this period, the Alboran domain moves rapidly towards the west by approximately 250 km (Platt *et al.*, 2003), the Internal Zones are simultaneously subjected to E-W directed extension, the Algerian basin opens, and coeval (latest Oligocene - early Miocene) folding and thrusting affects the External zones of the Betics and Rif, in WNW to NW and SW directions, respectively. According to several authors (e.g., Mazzoli and Helman, 1994; Frizon de Lamotte *et al.*, 2000; Jolivet and Faccenna, 2000; Rosenbaum *et al.*, 2002a) the sudden change in the relative motion between Africa and Eurasia led to, or gave way to the opening of the Western Mediterranean basins, the westward drift of the Alboran domain and the development of the Betics, Rif and Tell Mountains.

- In the late Miocene, extension in the Alboran domain comes slowly to an end and African-Eurasian plate convergence becomes again the dominant process, associated with tectonic structures both in the Atlas and Alboran domain suggesting approximately NW-SE shortening (Figure 2.6c). Since the late Miocene, African plate convergence has persisted towards the NW at a rate of 5.7 to 6.7 mm/yr, with an average present-day value of 5.2 mm/yr (Figure 2.6d). This convergence has been accommodated mainly in the Betics, Rif and Tell by continued thrusting towards the NW or SE in the External Zones and, at a late stage, by compression in the Internal Zones (Meijninger and Vissers, in press; chapter 6) and the Alboran basin floor (e.g., Watts *et al.*, 1993; Bourgois *et al.*, 1992; Comas *et al.*, 1992; Woodside and Maldonado, 1992). Plate motion reconstruction models estimate the amount of convergence accommodated in the Betics, Rif and Tell Mountains since the late Miocene, at 55 to 62 km.

Conclusions

Careful analysis of the history of Africa-Eurasia (Iberia) plate convergence based on plate motion reconstruction models, and comparison of these results with geological data leads to the following conclusions:

(1) Plate motion reconstruction models demonstrate that Africa-Iberia plate convergence slowed down and possibly came to a halt during the Neogene in the same period in which the western Mediterranean region began to develop. This involved the opening of the Algerian basin and the westward migration and extensional collapse of the Betic-Alboran-Rif Internal Zone, coeval with outward thrusting and folding in the External Zones of the system.

(2) There is a marked discrepancy between the convergence between Africa-Iberia since the late Oligocene and early Miocene calculated on the basis of plate motion reconstruction models, and the amount of shortening seen in the external parts of the Betic-Rif-Alboran system: 150 km up to possibly more than 400 km of shortening in the External Betics and Rif is not accounted for in the plate motion reconstruction models. It follows that the excess shortening must be compensated by extension known to have taken place in the internal parts of the system during the late Oligocene and early-middle Miocene.

(3) The results of plate motion reconstruction models support geological observations that Africa-Iberia plate convergence is the dominant process in the Alboran region since the late Miocene and that this convergence is responsible for the late Miocene to recent compressive deformation in the Internal Betics and Alboran crust. This is substantiated by the fact that late Miocene to recent tectonic transport directions and shortening directions in the fold and thrust belts of the External Zones are consistent with late Miocene to recent plate motion vectors, as opposed to trends of Oligocene and early Miocene slip vectors and fold axes in the External Zones which deviate from concurrent plate motion directions.

Table 2.1 – Total reconstruction and stage poles. Rotation parameters from Dewey et al. (1989), Srivastava et al. (1990a,b), Müller and Roest (1992), Mazzoli and Herman (1994), Rosenbaum et al. (2002) and DeMets et al. (1994).

DeMets et al. (1994) - NUVEL-1A - Instantaneous rotation pole AF-EU

Age	Latitude	Longitude	Angular velocity (deg/Myr)		Error ellipse major axis	minor axis	azimuth major axis
0	21	-20.6	0.12	± 0.02	6	0.7	-4

Total reconstruction poles Africa-Europe from Dewey et al. (1989)

Isochrons	Old ages (Ma)	New ages (Ma)	Latitude	Longitude	Rotation
5	8.9	10.1	0.55	-15.78	-0.94
6	19.4	19.2	24.04	-17.32	-2.33
13.2	35.5	33.1	29.26	-20.67	-6.65
21	48.8	46.3	35.08	-15.54	-10.39
24.2	55.7	52.8	33.04	-14.59	-10.77
30	66.7	65.6	31.52	-10.73	-11.29
33	74.3	73.6	33.51	-10.42	-11.61
34	84	83	34.82	-11.66	-14.64
M0	118	120.2	43.9	-9.08	-40.51
FIT	175	176	52.88	0.16	-59.86

Calculated forward motion stage poles

Latitude	Longitude	Rotation	angular velocity (deg/Myr)
-0.55	164.22	0.94	0.093
-38.36	161.83	1.52	0.167
-32.12	157.58	4.34	0.312
-43.62	176.28	3.89	0.294
11.30	176.60	0.55	0.085
1.26	-149.09	0.87	0.068
-77.66	-133.95	0.51	0.064
-40.17	164.07	3.05	0.325
-52.35	-164.82	7.46	0.279
-55.74	-144.46	21.36	0.379

Source: re-identify magnetic anomalies using the Lamont-Doherty data bank and remapping the fracture zones using bathymerty maps and SEASAT altimetry data.
Old ages after Klitgord & Schouten (1986) / Kent & Gradstein (1986). New ages after Huestis & Acton (1997), Cande & Kent (1995) and Gradstein et al.(1994).
Isochron lines positioned at the end of the normal polarity intervals. Corrections in the age result in very small changes of the angular velocity.

Srivastava et al. (1990)

Isochrons	Old ages (Ma)	New ages (Ma)
6	20	19.7
13	35.5	33.3
21	49.5	46.3
24	55.6	52.9
25	59	56.1
31	69	68.2
33o	80.2	79.1
34	84	83
M0	118	120.2
M10	131.5	130.2
M25	156.5	154

Finite rotation poles AF relative to NAM

Latitude	Longitude	Rotation	their reference
81.07	56.51	-5.21	(1)
76.28	2.22	-9.96	(1)
73.69	-6.11	-15.46	(1)
78.33	-2.64	-16.91	(1)
80.02	-0.73	-18.11	(1)
82.51	-0.63	-20.96	(4)
78.30	-18.35	-27.06	(4)
76.55	-20.73	-29.60	(4)
66.09	-20.18	-54.45	(1)
65.95	-18.50	-57.40	(4)
66.70	-15.85	-64.90	(1)

Finite rotation poles IB relative to NAM

Latitude	Longitude	Rotation	their reference
68.00	138.2	-4.75	(3)
76.34	117.33	-7.98	(1)
74.7	126.96	-11.05	(2)
72.98	133.28	-12.94	(2)
73.29	133.88	-14.25	(2)
74.96	135.34	-17.19	(2)
85.49	110.28	-22.41	(2)
87.18	57.43	-24.67	(2)
68.88	-15.00	-50.62	(1)
68.57	-13.11	-53.64	(1)
66.9	-12.93	-60.45	(1)

Calculated total reconstruction poles AF-IB

Latitude	Longitude	Rotation
-21.54	166.42	1.99
-27.61	158.14	4.07
-31.41	161.42	7.87
-31.46	161.42	7.87
-31.44	161.42	7.87
-31.4	161.42	7.87
-31.46	161.43	7.87
-31.44	161.42	7.87
-29.37	155.83	4.88
-27.91	156.38	4.88
-54.94	145.43	4.61

Calculated forward motion stage poles

Latitude	Longitude	Rotation	angular velocity (deg/Myr)
-21.54	166.42	1.99	0.101
-33.03	149.83	2.14	0.157
-35.12	165.53	3.83	0.294
-64.13	-27.58	0.01	0.001
66.55	151.59	0.00	0.001
62.50	152.90	0.01	0.001
-64.83	-47.53	0.01	0.001
50.98	115.24	0.00	0.001
33.67	-8.93	3.04	0.082
57.12	-173.68	0.13	0.013
-40.42	-10.14	2.33	0.098

Source: either (1) best fit or (2) calculated using correction pole or from (3) Olivet et al. (1984) or (4) Klitgord & Schouten (1986).
Old ages after Klitgord & Schouten (1986) / Kent & Gradstein (1986). New ages after Huestis & Acton (1997), Cande & Kent (1995) and Gradstein et al.(1994).
Isochron lines (5-31) positioned in the middle of the normal polarity intervals; ages shown are average ages of the normal polarity interval. Other ischron lines (34-M0) positioned at the end of the polarity intervals.
Uncertainties determined according to method of Stock and Molnar (1983); for each pole a maximum misfit of 7.5 km was allowed.

Table 2.1 continued – Total reconstruction and stage poles. Rotation parameters from Dewey et al. (1989), Srivastava et al. (1990a,b), Müller and Roest (1992), Mazzoli and Herman (1994), Rosenbaum et al. (2002) and DeMets et al. (1994).

Müller & Roest (1992)			Finite rotation poles AF relative to NAM				Finite rotation poles EU relative to NAM				Calculated total reconstruction poles AF-EU			Calculated forward motion stage poles			
Isochrons	Old ages (Ma)	New ages (Ma)	Latitude	Longitude	Rotation	their reference	Latitude	Longitude	Rotation	their reference	Latitude	Longitude	Rotation	Latitude	Longitude	Rotation	angular velocity (deg/Myr)
5.2	10	10.5	80.12	50.80	-2.52	(5)	65.38	133.58	-2.44	(4)	-13.88	158.83	1.09	-13.88	158.83	1.09	0.103
6	20	19.7	79.57	37.84	-5.29	(1)	68.92	136.74	-4.97	(4)	-14.30	165.31	2.23	-14.42	171.43	1.15	0.125
13.2	35.5	33.3	75.37	1.12	-10.04	(5)	65.64	136.95	-7.51	(4)	-28.30	160.93	5.96	-36.41	158.40	3.84	0.283
25	59	56.1	79.68	-0.46	-18.16	(5)	63.14	141.66	-14.22	(3)	-28.66	162.27	10.54	-28.96	164.06	4.59	0.201
31	69	68.2	82.46	-0.46	-21.39	(7)	64.84	143.96	-16.95	(3)	-30.72	163.53	11.23	-53.92	-166.82	0.82	0.068
34	84	83	76.55	-20.37	-29.60	(1)	66.54	148.91	-19.70	(2)	-35.98	165.82	18.08	-43.66	171.97	6.98	0.472
M0	118	120.2	66.09	-20.17	-54.45	(6)	68.99	154.75	-23.05	(3)	-43.63	173.18	41.20	-46.98	-177.58	23.55	0.660

Source: (1) Klitgord & schouten (1986), (2) Srivastava et al. (1988), (3) Srivastava & Roest (1989), (4) Lawver et al. (1990), (5) Mueller et al. (1991), (6) Roest et al. (1991), (7) interpolated from chron 30 and 32 remapping the fracture zones using com GEOSAT and SEASAT altimetry data.
Old ages after Kent & Gradstein (1986). New ages after Huestis & Acton (1997), Cande & Kent (1995) and Gradstein et al.(1994).
Isochron lines (5-31) positioned at the peak of the normal polarity intervals; ages shown are average ages of the normal polarity interval. Other ischron lines (34-M0) positioned at the end of the polarity intervals.

Total reconstruction poles Africa-Europe from Mazzoli & Helman (1994)						Calculated forward motion stage poles			
Isochrons	Old ages (Ma)	New ages (Ma)	Latitude	Longitude	Rotation	Latitude	Longitude	Rotation	angular velocity (deg/Myr)
2	1.66	1.79	2.39	162.74	0.16	2.39	162.74	0.16	0.089
2A.1	2.47	2.61	1.20	-16.52	-0.24	-8.30	164.97	0.08	0.099
3	3.88	4.1	11.04	-14.56	-0.39	-25.93	168.78	0.16	0.107
3A.1	5.35	5.91	7.49	-15.01	-0.55	1.05	163.89	0.16	0.090
4.1	6.70	7.48	10.14	-14.33	-0.69	-20.35	168.50	0.14	0.091
4A.1	7.90	8.8	1.55	163.68	0.81	47.08	153.05	0.20	0.148
5	8.92	9.91	0.55	-15.78	-0.94	-13.31	167.68	0.13	0.121
5A.2	11.86	12.44	6.72	-14.34	-1.18	-28.88	171.72	0.27	0.105
5C.1	16.22	16.04	12.03	-19.83	-1.87	-20.69	150.71	0.72	0.199
5D.1	17.57	17.4	15.97	-18.96	-2.08	-46.33	171.01	0.25	0.185
6A.1	20.88	20.59	23.38	-17.17	-2.58	-50.11	173.31	0.59	0.184
6B	22.57	22.44	25.66	-16.55	-2.79	-50.82	174.27	0.24	0.128
7.1	25.50	24.81	27.06	-15.96	-3.11	-38.75	170.24	0.33	0.139

Their source: Helman (1989).
Old ages after Berggren et al. (1985). New ages after Huestis & Acton (1997), Cande & Kent (1995) and Gradstein et al.(1994).
Isochron lines positioned at the end of the normal polarity intervals
Corrections in the age result in very small changes of the angular velocity

Table 2.1 continued – Total reconstruction and stage poles. Rotation parameters from Dewey et al. (1989), Srivastava et al. (1990a,b), Müller and Roest (1992), Mazzoli and Herman (1994), Rosenbaum et al. (2002) and DeMets et al. (1994).

Rosenbaum et al. (2002)		Finite rotation poles AF relative to NAM				Finite rotation poles IB relative to NAM				Calculated total reconstruction poles AF-IB			Calculated forward motion stage poles			
Isochrons	Ages (Ma)	Latitude	Longitude	Rotation	their reference	Latitude	Longitude	Rotation	their reference	Latitude	Longitude	Rotation	Latitude	Longitude	Rotation	angular velocity (deg/Myr)
5	9.9	80.12	50.80	-2.52	(5)	65.38	133.58	-2.44	(3)	-13.88	158.83	1.09	-13.88	158.83	1.09	0.110
6	19.2	81.07	56.51	-5.21	(4)	68.00	138.20	-4.75	(4)	-21.54	166.42	1.99	-29.74	176.40	0.94	0.101
13	33.1	75.37	1.12	-10.04	(5)	76.34	117.33	-7.98	(4)	-26.94	158.73	4.24	-31.48	151.68	2.30	0.166
21	46.3	75.30	-3.88	-15.25	(5)	74.70	126.96	-11.05	(4)	-32.88	161.39	7.40	-40.38	166.15	3.22	0.244
24	52.4	78.33	-2.64	-16.91	(4)	72.98	133.28	-12.94	(4)	-31.46	161.42	7.87	-10.09	160.34	0.50	0.082
25	55.9	79.68	-0.46	-18.16	(5)	73.29	133.88	-14.25	(4)	-31.24	161.94	7.97	-10.26	-168.05	0.12	0.034
31	67.7	82.51	-0.63	-20.96	(1)	74.96	135.34	-17.19	(4)	-31.40	161.42	7.87	14.06	13.11	0.12	0.010
33(old)	79.1	78.30	-18.35	-27.06	(1)	85.49	110.28	-22.41	(4)	-31.46	161.43	7.87	-64.83	-47.53	0.01	0.001
34	83	76.55	-20.73	-29.60	(1)	87.18	57.43	-24.67	(4)	-31.44	161.42	7.87	50.98	115.24	0.00	0.001
M0	120.2	66.09	-20.18	-54.45	(4)	68.88	-15	-50.62	(4)	-29.37	155.83	4.88	33.67	-8.93	3.04	0.082
M25	154	66.70	-15.85	-64.90	(4)	66.90	-12.93	-60.45	(4)	-54.94	145.43	4.61	-39.40	-10.85	2.20	0.065
ECMA	175	65.97	-12.76	-76.44	(4)	65.72	-12.82	-66.32	(6)	-67.27	165.07	10.12	-72.21	-162.12	5.81	0.277

Rosenbaum et al. (2002)		Finite rotation poles AF relative to NAM				Finite rotation poles EU relative to NAM				Calculated total reconstruction poles AF-EU			Calculated forward motion stage poles			
Isochrons	Ages (Ma)	Latitude	Longitude	Rotation	their reference	Latitude	Longitude	Rotation	their reference	Latitude	Longitude	Rotation	Latitude	Longitude	Rotation	angular velocity (deg/Myr)
5	9.9	80.12	50.80	-2.52	(5)	65.38	133.58	-2.44	(3)	-13.88	158.83	1.09	-13.88	158.83	1.09	0.110
6	19.2	81.07	56.51	-5.21	(4)	68.92	136.74	-4.97	(3)	-15.14	165.06	1.90	-16.40	173.35	0.83	0.089
13	33.1	75.37	1.12	-10.04	(5)	65.64	136.95	-7.51	(3)	-28.30	160.93	5.96	-34.36	159.09	4.14	0.297
21	46.3	75.30	-3.88	-15.25	(5)	66.15	135.40	-10.87	(7)	-31.14	160.65	9.11	-36.50	160.60	3.17	0.240
24	52.4	78.33	-2.64	-16.91	(4)	63.89	139.27	-12.89	(7)	-29.35	160.79	9.94	-10.61	160.42	0.89	0.145
25	55.9	79.68	-0.46	-18.16	(5)	63.14	141.66	-14.22	(2)	-28.66	162.27	10.54	-14.61	-178.17	0.65	0.187
33(old)	79.1	78.30	-18.35	-27.06	(1)	66.17	147.74	-19.00	(2)	-34.62	164.88	15.87	-45.03	173.25	5.51	0.238
34	83	76.55	-20.73	-29.60	(1)	66.54	148.91	-19.70	(2)	-35.99	165.65	18.08	-44.53	173.93	2.26	0.579
M0	120.2	66.09	-20.18	-54.45	(4)	69.67	154.26	-23.17	(8)	-43.61	173.06	40.90	-46.98	-177.57	23.25	0.625
M25	154	66.70	-15.85	-64.90	(4)	69.03	155.44	-23.26	(9)	-48.82	177.70	50.58	-55.78	-145.28	10.77	0.319
ECMA	175	65.97	-12.76	-76.44	(4)	71.61	156.70	-25.27	(9)	-50.57	-178.00	59.82	-47.86	-152.51	9.73	0.463

Rosenbaum et al. (2002)		Finite rotation poles IB relative to NAM				Finite rotation poles EU relative to NAM				Calculated total reconstruction poles IB-EU			Calculated forward motion stage poles			
Isochrons	Ages (Ma)	Latitude	Longitude	Rotation	their reference	Latitude	Longitude	Rotation	their reference	Latitude	Longitude	Rotation	Latitude	Longitude	Rotation	angular velocity (deg/Myr)
5	9.9	65.38	133.58	-2.44	(3)	65.38	133.58	-2.44	(3)		0	0				0
6	19.2	68.00	138.20	-4.75	(4)	68.92	136.74	-4.97	(3)	77.93	59.14	0.2378	77.93	59.14	0.24	0.012
13	33.1	76.34	117.33	-7.98	(4)	65.64	136.95	-7.51	(3)	-31.21	166.79	1.7259	-37.04	168.72	1.87	0.135
21	46.3	74.70	126.96	-11.05	(4)	66.15	135.40	-10.87	(7)	-23.85	157.12	1.7236	34.86	92.59	0.34	0.026
24	52.4	72.98	133.28	-12.94	(4)	63.89	139.27	-12.89	(7)	-21.60	157.88	2.0995	-11.36	160.87	0.38	0.063
25	55.9	73.29	133.88	-14.25	(4)	63.14	141.66	-14.22	(2)	-20.72	162.40	2.6064	-15.79	179.64	0.54	0.153
33(old)	79.1	85.49	110.28	-22.41	(4)	66.17	147.74	-19.00	(2)	-37.17	169.00	8.0377	-44.33	173.73	5.61	0.242
34	83	87.18	57.43	-24.67	(4)	66.54	148.91	-19.70	(2)	-38.86	169.85	10.2789	-44.56	173.97	2.26	0.579
M0	120.2	68.88	-15	-50.62	(4)	69.67	154.26	-23.17	(8)	-44.46	176.56	36.3419	-45.78	-179.68	26.18	0.704
M25	154	66.90	-12.93	-60.45	(4)	69.03	155.44	-23.26	(9)	-47.12	179.45	46.2876	-51.62	-163.81	10.22	0.302
ECMA	175	65.72	-12.82	-66.32	(6)	71.61	156.70	-25.27	(9)	-46.80	-178.90	50.3253	-37.59	-166.82	4.15	0.198

Source: (1) Klitgord and Schouten (1986), (2) Srivastava and Roest (1989), (3) Lawver et al. (1990), (4) Srivastava et al. (1990a), (5) Muller et al. (1990), (6) Srivastava and Verhoef (1992), (7) Srivastava and Roest (1996), (8) Srivastava et al. (2000), and (9) Torsvik et al. (2001). Ages after Huestis & Acton (1997), Cande & Kent (1995) and Gradstein et al.(1994). Isochron lines positioned at the end of the normal polarity intervals. ECMA = East coast magnetic anomaly.

Table 2.2 – Geomagnetic Polarity Time Scale (GPTS).

Isochrons	Gradstein et al. 1994 (Ma)	Cande & Kent 1995 (Ma)	Huestis & Acton 1997 (Ma)	Composite (Ma)
2			1.79	1.79
2A.1			2.61	2.61
3			4.1	4.1
3A.1			5.91	5.91
4.1			7.48	7.48
4A.1			8.8	8.8
5			9.91	9.91
5A.1			12.44	12.44
5C.1			16.04	16.04
5D.1			17.4	17.4
6			19.16	19.16
6A.1			20.59	20.59
6B			22.44	22.44
7.1			24.81	24.81
13			33.06	33.06
21		46.26		46.26
24		52.36		52.36
25		55.9		55.9
30		65.58		65.58
31		67.74		67.74
33		73.6		73.6
33old		79.08		79.08
34		83		83
M0	120.2			120.2
M10	130.2			130.2
M25	154			154
Closure	*176*			*176*

Ages represent the ends of the normal polarity intervals of the magnetic anomalies (chrons). The ages of the magnetic anomalies used in this study are shown.

Table 2.3 – Stage pole rotations of Africa relative to Iberia and Iberia relative to Eurasia. Stage pole parameters are in Table 2.1.

		Africa - Iberia				Iberia - Eurasia		
		Srivastava et al. (1990a,b)		Rosenbaum et al. (2002)		Rosenbaum et al. (2002)		
chrons	Age (Ma)	rotation angle (deg)	rotation rate (deg/Myr)	rotation angle (deg)	rotation rate (deg/Myr)	rotation angle (deg)	rotation rate (deg/Myr)	
5	9.91	-	-	1.09	0.110	0	0	Iberia part of Eurasia
6	19.7	1.99	0.101	0.94	0.101	0.24	0.012	Iberia part of Eurasia
13	33.3	2.14	0.157	2.30	0.166	1.87	0.135	Iberia independent
21	46.3	3.83	0.294	3.22	0.244	0.34	0.026	Iberia independent
24	52.9	0.01	0.001	0.50	0.082	0.38	0.063	Iberia part of Africa or independent?
25	56.1	0.00	0.001	0.12	0.034	0.54	0.153	Iberia part of Africa
31	68.2	0.01	0.001	0.12	0.010	-	-	Iberia part of Africa
33(old)	79.1	0.01	0.001	0.01	0.001	5.61	0.242	Iberia part of Africa
34	83	0.00	0.001	0.00	0.001	2.26	0.579	Iberia part of Africa
M0	120.2	3.04	0.082	3.04	0.082	26.18	0.704	Iberia independent
M10	130.6	0.13	0.013	-	-	-	-	Iberia independent
M25	154	2.33	0.098	2.20	0.065	10.22	0.302	Iberia independent
ECMA	176	-	-	5.81	0.277	4.15	0.198	Iberia independent

Table 2.4 – Overview of plate motion vectors and amounts of plate convergence.

			Srivastava et al. 1990a,b			Rosenbaum et al. 2002			Rosenbaum et al. 2002			Rosenbaum et al. 2002			Mazzoli & Helman 1994			Mueller & Roest 1992			Dewey et al. 1989		
			Af-Ib	(Betic - Atlas)		Af-Ib	(Betic - Atlas)		Ib-Eu	(Pyrenees)		Af-Eu			Af-Eu			Af-Eu			Af-Eu		
Isochrons	**Composite**	**Plates**	**azimuth**	**km (az)**	**km (ns)**	**azimuth**	**km (az)**	**km (ns)**	**azimuth**	**km (az)**	**km (ns)**	**azimuth**	**km (az)**	**km (ns)**	**azimuth**	**km (az)**	**km (ns)**	**azimuth**	**km (az)**	**km (ns)**	**azimuth**	**km (az)**	**km (ns)**
	(Ma)																					
2	1.79	IB + EU													298	11.10	5.26						
2A.1	2.61	IB + EU													303	4.26	2.32						
3	4.1	IB + EU													328	3.66	3.11						
3A.1	5.91	IB + EU													297	10.93	5.03						
4.1	7.48	IB + EU													312	4.41	2.97						
4A.1	8.8	IB + EU													288	21.61	6.71						
5	9.91	IB + EU				321	55.02	42.51				320	55.02	42.51	303	5.71	3.11	321	54.64	42.22	298	60.68	28.44
5A.2	12.44	IB + EU													334	4.16	3.73						
5C.1	16.04	IB + EU													343	38.28	36.51						
5D.1	17.4	IB + EU													66	7.36	3.02						
6	19.16	IB + EU	323	62.75	48.39	317	7.85	5.70	286	8.22	2.21	292	27.59	10.24				295	43.63	18.48	26	46.01	41.38
6A.1	20.59	IB													76	20.25	4.88						
6B	22.44	IB													79	8.39	1.66						
7.1	24.81	IB													40	6.32	4.85						
13	33.06	IB	9	101.41	100.18	5	104.30	103.95	330	40.15	34.76	11	137.99	135.44				18	133.26	126.97	4	156.41	155.99
21	46.26	IB/IB + AF	15	90.12	86.98	38	83.50	65.40	332	35.47	31.34	19	99.41	94.19							76	84.33	20.30
24	52.36	IB + AF	-	0.73	-0.15	313	27.01	18.45	304	25.30	14.27	314	47.06	32.44							275	42.87	3.58
25	55.9	IB + AF	-	0.35	0.07	61	5.61	-2.70	272	27.51	1.11	264	22.78	-2.25				349	125.03	122.62			
30	65.58	IB + AF																			223	68.30	-49.78
31	67.74	IB + AF	-	1.34	0.28	54	4.96	2.89										110	36.02	-12.30			
33	73.6	IB + AF																			102	43.17	-8.77
33old	79.08	IB + AF	-	1.18	-0.38	-	1.23	-0.40	14	56.44	54.66	69	141.91	51.07									
34	83	IB + AF	-	0.43	0.25	-	0.43	0.25	17	22.16	21.15	70	55.23	18.95				62	169.53	78.61	35	86.74	71.34
M0	120.2	IB																					
M10	130.2	IB																					
M25	154	IB																					
Closure	*176*	IB																					
Total				258.30	235.62		289.90	236.05		215.25	159.50		586.99	382.60		146.46	83.17		562.12	376.60		588.50	262.48

IB + EU = Iberia part of Eurasia
IB + AF = Iberia part of Africa
IB = Iberian plate independent
with respect to point on African plate (lat;lon) = (32.75;0)
for Ib-Eu wrt point on Iberian plate (lat; lon) = (43.25;0.75)

3

Miocene basins in the Betic fold and thrust zone

Introduction

The Betic Cordillera of southern Spain together with the Rif in Morocco and the Tell Mountains in northern Algeria form a morphologically distinct, arc-shaped orogen, which constitutes the western end of the Mediterranean Alpine chain (Fig. 3.1). The outer arc of this orogen consists of a fold and thrust belt (the Betic and Rif External Zones), whilst the inner arc is made up of an allochtonous pile of mostly metamorphic rocks exposed in the Betic and Rif Internal Zones. Part of the Internal Zone is presently submerged in the Alboran Sea. The Betic-Rif arc geometry developed during the latest Oligocene and early to middle Miocene, when a combination of westward motion plus extensional deformation of the Internal Zone and slow but continuous African – European plate convergence resulted in outward thrusting and folding of the Mesozoic – Cenozoic cover in front of the migrating Internal Zone (Fig. 3.2). A number of hypotheses have been proposed in the literature to explain the extensional collapse and westward drift of the Internal Zone, and the simultaneous folding and thrusting in the External Zones, in terms of orogenic processes at the African – European plate boundary (e.g., Platt and Vissers, 1989; García Dueñas *et al.*, 1992; Royden, 1993; Seber *et al.*, 1996; Vissers *et al.*, 1995; Lonergan and White, 1997; Spakman and Wortel, 2004).

During the Miocene, basins developed both on top of the growing fold and thrust belt of the External Zone and within the extending Internal Zone. This chapter focuses on Miocene basins in the fold and thrust belt, in particular on those in the eastern part of the Betic External Zone (Fig. 3.1). During the Neogene, the External Zone (Pre- and Subbetics) formed in essence a foreland domain, in which the Miocene is represented by a marine "Flysch" series (or "Tap" facies, or Moratalla Formation; e.g., Hermes, 1978; García-Hernández *et al.*, 1980; Ott d'Estevou *et al.*, 1988; Sanz de Galdeano and Vera, 1992). The flysch deposits pass upwards into late Miocene molasse type continental deposits (e.g., Dabrio, 1972; Calvo *et al.*, 1978; Ott d'Estevou *et al.*, 1988; Sanz de Galdeano and Vera, 1992). Both the Miocene and underlying Mesozoic – Cenozoic rocks are folded along approximately ENE to NE trending axes or are cut by generally northwest directed thrusts. Some of the Miocene basins, e.g., the Pontones basin (Figs. 3.2c and 3.3), have (partially) been overridden by thrust units and have been disconnected from the surrounding basins. But within the Betic External Zone, and in the Prebetics in particular, there are also clearly extensional structures, which run parallel to the general ENE-WSW trend of the compressional structures as indicated on the geological maps of the Instituto Geologico y Minero de España (IGME). Some of the Miocene basins in the Prebetics are bounded by these extensional structures, such as for example the Santiago de la Espada basin (Figs. 3.2c and 3.3) which is bounded along its northern margin by a morphologically distinct normal fault. At first inspection, the geometry of this basin suggests an extension-related origin with significant displacements along the extensional faults, and a direct relationship between the compressional structures (the folds and thrusts) and the extensional faults is not immediately obvious. Except of a study by Luján *et al.* (2000) and by Crespo-Blanc and Campos (2001), both in the Gibraltar fold and thrust belt, earlier structural studies of the External Betics (e.g., De Smet, 1984; Ott d'Estevou *et al.*, 1988; Banks and Warburton, 1991; Platt *et al.*; 2003) seem to have either overlooked or ignored the existence and significance of these extensional structures.

At least four different explanations may account for the development of extensional structures such as those in the Santiago de la Espada basin: (1) collapse of an overthickened fold and thrust belt or orogenic wedge (e.g., Davis *et al.*, 1983; Platt, 1986; Dahlen, 1990), (2) displacement of the locus of extension from the Internal towards the External Zone (e.g., Crespo-Blanc and Campos, 2001), (3) stratal extension in the footwalls of thrust faults (Platt and Leggett, 1986), (4) hanging-wall collapse in response to a specific fault plane geometry (a shallowing-upward fault; Coward, 1983). The first two explanations imply that the extensional structures should accommodate regional,

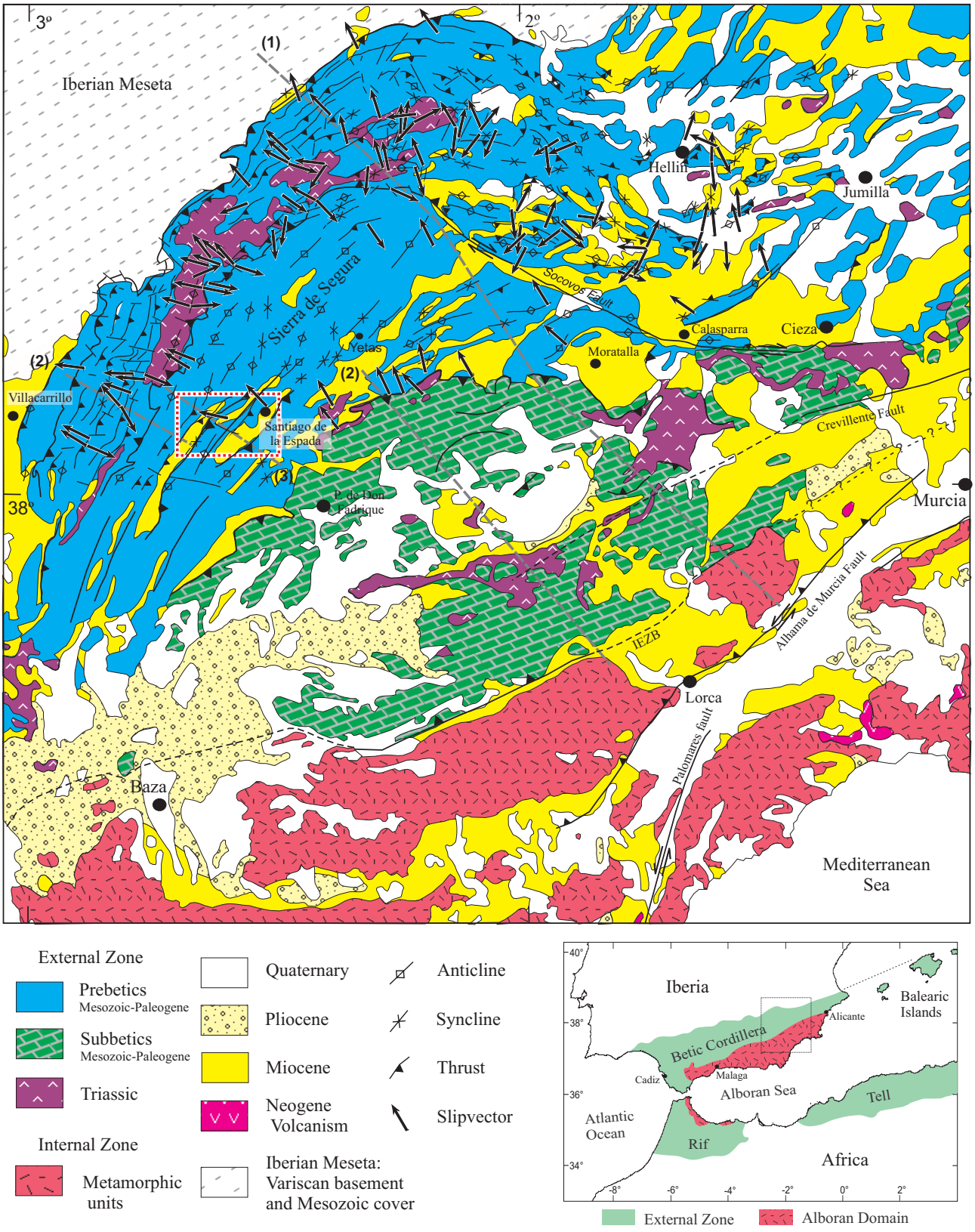

Figure 3.1. Geological map of part of the External Zone of the Betic Cordillera in southern Spain, modified from Mapa Geologico de la Peninsula Iberica (IGME, 1:1.000.000, 1981). Structural data in the Prebetics after Platt et al. (2003). Rectangle marks area of interest in western Prebetic Miocene basins (Pontones and Santiago de la Espada basins). IEZB - Internal-External Zone Boundary. (1) External Betics profile from Banks and Warburton (1991); (2) Carzola and Nerpio-Fuensante sections from Platt et al., (2003); (3) Pontones-Santiago de la Espada section (this study); for sections, see Figure 3.2.

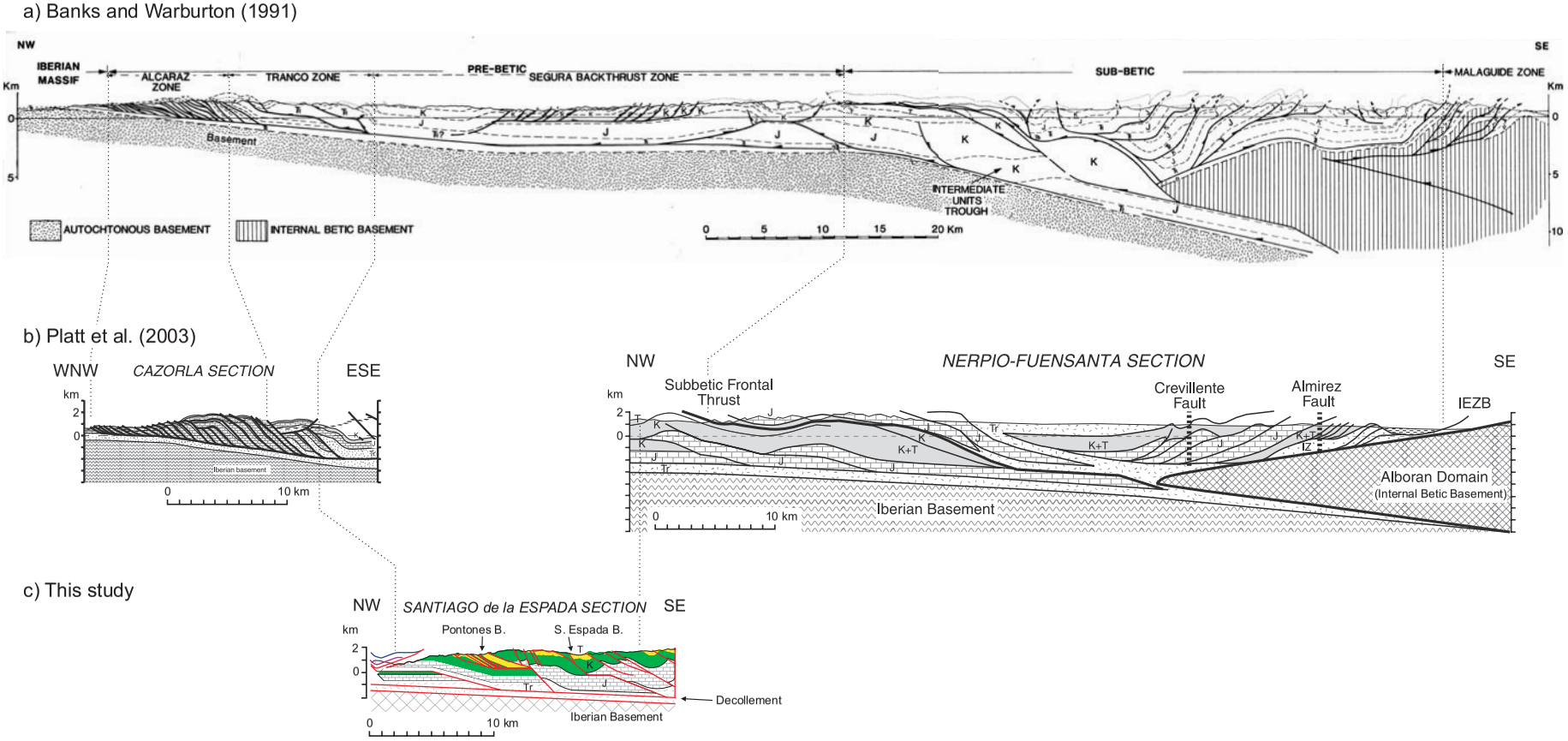

Figure 3.2. Balanced cross-sections of the Betic External Zone. For locations of sections see Figure 1. a) Cross-section from Banks and Warburton (1991). b) Cross-sections from Platt et al. (2003). c) Pontones-Santiago de la Espada section constructed in this study; for restored section see Figure 3.9. All cross-sections shown at same scale; Tr, J, K, and T denote Triassic, Jurassic, Cretaceous and Tertiary, respectively. Note that stratigraphic thickness of the Mesozoic units increases towards the south, and that shortening is accommodated by a gently southward dipping decollement within Triassic evaporites above the Iberian Paleozoic basement. Total amount of shortening since the early Miocene estimated at 200 or 212±76 km (Banks & Warburton, 1991; Platt et al., 2003), of which 40 or 48±11 km in the Alcaraz / Carzola imbricate fan (Banks & Warburton, 1991; Platt et al., 2003) plus a minimum of 6.3 km in the Santiago de la Espada cross-section (this study) since the late Miocene.

presumably crustal-scale extension of the Pre- and Subbetic domain. The latter two explanations imply that the extensional structures have developed due to local extension within a compressive setting in the Betic fold and thrust belt, and that they are inherent to the development of the thrust structure. The geometry of the extensional structures in the Santiago de la Espada basin indeed suggest that they formed in response to late Miocene thrusting, hence that the Miocene basins in essence developed in a compressive tectonic setting.

Main characteristics of the Betic External Zone

Primarily on the basis of its Mesozoic stratigraphy and facies, the Betic External Zone is divided into two geological domains, namely the Prebetic zone and the Subbetic zone (Hermes, 1978; García-Hernández *et al.*, 1980). The Prebetic zone, exposed in the eastern part of the Betic External Zone, mainly consists of Mesozoic up to Miocene continental to shallow marine deposits originating from the former southern Iberian margin. The rocks of the Subbetic zone, on the other hand, constitute a thicker and more complete Mesozoic sedimentary record with facies commonly indicating deeper marine conditions, most likely more distal with respect to the Iberian Meseta and south of the Prebetics. Relic Mesozoic extensional structures and lateral thickness variations of the Mesozoic cover suggest that during the Mesozoic both the Prebetics and Subbetics have intermittently been subjected to extension in response to the opening of the Atlantic Ocean in the west and opening of the Piemonte-Ligurian (or Alp-Tethys) Ocean in the east, eventually resulting in the separation of Iberia from Africa (Banks and Warburton, 1991, Reicherter *et al.*, 1994; Hanne *et al.*, 2003). These events led to the development of the various palaeogeographic realms and complex rift and wrench basin configurations identified on the thinned Iberian continental crust (García-Hernández *et al.*, 1980; De Ruig *et al.*, 1987; Reicherter *et al.*, 1994; Hanne *et al.*, 2003). In the subsequent post-rift stage, i.e., in the late Cretaceous and Paleogene to earliest Miocene, sediments were deposited in continental and shallow marine environments in the Prebetics and in a deep marine setting in the Subbetics (Hermes, 1978; Banks and Warburton, 1991). All of these deposits are overlain by a transgressive marine series of early to middle Miocene age, referred to as the Flysch deposits, the "Tap" facies, or the Moratella Formation, and lie unconformably on earlier Miocene or pre-Miocene rocks (e.g., Hermes, 1978; García-Hernández *et al.*, 1980; Sanz de Galdeano and Vera, 1992; Montenat *et al.*, 1996). The Miocene marine series pass upwards into an upper Miocene continental series (e.g., Calvo *et al.*, 1978; Montenat *et al.*, 1996).

The Betic fold and thrust belt is made up of NE to ENE trending folds, NW directed thrusts and SE directed back-thrusts (e.g., De Ruig, 1987; Ott d'Estevou *et al.*, 1988; Banks and Warburton, 1991; Frizon de Lamotte *et al.*, 1991; Van der Straaten, 1993; Lonergan *et al.*, 1994; Platt *et al.*, 2003; see Fig. 3.1). Shortening was accommodated along a gently southward dipping detachment in the Triassic horizon at the base of the External Zone stratigraphy, which probably continues underneath the Internal Zone (Banks and Warburton, 1991; Fig. 3.2). From the cross-sections (Fig. 3.2) it is evident that the thrusts form part of a complex structure, which is a result of piggy-back, overstep, out-of-sequence and break-back thrusting (e.g., Sabat *et al.*, 1988; Banks and Warburton, 1991; structural terms cf. Butler, 1982, 1987). On the other hand, De Smet (1984) has proposed that the Subbetic zone is part of a major flower structure associated with the motion on a crustal-scale strike-slip fault (the Crevillente fault) in the Betic (and Iberian?) basement, but structural evidence to support this interpretation seems to be lacking (Banks and Warburton, 1991; Platt *et al.*, 2003). Along the entire length of the Betic External Zone including the Balearic Islands, thrusting and folding initiated in the latest Oligocene – early Miocene, and has continued till the present (e.g., Sabat *et al.*, 1988; Geel *et al.*, 1992; Lonergan *et al.*, 1994; Geel, 1996; Crespo-Blanc and Campos, 2001). Beets and De Ruig (1992) have recognized unconformities in the Miocene stratigraphy, which they interpret in terms of the northward migration of a peripheral or fore-bulge and foreland basin. Several of these unconformities and associated stages of folding and thrusting have been identified: the stages have been dated as latest Oligocene – Aquitanian, Aquitanian – Burdigalian, Burdigalian - Langhian and Serravallian – early Tortonian (e.g., Calvo *et al.*, 1978; De Ruig *et al.*, 1987; Beets and De Ruig, 1992; Montenat *et al.*, 1996). These data are in agreement with data from the geological maps (IGME) and recent studies (e.g., Calvo *et al.*, 1978; De Ruig *et al.*, 1987; Ott d'Estevou *et al.*, 1988; Lonergan *et al.*, 1994; Geel, 1996; Platt *et al.*, 2003), showing that compressional deformation initiated in the early Miocene in the most internal parts of the External zone (the Internal-External Zone

Boundary, Lonergan *et al.*, 1994; and Fig. 3.1), whilst it became progressively younger (up to Tortonian – Messinian) near the outer parts of the External Zone. Thrusting and folding in the most external parts of the Prebetics eventually led to uplift and closure, in the late Miocene, of the northern Atlantic – Mediterranean corridor (also known as the "North Betic Strait"; e.g., Calvo *et al.*, 1978; Sanz de Galdeano and Vera, 1992; Soria *et al.*, 1999; Martín *et al.*, 2001; Braga *et al.*, 2003; Sanz de Galdeano and Alfaro, 2004). It should be emphasized that most of the Miocene basins in the Prebetics at present occur at an altitude of several hundreds up to 1500 meters above sea level (see also Sanz de Galdeano and Alfaro, 2004).

The basins chosen in the context of this study, i.e. the Pontones and Espada basins (Figs. 3.1 and 3.3), lie in the western part of the Prebetics. The Pontones basin, the Santiago de la Espada basin, and the basin in between, here referred to as the Almorchón basin, contain an almost complete record from the early to the late Miocene (Dabrio, 1970; Dabrio *et al.*, 1971; Dabrio, 1972). These Miocene sediments are considered part of the Santiago de la Espada Formation and lie in general unconformably on marine Cretaceous or shallow marine Paleocene-Eocene deposits (Dabrio, op. cit.). The total stratigraphic thickness of the Miocene sediments appears to increase from at least 140 meters in the Pontones basin up to about 600 meters in the Almorchón and Santiago de la Espada basins (Fig. 3.3). Currently, these basins are narrow, elongate structures separated from each other. The Miocene basin fill is folded and disrupted by both extensional and thrust faults. In case of the Pontones basin, it is disrupted and overridden from the southeast by a number of discontinuous thin-skinned thrusts, which has resulted in an imbricate structure of repeatedly stacked uppermost Cretaceous and Miocene rocks (Fig. 3.2). Both the Santiago de la Espada basin and the Almorchón basin are overridden from the southeast by thrust units and are cut by a major extensional fault along their north-western margins. The basins are underlain by a gradually southward thickening sequence of over a kilometre thick, ranging from the Triassic up to the Oligocene.

Methods

The structural and stratigraphical data for this study were collected in the Pontones basin, in outcrops along the road from Pontones to Santiago de la Espada, and in the Santiago de la Espada basin. Geological maps and stratigraphic data from earlier studies by Dabrio (1970, 1972) and Dabrio *et al.* (1971) were used in this study and modified where needed.

Rock or clay samples were collected about every 5 to 10 meters of section for biostratigraphic studies which were performed by G.J. van der Zwaan and W.J. Zachariasse (Stratigraphy and Paleontology group of the Department of Earth Sciences at the Utrecht University). Paleobathymetry analyses of individual marine clay samples using the ratio of planktonic and benthic foraminifera (P-B ratio) were performed by D.J.J. van Hinsbergen. An explanation of the methods of this paleobathymetry measurement is described in Van Hinsbergen *et al.* (2005).

Kinematics and slip directions of faults were determined on the basis of both structures on fault planes (such as tensile fractures, Riedel fractures, striations) and shear structures in fault gouges (Riedel, P, Y, R_2 and X shears and striations on these shear planes) as described by e.g., Logan *et al.* (1979), Rutter *et al.* (1986), Gamond (1987), Hancock and Barka (1987), Petit (1987), Means (1987), Sylvester (1988), and Woodcock and Schubert (1994). In the absence of lineations on a fault plane, the slip direction along the fault was inferred on the basis of the geometrical relationship between the main fault and secondary shear fractures, e.g., Riedel fractures.

A cross-section along the Pontones and Santiago de la Espada basins, parallel to the general direction of shortening, was constructed on the basis of both outcrop and published map data (Dabrio, 1972). Construction and restoration of this cross-section was performed by conventional principles, methods and techniques following Dahlstrom (1969), Hossack (1979) and Groshong (2002). In general, line length and, if permitted, area balance techniques were used in the reconstruction and restoration of the cross-section. The restoration and balancing of the deformed section was performed using the software program 2D-Move, kindly provided by Midland Valley Exploration Ltd [*1]. This program provides a number of restoration tools for balancing and restoration of a constructed (scanned and digitized) profile as well as tools for forward and backward modelling of restored and deformed cross-sections, respectively.

*1 Midland Valley Exploration Ltd: main office in Glasgow, United Kingdom. Website: www.mve.com.

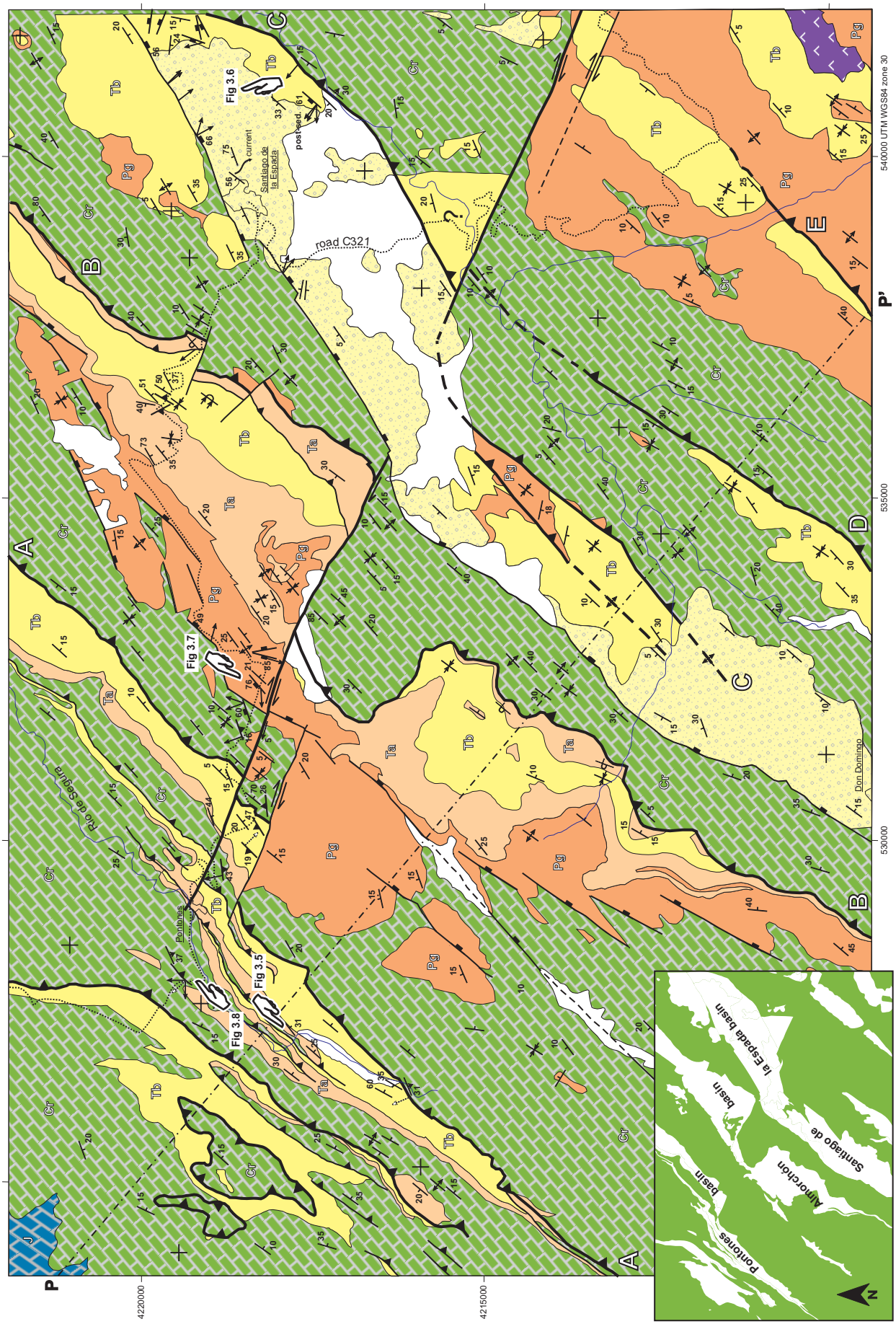
P
P'
A
B
C
D
E
Fig 3.6
Fig 3.7
Fig 3.5
Fig 3.8
road C321
current
Santiago de la Espada
post-sed.
Pontones
Río de Segura
Don Domingo
Tb
Ta
Pg
Cr
J
4220000
4215000
530000
535000
540000 UTM WGS84 zone 30
N
Pontones basin
Alhorchon basin
Santiago de la Espada basin

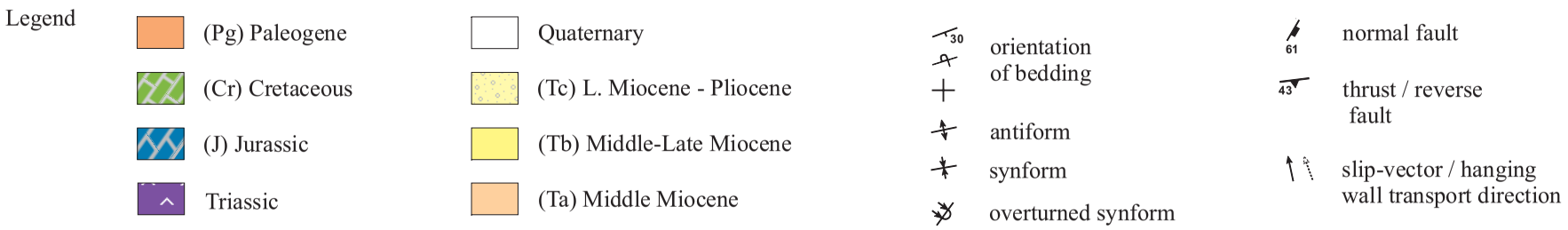

Figure 3.3. Geological map of the region of Santiago de la Espada and Pontones in the Prebetic Zone of the Betic Cordillera, modified after Dabrio (1972). Roman letters refer to large-scale thrust sheets. Profile P-P' is shown in Figures 3.2 and 3.9.

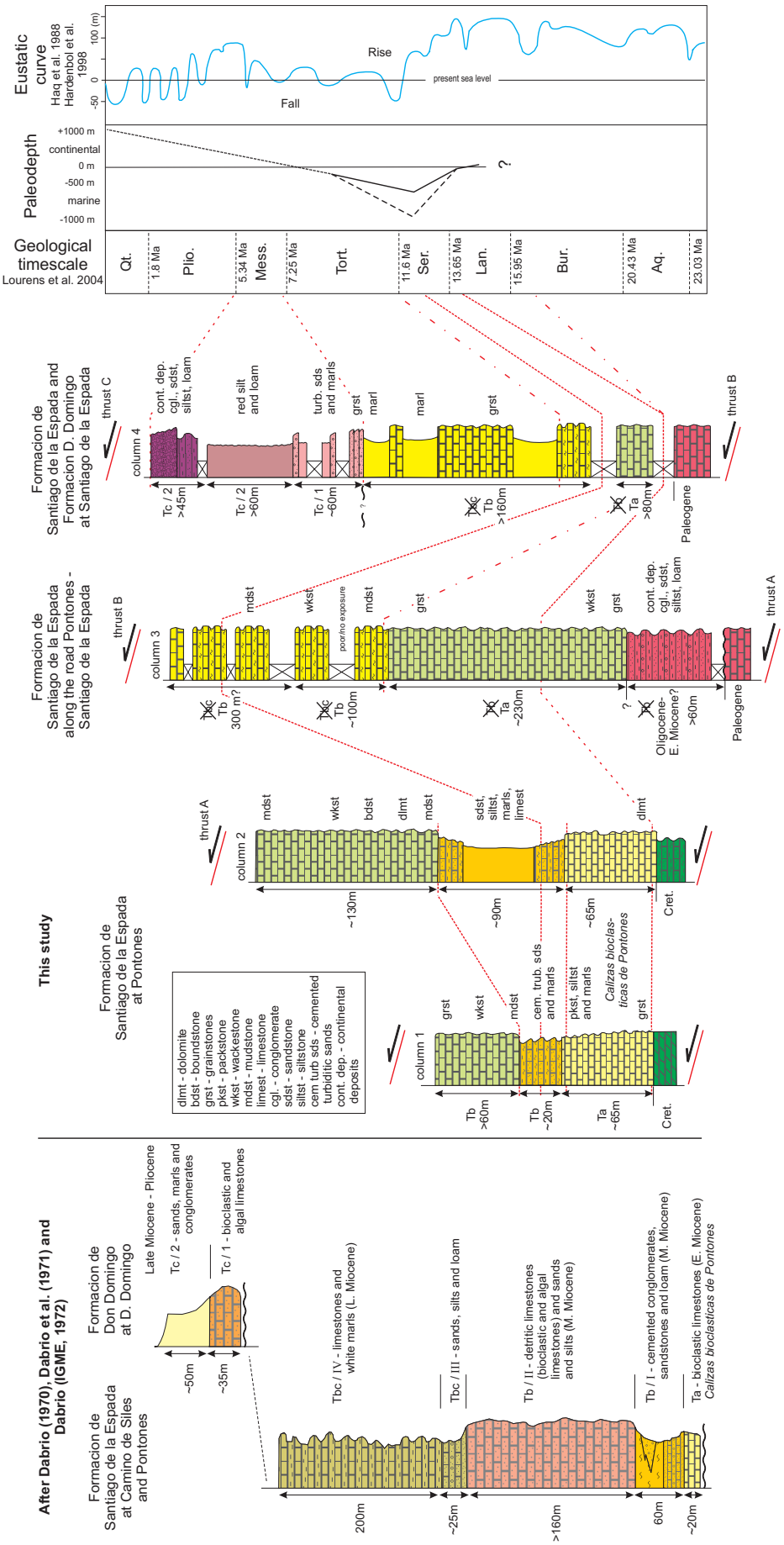

Figure 3.4. Stratigraphic correlation diagram of the Pontones and Santiago de la Espada region, after earlier studies by Dabrio et al. and after this study. Some earlier documented ages have been rectified based on new biostratigraphic study, resulting in improved correlations between the Miocene deposits of the Pontones, Almorchón and Santiago de la Espada basins. The paleo-depth curve is based on sedimentary facies study and paleo-bathymetry of individual samples.

Miocene stratigraphy of the Pontones and Santiago de la Espada basins

The oldest Neogene sediments consist of an at least 60 meter thick sequence of alternating grey-red lime and yellow sandstone and conglomerate beds of fluvial-continental origin. This unit is mainly exposed in the Almorchón basin, and (unconformably?) overlies Paleocene-Eocene shallow marine deposits (column 3 in Fig. 3.4).

The continental sediments pass upwards into a marine sequence that forms part of the "Formacion de Santiago de la Espada". Biostratigraphic analysis suggests that these marine sediments in the Pontones, Almorchón and Santiago de la Espada basins are of middle Miocene age (Fig. 3.4). This result is at variance with earlier studies by Dabrio (1970, 1972) and Dabrio *et al.* (1971), who claim that the marine sediments at the base of the "Formacion de Santiago de la Espada" are early Miocene. We therefore assume that the underlying fluvial-continental series is most likely of Oligocene to early Miocene age, which is in agreement with observations in other parts of the western Prebetics (e.g., Jerez Mir and Abril Hurtado, 1979). The middle Miocene marine series (unit Ta, Fig. 3.4) consist of a 65 up to a possibly 230 meter thick unit of bioclastic and algal limestone beds occasionally intercalated with a marl or silt bed. The massive limestone unit at the base is referred to as the "Calizas bioclasticas de Pontones" (Dabrio, 1970 and 1972; Dabrio *et al.*, 1971; and Fig. 3.5) and could be time equivalent to the "Roble Limestone" of Hermes (1978). The 230 meter stratigraphic thickness is most likely overestimated due to folding and thrusting. The occurrence of benthic foraminifera, such as representatives of *Amphistegina*, *Elphidium*, *Miogypsina*, *Bolivina*, and *Borelis*, and few planktonic foraminifera, such as *Orbulina* spp., *G. trilobus* and *G. scitula*, point to a middle Miocene age (pers. comm. G.J. van der Zwaan, W.J. Zachariasse and W. Renema). The lower limestone beds contain high percentages of quartz detritus and fragments of algae, brachiopods, echinoderms, gastropods and undeterminable larger foraminifera. According to Dabrio *et al.* (1971) the siliciclastic material was most likely derived from metamorphic and igneous sources on the Iberian Meseta. The litho-facies suggests a gradual transition from shallow marine near the base, to shelf conditions at the top of this unit.

The middle Miocene unit (Ta) changes upwards into a series of white marls intercalated with mudstone, turbiditic calcarenite beds and mass flow deposits (unit Tb), which reach a thickness of up to 300 meters (Fig. 3.4). This value, again, is most likely overestimated due to folding and thrusting. The occurrence of *Orbulina spp.*, *G. trilobus*, *G. menardii 3*, *P. mayeri* and *G. partimlabiata* suggest a Serravallian age (pers. comm. G.J. van der Zwaan and W.J. Zachariasse), which in terms of geochronology corresponds with the time interval 12.77 to 12.07 Ma (Lourens *et al.*, 2004). Paleodepth estimates using P-B ratios in individual samples indicate a water depth of 750 – 1000 m. Independent depth markers, e.g., *S. reticulata* and *P. araminensis*, suggest a depth of 500 to 600 meters, however (pers. comm. D.J.J. van Hinsbergen). The lithofacies includes mass flow deposits, and point to a relatively deep marine environment. These mass flow deposits of the Santiago de la Espada Formation are time equivalent with the 200 to 275 meter thick flysch-type deposits of the Moratalla Marlstone member near Moratalla to the east (Hermes, 1978; for location see Fig. 3.1).

The marls with intervening calcarenites pass upward into a thick and relatively massive unit of dolomites or crystalline limestones, wackestones and grainstones with large coral and bryozoa fragments. At Santiago de la Espada, however, these limestones alternate with marl beds. The presence of *menardii*-type globorotalids in thin sections suggests a late Serravallian – Tortonian age for this part of the sequence (pers. com. G.J. van der Zwaan). This limestone unit passes upwards into a series of silty clays and calcareous turbidite beds rich in siliciclastic detritus (unit Tc/1). The dominance of algae and benthic foraminifera, such as representatives of *Elphidium*, *Amphistegina*, *Ammonia*, *Borelis*, *Cibicides* and *Spiroplectammina* may suggest that relatively shallow marine conditions prevailed during this time.

In the Pontones and Almorchón basins these marine series are tectonically sealed by thrusts. In the Santiago de la Espada basin (Fig. 3.6), however, the shallow marine series changes abruptly into a thick homogeneous unit of red loam and fluvial silts, sands, and poorly sorted, angular conglomerates and breccias of the Don Domingo Formation (unit Tc). According to Dabrio (1972), an angular unconformity separates the marine sediments from these molasse-type continental deposits above, however, in the region of Santiago de la Espada we have found no evidence of this unconformity. We assume, therefore, that the continental deposits are of most likely Tortonian age, and that they may be time equivalents of the lacustrine deposits seen to the northeast near Yetas (Jerez Mir and Abril Hurtado, 1979) and of the

continental-lacustrine deposits near Hellin (for locations see Fig. 3.1). The latter deposits contain micromammal fossils which point to a late Turolian (Messinian) age (Calvo *et al.*, 1978). Note that in the most external parts of the Prebetics, towards the northwest near Villacarrillo, fluvial-continental deposits intercalate with marine limestones and marls containing micro-faunas indicative of Tortonian and Messinian age (Martínez del Olmo and Nuñez Galiana, 1973).

Structures in the Pontones and Santiago de la Espada basins

The structures observed in outcrops of the Cretaceous, Paleogene and Miocene rocks comprise both compression and extension-related structures, i.e., thrusts and folds, as well as low-angle to steeply dipping normal faults. In addition, there are few NW-SE oriented strike-slip faults (Figs. 3.7 and 3.8). In the Miocene deposits in particular, these structures are neither soft-sediment nor syn-sedimentary structures, i.e., the folds and most of the faults clearly developed after sediment deposition. In the uppermost Miocene deposits of the Santiago de la Espada formation (units Tb) at Santiago de la Espada, however, small-scale extensional faults show evidence of syn-sedimentary displacements.

Folds, in outcrops as well as on the scale of the geological map, commonly have NE-SW trending fold-axes, they are upright to inclined and their true profiles vary from close to open. The limbs of folds, in particular in the turbidite deposits of the Miocene Tb unit, are often stretched and boudinaged. Few folds are evidently thrust-related, such as in the case of drag folds in the footwall, and fault-bend or fault propagation folds in the hanging wall. Thrust planes in general dip at low to gentle angles, and kinematic indicators suggest hanging wall transport to the northwest. In a few examples, however, hanging wall transport is to the southeast. The strike-slip faults, both dextral and sinistral, have steeply inclined to vertical, NW-SE trending fault planes (Fig. 3.7b), i.e., they are parallel to the general transport direction of the fold and thrust belt, and clearly accommodate differential displacements between adjacent structural units. The slip-vectors on these fault planes vary in plunge from horizontal to oblique (66°), which makes these faults either tear / transcurrent faults (Sylvester, 1988) or hanging wall drop faults (Butler, 1982), respectively. The compressional structures are associated with a NW-SE direction of shortening (Figs. 3.3 and 3.7b).

The extensional faults are mainly located along the north-western margins of the Almorchón and Santiago de la Espada basins (Fig. 3.3). They have developed in Cretaceous, Paleogene and Miocene rocks and apparently cut earlier (outcrop-scale) compressional structures (Fig. 3.7a). The extensional faults run parallel to the main trend of the compressional structures in the region. The larger-scale extensional faults in particular dip to the southeast at moderate to high angles (Figs. 3.3 and 3.6). Slip vectors, such as grooves and lineations indicate hanging-wall movement to the southeast, which is opposite to the main transport direction of the fold and thrust belt. In the Almorchón basin, extensional faults form a network reminiscent of a relay pattern in the sense of Biddle and Christie-Blick (1985). Paleogene and Miocene marker beds on both sides of these faults (observed in the field and on the geological map; Dabrio, 1972) indicate that several tens up to 80 meters of throw (vertical displacement) has occurred along each of these faults, leading to a total of at least 500 meters of throw. In the Santiago de la Espada basin, on the contrary, displacement is accommodated along a single extensional fault, that may have up to several hundreds (>600) of meters of throw (Fig. 3.6). The extensional structures in these basins are associated with NW-SE directed extension, which clearly conflicts with the NW-SE direction of shortening deduced from the compressional structures.

The cross-cutting relationships of extensional and compressional structures, as shown in Fig. 3.7, suggest an extensional overprint on earlier compressional events. Fig. 3.8, however, shows a clear example of a geometric and genetic relationship between thrust tectonics and the local development of normal faults in the hanging wall. This kind of structural relationship, in which normal faults develop in the hanging wall in response to a change in the fault plane geometry of the thrust or reverse fault, has been described previously by Coward (1983) and will be discussed below.

Restoration of the section constructed across this part of the Prebetic zone leads to a viable solution (i.e., a viable cross section in the sense of Elliott, 1983) as shown in Figure 3.9. In the restoration, the base of the Miocene, which is in essence a pre-Miocene erosion surface, has been used as a reference level. The stratigraphic thickness of the different Mesozoic and Cenozoic units, as well as the depth to, and dip of the decollement zone in the Triassic evaporite, were estimated from surface data on the geological map, as well as from published seismic

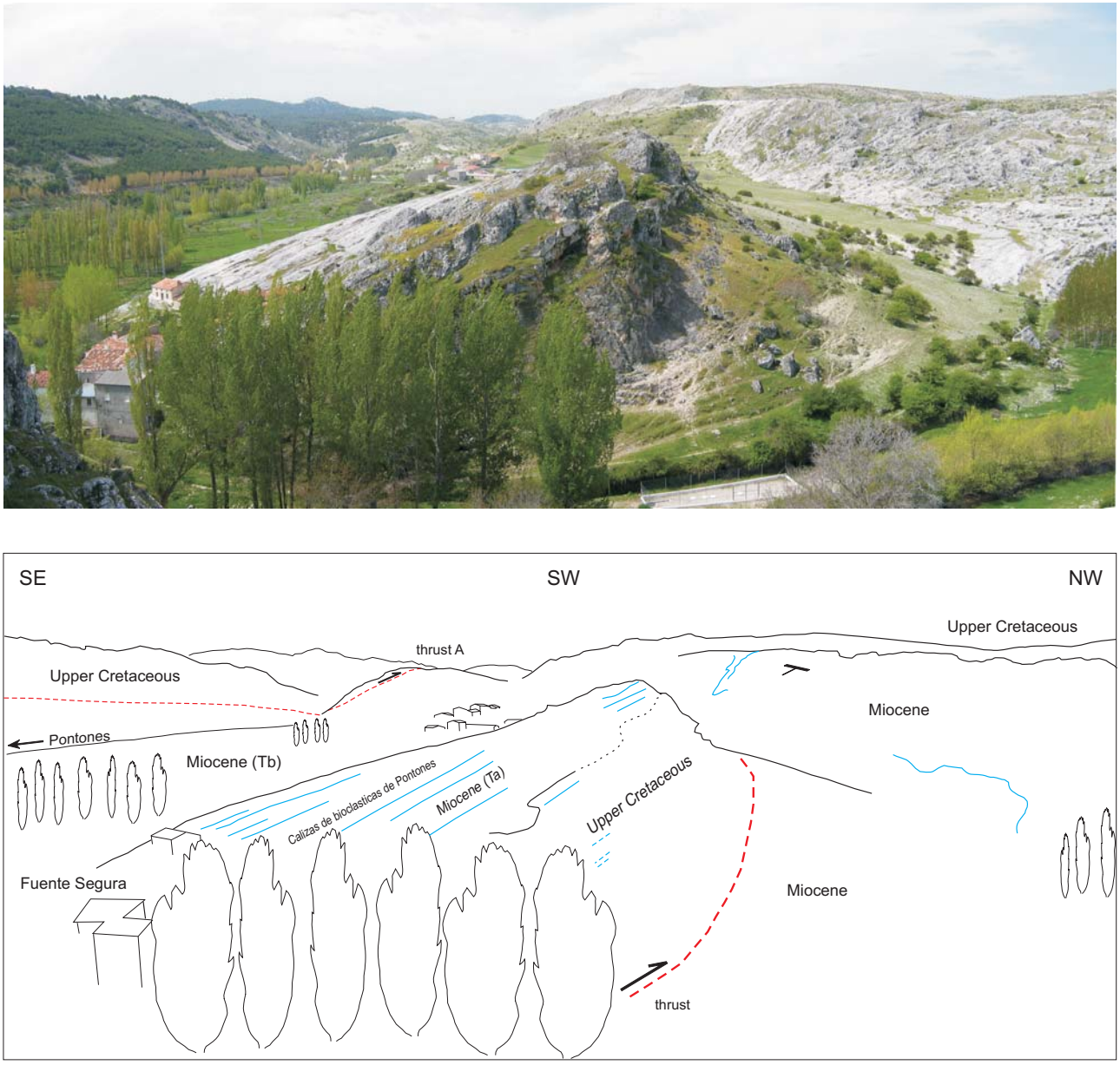

Figure 3.5. Panoramic view of the Pontones basin as seen from the NE along strike of the major thrust faults. On the left a NW-vergent thrust (labelled A on Figure 3.3) emplacing upper Cretaceous rocks on top of Miocene sediments. Foreground shows upper Cretaceous and Miocene deposits in the hanging wall emplaced on Miocene sediments in the footwall. The thrust forms part of an imbricate structure (Figure 3.3).

profiles and well data (Banks and Warburton, 1991). These estimates are to a large extent in agreement with Banks and Warburton (1991) and Platt *et al.* (2003), as shown in Figures 3.2a and b. The stratigraphic thickness of the Mesozoic units north of Pontones is approximately 1000 to 1400 meters (Fig. 3.9) and increases towards the south to values of up to 2500 to 3000 meters. This increase in thickness occurs stepwise across thrust faults, such as for example at fault A on the map and cross-section (Figs. 3.3 and 3.9). These faults apparently are Mesozoic extensional faults, as shown in the restored cross-section (Fig 3.9b), which were reactivated during the Neogene.

From the restored section (Fig. 3.9b) it is evident that, prior to the folding and thrusting in the Prebetics, the Pontones, Almorchón and Santiago de la Espada basins formed part of a single large basin. Estimates of the amount of shortening in the Tranco zone north of Pontones are up to 13 km, while compressional structures in the Pontones – Santiago de la Espada section (P-P') indicate that approximately 6.3 km of shortening has occurred in this part of the Prebetics. This latter estimate is of the same order as the about 4

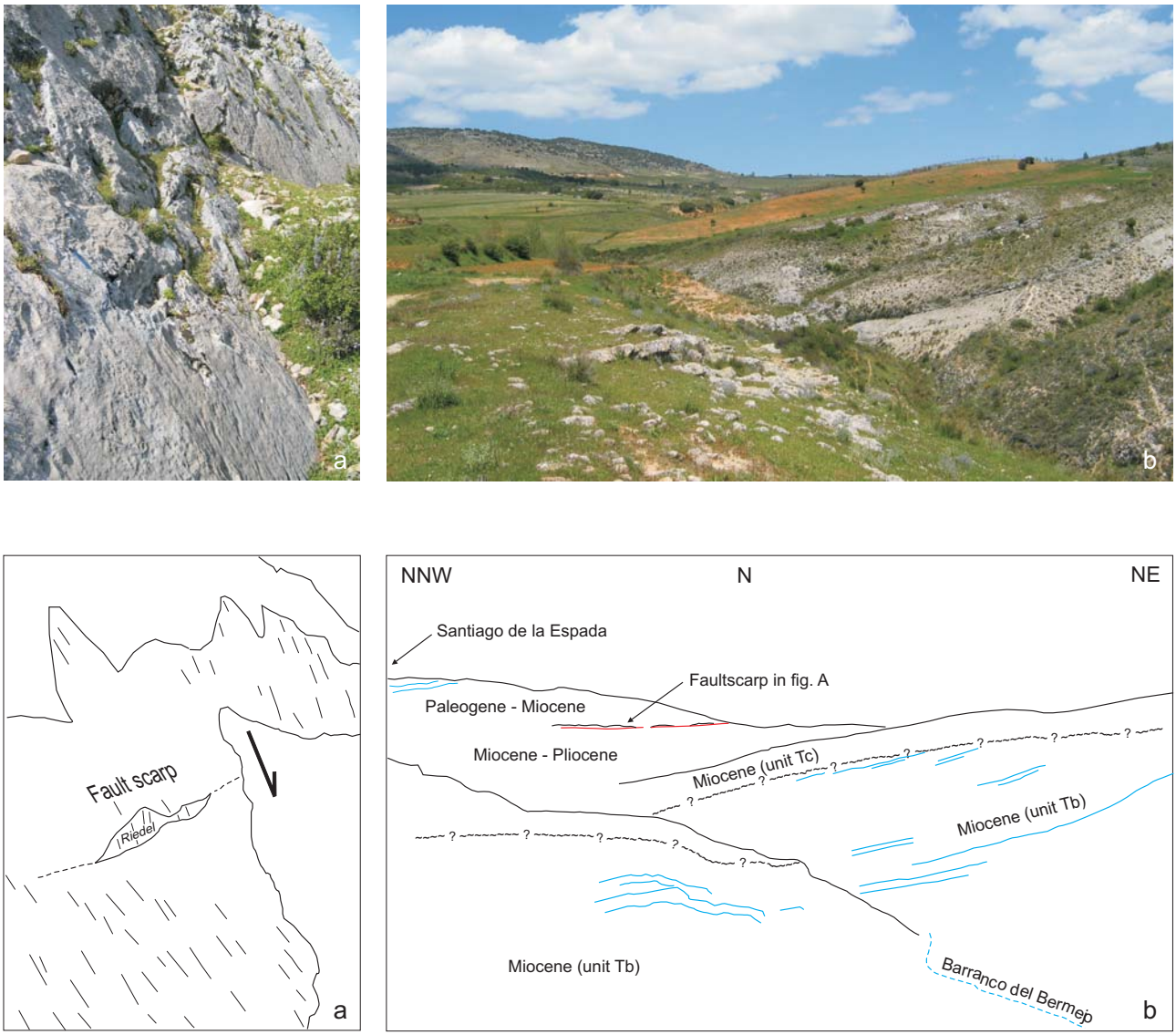

Figure 3.6. Main features of the Santiago de la Espada basin. a) Fault scarp of the extensional fault along the northwestern margin of the basin. Scarps reveal clear kinematic features such as Riedel fractures (136/76) and down-dip grooves (141/56 on 141/57) and slickenside lineations (142/41 on 148/41) on the fault surface, indicating dip-slip motion. b) Panoramic view of the basin seen from the south. To the northwest tilted middle-late Miocene marine deposits (unconformably?) overlain by late Miocene - Pliocene continental sediments of unit Tc. Note exposed fault plane of Figure 3.6a in far distance.

km of shortening estimated by Banks and Warburton (1991) and Platt *et al.* (2003) in the corresponding parts of their sections.

Discussion

Four different explanations were proposed in the introduction that may account for the development of extensional structures in the Betic fold and thrust belt. The first two would imply crustal-scale extension of the Betic fold and thrust belt for which there is clearly no evidence. The other two explanations (i.e., stratal extension in thrust-fault footwalls, or hanging-wall collapse above shallowing-upwards reverse faults) both imply that the extensional structures are in some way inherent to the process of thrusting in the developing fold and thrust belt. The available data lend support to such a thrust-related origin of the extensional faults as follows.

Platt and Leggett (1986) explain the development of extensional faults in the footwall of a thrust plane in terms of small-scale stratal extension, due to variations in sliding resistance along the thrust plane, whilst the hanging wall block remains undeformed. These extensional faults are in essence low-angle nor-

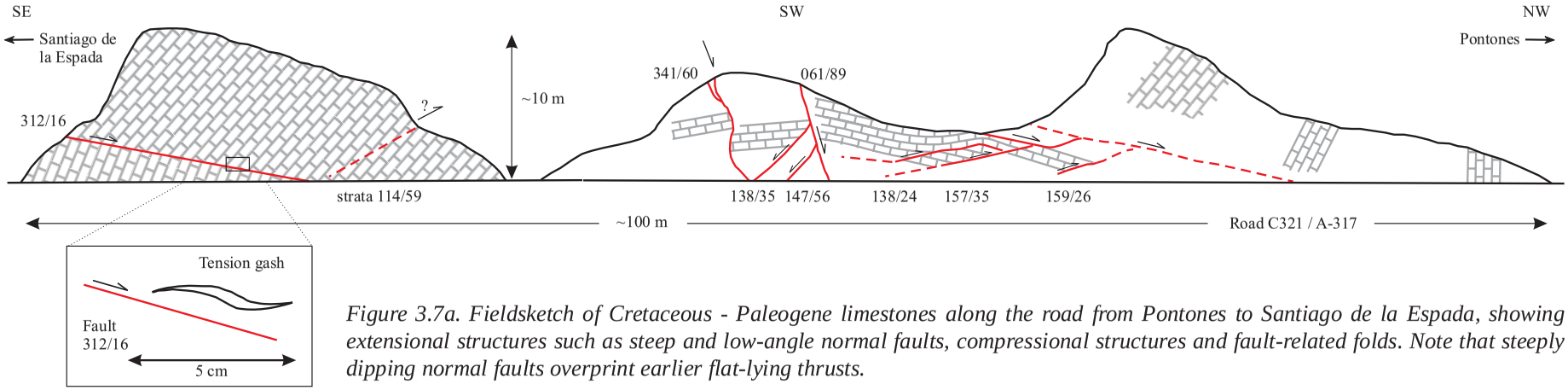

Figure 3.7a. Fieldsketch of Cretaceous - Paleogene limestones along the road from Pontones to Santiago de la Espada, showing extensional structures such as steep and low-angle normal faults, compressional structures and fault-related folds. Note that steeply dipping normal faults overprint earlier flat-lying thrusts.

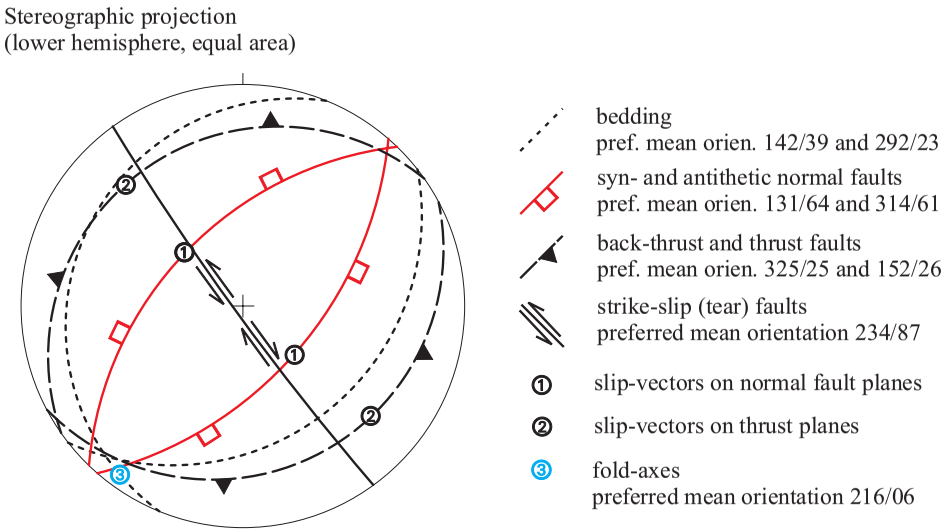

Figure 3.7b. Lower hemisphere, equal area stereoplot of structural data from Cretaceous, Paleogene and Miocene rocks along the road from Pontones to Santiago de la Espada. The data are preferred mean orientations (Fisher et al., 1987) of 115 measurements of bedding (15), normal faults (24), thrusts (33), strike-slip faults (10), lineations (or slip-vectors: 29) and fold-axes (4). Syn- and antithetic normal faults, back-thrust and thrust faults are defined with respect to the large-scale thrust nappes, as shown on the map and in the profile. Bedding, fault planes and fold-axes have an unmistakably NE-SW trend. Both slip-vectors on fault planes and dextral and sinistral strike-slip (tear) faults are orthogonal to the general structural trend.

mal faults dipping in the transport direction of the thrust, i.e., they have the same orientations as Riedel faults or shears. However, the extensional structures seen in the Prebetic fold and thrust belt have developed in the hanging walls of the thrust faults. Stratal extension of the kind described by Platt and Legget (1986) seems therefore inadequate to explain the structures observed.

According to Coward (1983), normal faults may develop in the hanging wall of a thrust in response to a change in fault plane geometry of the thrust or reverse fault, in a way that the dip-angle of the fault decreases with decreasing depth. Movement on such a fault, referred to as a shallowing-upwards fault, can result in stretching of the hanging wall block directly above the ramp-flat structure (Fig. 3.8b) in particular if there is no layer-parallel slip along the bedding planes in the hanging wall. Stretching in the hanging wall inevitably leads to the development of normal faults, which include synthetic but mostly antithetic faults, i.e., with respect to the sense of displacement of the thrust fault. The stretched hanging wall block as well as the geometrical relationships of the normal and thrust faults in outcrops, such as the one shown in Figure 3.7, are clearly consistent with the structures expected for a shallowing upwards fault. The structural and geometrical relationships of the large-scale thrust faults A and B, indicated on the map in Figure 3.3 and in the profiles of Figure 3.9, and the main extensional faults along the north-western margins of the Almorchón and Santiago de la Espada basins are quite similar to the smaller-scale structures seen in outcrop as shown in Figure 3.7. This strongly suggests the presence of a shallowing upwards fault at the scale of the thrust wedge, as shown in the profiles in Figure 3.9. The present interpretation is possibly strengthened by the fact that fault A initially developed as a Mesozoic extensional fault, which was reactivated as a reverse fault in the late Miocene, and became progressively shallower upwards during continued thrusting.

Both structural and stratigraphic data, such as the lithological correlations in the Miocene stratigraphy, indicate that the Pontones, Almorchón and Santiago de la Espada basins, prior to folding and thrusting in this part of the Betic External Zone, have been part of a single and large marine basin during the (early-) middle Miocene. This large marine basin most likely formed a connection between the Atlantic Ocean and the Mediterranean Sea, often referred to as the "North Betic Strait" (e.g., Calvo *et al.*, 1978; Sanz de Galdeano and Vera, 1992; Soria *et al.*, 1999; Martín *et al.*, 2001; Braga *et al.*, 2003; Sanz de Galdeano and Alfaro, 2004).

The "abrupt" facies change from a continental – shallow marine facies in the late Oligocene – earliest Miocene to a deep marine setting in the middle Miocene can not be explained with a global (eustatic) sea level change. As a matter of fact, the middle Miocene period is characterised by a high (up to 100-150 m) but decreasing eustatic sea level (Haq *et al.*, 1988, and Fig. 3.4). However, paleobathymetry estimates of the middle Miocene sediments show a rapid relative sea level rise (up to 500-600 meters of water depth) in an evidently underfilled basin. Both the magnitude of the relative sea level rise inferred from paleobathymetry and the sedimentary facies dominated by mass flow and turbidite deposits imply a tectonic cause for the rapid basin subsidence. These observations are in agreement with the Miocene subsidence histories inferred for both the Jumilla – Cieza region by Kenter *et al.* (1990) and for the western Prebetics, in particular the Santiago de la Espada region, by Hanne *et al.* (2003). Two obvious candidates for such a tectonic cause are: (1) the migrating depocenter of the foredeep domain ahead of the moving thrust mass of the fold and thrust belt (Kenter *et al.*, 1990; Beets and De Ruig, 1992; Hanne *et al.*, 2003) and (2) a rapid ("instantaneous") loading of the Iberian plate due to the emplacement of both the Subbetic and the Betic Internal Zones. According to Beets and De Ruig (1992) and Hanne *et al.* (2003) the first foreland basins already developed in the late Oligocene in the south due to loading of the Iberian plate by the Betic Internal Zone. This foreland basin system progressively migrated towards the northwest during the early and middle Miocene when it reached the realm of Santiago de la Espada and Pontones. The rapid subsidence of the Pontones – Santiago de la Espada basins, therefore, most likely reflects the approaching foredeep basin in front of the moving thrust mass. It is noted, however, that according to Van der Beek and Cloetingh (1992) the load of the Betic External and Internal Zones is insufficient to explain the flexure of the Iberian lithosphere as observed today.

The subsequent change in the basins from marine to continental facies and allied basin uplift in the Tortonian is almost coeval with the initiation of folding and thrusting in the western part of the Prebetic Zone, and evidently marks the moment that the forward propagating deformation front of the fold and thrust belt has approached the realm of Pontones and Santiago de la Espada. Since the Tortonian (~10 Ma), approximately 50 to 60 km of shortening has been accommodated in the western Prebetics, and the region

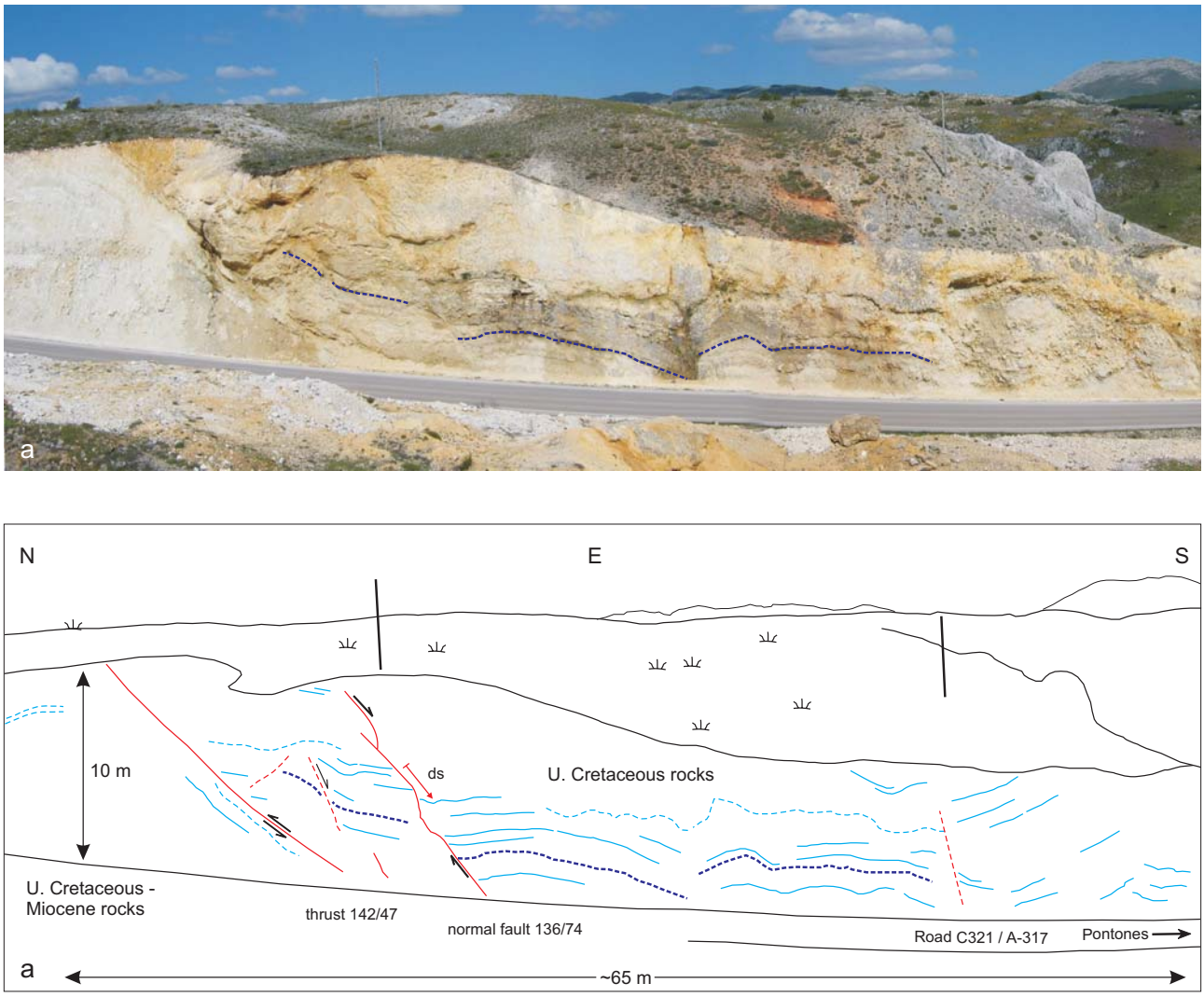

Figure 3.8. a) Deformational structures in Upper Cretaceous rocks north of Pontones. Thrust to the left emplaces Upper Cretaceous rocks in the hanging wall on Upper Cretaceous and Miocene deposits in the footwall. In the hanging wall, a normal fault transports material over a distance (ds) of ~2 m in a direction opposite to the movement direction of the thrust. The normal and thrust faults appear to be genetically and geometrically related. b) Diagram taken from Coward (1983), showing how extensional strains are developed above a shallowing-upwards fault. If bed A would be displaced to point D and there is no change in length of the beds along the hanging wall of the fault, then for a supposed kink band geometry, bed length CD will have to expand to length A'C. Stretching of the hanging wall over the top of such a shallowing-upwards fault increases with increase of α and decrease in β. This extension may occur over a broad zone in the hanging wall, leading either to ductile extension of the upper layers or to the development of brittle extensional faults.

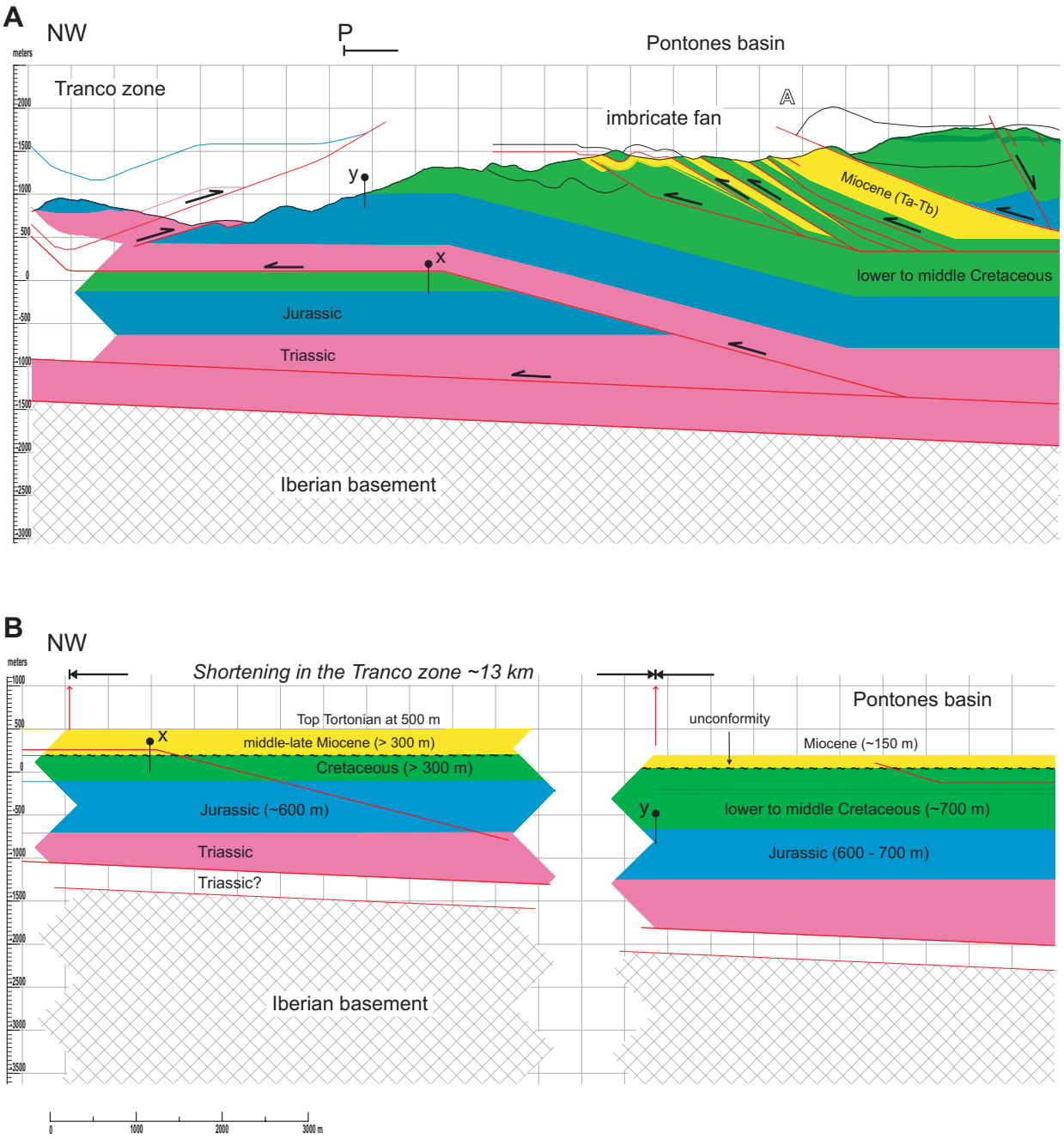

Figure 3.9. a) Balanced section across the region of Santiago de la Espada. For location of section see Figures 3.1 (profile 3) and 3.3 (profile P-P'). b) The Santiago de la Espada cross-section restored. Marker pins X, Y and Z refer to common points in the deformed and undeformed sections. White Roman letters refer to large-scale thrusts shown on the map in Figure 3.3. Stratigraphic thickness of the Mesozoic and Cenozoic units increases towards the SE as evident from field observations, the IGME geological map (Dabrio, 1972), and documented by, e.g., Hernandez et al. (1980), Hermes (1978), and Banks and Warburton (1991). Folding and thrusting initiated after deposition of the Miocene sediments, i.e., in latest Miocene and Pliocene period. Mesozoic extensional structures were reactivated as reverse faults (e.g., fault A), which shallow upwards. Tectonic transport direction is in general towards the NW. Normal faults, however, move with opposite movement sense. Total throw along sets of normal faults is up to 500-600 meters. Main decollement is located within the Triassic horizon, which dips at ~2.5° to the SE. The minimum amount of shortening in the Santiago de la Espada region is estimated at 6.25 km.

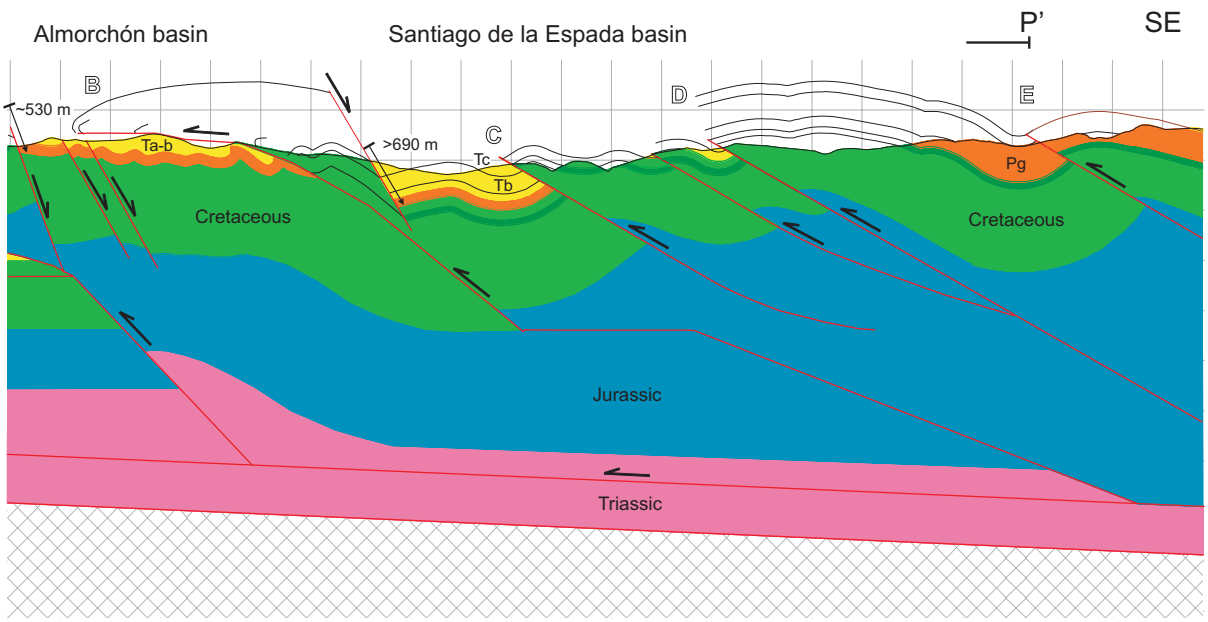

Shortening in the Santiago de la Espada section at least 6.25 km

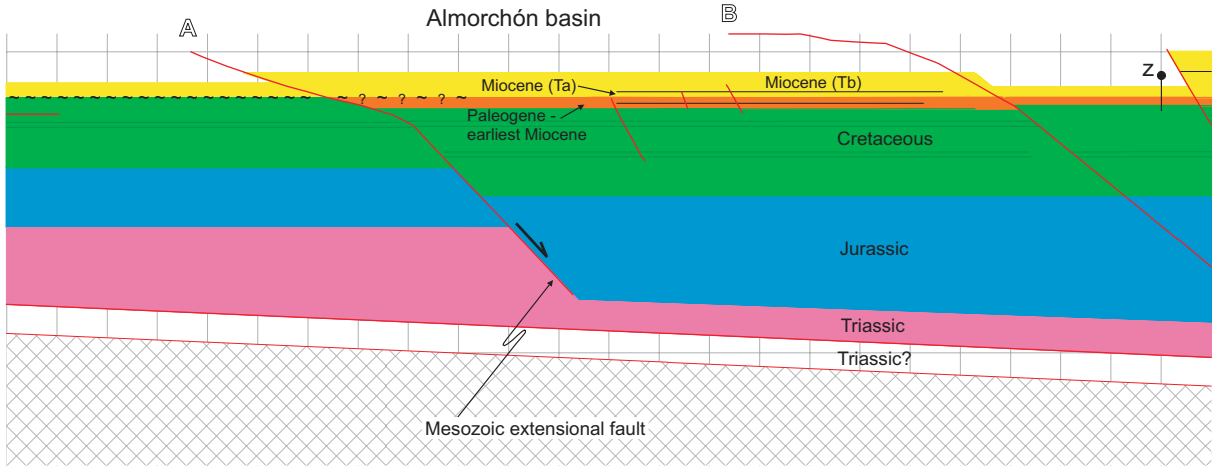

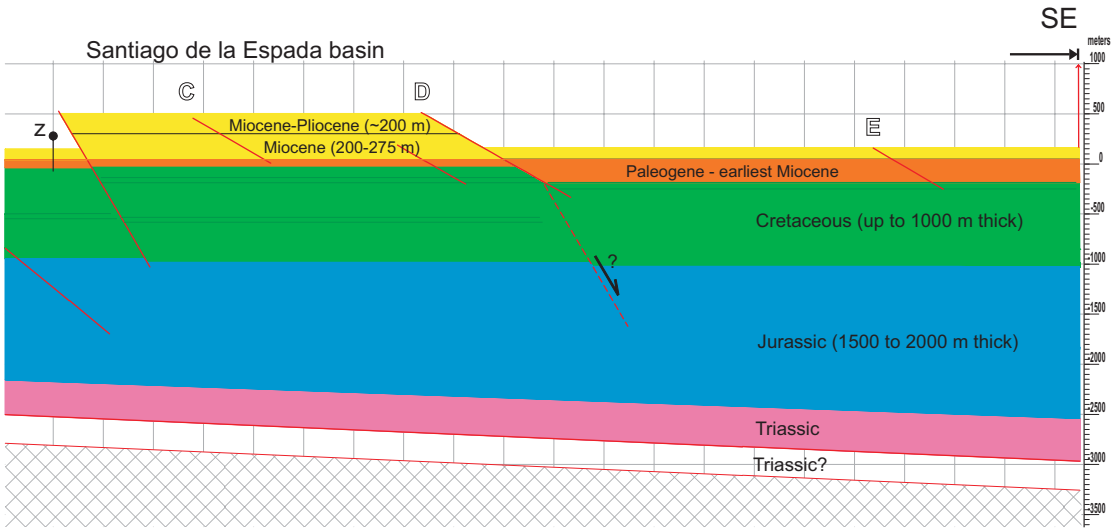

has experienced an uplift of up to 2000 meters. As suggested in chapter 2, African-Eurasian plate convergence is most likely responsible for this late Miocene to recent compressional deformation in the Betic External Zone. Regional uplift of the Betic Cordillera continues still today (e.g., Giménez *et al.*, 2000; Braga *et al.*, 2003; Sanz de Galdeano and Alfaro, 2004). A study of the causes of this uplift lies beyond the scope of this study, however, part of the late Miocene to recent uplift may well be related to flexural isostatic processes (e.g., Watts, 1992) of the Iberian lithosphere beneath.

Conclusions

Careful analysis of the structure and stratigraphy in the Miocene basins in the western part of the Prebetic Zone near Santiago de la Espada leads to the following conclusions:

The development of outcrop and map-scale extensional structures is related to the process of thrusting and reverse faulting. Some of these reverse faults were probably initiated as Mesozoic extensional faults, and were reactivated as reverse faults in the late Miocene in response to continued thrusting and folding in the Betic External Zone. During fault propagation upwards, the reverse faults became progressively shallower (i.e., less inclined), which inevitably led to extension in the hanging wall block and the subsequent development of normal faults. This implies that irrespective of the extensional nature of some of the faults, the Miocene basins in the Prebetics in essence developed in a compressive setting.

Prior to the late Miocene folding and thrusting in the Prebetics, the Pontones, Almorchón and Santiago de la Espada basins formed part of a large marine basin in the early-middle Miocene. The abrupt subsidence of this basin during the middle Miocene was likely associated with the migrating foredeep part of the foreland basin, in front of the growing thrust mass of the External Zone. Shallowing of the basin in the late Miocene was immediately followed by the onset of folding and thrusting in the western Prebetics, which led to segmentation of the large basin into smaller basins and closure of the northern Atlantic-Mediterranean connection.

4

Stratigraphy of the Miocene basins in the Internal Zone

Introduction

The Internal Zone of the Betic Cordillera has a characteristic "Basin and Range" type morphology defined by ENE trending, elongate mountain ranges of intensely deformed and mostly metamorphosed Palaeozoic and Mesozoic rocks (e.g., Egeler and Simon, 1969; Platt and Vissers, 1989; Fig. 4.1), flanked by narrow, elongate basins generally referred to as intramontane or intermontane basins. In the eastern Betics, the intramontane basins are in part bounded by major faults which form a network that has been interpreted as the upper-crustal expression of a crustal-scale transcurrent shear zone that crosses the eastern part of the Internal Zone (De Larouzière *et al.*, 1988).

The intramontane basins are filled with Neogene to recent continental siliciclastics and marine mixed siliciclastic / carbonate facies, marls and evaporites (e.g., Montenat and Ott d'Estevou, 1990; Sanz de Galdeano, 1990) showing highly variable facies and thicknesses. It is, however, generally accepted that the stratigraphy of the different basins show very similar trends (e.g., Montenat *et al.*, 1987; Montenat and Ott d'Estevou, 1990, 1996 and 1999; Sanz de Galdano, 1990). A number of hypotheses have been proposed in the literature to explain the geology and geometry of the Betic Cordillera as well as the development of the intramontane basins. Irrespective of the details of these scenarios, however, it is generally believed that the present-day geomorphology of the Betic Internal Zone including the (elongate) rectangular geometry of the intermontane basins was already acquired in the late Serravallian-earliest Tortonian, i.e., at the end of the middle Miocene (e.g., Geel, 1976; Briend, 1981; Briend *et al.*, 1990; Sanz de Galdeano and Vera, 1992; Guerra-Merchán and Serrano, 1993; Mora-Gluckstadt, 1993; Geel and Roep, 1998 and 1999). This assumption is substantiated by the fact that upper Miocene, Pliocene and Quaternary sediments dominate the basin fills and lie unconformably on pre- and early Miocene deposits, as well as on both metamorphic basement units of the Internal Zone and rocks of the Betic External Zone. The upper Miocene and younger sediments therefore clearly postdate early Miocene tectonic structures. In contrast, the early and middle Miocene stages are represented by few scattered and highly fragmentary outcrops, and most of these deposits are considered part of either the Betic External Zone, the Campo de Gibraltar Complex (or North African Flysch Trough), or the Malaguide units of the Betic Internal Zone (e.g., Rodríguez-Fernández and Sanz de Galdeano, 1992; Sanz de Galdeano and Vera, 1992; Lonergan *et al.*, 1994; Geel and Roep, 1998 and 1999).

There are several unconformities and stratigraphic trends identified in the late Miocene and Pliocene stratigraphy of the different basins, which are commonly accepted as regional, synchronous phenomena, reflecting regional eustatic changes or tectonic "events" (e.g., Montenat *et al.*, 1987; Montenat and Ott d'Estevou, 1990, 1996 and 1999; Sanz de Galdeano and Vera, 1992). An example of such a tectonic event is the evaporite succession present in several of the Betic basins and which is considered late Miocene in age. These evaporites reflect a hypersaline environment, which was presumably the result of restriction of the connection between the Atlantic and the Mediterranean Sea at that time (Müller and Hsü, 1987). This restriction or closure of the Atlantic-Mediterranean connection occurred most likely due to tectonics in the Betic Cordillera and other parts of the Alboran region (e.g., Sanz de Galdeano and Vera, 1992) with an inevitably catastrophic impact on the entire Mediterranean region. There is, however, ongoing debate on the exact age (either late Tortonian and/or Messinian) and significance of the evaporite successions in the Cartagena, Fortuna, Lorca, Sorbas and Nijar basins (e.g., Müller and Hsü, 1987; Garcés *et al.*, 1998; Rouchy *et al.*, 1998; Wrobel and Michalzik, 1999; Krijgsman *et al.*, 2000; Krijgsman *et al.*, 2001).

In this study we focus on three areas in the eastern part of the Betic Internal Zone, i.e., from west to east: (1) the Almanzora, Huercal Overa and Puerto Lumbreras basins, (2) the Lorca basin, and (3) the Fortuna basin (Fig. 4.1). The Almanzora, Huercal Overa and Puerto Lumbreras basins are located en-

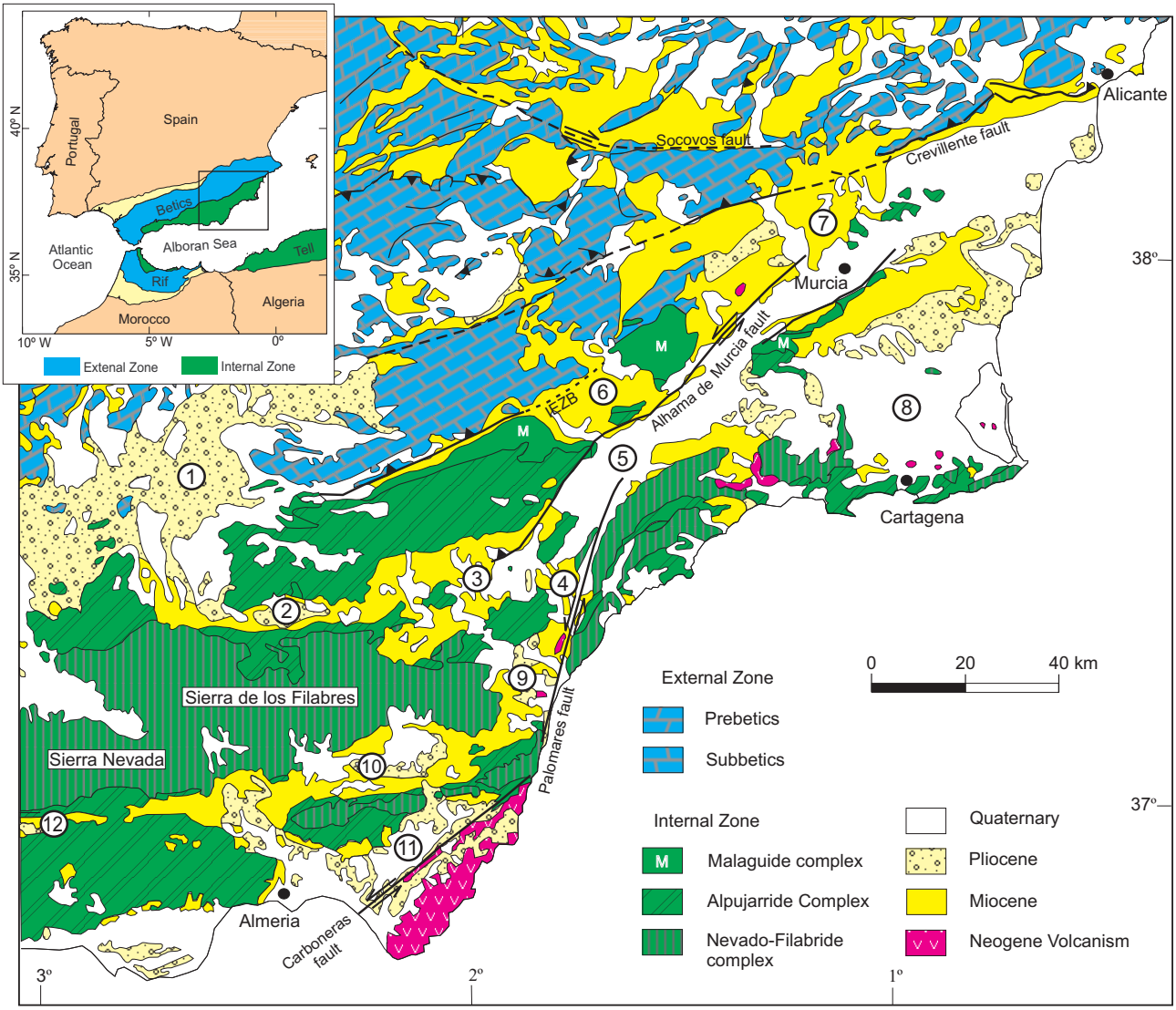

Figure 4.1. Geological map of the eastern part of the Betic Cordillera, modified from Mapa Geologico de la Peninsula Iberica (IGME, 1:1.000.000, 1981). Numbers refer to basins: 1) Guadix-Baza basin, 2) Almanzora corridor, 3) Huercal Overa basin, 4) Pulpi basin, 5) Puerto Lumbreras and Guadalentin-Hinojar basins, 6) Lorca basin, 7) Fortuna basin, 8) Alicante-Cartagena basin, 9) Vera basin, 10) Tabernas-Sorbas basin, 11) Nijar-Carboneras basin, 12) Alpujarran Corridor. IEZB - Internal-External Zone Boundary. The Carboneras, Palomares, Alhama de Murcia and Crevillente faults are considered part of a crustal scale shear zone.

tirely within the Betic Internal Zone, whilst the Lorca and Fortuna basins straddle the contact of the Internal and External Zones. In addition, these basins have been chosen because they are all located immediately adjacent to the Alhama de Murcia Fault, one of the major faults belonging to the crustal scale shear zone that crosses the south-eastern part of the Betic Cordillera. The relationship with this major fault structure is addressed in chapters 5 and 6 below.

In this chapter, an overview is presented of the Miocene and Pliocene stratigraphy of the three selected basins that incorporates new litho- and biostratigraphic data. This improved data set allows new basin-scale and regional correlations, in particular by using biostratigraphic correlations to disclose hitherto unidentified, syn- and/or diachronic regional trends in the development of the basins that may be associated with eustatic changes and/or lithospheric

Figure 4.2. Detailed time table for the Neogene showing some of the main characteristic planktonic foraminiferal datum events used here in this study. Column to the left shows biostratigraphic events mostly after Bizon (1978). The column to the right shows biostratigraphic events according to the astronomically tuned Neogene time scale of Lourens et al. (2004) and used in this study.

Planktonic foraminiferal events in the Mediterranean Neogene

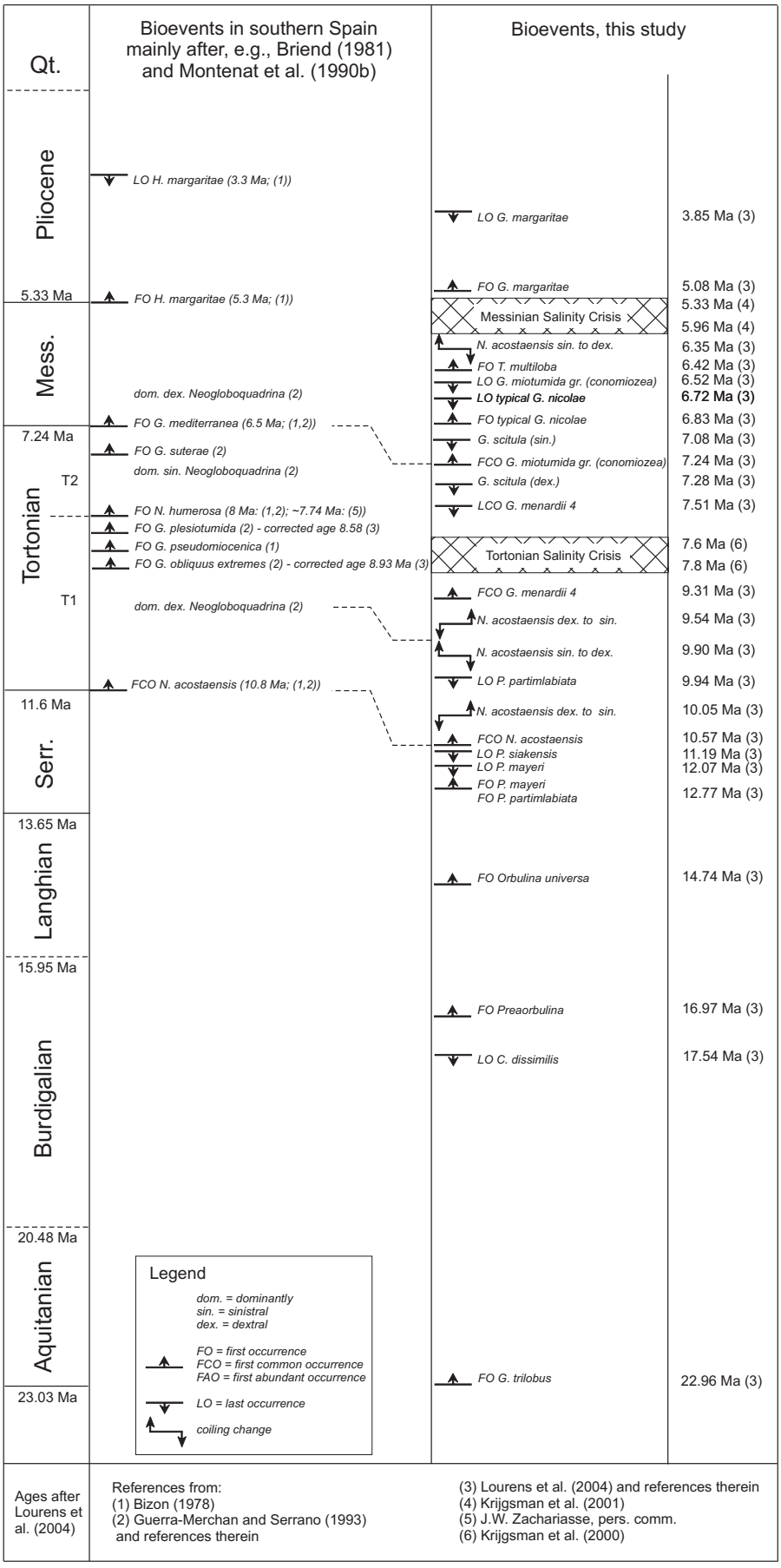

processes in the Betic crust. In addition, the improved time frame, in combination with the thicknesses of the various formations in the Miocene basins, are used to make quantitative estimations of both vertical and horizontal motions (stretching or compression) of these basins addressed in chapter 5.

Methods

The stratigraphic data for the research described in this chapter were collected in the Huercal Overa, Lorca and Fortuna basins. Geological maps and stratigraphic data from earlier studies were used in this study and modified where needed. Rock or clay samples were collected for biostratigraphic studies, either as individual samples, or as series of samples with a sampling distance of 2 to 3 meters of section. The samples were studied by W.J. Zachariasse, G.J. van der Zwaan, F.J. Hilgen and T.J. Kouwenhoven (Stratigraphy and Paleontology group of the Department of Earth Sciences at the Utrecht University, The Netherlands) and A. di Stefano (Geology and Geophysics group of the Department of Geological Science at the University of Catania, Italy). Ages for bioevents are according to the latest Astronomical Tuned Neogene Time Scale of Lourens *et al.* (2004) and shown in Fig. 4.2. Paleobathymetry analyses of (individual) marine clay samples using the ratio of planktic and benthic foraminifera (P-B ratio) were performed by D.J.J. van Hinsbergen (Department of Earth Sciences, Utrecht University, The Netherlands). Details of this paleobathymetry technique are given in Van Hinsbergen *et al.* (2005).

Almanzora, Huercal Overa and Puerto Lumbreras basins

Introduction

The Huercal Overa basin is an ENE trending elongate basin, which merges with the Guadalentin-Hinojar and Pulpi basins in the east and is connected through the E-W trending Almanzora corridor with the Guadix-Baza basin to the west (Figs. 4.1 and 4.3). In contrast, the Puerto Lumbreras basin is an isolated and very small (few km) rhomboidal shaped basin located within the Sierra de las Estancias, northeast of the Huercal Overa basin. The western part of the Huercal Overa basin is occasionally referred to as the Albox basin (e.g., Dubelaar, 1980; Mora Gluckstadt, 1993).

The mountain ranges surrounding and bounding the Almanzora and Huercal Overa basins are mainly made up of metamorphic rocks of the Nevado-Filabride and Alpujarride complexes of the Betic Internal Zone, with occasional small outcrops of non-metamorphic Malaguide rocks (De Booy and Egeler, 1961; Egeler and Simon, 1969). This metamorphic basement also underlies the basin sediments, as evident from outcrops of Alpujarride and/or Nevado–Filabride units that occur as basement highs within the Huercal Overa and Almanzora basins.

Small outcrops of limestones and conglomerates along the southern margins of the Almanzora, Huercal Overa and Puerto Lumbreras basins (De Booy and Egeler, 1961; Voermans *et al.*, 1972; Briend, 1981; Briend *et al.*, 1990; Mora-Gluckstadt, 1993, Fig. 4.3) are believed to be of Oligocene and early – middle Miocene age. The basin fill is dominated, however, by upper Miocene sediments, whilst in the eastern part of the Huercal Overa basin the upper Miocene sediments are covered with Pliocene to recent alluvial fan deposits (García-Meléndez *et al.*, 2002 and 2003). The stratigraphy of the upper Miocene sediments of the Almanzora, Huercal Overa and Puerto Lumbreras basins has been thoroughly studied and described by Voermans *et al.* (1972), Simon *et al.* (1978), Briend (1981), Dabrio and Polo (1988), Briend *et al.* (1990), Montenat *et al.* (1990a), Mora-Gluckstadt (1993), Guerra-Merchán and Serrano (1993), Poisson *et al.* (1999) and Augier (2004) as shown in Fig. 4.4.

Stratigraphy

Early and middle Miocene

The lower-middle Miocene basin sediments are exposed in few scattered outcrops along the south-eastern margins of Almanzora, Huercal Overa and Puerto Lumbreras basins (De Booy and Egeler, 1961; Briend, 1981; Guerra Merchán and Serrano, 1993; Mora-Gluckstadt, 1993; Figs. 4.3, 4.4 and 4.5). These lower Neogene sediments include 170 meters of purple alluvial breccias and mass flow deposits (Poudingue lie-de-vin unit of Briend, 1981), as well as approximately 60 meters of varicoloured conglomerates, sands, silts, calcarenites, foraminiferal limestones and reef limestones (Santa Barbara formation of Briend, 1981, equivalent to Tectosedimentary Unit 1 (TSU1) of Guerra-Merchán and Serrano, 1993). The sediments of the latter formation were deposited in a very shallow marine to coastal facies, passing upwards into a continental facies of fluvial and alluvial

conglomerates (Guerra-Merchán and Serrano; 1993). Both formations lie unconformably on rocks of the Malaguide or Alpujarride complex (De Booy and Egeler, 1961). It is emphasized, however, that the purple alluvial breccias of the Poudingue lie-de-vin unit and the shallow marine deposits of the Sta. Barbara formation do not occur in one and the same outcrop, such that their lateral relationship and relative age are difficult to substantiate.

Representatives of *G. trilobus*, *C. dissimilis*, and *G. dehiscens* in the shallow marine deposits of the Sta. Barbara formation suggest an early Miocene age (Voermans *et al.*, 1972; Mora-Gluckstadt, 1993), but representatives of *Orbulina spp.* encountered in this study point to a middle Miocene age (G.J. van der Zwaan and W.J. Zachariasse, pers. comm.; Fig 4.2.), i.e. *C. dissimilis* must have been reworked. Furthermore, the nature and facies of the sediments of the Sta. Barbara formation and Poudingue lie-de-vin unit as well as their detrital content (i.e., derived mostly from the Malaguide and some from the Alpujarride complex) strongly support correlation with the sediments of, respectively, the Serravallian Umbria and Mofar formations in the Vera and Sorbas basins (Völk, 1964; Völk and Rondeel, 1964; Hodgson *et al.*, in review). It is noted that the fauna, described by Völk (1964) from the Umbria formation, and interpreted according to the astronomical tuned biostratigraphic ages of Lourens *et al.* (2004), yields a Serravallian age with a presumable age range of 12.77 to 12.07 Ma.

Late Miocene and Pliocene

The middle Miocene sediments of the Poudingue lie-de-vin unit and Sta. Barbara formation are unconformably overlain by upper Miocene red continental breccias and conglomerates. These continental deposits consist of an up to 1200 meter thick series of alluvial fan and mass flow deposits exposed along the basin margins and fringing basement highs (Figs. 4.3 and 4.5). They belong to the Brèche rouge (Plate 4.1) and Conglomérats et limons rouges (Plate 4.2) units of Briend (1981) and Briend *et al.* (1990), equivalent to the TSU2a of Guerra-Merchán and Serrano (1993), to the Basal red clastics and Abejuela unit of Mora-Gluckstadt (1993) and Augier (2004), and to the Red lower clastics as defined by Poisson *et al.* (1999), as shown in Fig. 4.4. The Conglomérats et limons rouges unit lies unconformably on the Alpujarride rocks of the Sierra de las Estancias, and in some outcrops there is clear evidence of onlap on these basement rocks (Plates 4.3 and 4.4). The typical breccias of the Brèche rouge unit are only exposed in the southern part of the Almanzora and Huercal Overa basins, where they lie unconformably on lower Tertiary rocks of the Malaguide complex and on rocks of the Alpujarride and Nevado-Filabride complex, or are juxtaposed with these basement rocks along faulted contacts. An additional aspect of these continental deposits is that they are in general pervasively cut by extensional faults, which may partially explain existing discrepancies in the estimated accumulated thickness of these units.

The precise age of the continental fan deposits is difficult to establish, however, the detritus of these continental deposits comprises e.g. blocks of micaschist, tourmaline-bearing gneiss, marble, serpentinite and gypsum, and is mostly derived from metamorphic basement rocks, and part of the metamorphic detritus clearly originates from the Sierra de Los Filabres, south of the Almanzora and Huercal Overa basins (Vissers, 1975; Dubelaar, 1980; Montenat *et al.*, 1990a). According to Johnson *et al.* (1997), the greenschist facies metamorphic rocks of the Sierra de Los Filabres cooled to near-surface temperatures during the mid-Serravallian (12±1 Ma), which is consistent with a late Serravallian to early Tortonian age for the continental sediments containing this Filabride detritus. The flow directions seen in the continental fan deposits are in general towards the N, E and SE (Vissers, 1975; Dubelaar, 1980; this study) and NW (Montenat *et al.*, 1990a), which is consistent with the inferred Filabride source of the detritus and distribution areas. Note, however, that Mora-Gluckstadt (1993) and Augier (2004) have documented flow directions which are in part at variance with those observed in this study and those of Vissers (1975) and Dubelaar (1980).

The continental fan deposits of the Conglomérats et limons rouges unit pass upwards and laterally into a variously coloured and lithologically diverse sequence of conglomerates, sands, homogenous grey silts, clays, marls, caliches, paleosoils and evaporites, as well as conglomeratic and sandy mass flow beds. These deposits roughly coincide with the Turbidites micacées et gypseuses unit of Briend (1981) and Briend *et al.* (1990), with the TSU2b of Guerra-Merchán and Serrano (1993), and with the Santopetar formation of Mora-Gluckstadt (1993) and Augier (2004). According to Dabrio and Polo (1988), Guerra-Merchán and Serrano (1993) and Mora-Gluckstadt (1993), these sediments were deposited under fluvial-lacustrine, sabkha and shallow marine conditions in aggradational and progradational developing, fluvial-

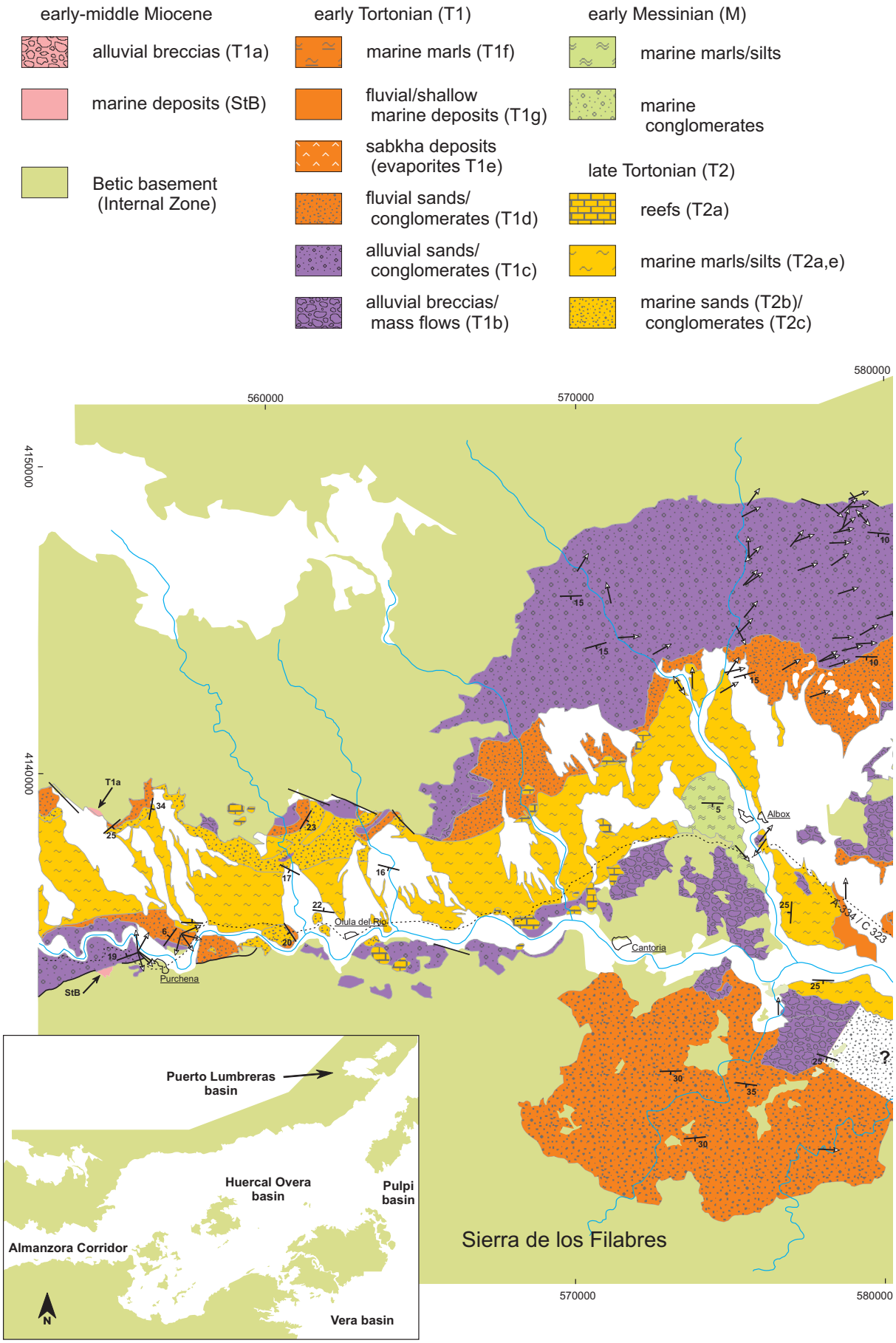
early-middle Miocene
alluvial breccias (T1a)
marine deposits (StB)
Betic basement (Internal Zone)
early Tortonian (T1)
marine marls (T1f)
fluvial/shallow marine deposits (T1g)
sabkha deposits (evaporites T1e)
fluvial sands/ conglomerates (T1d)
alluvial sands/ conglomerates (T1c)
alluvial breccias/ mass flows (T1b)
early Messinian (M)
marine marls/silts
marine conglomerates
late Tortonian (T2)
reefs (T2a)
marine marls/silts (T2a,e)
marine sands (T2b)/ conglomerates (T2c)
560000
570000
580000
4150000
4140000
T1a
StB
Purchena
Olula del Río
Albox
Cantoria
A-334
C-323
Sierra de los Filabres
Puerto Lumbreras basin
Huercal Overa basin
Pulpi basin
Almanzora Corridor
Vera basin
N

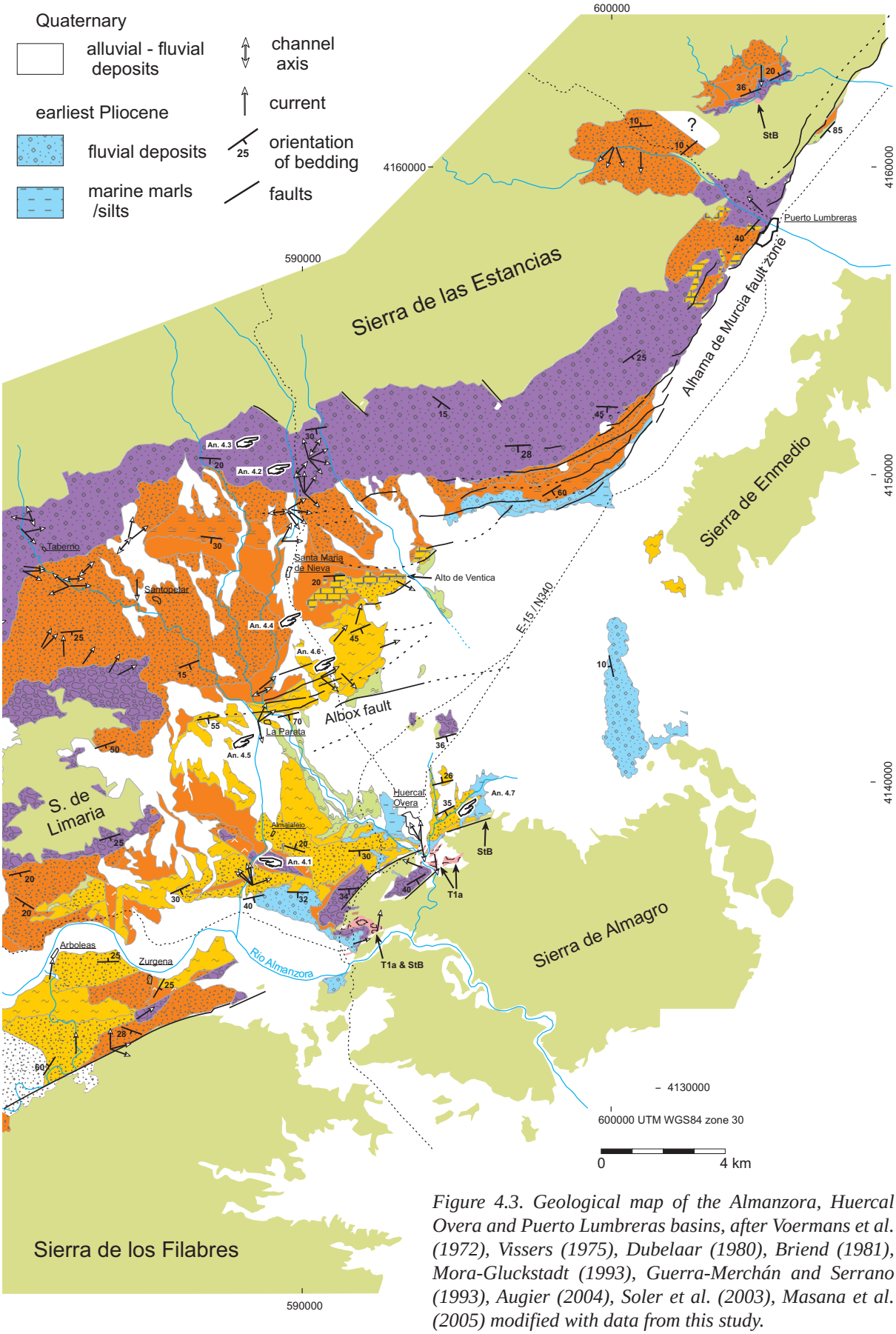

Figure 4.3. Geological map of the Almanzora, Huercal Overa and Puerto Lumbreras basins, after Voermans et al. (1972), Vissers (1975), Dubelaar (1980), Briend (1981), Mora-Gluckstadt (1993), Guerra-Merchán and Serrano (1993), Augier (2004), Soler et al. (2003), Masana et al. (2005) modified with data from this study.

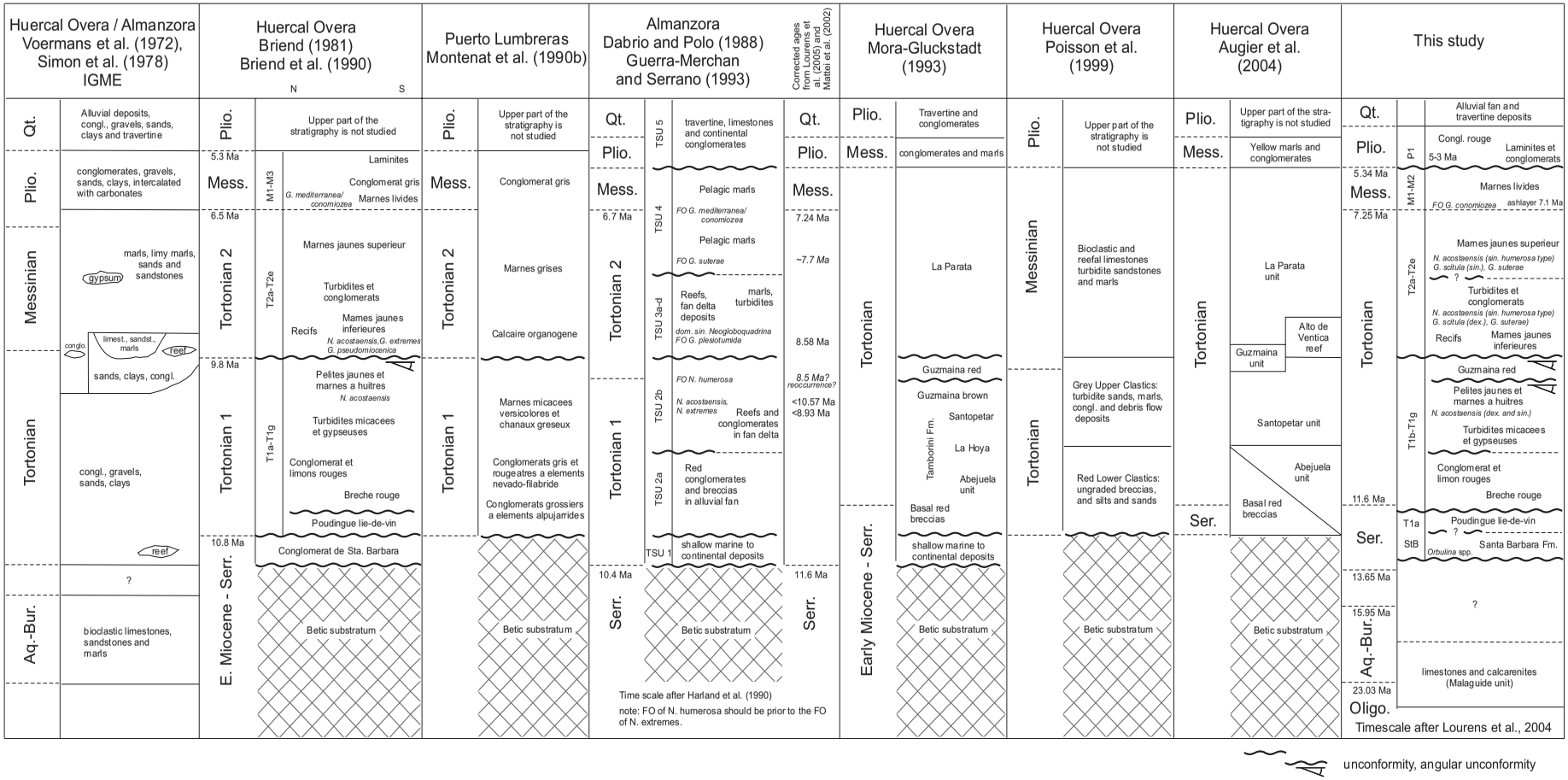

Figure 4.4. Stratigraphy of the Almanzora, Huercal Overa and Puerto Lumbreras basins. This study mainly follows the stratigraphic subdivision of Briend (1981).

dominated Gilbert-type fan deltas, located along the basin margins and receiving detritus from the adjacent ranges. These fan deltas developed outward in the shallow marine environment of the corridor, whilst patch and fringing reefs developed on the basin margins and fan deltas.

According to Briend (1981) and Briend *et al.* (1990), the fluvial-lacustrine sediments are overlain with an angular unconformity by a relatively thin interval of shallow marine sandy marls referred to as the "Pélites jaunes" (Briend, 1981; Briend *et al.*, 1990), equivalent to the La Parata formation (Mora-Gluckstadt, 1993; Augier, 2004), exclusively exposed along the north-eastern margin of the Huercal Overa basin (Fig. 4.3). According to Briend (1981), these marls mainly contain benthic foraminifera but also few planktonic foraminifera, such as representatives of *N. acostaensis*, which point to a Tortonian age. However, the alternating occurrence of intervals of dominant dextral and sinistral coiled *N. acostaensis* suggest an early Tortonian age (W.J. Zachariasse, pers. comm.; Fig. 4.2). Using Lourens *et al.* (2004), then rapid changes in coiling of *N. acostaensis* would point to an age range of 10.57 to 9.54 Ma. Paleobathymetry of individual samples from these marine sediments suggests shallow water depths of 50 to 100 meters (D.J.J. van Hinsbergen, pers. comm.). It should be noted that Mora-Gluckstadt (1993) and Augier (2004) consider these marls as part of the "marnes jaunes inferieurs et recifs" described below, which is at variance with this study.

The sandy marl interval passes upward into a regressive interval again made up of a varicoloured, lithologically diverse sequence of sandstones, graded conglomerates, blue and red clays, marls and oyster beds deposited in a fluvial dominated delta to lacustrine and shallow marine environment. These rocks form part of the Turbidites micacées and Marnes à Huîtres unit of Briend (1981) and Briend *et al.* (1990), and of the Santopetar formation and Guzmaina Brown and Red units (Mora-Gluckstadt, 1993; Augier, 2004). The upper part of this unit, which is considered as a separate unit referred to as the Guzmaina Red unit by Mora-Gluckstadt (1993) and Augier (2004), consists of a series of reddish silts and clays intercalated with conglomerate and sand beds. According to Mora-Gluckstadt (1993), the contact between the Guzmaina Red unit and the overlying marine sediments is an erosive contact as indicated by onlap of marine sediments. Fossil plant roots, raindrop imprints and the reddish colour all suggest a continental depositional environment (Augier, 2004). Paleo-current directions within the channels are mostly towards the NE and E (Vissers, 1975; Dubelaar, 1980; this study) which is, again, at variance with the flow direction data reported by Mora-Gluckstadt (1993). The marine sediments within this regressive interval contain a variety of macrofossils as well as planktic but dominantly benthic foraminifera (Briend, 1981). The planktic foraminiferal assemblage consists mostly of representatives of dextral and sinistral coiled *N. acostaensis.* Absence of late Tortonian and Messinian biostratigraphic markers suggests an early Tortonian age for these sediments.

Outcrops along roads and dry riverbeds host ubiquitous examples of sedimentary structures (channel structures, graded and ungraded mass flow beds, a large olistostrome) within the fluvial-shallow marine deposits, as well as large and small scale (syn-sedimentary) deformational structures reflecting the tectonic context of the basin development, addressed below in chapter 5. The total accumulated thickness of the Turbidites micacées et gypseuses unit / Santopetar formation in the Huercal Overa basin is estimated between 540 meters (Augier, 2004; this study) and 1500 meters (Briend, 1981; Mora-Gluckstadt, 1993), and in the Almanzora basin up to 300 meters (Dabrio and Polo, 1988; Guerra-Merchán and Serrano, 1993). The estimated thickness of the different lithologies making up these fluvial-shallow marine deposits varies (abruptly) along strike, and some may disappear along strike, possibly as a result of lateral variations in depositional system or erosion, or due to deformation.

The lower Tortonian continental and fluvial-shallow marine sediments are overlain by a transgressive unit of shallow to deeper marine deposits of late Tortonian and early Messinian age, referred to as the Marnes jaunes inférieur et récifs, Turbidites et Conglomérats jaunes, Marnes jaunes supérieur and Marnes livides units of Briend (1981) and Briend *et al.* (1990), the TSU3 and TSU4 of Guerra-Merchán and Serrano (1993), or the La Parata unit of Mora-Gluckstadt (1993) and Augier, (2004), as shown in figure 4.4 and plate 4.5. According to Briend (1981), the transgressive series of in the northern part of the Huercal Overa basin lies concordantly on the lower Tortonian sediments, whilst in the southern part of the basin they lie on basement and earlier deposits with an angular unconformity. Dabrio and Polo (1988), Guerra-Merchán and Serrano (1993) and Mora-Gluckstadt (1993), on the other hand, suggest that both in the north and south of the Huercal Overa and Almanzora basins the transgressive series lie

unconformably, with an onlappping contact, on the lower Tortonian rocks. This contact between the lower and upper Tortonian sediments is identified as a prominent regional unconformity, also observed in several other Miocene basins in the Betic Cordillera (Montenat and Ott d'Estevou, 1990, 1996 and 1999; Sanz de Galdeano and Vera, 1992). However, as emphasized by Guerra-Merchán and Serrano (1993) in their study of the Almanzora basin where an uninterrupted biostratigraphy occurs across the unconformity, it is possible that this unconformity does not represent a substantial hiatus.

The marine series comprise reef complexes (e.g., at Alto de Ventica) and submarine fan delta and floodplain deposits at the basin margins, which laterally interfinger with shallow marine marls and turbidites in the central part of the Huercal Overa basin (Figs. 4.3 and 4.5, Plates 4.5 and 4.6). A late Tortonian age of these sediments is substantiated by representatives of left coiled *N. acostaensis* (including *humerosa types*), *G. pseudomiocenica*, *G. menardii*, *G. ventriosa* (rare), and *G. extremus* (Briend, 1981) as well as, dextral coiled *G. scitula* and *G. suterae types* (W.J. Zachariasse, pers. comm.). Paleodepth estimates on individual samples indicate a gradual deepening to 150-200 meter at the top of the upper Tortonian marine sediments (D.J.J. van Hinsbergen, pers. comm.). Cross bedding and flute casts in the turbidite beds suggest transport towards the east, north and south, implying clastic input from the western basin margins. Upwards, the shallow marine marls change rapidly into pelagic marls, which according to Briend (1981) were deposited under deeper marine (epibathyal) conditions. Representatives of dominant left coiled *N. acostaensis* and dextral coiled *G. scitula* in the marine marls and the occurrence of *G. mediterranea / conomiozea* in the upper part of the marls (W.J. Zachariasse and F.J. Hilgen, pers. comm.) suggest a latest Tortonian – early Messinian age for these marls, which is in agreement with Briend (1981) and Briend *et al.* (1990). An early Messinian age of these marine sediments is substantiated by a $^{40}Ar/^{39}Ar$ age of an ash-layer of 7.10 Ma (K.F. Kuiper, pers. comm.; Meijninger *et al.*, in prep.; see Figs. 4.4 and 4.5). Paleodepth estimates suggest a relatively constant water depth of 100-200 meter in the lower Messinian marine sediments (D.J.J. van Hinsbergen, pers. comm.). It should be noted that the samples show abundant evidence of down-slope transport and poor basin "ventilation". The total accumulated thickness of the upper Tortonian and lower Messinian marine sediments is estimated at 200 to 300 meters in the Almanzora corridor (Dabrio and Polo, 1988; Guerra-Merchán and Serrano, 1993) and 500 m (Mora-Gluckstadt, 1993; Augier, 2004) up to 1000 m (Briend, 1981; Briend *et al.*, 1990; this study) in the Huercal Overa basin.

It must be emphasized that massive upper Miocene evaporites, such as exposed in the Lorca and Sorbas basins, are entirely absent in the Almanzora, Huercal Overa and Puerto Lumbreras basins. It follows that either the conditions in these basins were in some way unfavourable for evaporite deposition, or that shortly after their deposition these evaporites were entirely removed by erosion.

Near the southern margin of the Huercal Overa basin, fluvial conglomerates and silts lie unconformably on upper Tortonian shallow marine deposits and laterally interfinger with an approximately 60 meter thick laminated series of shallow marine marls, clays and silts (Figs. 4.4 and 4.5, Plate 4.7). Biostratigraphic studies of the planktonic foraminiferal assemblages by Briend (1981) suggest that these deposits are Messinian in age. Our analysis shows that the sediments hold representatives of dominantly dextral coiled *N. acostaensis*, poorly preserved though abundant *G. siphonifera* (W.J. Zachariasse and F.J. Hilgen, pers. comm.) and benthic fauna (T.J. Kouwenhoven, pers. comm.), which are not age diagnostic, i.e. the age of the sediments is not conclusive. However, both Messinian (*G. conomiozea* and *G. nicolae*) and early Pliocene (*G. margaritae*) markers are clearly absent. Calcareous nannoplanktonic studies (A. di Stefano) on this section are in progress. Magneto-stratigraphic analysis of the upper 44 meters laminated marine marls show a single reversed polarity (Meijninger *et al.*, in prep). Biostratigraphy may suggest that these deposits are of late Messinian - earliest Pliocene age (W.J. Zachariasse, F.J. Hilgen and T.J. Kouwenhoven, pers. comm.), which is substantiated by the fact that, using Lourens *et al.* (2004), the late Messinian – earliest Pliocene period coincides with the reversed polarity chron 3Cr. Paleodepth estimates on the basis of P-B ratios indicate a water depth of 100-150 meter (D.J.J. van Hinsbergen, pers. comm.). All lithological and microfauna data seem to support correlation with the Cuevas and Espiritu-Santo formations in the Vera basin (Völk and Rondeel, 1964).

Along the north-eastern and southern margins of the Huercal Overa basin, red and grey fan conglomerates lie unconformably on basement and on Tortonian continental and shallow marine deposits, and they fill and cover a Tortonian paleorelief. In fact, a morpho-

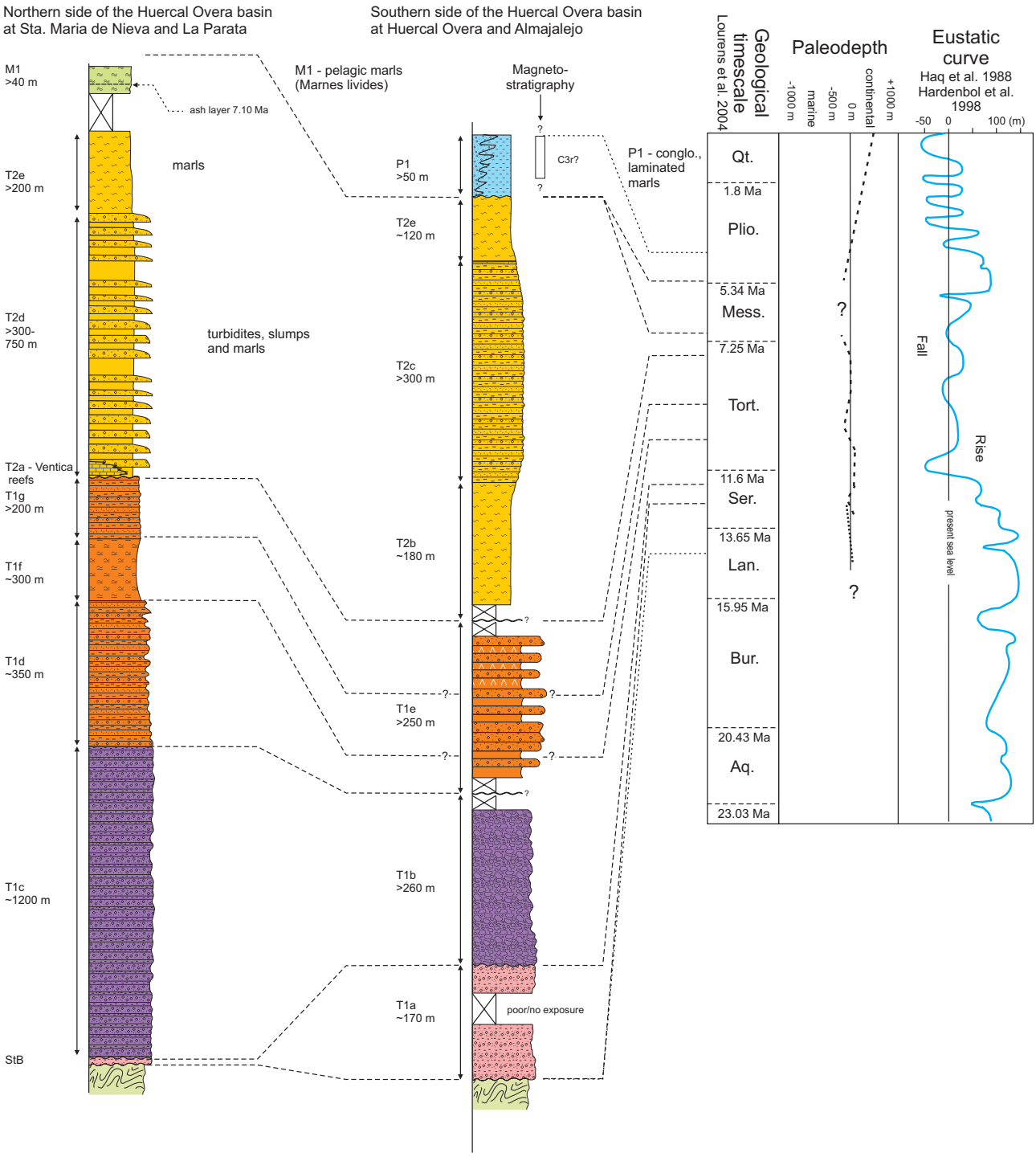

Figure 4.5. Stratigraphic columns for the northern and southern parts of the Huercal Overa basin. Paleomagnetic data after Meijninger et al. (in prep.).

logical study of the Huercal Overa basin (García-Meléndez, 2002 and 2003) has revealed a Pliocene depocenter in the eastern part of the Huercal Overa basin filled with up to 340 meters of Pliocene continental fan and fluvial deposits. These sediments are tentatively correlated with the Pliocene continental deposits of the Salmerón formation in the Pulpi and Vera basins (Völk and Rondeel, 1964; Veeken, 1983).

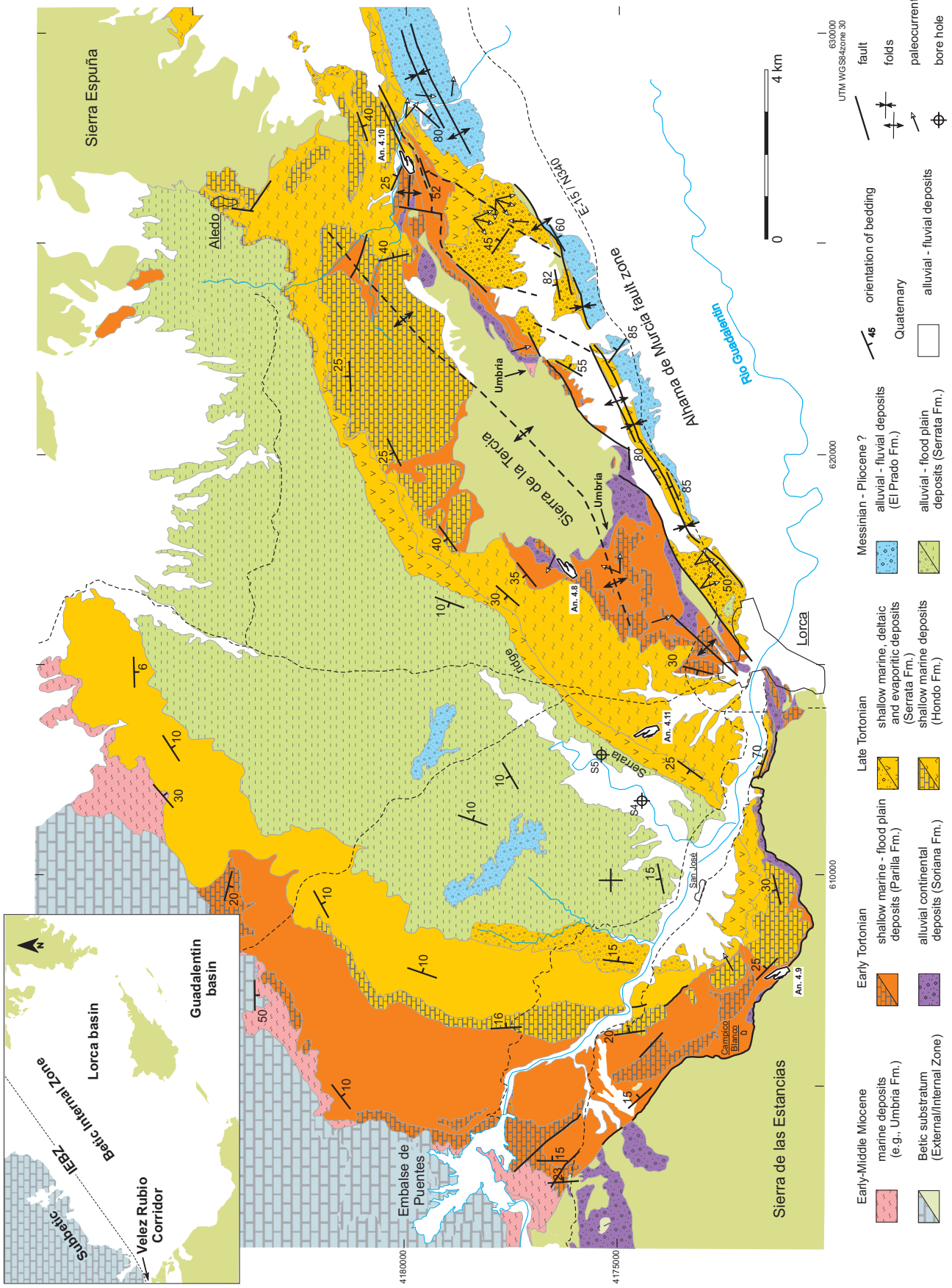
Sierra Espuña
Aledo
Sierra de la Tercia
Umbria
Umbria
Alhama de Murcia fault zone
E-15 / N340
Río Guadalentín
Lorca
Serrata
San José
Embalse de Puentes
Sierra de las Estancias
Campico Blanco
An. 4.8
An. 4.9
An. 4.10
An. 4.11
S4
S5
4 km
0
630000
UTM WGS84zone 30
620000
610000
4180000
4175000
Guadalentin basin
Lorca basin
Betic Internal Zone
IEBZ
Subbetic
Velez Rubio Corridor
Early-Middle Miocene
marine deposits (e.g., Umbria Fm.)
Betic substratum (External/Internal Zone)
Early Tortonian
shallow marine - flood plain deposits (Parilla Fm.)
alluvial continental deposits (Soriana Fm.)
Late Tortonian
shallow marine, deltaic and evaporitic deposits (Serrata Fm.)
shallow marine deposits (Hondo Fm.)
Messinian - Pliocene ?
alluvial - fluvial deposits (El Prado Fm.)
alluvial - flood plain deposits (Serrata Fm.)
Quaternary
alluvial - fluvial deposits
orientation of bedding
fault
folds
paleocurrent
bore hole

Lorca basin

Introduction

The Lorca basin forms an isolated, rhomboidal shaped topographic depression, about 15 km wide, with a NE trending basin axis, and is surrounded by the mountains of the External Zone to the northwest, and those of the Internal Zone (Sierra de Espuña, Sierra de la Tercia and Sierra de las Estancias) to the northeast, south and southwest (Fig. 4.6). The basin is connected through the ENE trending Velez Rubio corridor with the Guadix-Baza basin to the west, and via narrow corridors with basins in the External Zone to the north and the Guadalentin basin to the southeast. The mountains of the External Zone in the north consist of folded and thrusted, marine Mesozoic and Tertiary sediments of the Subbetic. The mountains bounding the Lorca basin to the northeast, south and southwest consist of non-metamorphic Mesozoic and Tertiary rocks of the Malaguide complex as well as intensely deformed and metamorphosed rocks of the Alpujarride complex (e.g., Egeler and Simon, 1969; Kampschuur *et al.*, 1972).

The basin sediments are in general exposed along the margins of the Lorca basin and around the Sierra de la Tercia, except for the north-eastern margin where they are covered with recent alluvial fan deposits. Most of the sediments in the Lorca basin are of late Miocene, Pliocene and Quaternary age, and these were deposited in non-marine and shallow marine-lagoonal environments. However, marine sediments of early and middle Miocene age crop out along the western and north-western basin margins (Geel, 1976; Montenat *et al.*, 1990b; Wrobel and Michalzik, 1999; Wrobel, 2000). According to Geel (1976) and Geel and Roep (1998, 1999), the basin obtained its present-day geometry in the late Serravallian and Tortonian, but was preceded by a much larger, presumably NE-SW trending Burdigalian - early Serravallian turbidite-olistostrome basin.

The basin stratigraphy has been studied extensively in the past decades by e.g., Montenat *et al.* (1990b), Geel and Roep (1998, 1999), Wrobel and Michalzik (1999), Wrobel (2000) and Vennin *et al.* (2004), with particular attention for the upper Miocene evaporite succession exposed in the prominent NE trending Serrata ridge along the south-eastern margin of the basin (e.g., Geel, 1976; Orti *et al.*, 1993; García-Veigas *et al.*, 1994 and 1995; Dinares-Turell *et al.*, 1997; Rouchy *et al.*, 1998; Steffahn and Michalzik, 2000; Krijgsman *et al.*, 2000; Fig. 4.7).

Stratigraphy

Early and middle Miocene

The lower and middle Miocene sediments are exposed along the western and north-western margins of the Lorca basin, in the Velez Rubio corridor and north of the Sierra Espuña. These sediments were deposited in basin geometries that were markedly different from the geometry of the present-day Lorca basin (Geel 1976; Geel and Roep, 1998 and 1999).

The lower Miocene marine deposits of the Solana, Fuente and Espejos formations unconformably or tectonically overlie allochtonous units of the Subbetic Zone and the Malaguide Complex, (Geel and Roep, 1998 and 1999; Fig. 4.7). In turn these lower Miocene sediments are tectonically overlain by rocks of the Subbetic Zone (i.e., the Internal-External Zone Boundary).

The middle Miocene marine deposits of the Cañada del Maiz, Campico de Flores, Pantano de Lorca and Bernabeles formations (Geel and Roep, 1998 and 1999; Fig. 4.7), lie unconformably on the lower Miocene sediments as well as on the Subbetic limestones and rocks of the Malaguide Complex. This implies that the middle Miocene rocks seal the earlier thrust structures associated with the Internal-External Zone Boundary (Lonergan *et al.*, 1994; Geel and Roep, 1998 and 1999).

The lower Miocene sediments of the Fuente, Espejos and Solana formations consist of a mixture of planktonic foraminiferal packstones, varicoloured marls, conglomerates, sandstones and oolites, in part developed as mass flow deposits. The sediments were deposited in the proximal and distal parts of submarine fans and, in the case of the Burdigalian Espejos formation, in a deep marine basin (~1000 m by P-B ratio; D.J.J. van Hinsbergen, pers. comm.). The sediments of the Espejos formation contain polymict detritus from both the Internal (Malaguide and Alpujarride components) and the External Zones which reflects, first, the juxtaposition of the Internal and External zones at that time, and secondly, the erosional unroofing and exhumation of the basement

Figure 4.6. Geological map of the Lorca basin, after Kampschuur et al. (1972), Geel (1976), Montenat et al. (1990), Wrobel and Michalzik (1999), Wrobel (2000), modified with data from this study. Locations of boreholes S4 and S5 after Garcia-Veigas et al. (1994).

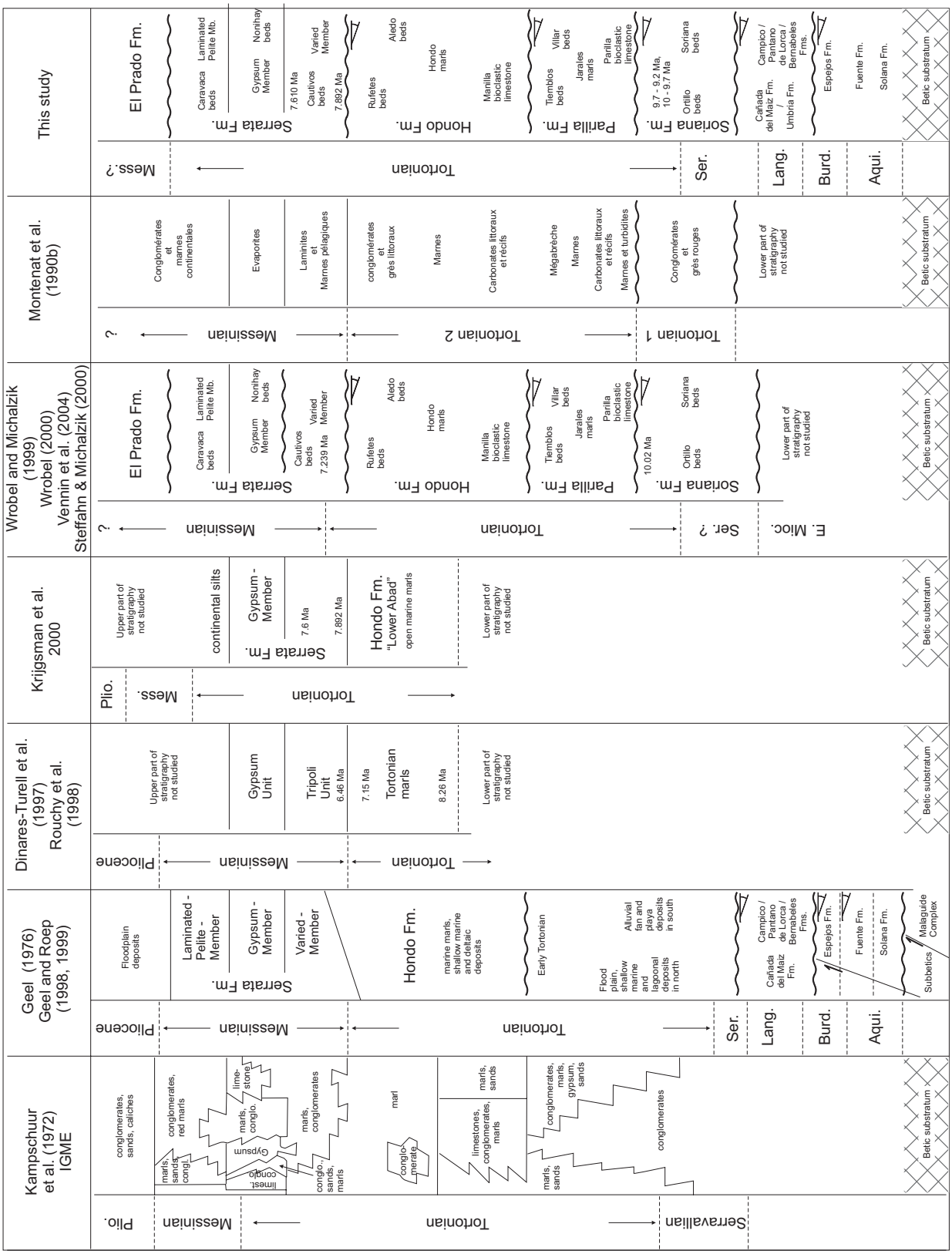

Figure 4.7. Stratigraphy of the Lorca basin. This study mainly follows the stratigraphic subdivision of Wrobel (2000).

rocks of the Betic Internal Zone (Geel and Roep, 1998 and 1999). The middle Miocene sediments of the Cañada del Maiz, Campico de Flores, Pantano de Lorca and Bernabeles formations were deposited in a southward prograding delta in a new suite of basins, consisting of approximately 500 meters of bioclastic packstones, polymict conglomerates, and marls, which are part of a series of turbidites and mass flows. Representatives of *P. mayeri* suggest a Serravallian age for these sediments (W.J. Zachariasse, pers. comm.; Fig. 4.2). Furthermore, paleodepth estimates indicate water depths of 500 to 1000 meter (D.J.J. van Hinsbergen, pers. comm.). According to Geel and Roep (1998 and 1999), the middle Miocene basins show rapid shoaling in the early Serravallian. The deltaic sediments of the Campico de Flores and Pantano de Lorca formations are unconformably (transgressively) overlain by late Serravallian - early Tortonian shallow marine bioclastic limestones and marls, which are the Ortillo beds of the Soriana formation (Geel and Roep, 1999; Wrobel, 2000; Figs. 4.6 and 4.7).

It should be noted that, similar to the middle Miocene sediments in the Huercal Overa basin, the nature and facies of the middle Miocene sediments in outcrops north and south of the Sierra de la Tercia (Figs. 4.6 and 4.8) as well as their detrital content (i.e., derived mostly from the Malaguide and some from the Alpujarride complex) strongly support correlation with the sediments of the Serravallian Umbria formation in the Vera and Sorbas basins (Völk, 1964; Völk and Rondeel, 1964; Hodgson *et al.*, in review)

Late Miocene and Pliocene

The upper Miocene-Pliocene sediments crop out in the north-western, south-western and south-eastern margins of the Lorca basin (Figs 4.6 and 4.8). Because of the rapid lateral and vertical facies changes and consequent lithological heterogeneity it is difficult to substantiate any correlations across the basin. Wrobel (2000) has divided the late Miocene-Pliocene succession into five allostratigraphic formations (lower, middle and upper pre-evaporitic units, evaporitic unit and post-evaporitic unit), which are mappable units of sedimentary rocks characterized by lithological heterogeneity and separated by discontinuities. The total accumulated thickness of the upper Miocene-Pliocene sediments is estimated at a minimum of 1500 meters in the central part of the Lorca basin, but the accumulated thickness reduces markedly towards the margins of the basin.

The basal succession of the late Miocene in the Lorca basin consist of an at least 50 meter thick series of red coloured, coarse clastic alluvial fans passing upward into playa and marginal marine deposits and evaporites (Fig. 4.8 and Plate 4.8). These deposits, which fringe the Sierra de la Tercia and Sierra de las Estancias, are often strongly faulted and reflect initial basin subsidence whilst detritus was supplied from the surrounding emerging basement rocks of the Betic Cordillera. Current directions inferred from pebble imbrications suggest variable currents to the NE, E and S. In the western part of the Lorca basin, the continental clastics grade into an approximately 90 meter thick succession of shallow-marine bioclastic and calcareous sandstones, reefal limestones, calcarenites and silty marls (Geel 1976, Tortonian 1 of Montenat *et al.*, 1990b; Soriana formation of the lower pre-evaporite unit of Wrobel and Michalzik 1999; Unit 1 of Vennin *et al.*, 2004; Fig. 4.7). The precise age of the continental fan deposits is unknown, but part of the metamorphic detritus in the Lorca basin clearly originates from the Sierra de Los Filabres in the Internal Zone. Similar to the sediments of the Huercal Overa basin, the mid-Serravallian cooling ages of the Filabride rocks (12±1 Ma; Johnson *et al.*, 1997) place an upper bound to the age of the pertinent sediments that may well be late Serravallian to early Tortonian. Representatives of dominant dextral coiled *N. acostaensis*, the rare occurrence of *G. scitula* and absence of *G. menardi 4* suggest an early Tortonian age of the shallow marine marls (W.J. Zachariasse, pers. comm.). Using Lourens *et al.* (2004), the biostratigraphy of these sediments would point to an age range of 9.90 to 9.54 Ma. However, Vennin *et al.* (2004) suggest an age of 10.55 to 10.02 Ma for the onset of the deposition of these marls. Paleodepth estimates in a series of samples from a stratigraphic section in the marls yield an approximate water depth of 250 to 500 meter (D.J.J. van Hinsbergen, pers. comm.). The alluvial fan deposits and shallow marine marls are unconformably overlain by a transgressive succession of prograding ridge-forming platform carbonates and coral reefs, grading basinward into shallow marine marls (Tortonian 2 of Montenat *et al.*, 1990b; Parilla formation of the lower pre-evaporite unit of Wrobel and Michalzik 1999; Unit 1-2 of Vennin *et al.*, 2004; Fig. 4.7 and Plate 4.9).

The basal succession passes upwards into a progradational and retrogradational series of mixed siliciclastic and carbonatic coastal and submarine deposits along the margins of the basin, comprising alluvial and submarine fan delta conglomerates, breccias and sandstones, calcarenitic sands, and bioclastic and

reef limestones of reef and carbonate platforms (Hondo formation of Geel, 1976 and Wrobel and Michalzik, 2000; Unit 2-3 from Vennin *et al.*, 2004; Fig. 4.7 and Plate 4.10). These sediments interfinger with approximately 1000 meter thick open marine marls in the central part of the Lorca basin (Hondo formation, Geel, 1976; Fig. 4.8). Both Worbel and Michalzik (1999) and Vennin *et al.* (2004) observed a progradational stacking pattern of these reef and deltaic facies successions, which they attribute to both allocyclic (eustatic) and autocyclic (basin dynamics) processes.

Representatives of sinistral and dextral coiled *N. acostaensis* and *G. menardii 4* in the marine marls of the Hondo formation in the eastern part of the Lorca basin point to a Tortonian age (W.J. Zachariasse, pers. comm.). Messinian biostratigraphic markers are clearly absent. Using Lourens *et al.* (2004), occurrence of *N. acostaensis* and common occurrence of *G. menardii 4* of would point to an age range of 9.31 to 7.51 Ma. The Hondo marls have in general a high detritus content and a low planktonic/benthic foraminifera ratio, which points to a shallow marine depositional environment (~100-200 m).

Stratigraphically upwards, the marls of the Hondo formation pass into an approximately 130 meter thick sequence of laminated diatomites, pelites, sandstones, carbonates and gypsum beds and a 50 meter thick massive gypsum unit, which belong to the Tripoli or Varied and Serrata Gypsum members, respectively (Geel, 1976; Rouchy *et al.* 1998; Serrata formation of the upper pre-evaporitic unit of Wrobel and Michalzik, 1999; Figs. 4.7 and 4.8, Plate 4.11). The laminated series and evaporites interfinger with alluvial and submarine fan delta conglomerates, breccias and sandstones, and bioclastic and reef limestones of reef and carbonate platforms (Serrata formation of the of the upper pre-evaporitic unit of Wrobel and Michalzik, 1999; Units 3-4-5 of Vennin *et al.*, 2004). Two boreholes in the centre of the Lorca basin north of the Serrata ridge (for locations see Fig. 4.6) have shown the presence of respectively 49 and 235 m thick halite units in the Serrata Gypsum member (García-Veigas *et al.*, 1994 and 1995). The precise age of the sediments of the Hondo and Tripoli units is still controversial. Biostratigraphic as well as magnetostratigraphic studies of these sediments by, e.g., Geel (1976), Montenat *et al.* (1990b), Dinares-Turell *et al.* (1997), Rouchy *et al.* (1998), Steffahn and Michalzik (2000) suggest that the Tortonian-Messinian boundary is located slightly beneath or above the base of the laminated sediments of the Tripoli unit reflecting the onset of basin restriction. These results imply that the evaporites of the Lorca basin are Messinian in age. However, on the basis of their study of the biostratigraphy and magnetostratigraphy of the same section, Krijgsman *et al.* (2000) suggest a late Tortonian age for the laminated sediments of the Serrata formation. A study of nannofossil assemblages in the upper 60 meters of these laminated sediments, in collaboration with A. di Stefano, suggests a Tortonian age as well, merely on basis of the absence of any Messinian markers and the occurrence of *Helicosphaera stalis* in one sample, which could be interpreted as the last occurrence (LO) of this species in this section (7.61 Ma, Raffi *et al.*, 2003). On the basis of the occurrence of *Reticulofenestra pseudoumbilicus*, which reappears in the stratigraphic record at 7.1 Ma, Rouchy *et al.* (1998) infer a Messinian age, but their findings are not substantiated by Krijgsman *et al.* (2000). There is strong evidence, however, for reworking in the sampled sections (Krijgsman *et al.*, 2000; W.J. Zachariasse and A. di Stefano, pers. comm.). Moreover, Wrobel and Michalzik (1999) and Wrobel (2000) mark the contact between the laminated sediments of the Tripoli unit and the Serrata gypsum member as an unconformity (a sequence boundary), which implies a hiatus, either small or large, in the stratigraphic record of the Serrata formation. At this stage it is emphasized, that the present study has yielded clear and unequivocal evidence for intense localized deformation along the base of the massive (Serrata) gypsum unit. Possible implications of these deformational structures are addressed in chapter 5.

The Serrata gypsum is followed by at least 30 meters of varicoloured laminated marly clays, sandy calcarenites and gypsum beds of the Laminated Pelite Member (Geel, 1976; post-evaporitic unit from Rouchy, 1998 and Wrobel and Michalzik, 1999; Wrobel, 2000). According to both Geel (1976) and Steffahn and Michalzik (2000), the biostratigraphy of the shallow marine marly clays of the Laminated Pelite Member suggests a Messinian age. Steffahn and Michalzik (2000) find a sinistral to dextral coiling change of *N. acostaensis* in the Laminated Pelite

Figure 4.8. Stratigraphic columns for the western and southern parts of the Lorca basin. Paleomagnetic data and biostratigraphic events after (1) Dinares-Turell et al. (1999) and (2) Krijgsman et al. (2000) and reinterpreted after Krijgsman et al. (2000) and Lourens et al. (2004).

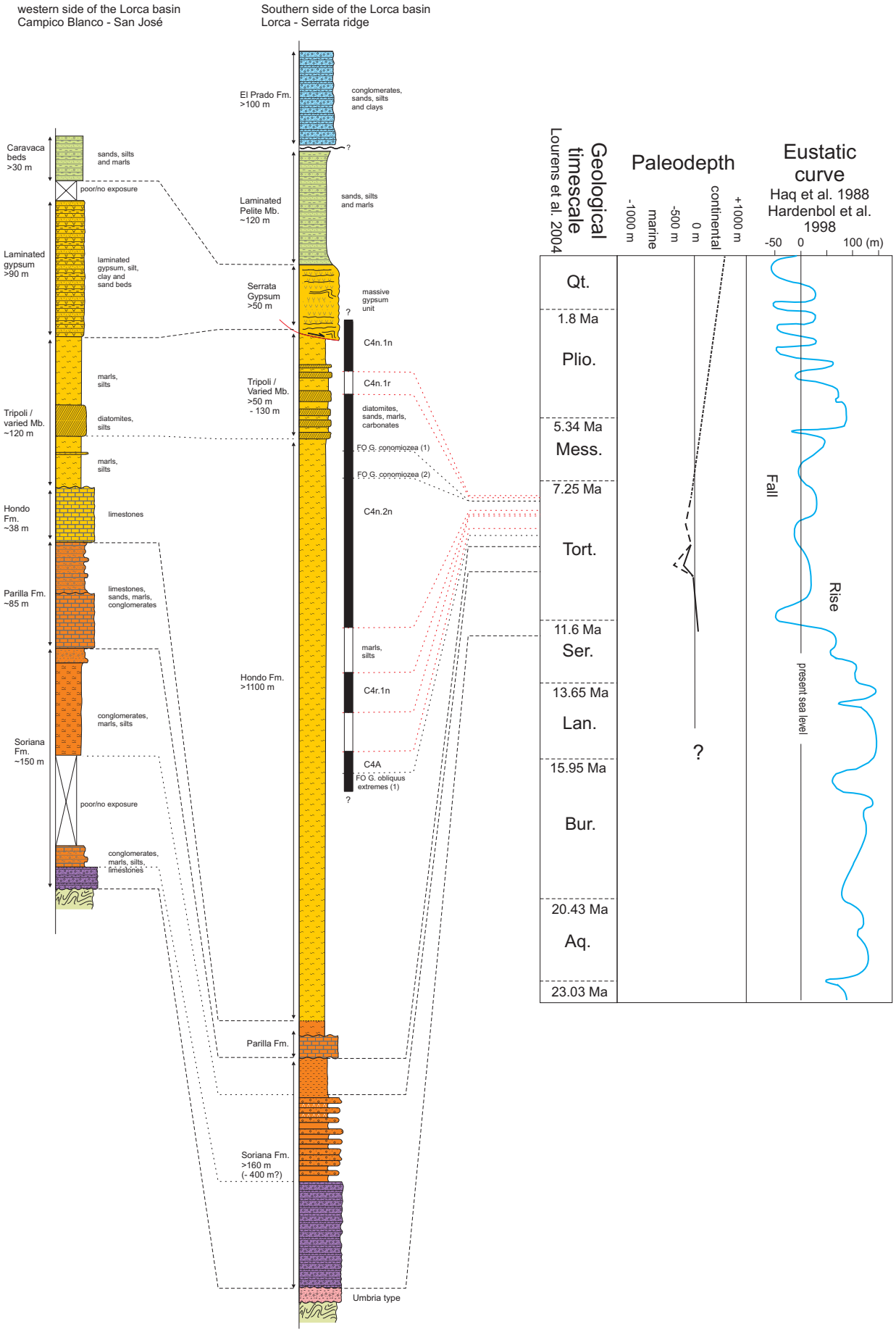
western side of the Lorca basin
Campico Blanco - San José
Southern side of the Lorca basin
Lorca - Serrata ridge
Caravaca beds >30 m
sands, silts and marls
poor/no exposure
Laminated gypsum >90 m
laminated gypsum, silt, clay and sand beds
marls, silts
Tripoli / varied Mb. ~120 m
diatomites, silts
marls, silts
Hondo Fm. ~38 m
limestones
Parilla Fm. ~85 m
limestones, sands, marls, conglomerates
conglomerates, marls, silts
Soriana Fm. ~150 m
poor/no exposure
conglomerates, marls, silts, limestones
El Prado Fm. >100 m
conglomerates, sands, silts and clays
Laminated Pelite Mb. ~120 m
sands, silts and marls
Serrata Gypsum >50 m
massive gypsum unit
Tripoli / Varied Mb. >50 m - 130 m
diatomites, sands, marls, carbonates
FO G. conomiozea (1)
FO G. conomiozea (2)
C4n.1n
C4n.1r
C4n.2n
marls, silts
C4r.1n
C4A
FO G. obliquus extremes (1)
Hondo Fm. >1100 m
Parilla Fm.
Soriana Fm. >160 m (- 400 m?)
Umbria type
Geological timescale
Lourens et al. 2004
Qt.
1.8 Ma
Plio.
5.34 Ma
Mess.
7.25 Ma
Tort.
11.6 Ma
Ser.
13.65 Ma
Lan.
15.95 Ma
Bur.
20.43 Ma
Aq.
23.03 Ma
Paleodepth
-1000 m
marine
-500 m
0 m
continental
+1000 m
?
Eustatic curve
Haq et al. 1988
Hardenbol et al. 1998
-50
0
100 (m)
Fall
Rise
present sea level

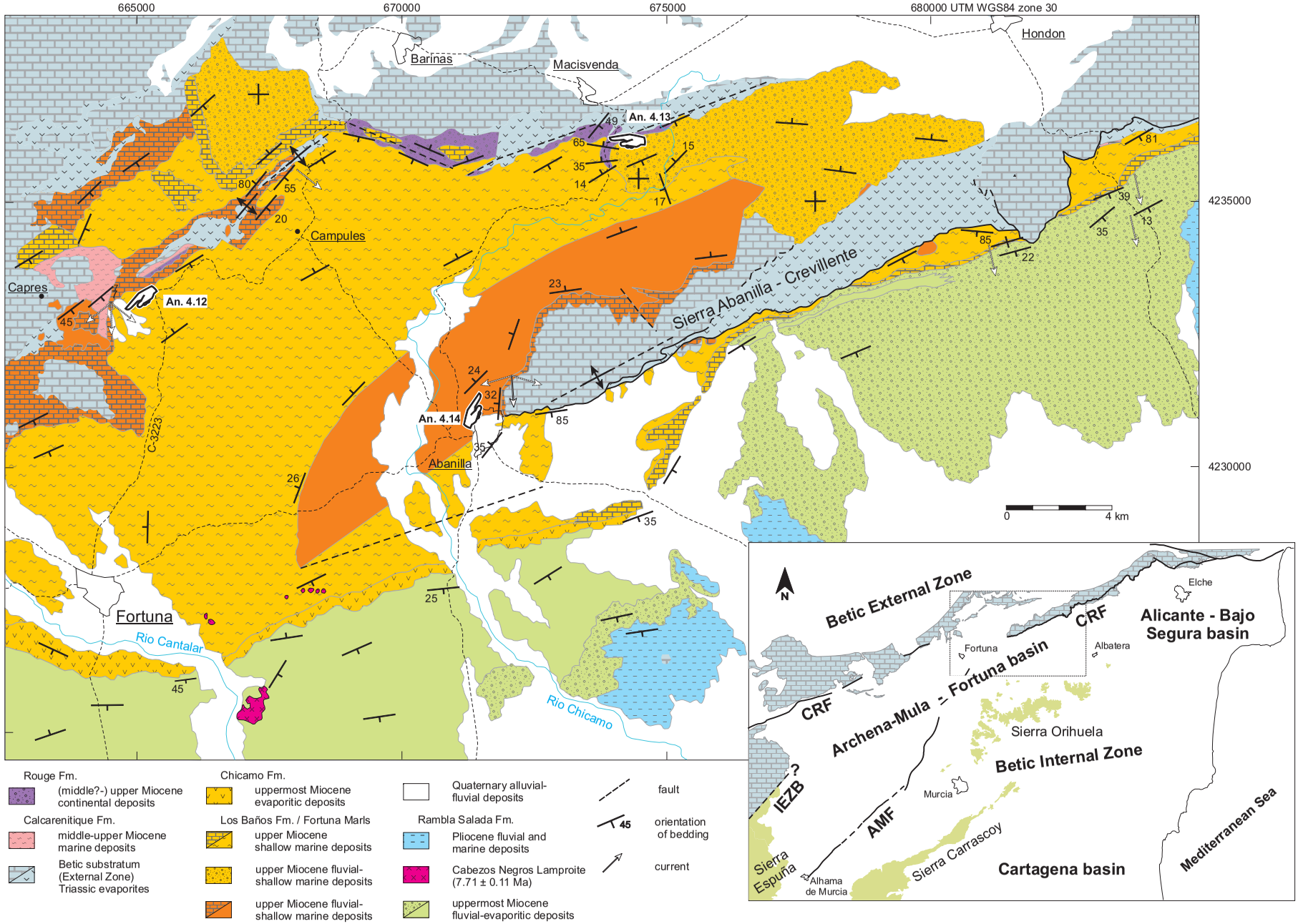
665000
670000
675000
680000 UTM WGS84 zone 30
4235000
4230000
Barinas
Macisvenda
Hondon
Campules
Capres
Abanilla
Fortuna
An. 4.12
An. 4.13
An. 4.14
Sierra Abanilla - Crevillente
C-3223
Rio Cantalar
Rio Chicamo
0
4 km
Rouge Fm.
(middle?-) upper Miocene continental deposits
Calcarenitique Fm.
middle-upper Miocene marine deposits
Betic substratum (External Zone) Triassic evaporites
Chicamo Fm.
uppermost Miocene evaporitic deposits
Los Baños Fm. / Fortuna Marls
upper Miocene shallow marine deposits
upper Miocene fluvial-shallow marine deposits
upper Miocene fluvial-shallow marine deposits
Quaternary alluvial-fluvial deposits
Rambla Salada Fm.
Pliocene fluvial and marine deposits
Cabezos Negros Lamproite (7.71 ± 0.11 Ma)
uppermost Miocene fluvial-evaporitic deposits
fault
45 orientation of bedding
current
N
Betic External Zone
CRF
Alicante - Bajo Segura basin
Elche
Fortuna
Albatera
Archena-Mula - Fortuna basin
CRF
Sierra Orihuela
Betic Internal Zone
IEZB ?
AMF
Murcia
Sierra Espuña
Alhama de Murcia
Sierra Carrascoy
Cartagena basin
Mediterranean Sea

Member, which actually suggests that this unit predates the Messinian Salinity Crisis (Fig. 4.2). Unless the fauna is reworked, the conclusions of Steffahn and Michalzik (2000) are in conflict with their own observations. The Laminated Pelite Member grades laterally and upwards into continental alluvial and fluvial conglomerates, sands and marls (El Prado formation of Wrobel, 2000; Figs. 4.7 and 4.8).

The Quaternary is represented by km-scale alluvial fans in the northern and north-eastern parts of the Lorca basin, covering Miocene and Pliocene sediments and structures. Along the western and southern margins of the basin, the Quaternary is represented by present-day riverbeds, such as those of the Guadalentin and the Lebor, incising tens or even hundreds of meters and eroding Miocene and Pliocene sediments.

Few attempts have been made to correlate the Miocene sediments of the Lorca basin with the sediments fringing the southern margin of the Sierra de la Tercia (e.g., Montenat *et al.*, 1990b). This may be the case for two reasons. First, the sediments in question are dominated by varicoloured conglomerates and breccias which, given the absence of any fauna, are difficult to date and correlate. However, along the south-eastern side of the Sierra de la Tercia these conglomerates are unconformably covered by a laminated series of sediments and a thick evaporite unit. These laminated sediments and evaporites are commonly correlated with the laminated rocks and evaporites of the Serrata formation (e.g. Geel, 1976; Montenat *et al.*, 1990b; Orti *et al.*, 1993; Wrobel, 2000) which, however, allows a relatively young, possibly Tortonian age of the underlying conglomerates. Secondly, due to progressive deformation along the Alhama de Murcia fault, the sediments along the southern margin of the Sierra de la Tercia are intensely faulted and folded, and they are covered by Quaternary alluvial deposits. As a consequence, detailed stratigraphic studies are virtually impossible. The deformational structures along the southern margin of the Sierra de la Tercia are discussed in chapters 5 and 6.

Fortuna basin

Introduction

The Fortuna basin is one of the largest Neogene basins in the south-eastern Betic Cordillera. The basin has an ENE trending elongate geometry and merges with the Alicante-Bajo Segura basin to the east, the Cartagena basin to the south and the Guadalentin-Hinojar basin to the southwest (see inset of Fig. 4.9). The Fortuna basin is connected via narrow corridors with smaller basins in the External Zone. The western part of the basin is occasionally referred to as the Archena-Mula basin (Loiseau *et al.*, 1990). The northern part of the Fortuna basin is crossed by the North Betic - Crevillente fault (e.g., Leblanc and Olivier, 1984; Montenat and Ott d'Estevou, 1996). Furthermore, the basin is diagonally transected by the Alhama de Murcia fault zone, which forms part of the crustal scale shear zone.

The sediments of the Fortuna basin cover parts of the Pre- and Subbetic Zone in the north as well as non- to low-grade metamorphic rocks of the Alpujarride and Malaguide units of the Internal Zone. The presence of these basement rocks underneath the Fortuna basin is evidenced by exposures of both Internal and External Zone rocks in basement highs: the Sierra de Abanilla and Sierra de Crevillente are made up of rocks of the External zone, the Sierra de Orihuela contains rocks of both the External and Internal Zone (O.J. Simon, pers. comm.) and the Sierra de Carrascoy exposes units of the Internal Zone.

The Miocene sediments are in general exposed in the northern half of the Fortuna (and Archena-Mula) basin. In the southern part of the basin, i.e. south of the Alhama de Murcia fault zone and south of the Sierra Abanilla-Crevillente, the upper Miocene sediments are covered by Pliocene and recent alluvial and fluvial deposits. The sediments in the Fortuna basin are late Miocene to Pliocene-Quaternary in age and have been deposited in a regressive sequence of marine towards shallow marine-lacustrine and non-marine environments (Garcés *et al.*, 2001). Lower and middle Miocene sediments (marls and limestones) are only exposed along the northern and western margins of the basin and they are considered to be part of the Subbetic Zone and of the Malaguide complex (Jerez Mir *et al.*, 1972; Azema and Montenat, 1973;

Figure 4.9. Geological map of the north-eastern part of the Fortuna basin, after Azema and Montenat (1973), Lukowski and Poisson (1990), Poisson and Lukowski (1990), and Garces et al. (2001). Age of the Fortuna lamproite after Kuiper et al. (2006) Inset: CRF - Crevillente fault, IEZB - Internal-External Zone Boundary, AMF - Alhama de Murcia fault.

Figure 4.10. Stratigraphy of the Fortuna basin. This study mainly follows the stratigraphic subdivisions of Lukowski and Poisson (1990) and Garces et al. (2001).

Pignatelli García *et al.*, 1972; Lonergan *et al.*, 1994; Geel and Roep, 1998 and 1999).

The stratigraphy of the Fortuna and Archena-Mula basins has been extensively studied by, e.g., Lukowski and Poisson (1990) and Loiseau *et al.* (1990) as shown in figure 4.10, whilst particular attention has been given to the upper Miocene evaporite succession by, e.g., Müller and Hsü (1987), Orti et al (1993), Dinares-Turell *et al.* (1999), Playa *et al.* (1999), Krijgsman *et al.* (2000), Playa *et al.* (2000) and Garcés *et al.* (2001).

This study focuses primarily on the north-eastern part of the Fortuna basin (Fig. 4.9).

Stratigraphy

Early and middle Miocene

Lower and middle Miocene deposits consisting of marls and limestones, as well as older Tertiary deposits, crop out along the northern and western margins of the Fortuna – Archena-Mula basin. According to Jerez Mir *et al.* (1972), Azema and Montenat (1973), Pignatelli García *et al.* (1972), Loiseau *et al.* (1990), Lonergan *et al.* (1994) and Geel and Roep (1998 and 1999) these deposits belong to allochtonous as well as autochthonous formations of the Pre- and Subbetic Zone and of the Malaguide Complex. According to these authors sedimentation in the basin was continuous from the late Oligocene to the early Miocene, which is evidenced by the influx of *G. trilobus* and *C. dissimilis* in the top part of the pelagic marine marls. In the westernmost part of the Fortuna basin, late Burdigalian – Langhian submarine fan deposits straddle the Internal-External Zone Boundary. These deposits lie unconformably on rocks of the External and Internal Zone, hence they seal and therefore postdate the juxtaposition of the Internal and External Zones (Lonergan *et al.*, 1994; Geel and Roep, 1998 and 1999).

The lower-middle Miocene deposits, as well as the underlying Mesozoic and lower Tertiary rocks of the Prebetic Zone and Malaguide complex, are folded and faulted, and they are tectonically overlain by lower Tertiary and Mesozoic rocks of the Subbetic Zone (Lonergan *et al.*, 1994; Geel and Roep, 1998). Like in the Lorca basin, the deformed Mesozoic to lower-middle Miocene rocks of the Internal and External Zones are unconformably overlain by late Miocene sediments, and earlier tectonic structures are consequently sealed.

Late Miocene and Pliocene

The upper Miocene – Pliocene sediments of the Fortuna basin can essentially be grouped into four units: (1) a basal shallow marine-continental unit, (2) a transgressive marine unit, (3) a regressive marine to transitional evaporitic unit, and (4) a thick continental alluvial-lacustrine unit (Dinares-Turell *et al.*, 1999; Krijgsman *et al.*, 2000; Garcés *et al.*, 2001); see figures 4.10 and 4.11.

The oldest lower Miocene deposits forming the basal shallow marine-continental unit crop out in narrow but elongate zones along the northern margin of the Fortuna basin. This basal unit consists of an at least 100 to 200 meter thick shallow marine series of alternating (reef) breccias, oyster beds, bioclastic grainstones and boundstones, referred to as the "Brèche de démantèlement" unit by Loiseau *et al.* (1990) and the "Brèchique" unit by Lukowski and Poisson (1990), as shown in figure 4.10 and Plate 4.12. Towards the top this unit gradually passes into alluvial and fluvial red conglomerates, sands and silts of the "Rouge" unit (Plate 4.13). The bioclastic grainstones contain coral fragments and a diverse benthic foraminiferal assemblage. According to Loiseau *et al.* (1990), some of the calcarenites contain *N. acostaensis*, which substantiate a Tortonian age for these sediments. The conglomerates consist mainly of limestone pebbles derived from the External Zone. Outcrops of the basal unit occasionally show a clearly unconformable contact of the marine breccias and continental conglomerates on the External Zone substratum. The rocks of the basal unit are strongly affected by large- and small-scale (syn-sedimentary) extensional faults that will be discussed in chapter 5.

The basal units are unconformably overlain by an approximately 500 to 600 meter thick transgressive marine unit of reefal and bioclastic limestones exposed along the basin margins which, towards the central part of the Fortuna basin, pass laterally into (pelagic) marls and turbidites (Plates 4.12 and 4.14). These latter rocks are known in the literature as the Fortuna Marls (Lukowski and Poisson, 1990) or Los Baños Formation (Müller and Hsü, 1987; Figs. 4.10 and 4.11). Samples from the basal part of these marls in the eastern part of the Fortuna basin reveal the presence of dextral coiled *N. acostaensis*, *G. menardii 4* and *G. scitula* indicating an early Tortonian age (W.J. Zachariasse, pers. comm.). The samples contain reworked Cretaceous, Eocene and middle Miocene planktonic microfauna as well. Using Lourens *et al.* (2004), the biostratigraphy of these sediments would point to an age range of 10.57 to 9.54 Ma. The upper

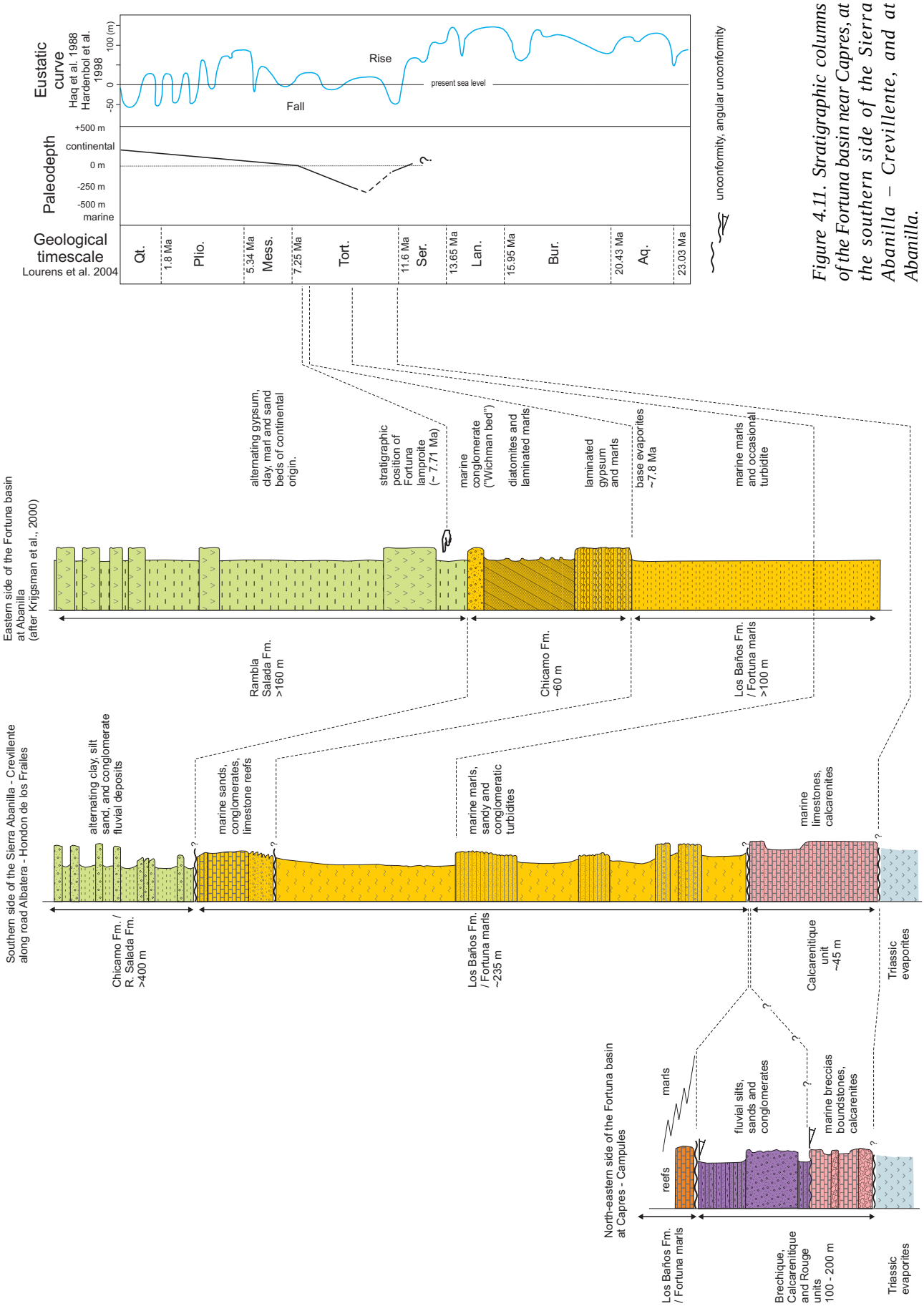

Figure 4.11. Stratigraphic columns of the Fortuna basin near Capres, at the southern side of the Sierra Abanilla – Crevillente, and at Abanilla.

part of the Fortuna marls in a section south of the Sierra Abanilla reveals high percentages of benthic foraminifera and a rather poor planktonic assemblage including dominant sinistral coiled *N. acostaensis* and occasionally *G. menardii 4* and *G. scitula*, as well as reworked middle Miocene forms (e.g., *P. partimlabiata*, *P. siakensis*, *N. atlantica* and *G. dehiscens*), suggesting a late Tortonian age for these shallow marine sediments (W.J. Zachariasse, pers. comm.; Fig. 4.2). Using Lourens *et al.* (2004), the biostratigraphy of these sediments would point to an age range of 9.54 to 7.51 Ma. These results are consistent with the observations of Montenat (1973) and Martín-Suarez *et al.* (2001), however, they are in conflict with the observations of Lukowski and Poisson (1990). Lukowski and Poisson (1990) noticed the presence of *N. humerosa* in the lower part and *T. multiloba* in the upper part of the Fortuna marls, and therefore suggest a late Tortonian to Messinian age for these sediments, although the Messinian marker *G. mediterranea* or *G. miotumida (conomiozea) gr.* is absent (Dinares-Turell *et al.*, 1999; W.J. Zachariasse, pers. comm.). Paleodepth estimates of a section in the upper marl series suggest a water depth of 150-200 meter (D.J.J. van Hinsbergen, pers. comm.).

The marine sequence passes upward into the regressive marine to transitional evaporitic unit, an approximately 200 meter thick series of mixed continental - shallow marine sediments of the Chicamo Formation (Müller and Hsü, 1987; Dinares-Turell *et al.* 1999; Krijgsman *et al.*, 2000; Garcés *et al.*, 2001; Figs. 4.10 and 4.11) consisting of diatomites, marls, evaporites and continental-lacustrine conglomerates, which outcrop in the southern and eastern parts of the Fortuna basin. The evaporites thin out laterally towards the east (Fig. 4.9). The sediments of the Chicamo Fm. in turn grade upwards into the continental alluvial-lacustrine unit, an approximately 1000 meter thick massive unit consisting of alluvial to lacustrine evaporitic deposits of the Rambla Salada Formation (Müller and Hsü, 1987; Dinares-Turell *et al.* 1999; Krijgsman *et al.*, 2000; Garcés *et al.*, 2001) and made up of thinly bedded alternating clays, evaporites, sandstones, conglomerates, lacustrine marls and limestones.

The regressive marine to transitional evaporite deposits have been studied intensively in the past decades and have been correlated through event stratigraphy (Müller and Hsü, 1987), lithostratigraphy (Orti *et al.*, 1993) and trace element (strontium) and (oxygen and sulphur) isotope geochemistry (Playa *et al.*, 2000) with other known Messinian evaporite units in southern Spain (e.g., Sorbas) as well as elsewhere in the Mediterranean (e.g., Sicily). However, recent integrated magnetostratigraphic and palaeontological studies by Dinares-Turell *et al.* (1999), Krijgsman *et al.* (2000), Martín-Suarez *et al.* (2001) and Garcés *et al.* (2001) suggest a late Tortonian age for the regressive sequence (Chicamo Fm.) and a late Tortonian to early Pliocene age for the massive continental unit (Rambla Salada Fm.), which are consistent with earlier studies by Montenat (1973). The onset of restriction in the Fortuna basin is estimated at 7.8 Ma which is at the base of the evaporite-diatomite series. The marine influence vanished from the Fortuna basin at about 7.6 Ma (Krijgsman *et al.*, 2000), except for a short period in the early Pliocene evidenced by 30 meters of shallow marine deposits and associated with a Pliocene flooding event or transgression, after which continental conditions re-established in the basin (Garcés *et al.*, 2001). The timing of basin restriction is substantiated by a recently obtained age of 7.71 ± 0.11 Ma of volcanic rocks intercalated with the marine marls immediately above the evaporites near Fortuna (Kuiper *et al.*, 2006; Figs 4.9 and 4.11).

Regional correlation between the basins studied

The available data summarized above indicate that the Huercal Overa, Lorca and Fortuna basins were initiated as true depocenters and obtained their present-day geometry in the latest Serravallian and earliest Tortonian. The initiation of the basins seems to have occurred synchronically (Fig. 4.12), however, accurate age constraints on the pertinent sediments are lacking: the pre-basin sediments are scarce and scattered, and the basal deposits of the basins are continental. The surrounding basins, such as the Vera, Sorbas-Tabernas, Nijar, Guadix, Murcia-Cartagena basins show a similar trend in their early-stage development (e.g., Sanz de Galdeano and Vera, 1992). The deposition of Serravallian to lower Tortonian continental sediments in the Betic basins seems to coincide with a significant eustatic sea level drop. In the Alboran basin the Serravallian/lower Tortonian and the Tortonian seismic stratigraphic units are separated by a regional unconformity (e.g., Comas *et al.*, 1992; Rodríguez-Fernández *et al.*, 1999; Comas *et al.*, 1999).

The subsequent continental to marine transition in the early Tortonian occurs gradually and manifests itself in lithologically diverse sediments deposited in mixed fluvial and shallow marine facies. In the

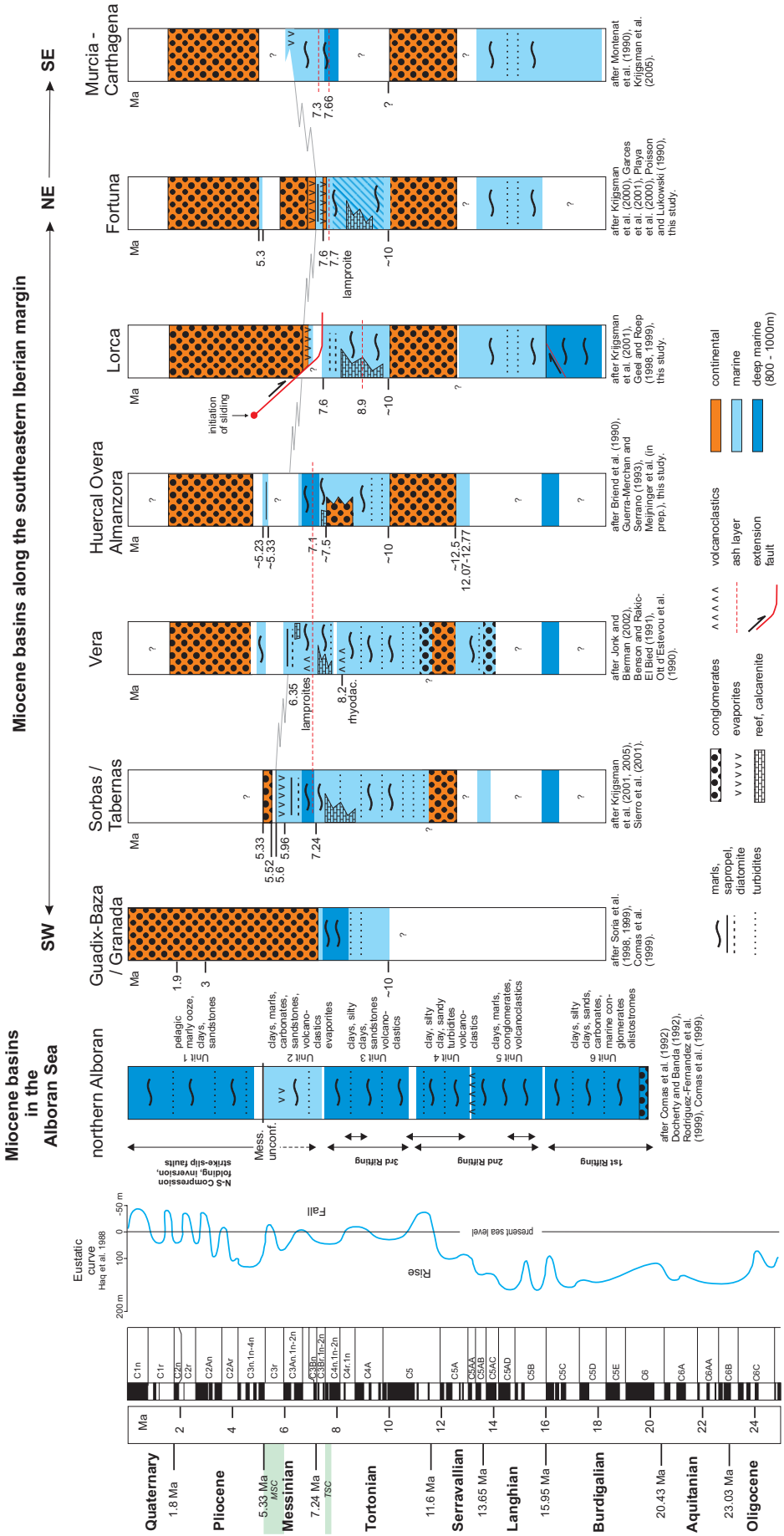

Figure 4.12. Stratigraphic correlation diagram for the different Miocene basins in the south-eastern part of the Betic Cordillera. For further explanation see text.

Huercal Overa and Lorca basins, a clear basin-wide dominance of marine conditions does not occur until approximately 10 Ma. In the Guadix-Baza, Fortuna and Murcia-Cartagena basins, the transgression probably occurred at the same moment, however, in the Vera and Sorbas-Tabernas basins the transgression seems to have occurred earlier. The marine dominance in the Betic basins seems to coincide with a transgression and high-stand in the early Tortonian. The marine transgression is characterized with the progradational and aggradational development of interfingering submarine delta fans and reef- and carbonate platforms, which pass laterally into marls and turbidites in the deeper parts of the basins.

From approximately 7.8 Ma (late Tortonian) till the late Messinian, a diachronic trend occurs in the basins of the south-eastern Betic Cordillera, which was detected first by Dinares-Turell *et al.* (1999). At about 7.7 Ma the depositional environment in the Fortuna basin changes from marine towards continental, with first the deposition of late Tortonian evaporites, followed by continental deposits (Krijgsman *et al.*, 2000). In contrast, the Huercal Overa basin as well as the Vera and Sorbas-Tabernas basins to the southwest, show clear evidence for continuing, relatively open marine conditions during the late Tortonian and early Messinian. The Lorca basin, located in between the Fortuna and Huercal Overa basins, becomes progressively shallower, but the precise age of the marine to continental transition remains unclear because the contact between the marl-diatomite sequence and the overlying evaporites is affected by localized deformation rather than being an undisturbed stratigraphic contact (see also chapter 5). In this context it is emphasized that there are no drastic eustatic sea level changes documented during the late Tortonian and early Messinian (Haq *et al.*, 1988, see also Fig. 4.9).

During the Messinian, the Lorca and Fortuna basins remain continental depocenters. It is unclear what happened in the Huercal Overa basin: like in the Vera basin, most of the Messinian is absent. The Sorbas and Tabernas basins, on the other hand, remained marine basins until the late Messinian (5.60-5.54 Ma; Krijgsman *et al.*, 2001), when massive evaporites mark the beginning of a marine-continental transition (the Sorbas evaporites of the Messinian Salinity Crisis; 5.96-5.60 Ma). Note that this transition from marine to continental conditions coincides with a drastic eustatic sea level drop in the latest Messinian (~5.5 Ma).

From the Pliocene onward, most of the Betic basins are mainly characterized by the deposition of continental, alluvial and fluvial, sediments. However, in the earliest Pliocene some of the basins, such as the Huercal Overa, Vera and Fortuna basins, may have experienced a short marine incursion. This event, which clearly postdates the Messinian Salinity crisis, coincides with a Pliocene eustatic transgression believed to be responsible for the flooding of the Neogene basins in the Mediterranean region, and is commonly referred to as the “Pliocene flooding event” (e.g., Garcés et al, 2001).

Plate 4.1) Steeply inclined alluvial and mass flow deposits of the Brèche rouge unit at Almajalejo, consisting of unsorted angular pebbles, blocks and boulders. Note geologist for scale.
Plate 4.2) Fluvial deposits of the Conglomérats et limons rouges unit at the northern margin of the Huercal Overa basin. Note hammer for scale.
Plate 4.3) Panoramic view of the northern basin margin near Sta. Maria de Nieva. Fluvial deposits of the Conglomérats et limons rouges unit dip gently towards the south.Inset shows detailed sedimentary structures; onlap on a paleo-relief of the basement rocks of the Sierra de las Estancias. Note geologist for scale.
Plate 4.4) Panoramic view of the continental – marine transition in the Hueral Overa basin: continental deposits of the Guzmaina red unit are unconformably overlain by upper Tortonian marls and Ventica reefs (marnes jaunes inferieurs et recifs unit).
Plate 4.5) Panoramic view of the late Tortonian - earliest Messinian marine marls and turbidites.

Plate 4.6) Turbidite beds in the late Tortonian marine marls. Transport towards the ENE,E and SE. Note hammer for scale.
Plate 4.7) Panoramic view of the southern basin margin, east of Huercal Overa. Earliest Pliocene shallow marine deposits lie unconformably on late Tortonian shallow marine deposits.

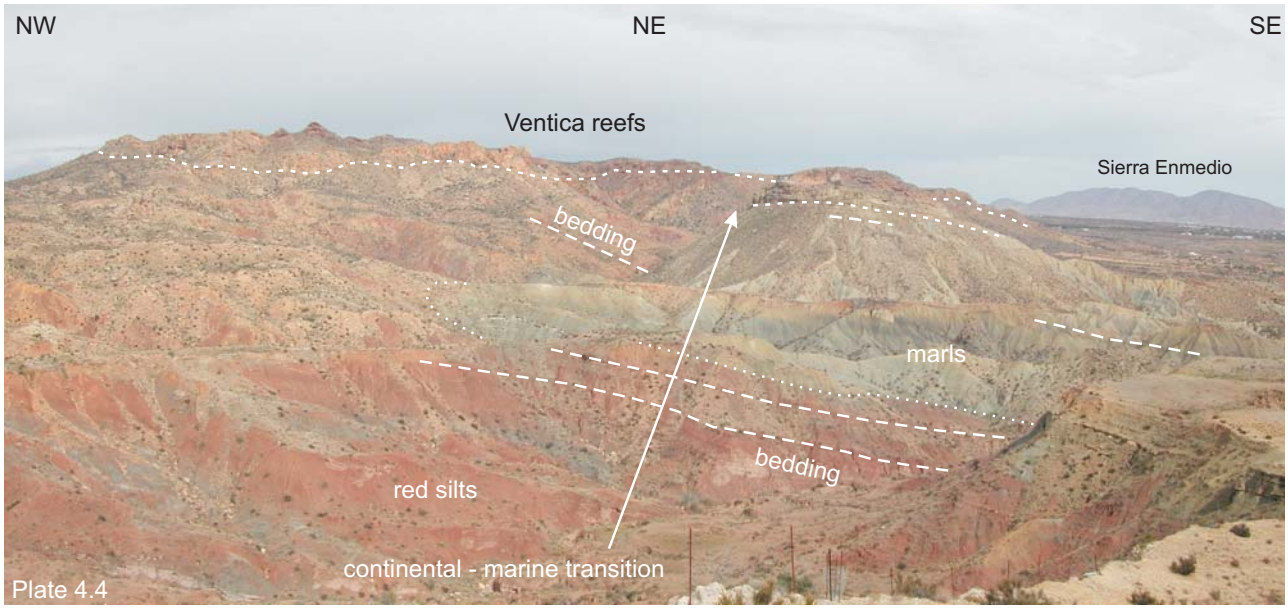

Plate 4.4

Plate 4.5


Plate 4.6

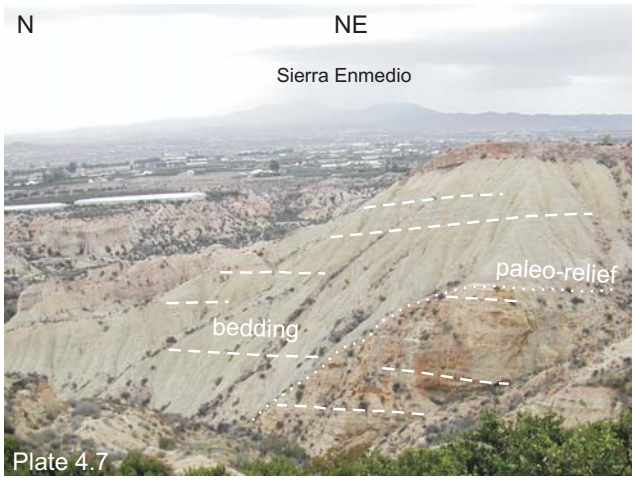

Plate 4.7

Plate 4.8) View of the northern side of the Sierra de la Tercia, showing alluvial deposits of the Soriana formation that pass upwards into playa and marginal marine deposits and evaporites. These deposits are unconformably overlain by the reef limestones of the Parilla formation.

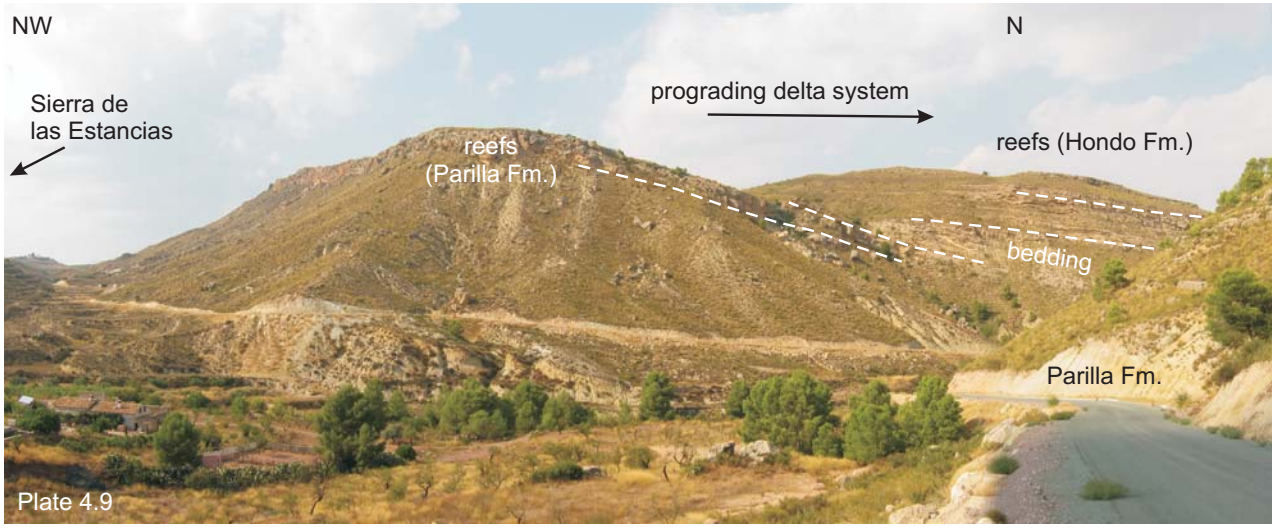

Plate 4.9) Panoramic view of the south-western margin of the Lorca basin, showing shallow marine deposits of the Parilla and Hondo formations in a basinward prograding-aggrading reef-delta system.

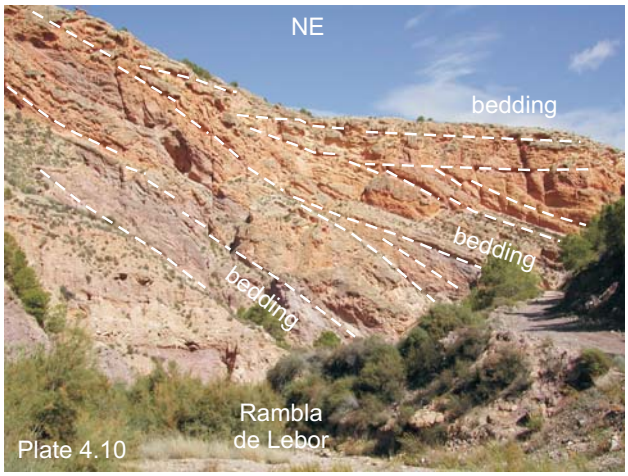

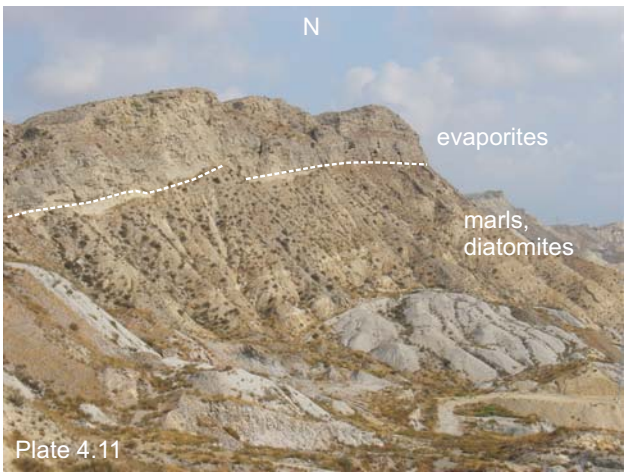

Plate 4.10) Large-scale outcrop of submarine fan deposits and reefs of the Hondo formation at the eastern side of the Sierra de la Tercia in the rambla de Lebor. Plate 4.11) Panoramic view of the Serrata ridge in the Lorca basin showing the marls and diatomites of the Serrata formation, which pass upwards into a thick unit of evaporites.

Plate 4.12) Panoramic view of the northern side of the Fortuna basin near Capres. Tortonian shallow marine and fluvial deposits are overlain by reef limestones which interfinger with the Fortuna marls towards the south.

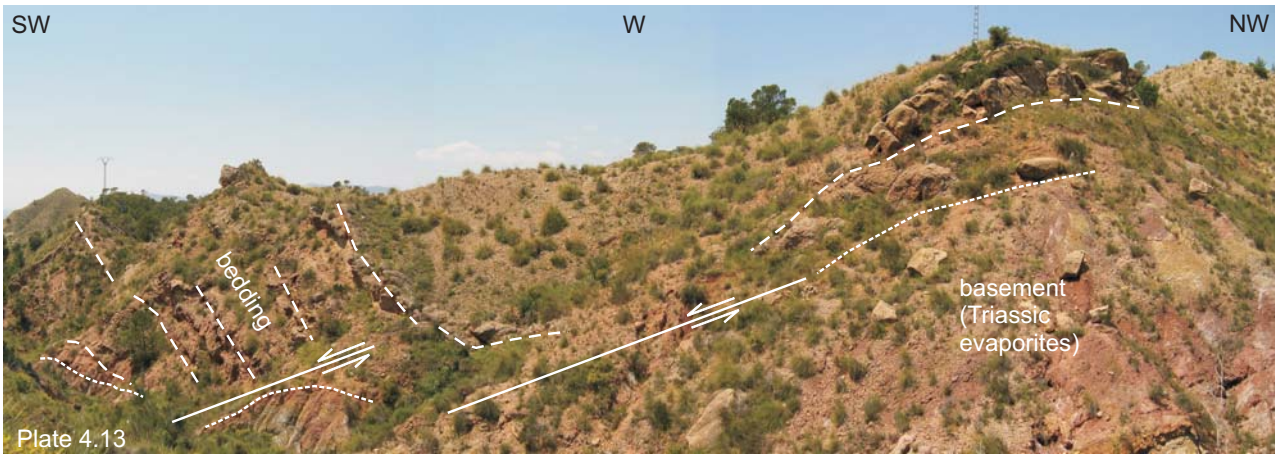

Plate 4.13) View of the northern side of the Fortuna basin near Macisvenda. Red conglomeratic alluvial deposits of the Rouge formation lie unconformably on Triassic evaporites. The conglomeratic beds and the evaporites have been tilted and faulted.

Plate 4.14) View of the north-western side of the Sierra Abanilla near Abanilla. The gently north-westward tilted Fortuna marls and marine conglomerates onlap on the Mesozoic basement of the Sierra Abanilla.

5

Deformational structures in the Neogene basins

Introduction

The Internal Zone of the Betic Cordillera is characterized by a "Basin and Range" type morphology, made up of ENE trending, elongate mountain ranges of intensely deformed and mostly metamorphosed Palaeozoic and Mesozoic rocks of the Nevado-Filabride, Alpujarride and Malaguide Complexes (e.g., Egeler and Simon, 1969; Platt and Vissers, 1989; Fig. 5.1) that are flanked by narrow, elongate basins. These intramontane basins are filled with Neogene, in particular late Miocene, Pliocene and Quaternary sediments. The basin sediments may show evidence of intense brittle, partly syn-sedimentary deformation, including in places spectacular extensional and occasionally also compressional tectonic structures (e.g., Briend, 1981; Montenat *et al.*, 1990b; Poisson and Lukowski, 1990; Mora-Gluckstadt, 1993; Vissers *et al.*, 1995; Augier, 2004). Detailed structural and sedimentological studies of, e.g., the Huercal Overa basin (Briend, 1981; Mora-Gluckstadt, 1993) as well as seismic studies of the Granada (Morales *et al.*, 1990; Ruano *et al.*, 2004) and Guadalentin basins (Amores *et al.*, 2001 and 2002) demonstrate the existence of late Miocene half graben structures. Seismic surveys of the Miocene sediments in the Alboran Sea (e.g., Comas *et al.*, 1992; Mauffret *et al.*, 1992; Watts *et al.*, 1993) have documented similar half graben structures offshore.

The rocks of the Nevado-Filabride, Alpujarride and Malaguide Complexes, which make up the mountain ranges as well as the basement underneath the Miocene basins in the Internal Zone, experienced an early Tertiary stage of crustal thickening, reflected by relics of high-pressure metamorphic assemblages in the Nevado-Filabride and locally Alpujarride rocks (e.g., de Roever and Nijhuis, 1964; Egeler and Simon, 1969; Vissers, 1981; de Jong, 1991). This was followed by large-scale E-W directed extension and exhumation during the latest Oligocene and early to middle Miocene, locally associated with early Miocene low-pressure, high-temperature metamorphism mainly observed in Alpujarride rocks of the western and central Betics, but locally also in the eastern Betic Zone (e.g., Platt and Vissers, 1989; Monie *et al.*, 1991 and 1994; Vissers *et al.*, 1995; Lonergan and Johnson, 1998; Comas *et al.*, 1999; Platt and Whitehouse, 1999; de Jong, 2003; Platt *et al.*, 2005). As a result of this history, the basement rocks commonly show evidence of ductile and brittle extension superimposed on earlier Alpine structures (e.g., Platt and Vissers, 1989; Vissers *et al.*, 1995; Augier, 2004; Platzman and Platt, 2004). Much of this extension, however, was localized along crustal-scale low-angle detachments, which clearly evolved through time from ductile to brittle (Platt and Vissers, 1989; Jabaloy *et al.*, 1992; Vissers *et al.*, 1995; Lonergan and Platt, 1995). The simultaneous exhumation and thinning of the metamorphic middle to upper crust and the deposition of late Miocene sediments in an extensional setting clearly suggest a dynamic link: the intramontane basins in fact developed on top of a previously thickened, thermally anomalous and locally hot, stretching continental crust.

The geology and morphology of the Betic Internal Zone is further complicated by a network of major faults such as the Alhama de Murcia, Palomares and Carboneras faults (Fig. 5.1), that has been interpreted as a left-lateral crustal-scale strike-slip corridor or transcurrent shear zone crossing the eastern part of the Internal Zone (e.g., Leblanc and Olivier, 1984; Montenat *et al.*, 1987; De Larouziere *et al.*, 1988). Several of these large faults make up the strongly deformed contacts between basement rocks of the ranges and the intramontane basin sediments. The position of the pertinent fault network approximately coincides with a transition from thick (> 30 km) crust to the west and northwest and thin (< 25 km) crust east and south of the faults (Banda and Ansorge, 1980; De Larouziere *et al.*, 1988; Torné and Banda, 1995) suggesting that they are the surface expression of a crustal-scale feature. Bousquet and Montenat (1974), Bousquet *et al.* (1975), Gauyau *et al.* (1977), Bousquet (1979), Silva *et al.* (1997), Martínez-Díaz *et al.* (2001), Soler *et al.* (2003) and Masana *et al.* (2004 and 2005) have provided evidence for intense deformation of Quaternary sediments close to the Alhama de Murcia, Palomares and Carboneras faults, which

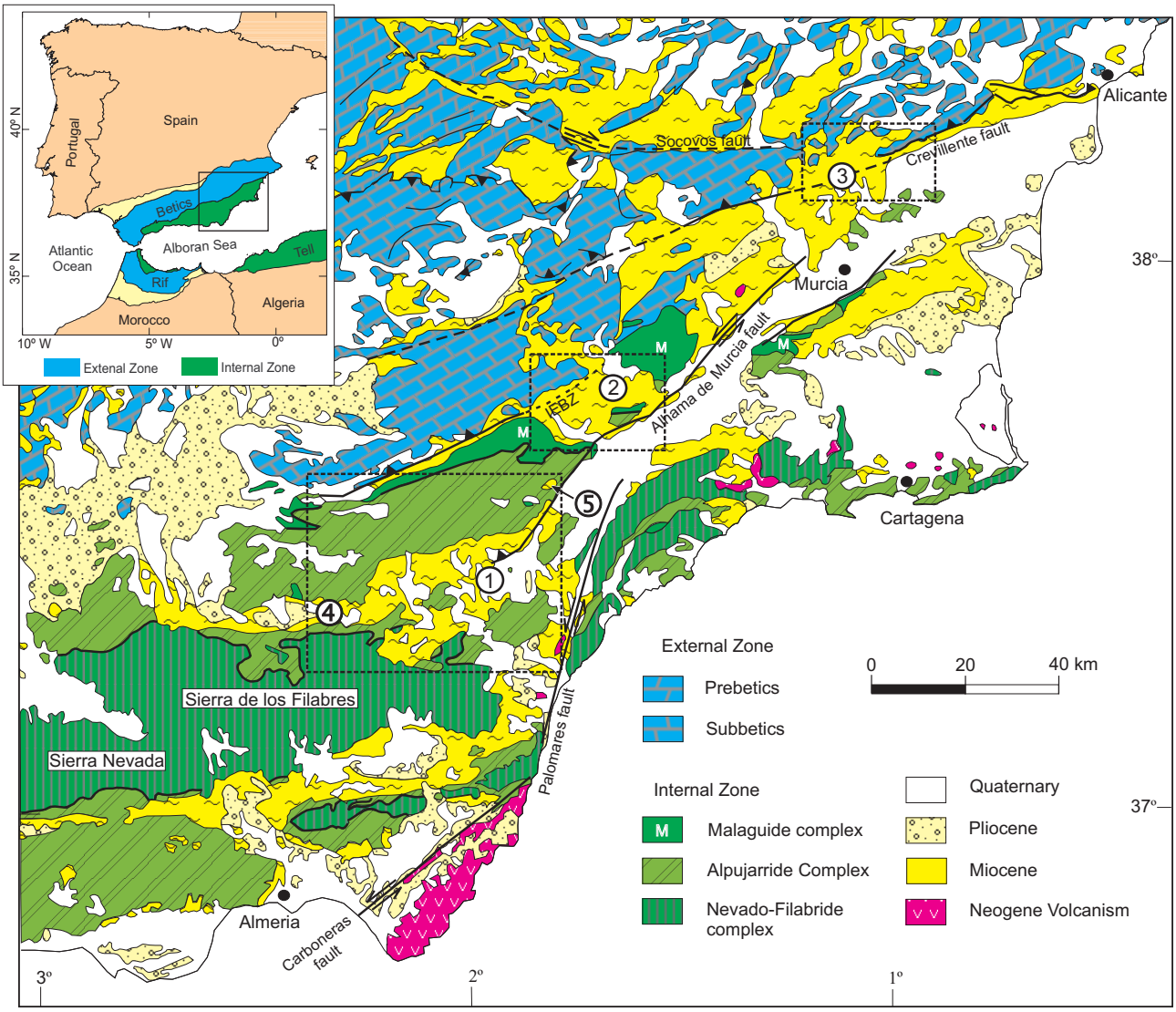

Figure 5.1. Geological map of the eastern Betic Cordillera, modified from Mapa Geologico de la Peninsula Iberica (IGME, 1:1.000.000, 1981), showing study areas (rectangles) and main faults. Numbers refer to basins: 1) Huercal Overa basin, 2) Lorca basin, 3) Fortuna basin, 4) Almanzora corridor, 5) Puerto Lumbreras basin. IEZB - Internal-External Zone Boundary.

demonstrates recent activity of these faults. According to, e.g., Bousquet (1979) and Masana *et al.* (2004) such activity may very well be associated with the present-day convergence of the African plate towards Eurasia (see also chapter 2). This interpretation is supported by seismological studies in the Betic – Alboran region providing evidence for present-day E-W directed extension and allied N-S to NW-SE directed shortening (e.g., Buforn, 1995; Stich *et al.*, 2003).

Principal questions arising from the above setting of the Neogene intramontane basins concern (1) the structural geometry and allied kinematics of the (mostly brittle) deformational structures in the basins and adjacent basin margins, (2) the role of the main faults such as the Alhama de Murcia fault in the development of the basins, and (3) relationships between the structure of the basins and the clearly extensional processes affecting the underlying Betic crust.

The data presented below strongly suggest that the Huercal Overa, Lorca and Fortuna basins investigated in this study in essence result from Tortonian crustal-scale extension, and that the resulting basin geometries were modified since the latest Miocene by NW-SE directed compression, giving rise to the present-day network of main faults. In this chapter, we present most of the pertinent structural data, with emphasis on the Tortonian extensional history. In order to explore relationships between basin development and processes in the Betic crust, we also address structures in the adjacent and underlying basement rocks, albeit that a detailed study of extensional proc-

esses in the Betic basement remains beyond the present scope. The compressional structures associated with crustal-scale NW-SE directed shortening, and the allied role and structural history of the main faults in the region are further discussed in detail in chapter 6.

Methods

The structural data for this study were collected in key areas and sections in the Almanzora, Huercal Overa, Puerto Lumbreras, Lorca and Fortuna basins, and partly in the basements rocks along the basin margins. Kinematics and slip directions of faults were de-

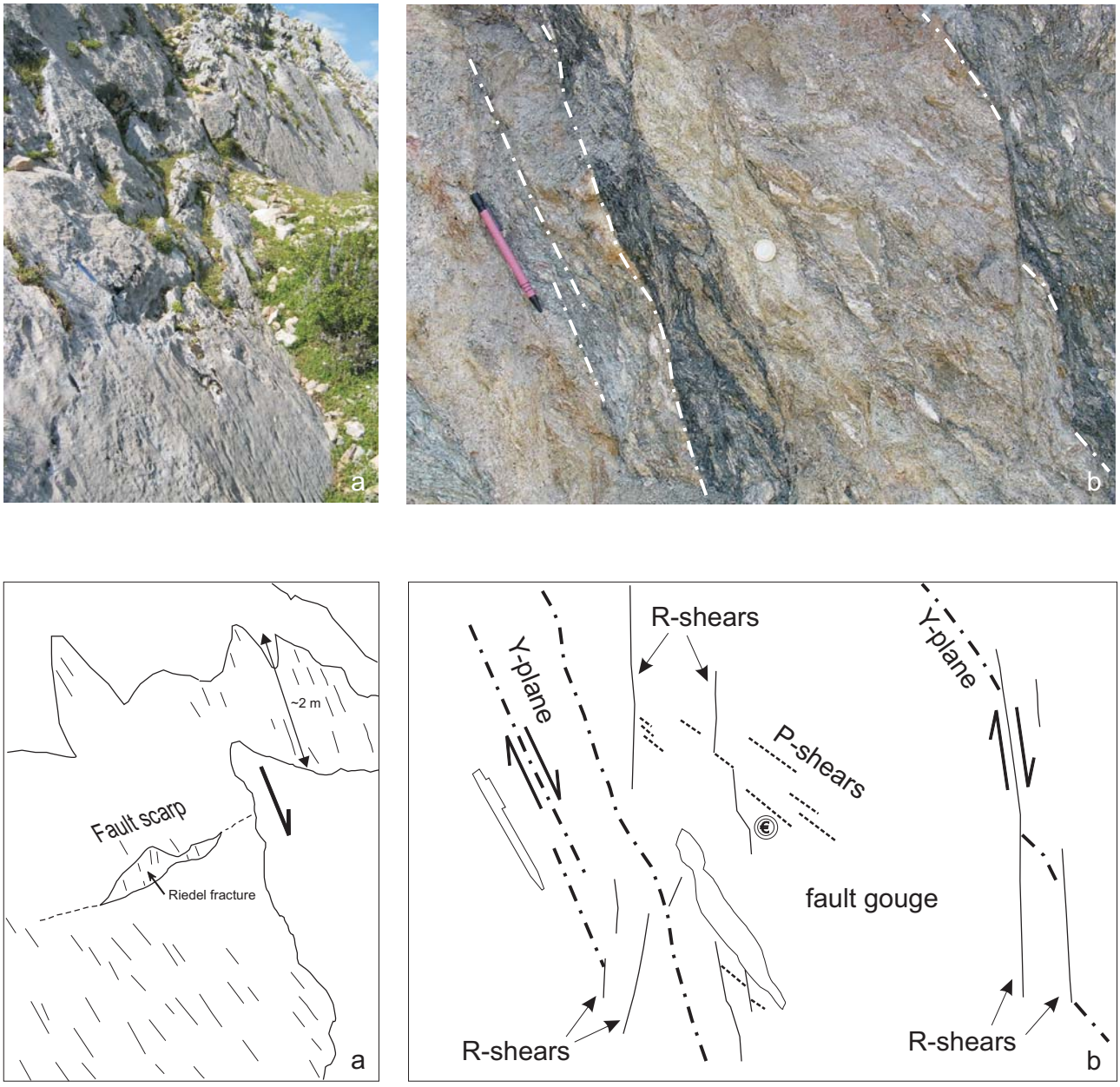

Figure 5.2. Structures on fault planes and in fault gouges used in kinematic analyses. a) Fault scarp of extensional normal fault. Scarp shows clearly grooved Riedel fractures, down-dip plunging grooves and slickenside lineations on the fault surface, indicating dip-slip motion. b) Fault gouge of extensional fault at basement-basin contact, southern margin of the Huercal Overa basin, showing steeply inclined main fault (Y-plane), subvertical Riedel shears (R-shears) and gently inclined P-shears. Down-dip lineations on shear surfaces and geometric relationships of the Y, R and P-shears indicate down-dip movement of the hanging wall.

termined on the basis of both structures on fault planes (such as tensile fractures, Riedel fractures, striations; see Fig. 5.2a) and shear structures in fault gouges (Riedel, P, Y, R_2 and X shears and striations on these shear planes; see Fig. 5.2b) as described by, e.g., Logan *et al.* (1979), Rutter *et al.* (1986), Gamond (1987), Hancock and Barka (1987), Petit (1987), Means (1987), Sylvester (1988), and Woodcock and Schubert (1994). In the case of fault planes without clearly developed linear structures, slip directions along such faults have been inferred on the basis of the geometrical relationship between the main fault and secondary fractures, e.g., Riedel fractures. Kinematic axes, i.e. the principal axes of incremental shortening and extension, were inferred from fault plane orientation, lineations on the fault plane and slip direction following Marrett and Allmendinger (1990).

Despite the wealth of studies carried out in the Neogene basins over the last few decades, there have been surprisingly few attempts to arrive at geometrically accurate basin-scale cross sections. Special attention has therefore been paid to the construction of admissible and viable (Elliott, 1983), basin-scale cross sections. Cross-sections along the Huercal Overa, Lorca and Fortuna basins, perpendicular to the general basin axis, were constructed on the basis of both new outcrop and published map data. Construction and restoration of these cross-sections was performed by conventional principles, methods and techniques following Dahlstrom (1969) and Groshong (2002). The geometries of listric normal faults and fault-bend folds, fault-propagation fold or detachment-folds and the depths to the associated decollements were determined following methods and techniques of, e.g., Suppe (1983), Davison (1986), White *et al.* (1986), Williams and Vann (1987), Dula (1991), Homza and Wallace (1995), Bulnes and Poblet (1999), Mitra (2002) and Poblet and Bulnes (2005). Construction of the basin structures (strata and faults) at depth was performed using the software program 2D-Move, kindly provided by Midland Valley Exploration Ltd [*1]. This program provides a number of tools for balancing and restoration of a constructed (scanned and digitized) profile as well as tools for forward and backward modelling of restored and deformed cross-sections, respectively. The resulting cross-sections presented below are considered viable and admissible solutions, i.e. they are viable cross-section in the sense of Elliot (1983) in that they can be restored to the undeformed state.

Where possible, bulk horizontal extension in different parts of the basins and in the basement near the basin margins has been quantified using â-factors calculated from the geometry of the extensional structures according to geometrical principles proposed by Thompson (1960) and Wernicke and Burchfiel (1982), as illustrated in figure 5.3. This is particularly interesting in the case of syn-sedimentary structures, because β-factors in such cases provide information

*1 Midland Valley Exploration Ltd: main office in Glasgow, United Kingdom. Website: www.mve.com.

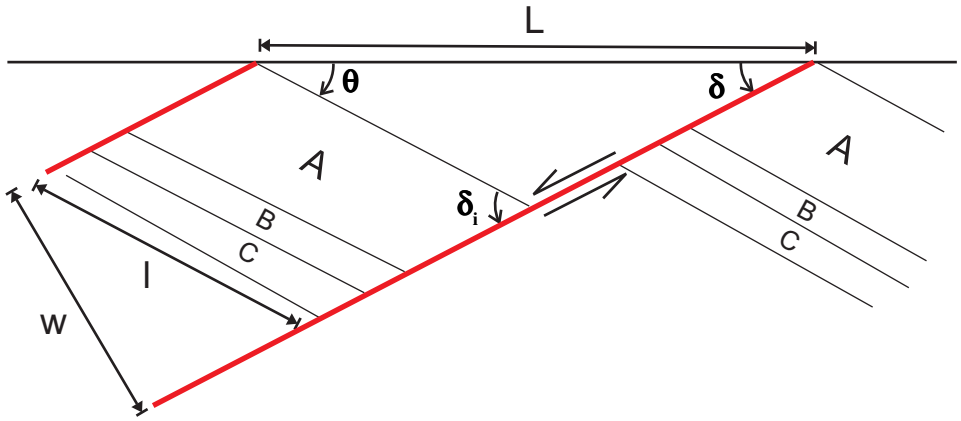

$$\beta = \frac{L}{l} = \frac{w/\sin\delta}{w/\sin\delta i} = \frac{\sin\delta i}{\sin\delta}$$

*or % extension = (β – 1) * 100%*

Figure 5.3. Determination of the amount of horizontal extension (i.e., stretching or β-factor) using the geometry of rotated planar faults, with fault dip (δ), dip of the bedding (θ), fault block width (w) and initial and final horizontal spacing (l and L) between the faults (modified after Wernicke and Burchfield, 1982).

on the incremental amount (percentage or fraction) of extension for the time slices in question.

Improved stratigraphic data (age, paleobathymetry and thickness in chapter 4) was used in order to determine subsidence and uplift episodes in the basin and underlying basement. The subsidence history of each of the basins was calculated using conventional backstripping techniques that allow to calculate tectonic subsidence by removing water and sediment load, according to principles described by, e.g., Van Hinte (1978), Steckler and Watts (1979), Bond and Kominz (1984), Bessis (1986), Allen and Allen (2005), and including corrections for compaction (e.g., Perrier and Quiblier, 1974; Sclater and Christie, 1980), eustatic sea level changes (Hardenbol *et al.*, 1998) and paleobathymetry. Local isostasy has been assumed in the calculation of the basement (or total) and tectonic subsidence curves. The motivation for this choice is discussed below.

Deformational structures in the basins and adjacent basement rocks

Almanzora, Huercal Overa and Puerto Lumbreras basins

The Huercal Overa basin is an elongate rectangular basin with an ENE trending basin axis. In general, the Miocene sediments in the basin dip towards the south and the stratigraphically lowest deposits are exposed in the northern part of the basin where they onlap on metamorphic basement rocks of the Sierra de las Estancias. The stratigraphically younger deposits occur mainly in the southern part of the basin, i.e., the basin is clearly asymmetric. Along the southern margin of the basin, the Miocene sediments are bounded by an ENE to NE trending network of extensional faults (Briend, 1981; Mora-Gluckstadt, 1993; Augier, 2004). In essence, the Huercal Overa basin thus forms an up to 14 km wide half-graben (Fig. 5.4). The late Miocene – Quaternary sediments dominate this basin, hence a Tortonian age was proposed for the initiation of the basin (see chapter 4). The eastern part of the basin is covered by a thick series of Pliocene – Quaternary alluvial deposits (García-Meléndez *et al.*, 2002 and 2003). Both the Almanzora corridor, west of the Huercal Overa basin, and the small Puerto Lumbreras basin, isolated in the Sierra de las Estancias northeast of the Huercal basin, have similar but smaller-scale basin geometries analogous to that of the Huercal Overa basin (e.g., Mora-Gluckstadt, 1993). The large-scale structure of the Huercal Overa basin is entirely comparable with similar half-graben structures seen at a same length scale in seismic studies of the Alboran Sea (e.g., Comas *et al.*, 1992). The basement underlying the Huercal Overa basin is largely made up of rocks of the Alpujarride complex like exposed in the Sierra de las Estancias immediately north of the basin (Fig. 5.1). On the basis of the geological maps, however, it may be inferred that in the southwestern part of the basin the basin sediments were locally deposited on Nevado-Filabride rocks.

Along the south-eastern side of the Sierra de las Estancias near Puerto Lumbreras, a narrow zone parallel to the basement – basin contact is marked by a NE trending network of faults belonging to the Alhama de Murcia fault zone (Fig. 5.4). This fault zone continues in the Huercal Overa basin and turns towards the west-southwest in the central part of the basin as suggested by earlier studies of Briend (1981) and Silva *et al.* (1992). This part of the fault zone, referred to as the Albox fault (Masana *et al.*, 2005) has been interpreted as a horsetail splay or contractional imbricate fan system at the south-western end of the Alhama de Murcia fault (e.g., Montenat *et al.*, 1987; De Larouziere *et al.*, 1988; Silva *et al.*, 1992). This horsetail splay or "Queue de cheval" has been an underlying argument to support interpretations of the Huercal Overa basin as a compressional basin (Montenat *et al.*, 1987, and references therein). However, studies of the Huercal Overa basin by, e.g., Briend (1981), Mora-Gluckstadt (1993), Vissers *et al.* (1995) and Augier (2004) have provided clear evidence of (syn-sedimentary) extensional structures in the Miocene basin sediments and have demonstrated the extensional nature of this basin.

As outlined above, the oldest sediments exposed along the northern margin of the Huercal Overa basin show onlap on the basement rocks of the Sierra de las Estancias. This unconformity provides some constraints on the development of deformational structures and their timing in the basement rocks of the Sierra de las Estancias, as compared with sedimentation and deformation in the Huercal Overa basin. We therefore first address the structure and microstructure of metamorphic rocks of the Sierra de las Estancias exposed in a limited number of outcrops immediately north of the Huercal Overa basin, mostly along the road from Huercal Overa to Velez Rubio. We then proceed to focus on the (brittle) structures at different stratigraphic levels in the sediments of the Huercal Overa basin proper.

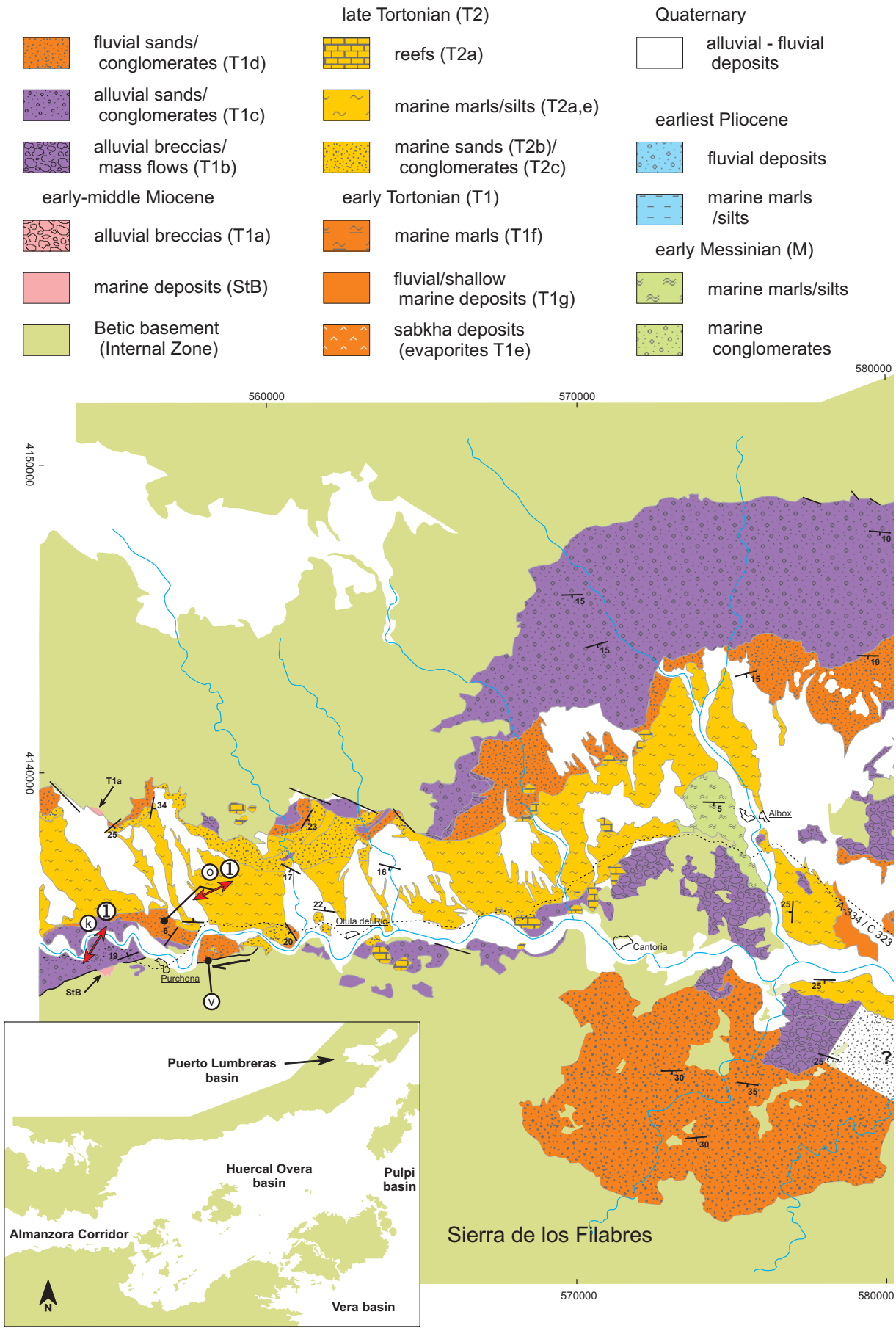
late Tortonian (T2)
Quaternary
fluvial sands/ conglomerates (T1d)
reefs (T2a)
alluvial - fluvial deposits
alluvial sands/ conglomerates (T1c)
marine marls/silts (T2a,e)
earliest Pliocene
alluvial breccias/ mass flows (T1b)
marine sands (T2b)/ conglomerates (T2c)
fluvial deposits
early-middle Miocene
early Tortonian (T1)
marine marls /silts
alluvial breccias (T1a)
marine marls (T1f)
early Messinian (M)
marine deposits (StB)
fluvial/shallow marine deposits (T1g)
marine marls/silts
Betic basement (Internal Zone)
sabkha deposits (evaporites T1e)
marine conglomerates
580000
560000
570000
4150000
4140000
T1a
StB
Purchena
Olula del Río
Albox
Cantoria
A-334 / C-323
Sierra de los Filabres
Puerto Lumbreras basin
Huercal Overa basin
Pulpi basin
Almanzora Corridor
Vera basin
N

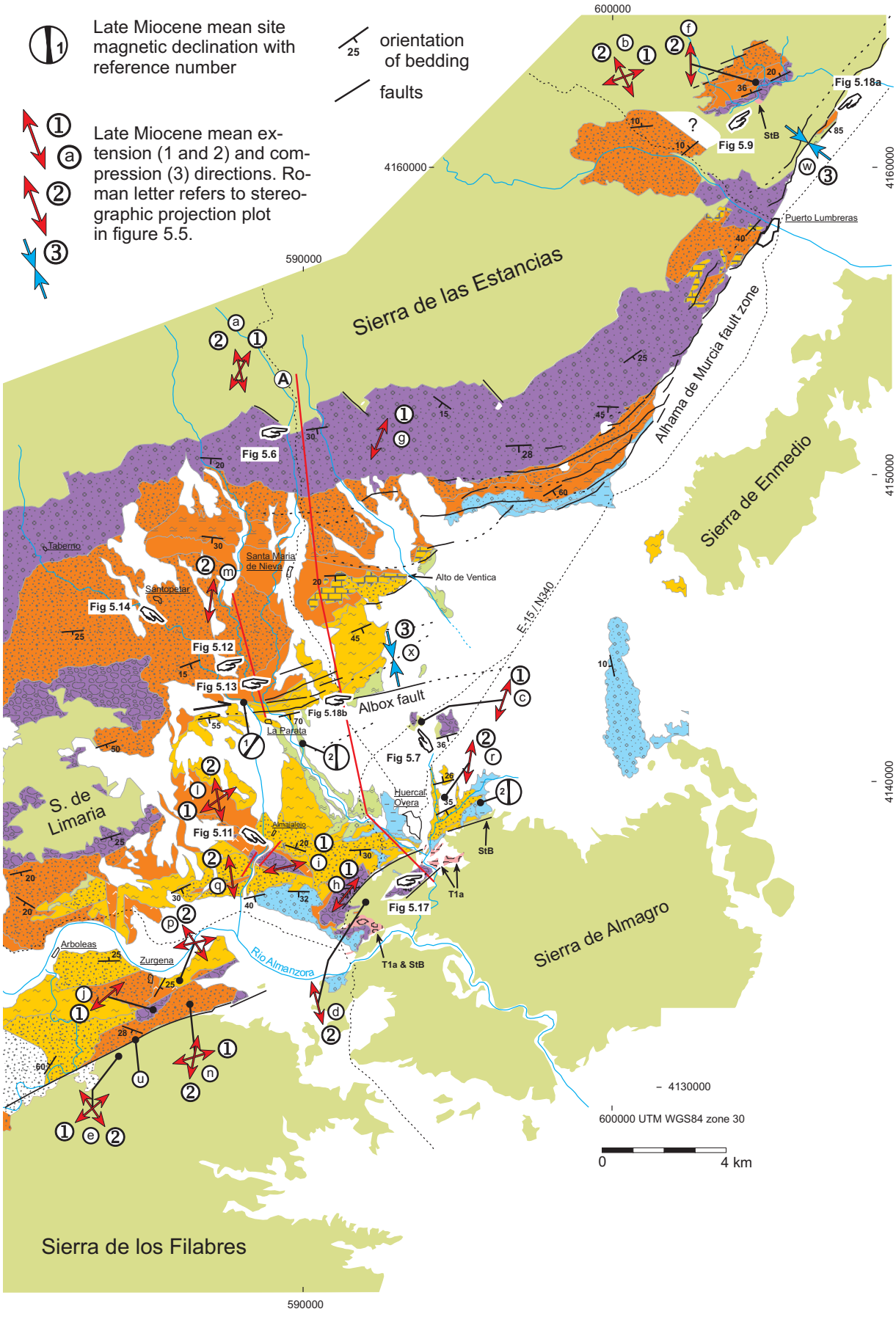
Late Miocene mean site magnetic declination with reference number
orientation of bedding
faults
Late Miocene mean extension (1 and 2) and compression (3) directions. Roman letter refers to stereographic projection plot in figure 5.5.
Sierra de las Estancias
Alhama de Murcia fault zone
Sierra de Enmedio
Sierra de Almagro
Sierra de los Filabres
S. de Limaria
Albox fault
E-15 / N340
Río Almanzora
Puerto Lumbreras
Alto de Ventica
Santa María de Nieva
Taberno
Santopetar
La Parata
Huercal Overa
Almajalejo
Arboleas
Zurgena
Fig 5.6
Fig 5.7
Fig 5.9
Fig 5.11
Fig 5.12
Fig 5.13
Fig 5.14
Fig 5.17
Fig 5.18a
Fig 5.18b
StB
T1a
T1a & StB
600000
590000
4160000
4150000
4140000
4130000
600000 UTM WGS84 zone 30
0
4 km

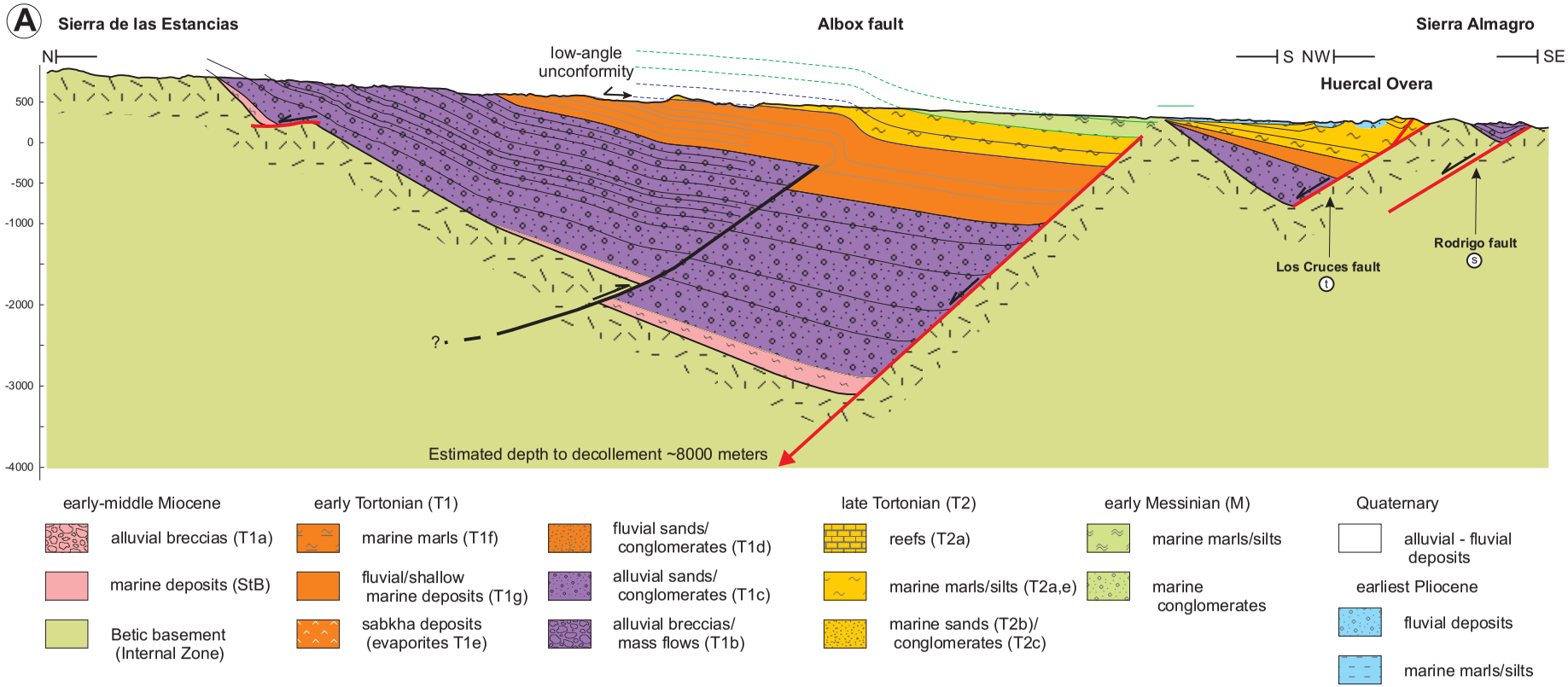

Figure 5.4. Geological map (previous page) and cross-section of the Almanzora, Huercal Overa and Puerto Lumbreras basins, after Voermans et al. (1972), Vissers (1975), Dubelaar (1980), Briend (1981), Mora-Gluckstadt (1993), Guerra-Merchán and Serrano (1993), Augier (2004), Soler et al. (2003), Masana et al. (2005) and this study. Paleomagnetic data from (1) Mora-Gluckstadt (1993) and (2) Meijninger et al. (in prep.).

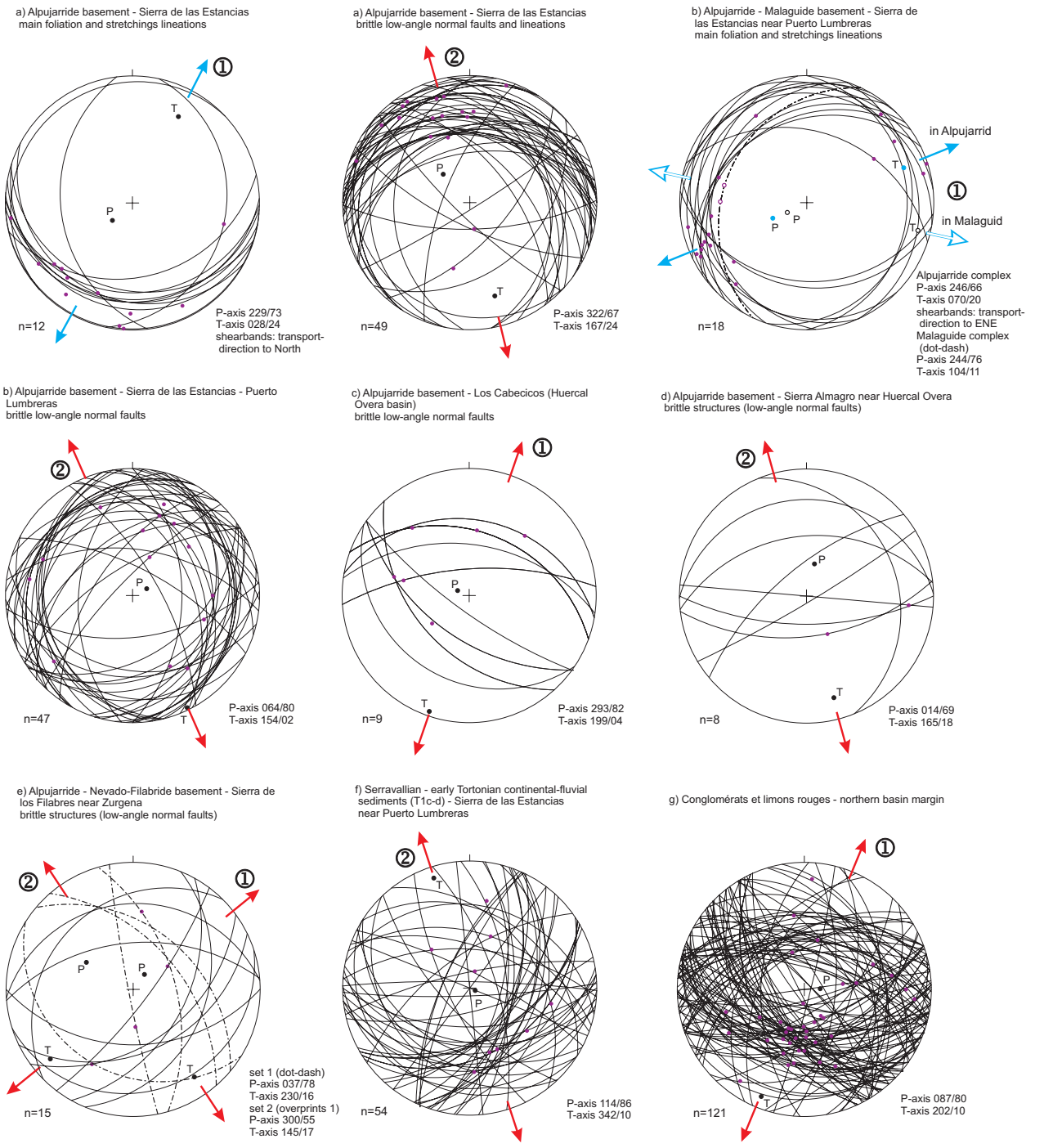

Figure 5.5. Stereographic projections (equal area, lower hemisphere) showing the orientations of the main foliation and stretching lineations in basement rocks and brittle faults and lineations in basement rocks and basin sediments. Locations of pertinent exposures are shown in figure 5.4. P- and T-axes represent mean axes of incremental shortening and extension.

h) Brèche rouge - near Huercal Overa

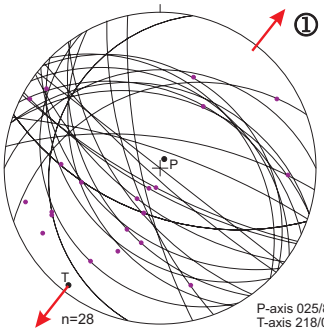

i) Brèche rouge near Almajalejo

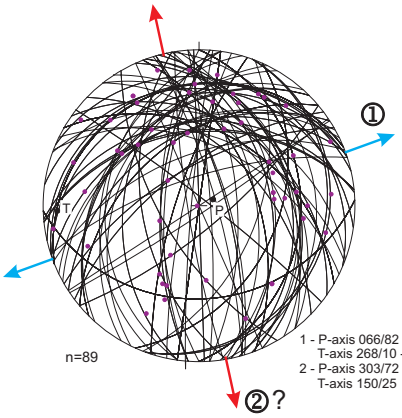

j) Brèche rouge near Zurgena

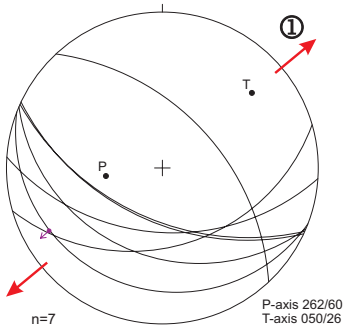

k) Brèche rouge near Purchena

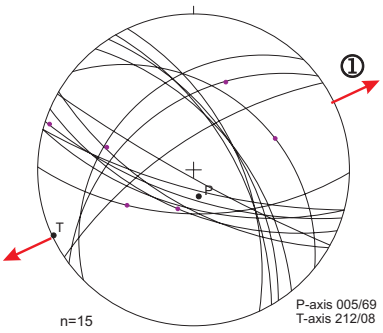

l) Turbidites micacées et gypseuses near Almajalejo

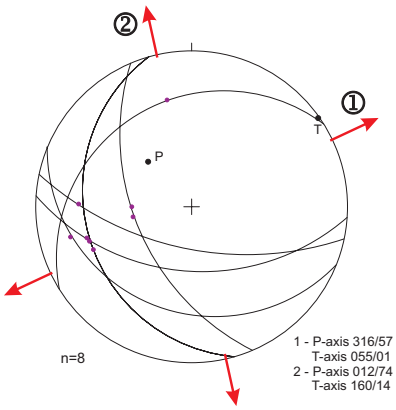

m) Turbidites micacées and Marnes à Huîtres unit in northern part of Huercal Overa basin

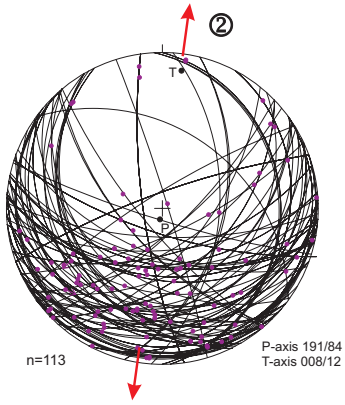

n) Turbidites micacées et gypseuses near Zurgena

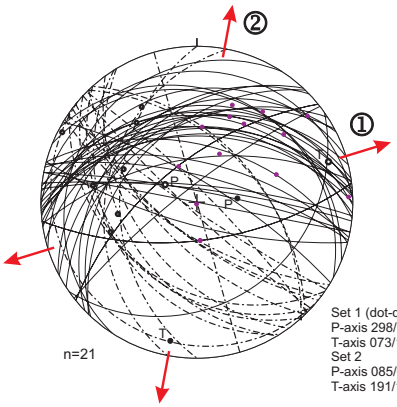

o) Turbidites micacées and Marnes à Huîtres unit near Purchena in Almanzora Corridor

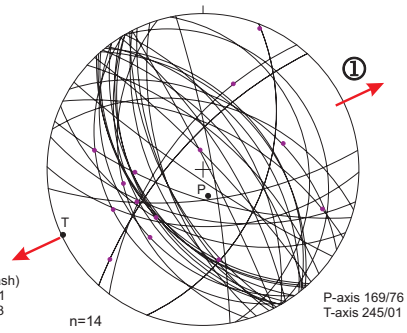

p) Conglomérats jaunes near Zurgena

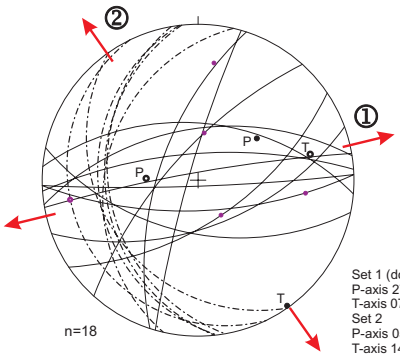

q) Conglomérats jaunes near Almajalejo

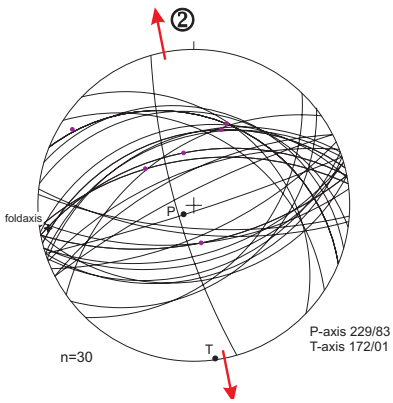

r) Conglomérats jaunes near Huercal Overa

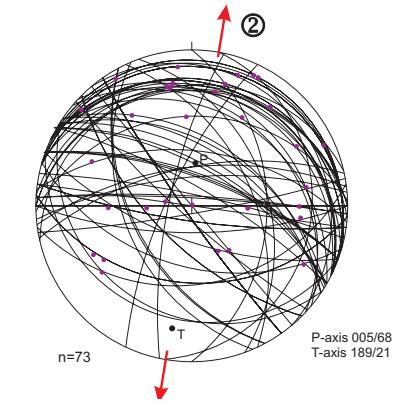

s) Rodrigo fault scarp at Huercal Overa, 1) dex-transtensioneel, 2) dip-slip, 3) compressie

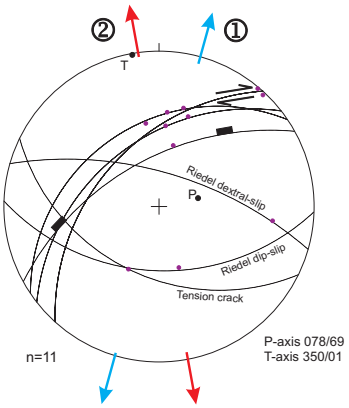

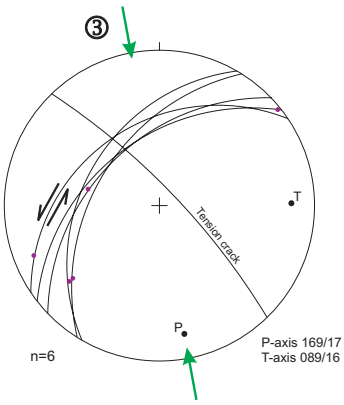

t) Los crucos fault at Huercal Overa, 1) dex-transtensioneel, 2) dip-slip

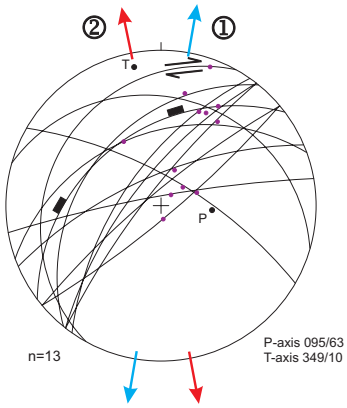

u) basin bounding fault near Zurgena

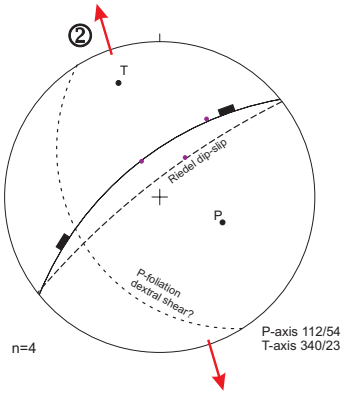

v) basin bounding fault at Purchena

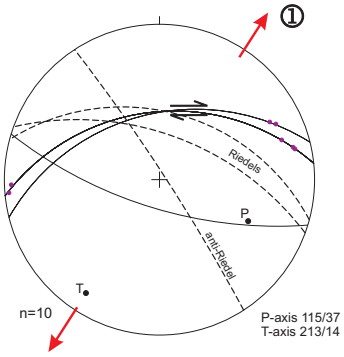

w) Thrusts and strike-slip faults in Miocene - Quaternary sediments and basement rocks part of the Alhama de Murcia fault along the Sierra de las Estancias near Puerto Lumbreras

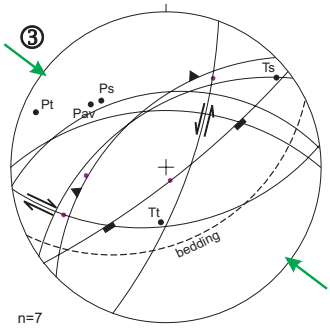

P-axis average 307/31
strike-slip faults
P-axis 316/40
T-axis 051/09
thrusts
P-axis 293/10
T-axis 185/61

x) Thrusts and strike-slip faults in Miocene - Quaternary sediments at the Albox fault near Huercal Overa

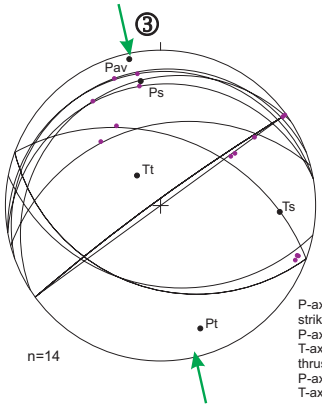

P-axis average 348/04
strike-slip faults
P-axis 351/20
T-axis 093/24
thrusts
P-axis 162/18
T-axis 322/70

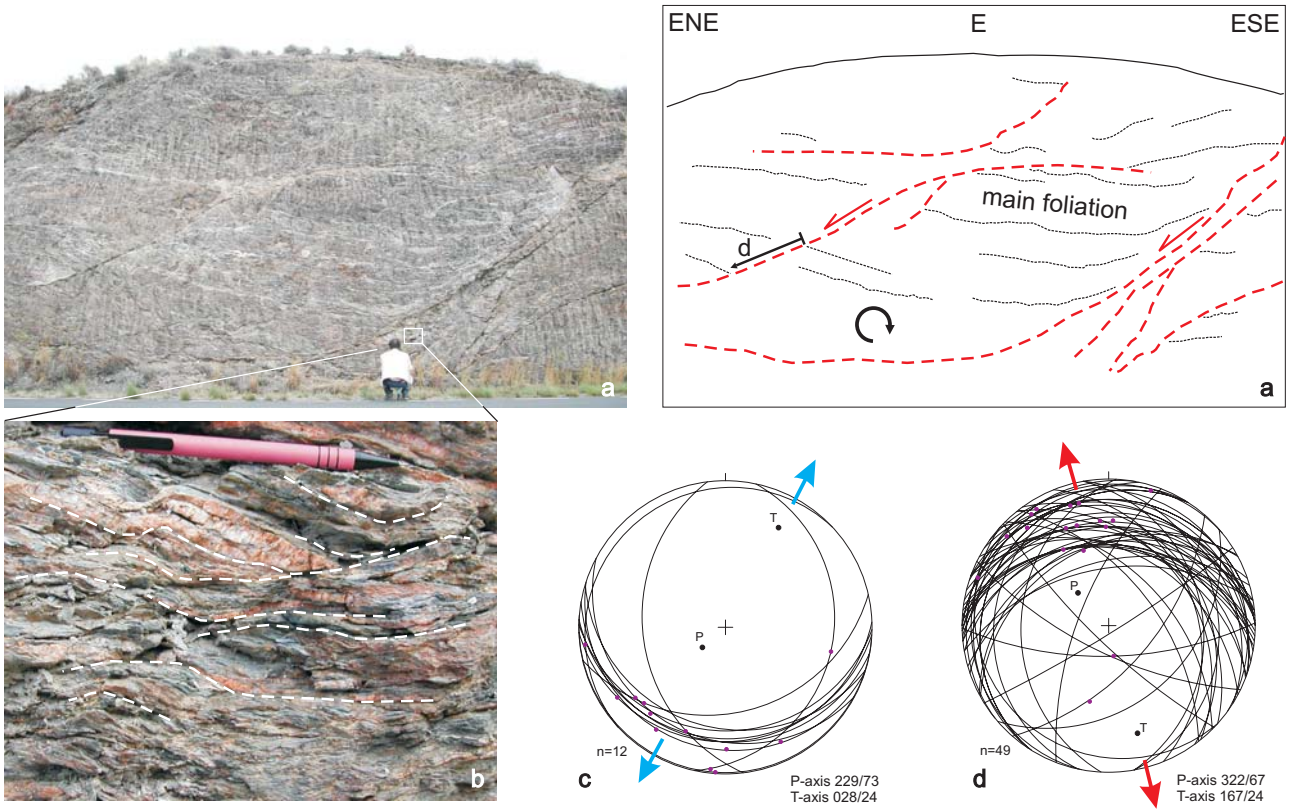

Figure 5.6. a) Outcrop of Alpujarride phyllites and quartzites in the Sierra de las Estancias near the northern margin of the Huercal Overa basin (for location see figure 5.4). Outcrop shows brittle extensional structures (low-angle normal faults) which overprint earlier ductile structures, shown in (b). b) Ductile shear bands in Alpujarride phyllite. c) Stereographic projection (equal area, lower hemisphere) showing orientations of main foliation and stretching lineations indicating NE-SW to NNE-SSW oriented ductile extension. d) Stereographic projection (equal area, lower hemisphere) showing orientations of brittle faults pointing to NNW-SSE directed extension.

Structures and metamorphism in basement rocks of the Sierra de las Estancias

The Alpujarride rocks of the Sierra de las Estancias north of the Huercal Overa basin are made up of light to dark grey and black fine-grained micaschists, phyllites and quartzites. The main foliation of the Alpujarride rocks in this part of the Sierra de las Estancias lies sub-horizontal or dips gently towards the south. In outcrop, the rocks show clear evidence of ductile and brittle extension. The main foliation is overprinted first by ductile NE-directed extensional shear bands suggesting N-S to NNE-SSW directed extension (Figs. 5.5a and 5.6). Towards the central and northern parts of the Sierra de las Estancias the ductile shear bands tend to gradually change orientation with associated extension directions turning to ENE-WSW (e.g., near Puerto Lumbreras, Figs. 5.4 and 5.5b). This result is consistent with observations by Platzman and Platt (2004) and Lonergan and Platt (1995). Like the ductile extensional structures in the Alpujarride rocks underneath, brittle extensional structures in outcrops of non-metamorphic rocks of the Malaguide Complex near Puerto Lumbreras point to an E-W to ESE-WNW direction of extension (Fig. 5.5b).

In some of the outcrops of the Alpujarride basement it is clear that structures have progressively developed from ductile shear bands into brittle low-angle normal faults. These low-angle normal faults, which clearly overprint all earlier structures (Fig. 5.6), generally show northerly dips indicating N-S to NW-SE directed extension (Fig. 5.5a and b). In this context it is noted that along the strongly faulted southern margin of the Huercal basin brittle extensional structures in the Alpujarride and Nevado-Filabride rocks of the Sierra de Almagro and Sierra de los Filabres generally indicate NNE-SSW to NNW-SSE directions of extension (Figs. 5.4, 5.5c-e and 5.6), i.e., the inferred extension directions seen along the southern margin are somewhat more variable but grossly consistent with the extension directions of the brittle structures in the north.

In thin section, the main foliation is commonly a

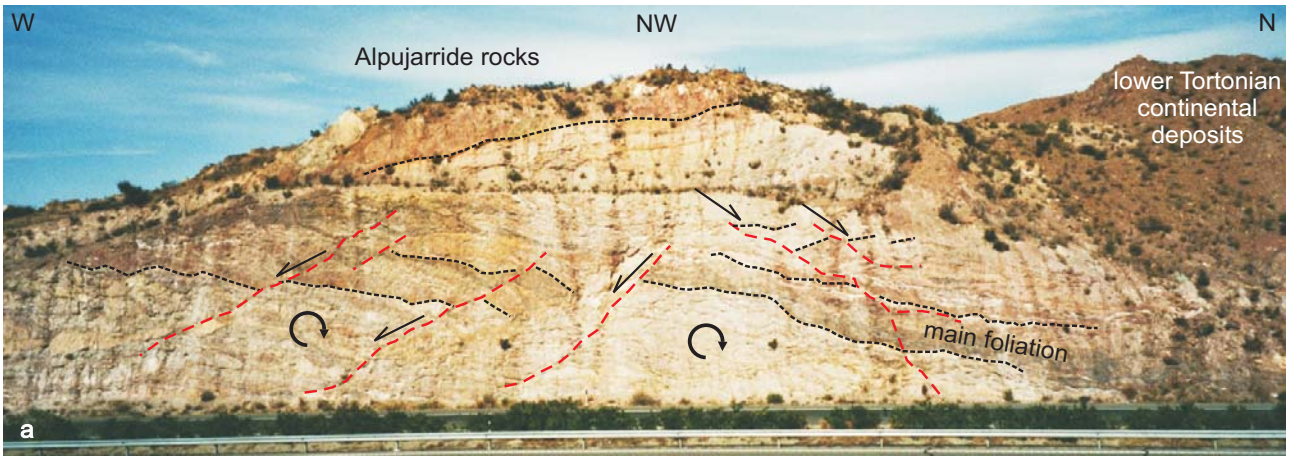

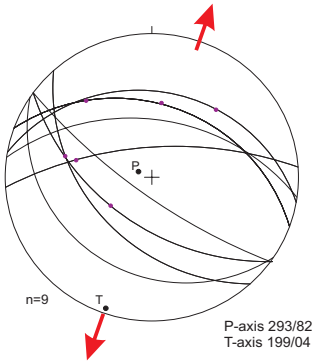

Figure 5.7. a) Outcrop of Alpujarride basement rocks along motorway E-15, north-east of Huercal Overa at Los Cabecicos (for location see figure 5.4) showing south-west and north-east dipping brittle extensional faults. b) Stereographic projection (equal area, lower hemisphere) showing pertinent orientations of brittle faults and associated lineations indicating NNE-SSW directed extension.

differentiated crenulation cleavage with alternating bands of muscovite plus rare biotite and quartz-rich microlithons. Occasionally, relics of (a)symmetrical microfolds are preserved. In places, this differentiated crenulation foliation passes into a pervasive schistosity (Fig. 5.8a). The main foliation is overprinted by ductile shear bands or extensional crenulations (Fig. 5.8a), and by sub-vertical brittle cracks filled with granular quartz. Furthermore, ubiquitous quartz veins have been stretched and boudinaged.

Outcrops approximately 1.5 km north of the basin margin, and structurally about 750 m below the onlapping middle Miocene sediments, in places contain chloritoid, staurolite, garnet and andalusite (Fig. 5.8b-f) indicating amphibolite facies metamorphism. Microstructural relationships between the deformational structures and porphyroblast growth (Zwart, 1962; Passchier and Trouw, 1998) suggest that garnet and part of the chloritoid formed pre- to synkinematic with the main foliation. Small, mostly euhedral grains of chloritoid and staurolite have grown over the early (S_1) schistosity in the limbs of mainphase F_2 microfolds, but in the samples studied their timing with respect to development of the mainphase crenulation foliation is somewhat unclear. Staurolite, however, is frequently enclosed in (and therefore predates) porphyroblasts of andalusite (Fig. 5.8c-f). These andalusites clearly overgrow the mainphase structure and in places show slightly rotational inclusion patterns (Fig. 5.8c) suggesting that they grew synkinematic with shearing on this foliation presumably related to the incipient development of ductile shear bands. Chloritoid may occur as small grains overgrowing the main foliation (Fig. 5.8g), whilst chlorite may have developed in pressure shadows adjacent to the andalusite crystals, as well as along shear bands.

The metamorphic assemblage is consistent with metamorphic conditions evolving from upper-greenschist to amphibolite facies (300-400 MPa and 550-600°C), producing early chloritoid, garnet and staurolite prior to and during development of the mainphase foliation, via lower pressure amphibolite facies conditions leading to andalusite growth, to greenschist facies retrogression associated with ductile extension

Studies in Alpujarride rocks of the western Betics as well as in the Sierra de las Estancias and Sierra Cabrera in the eastern part of the Betic Zone and in the Alboran Sea (e.g., Vissers *et al.*, 1995; Azañón and Goffé, 1997; Comas *et al.*, 1999; Platt *et al.*, 2005,) have shown that part of the Alpujarride rocks were initially deformed and metamorphosed at relatively high-pressure conditions associated with a main

contractional event in the Alpujarride Complex (*c*. 48 Ma; Platt *et al.*, 2005) leading to the mainphase foliation. This was followed by a marked LP-HT overprint leading to andalusite ± cordierite - sillimanite facies series. The age of this LP-HT metamorphism has been estimated at 22-20 Ma, i.e., an early Miocene, Aquitanian age (e.g., de Jong, 1991 and references therein; Comas *et al.*, 1999), whilst zircon dating in associated granitoids yields ages around 19 Ma (Platt and Whitehouse, 1999).

The structures and microstructures described above are fully consistent with those by Platzman and Platt (2004) and earlier work in the Sierra de las Estancias by de Vries and Zwaan (1967) who aside andalusite also reported late-stage cordierite, and with the structural and metamorphic studies of Alpujarride rocks elsewhere in the Betics. On the basis of these studies we infer that the early chloritoid, garnet and staurolite associated with the main phase foliation in the southern Sierra de las Estancias represent the early contractional event, and that the andalusite and locally cordierite producing metamorphism in these rocks is of the same early Miocene age as elsewhere in the Betic Zone.

The above results imply that, prior to the deposition of the onlapping Tortonian conglomerates, more than 10 km of Malaguide and Alpujarride rocks forming the overburden of the staurolite-andalusite bearing micaschists and phyllites must have been removed in approximately 7 Myrs (from *c*. 19 to 12 Ma), whilst the andalusite-bearing rocks cooled during that time span from around 550-600°C rocks to near-surface temperatures at a time-averaged rate of at least 80°C/Ma. This result reinforces the conclusion of previous workers, e.g., Lonergan and Johnson (1998), that early and middle Miocene cooling rates in the Betic crust were high. The exhumation must in part have occurred via erosion, but it also had a component of ductile to brittle thinning (Lonergan and Platt, 1995; Lonergan and Johnson, 1998). On the basis of the structures it is not possible to precisely quantify the amount of extensional strain, hence to determine how much exhumation was caused by tectonic thinning of the overburden, but the brittle extensional structures in a number of outcrops of the Alpujarride basement in the southern Sierra de las Estancias point to approximately 22% and occasionally up to 74% of extension (β = 1.22 to 1.74) which pose lower bound values to the magnitude of tectonic thinning.

Structures in the basin sediments

The basal continental conglomerates and breccias of the Poudingue lie-de-vin (T1a), Brèche rouge (T1b) and Conglomérats et limons rouges (T1c) units show ubiquitous normal faulting. These extensional structures are in general east-west trending planar faults, however, fault trends vary from NE to SE. In places, spectacular extensional structures such as domino - type faults, have developed (Fig. 5.9 and 5.10). In the northern part of the Huercal Overa basin, hanging-wall transport is in general towards the south, while in the southern half of the basin transport is in general towards the north. These extensional structures indicate a NNE-SSW to N-S direction of extension (Figs. 5.4 and 5.5f and g). However, outcrops of the basal deposits in the Puerto Lumbreras basin display few NNE trending extensional structures with minor displacement suggesting approximately E-W directed extension. The amount of extension along these extensional structures varies across the basin: in the northern half of the Huercal Overa basin the faults show minor displacements (dm to m scale; stretch factor β = 1.14 – 1.21). However, in the Puerto Lumbreras basin extension in the basal conglomerates may reach values of 54% (β = 1.54), and occasionally up to 101% (β = 2.01).

In the southern part of the Huercal Overa basin, the Brèche rouge unit is exposed in the up to 50 m high cliffs of the Rambla de Almajalejo, forming a 1.2 km long outcrop with spectacular normal fault structures (Fig. 5.11). In essence there are at least two sets of faults, i.e., shallow dipping to even horizontal faults (Fig. 5.11b) cut and displaced by younger steeply dip-

Figure 5.8. a) Photomicrograph showing pervasive schistosity that makes up main foliation, overprinted by ductile shear bands. b) cm-scale crystals of andalusite in fine-grained micaschist. c) Photomicrograph (crossed nickols) and sketch of fine-grained micaschist, showing pervasive schistosity defined by oriented mica and quartz, affected by isoclinal microfolds. Note that axial trace of the microfolds runs parallel to the main foliation indicating that the main foliation is in fact a crenulation cleavage. The main foliation is overgrown by porphyroblasts of andalusite and overprinted by shearbands. Slightly rotational inclusion pattern in the andalusite suggests growth during slip along the foliation. d and e) Photomicrograph (plane polarized light and crossed nickols) of same thin section as in (b), showing andalusite porphyroblast grown over the main foliation, with the foliation and porphyroblast deformed by a shearband. f) Detail of (d) showing staurolite enclosed in andalusite porphyroblast. Note chlorite developed along shear band and in pressure shadow. g) Detail of (d) showing small chloritoid grains grown over the main foliation.

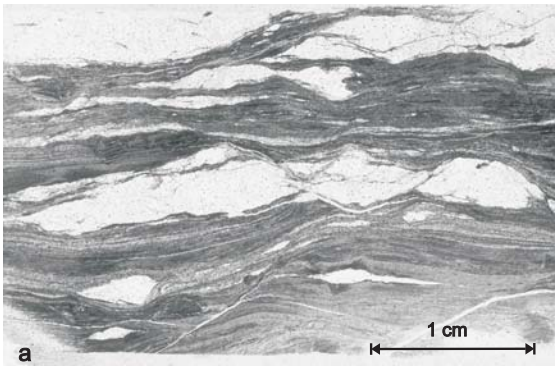
1 cm
a

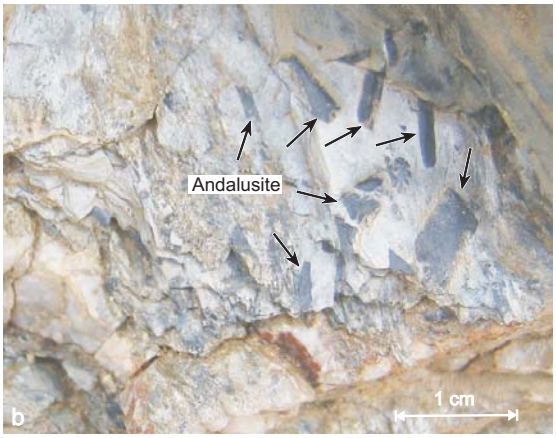
Andalusite
1 cm
b

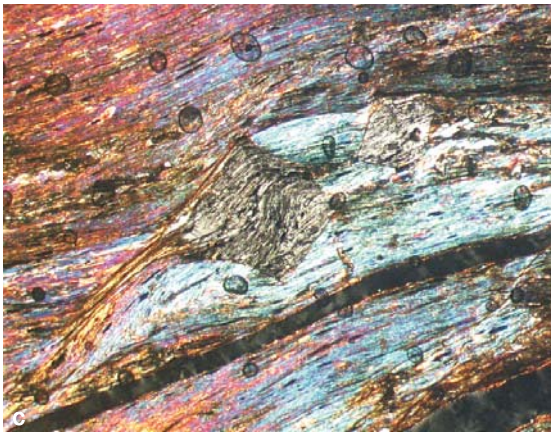
c

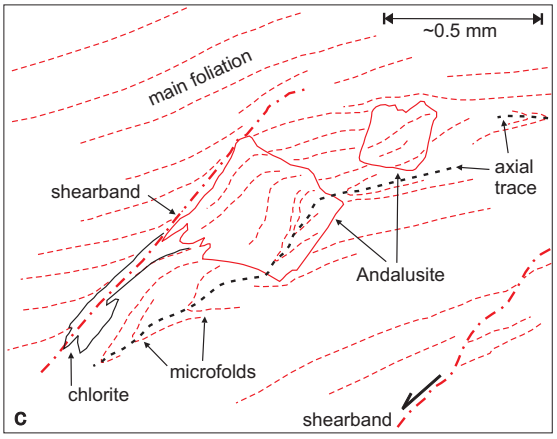
~0.5 mm
main foliation
shearband
axial trace
Andalusite
microfolds
chlorite
shearband
c

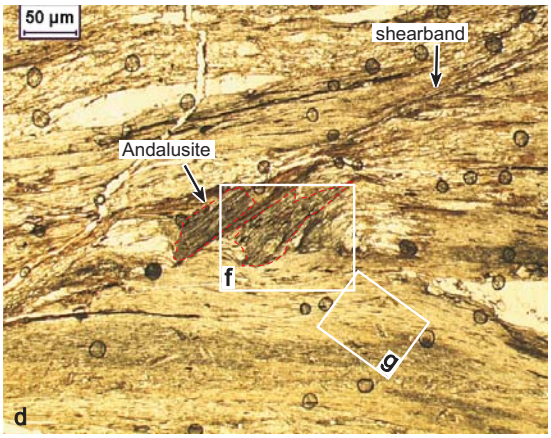
50 µm
shearband
Andalusite
f
g
d

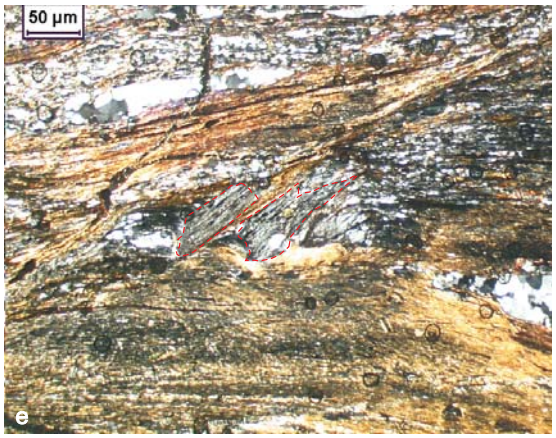
50 µm
e

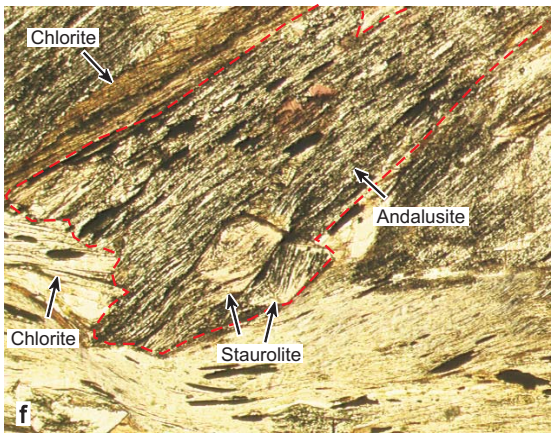
Chlorite
Andalusite
Chlorite
Staurolite
f

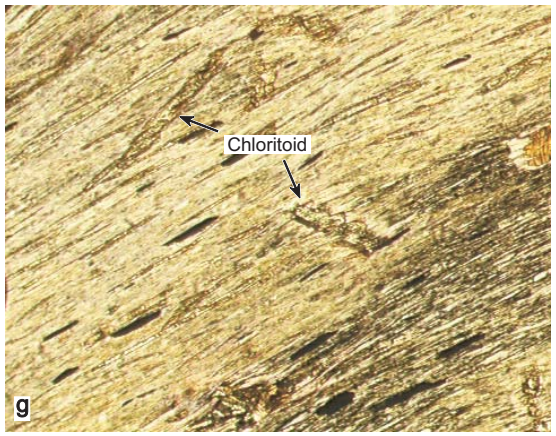
Chloritoid
g

Figure 5.9. Exposure of basal continental conglomerates of the Puerto Lumbreras basin, penetratively cut, displaced and rotated by domino-type extensional normal faults. Kinematic analysis of these faults point to N-S to NNW-SSE directed extension. Stretching estimates in this outcrop range from 54% up to 101%.

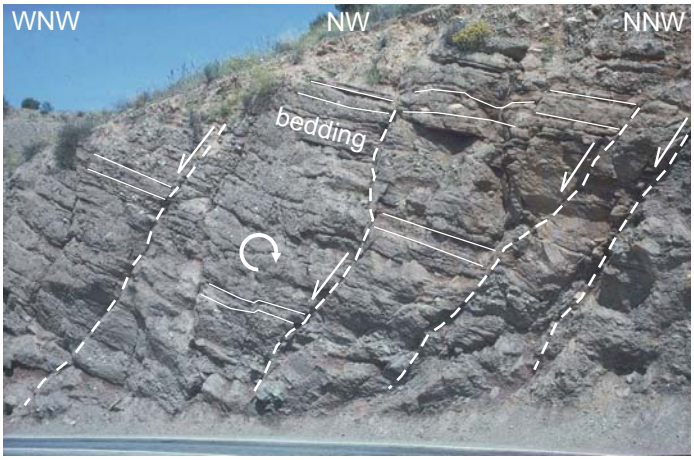

Figure 5.10. Exposure of lower Tortonian Brèche rouge unit affected by domino-type faults, southern part of the Huercal Overa basin. Kinematic analysis suggests NNE-SSW to NE-SW oriented extension. The exposure has unfortunately been destroyed for recent road construction purposes.

ping ones, suggesting that progressive normal faulting led to rotation of initially steep faults to flat-lying orientations. The bedding, often difficult to identify in the coarse breccia, concurrently rotates from relatively flat orientations in the northern part of the outcrop to steep orientations in the southern part. The resulting structure is a strongly faulted, moderately inclined anticline. Kinematic analysis on the steeply as well as the shallowly dipping faults clearly point to an ENE-WSW to NE-SW direction of extension (Fig. 5.11c). This large-scale structure in the Brèche rouge unit near Almajalejo has previously been considered by other workers as an anticline associated with compression or transpression (e.g., Poisson *et al.*, 1999). In view of the overwhelming evidence for normal faulting, this interpretation seems untenable. Instead, the Almajalejo structure is more appropriately interpreted as an extensional roll-over anticline above a NE to ENE dipping listric normal fault that must have accommodated a significant amount of displacement. The Almajalejo structure is further complicated by a set of relatively young, NW trending normal faults bounding the structure on the northern and southern margins of the Brèche rouge. As a result, the anticlinal structure of the Brèche rouge rocks is now exposed in what is essentially a horst, and the amount of extension that must have occurred before the development of the horst-bounding faults is difficult to quantify because of the lack of structural information on the precise position and orientation of the main fault plane underlying the inferred roll-over.

Similar to the inferred stretching directions in the Almajalejo section, normal fault structures in the breccias of the Brèche rouge unit near Huercal Overa and Zurgena in the southern part of the Huercal Overa basin and near Purchena in the Almanzora Corridor point to an ENE-WSW to NE-SW direction of extension (Figs. 5.5h to k).

The fluvial to shallow marine sediments of lower Tortonian age (i.e., the Turbidites micacées (T1d), Turbidites micacées et gypseuses (T1e), Pélites jaunes

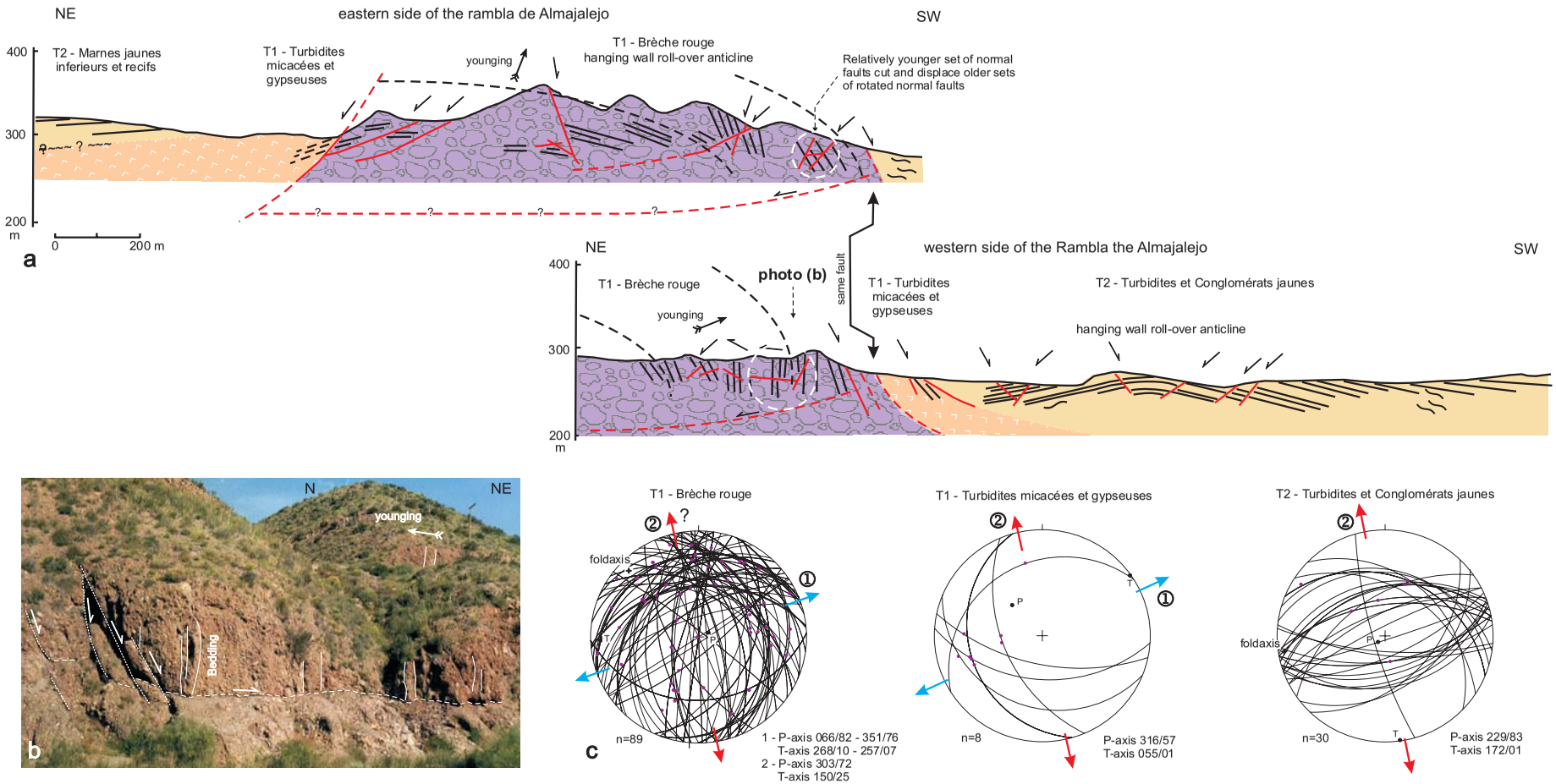

Figure 5.11. Structures and orientation data from the late Miocene rocks near Almajalejo (for location see figure 5.4). a) Cross section showing lower Tortonian Brèche rouge deposits flanked by the upper Tortonian Turbidites micacées et gypseuses and Turbidites et Conglomérats jaunes units. In the Brèche rouge unit, shallowly dipping normal faults are cut and displaced by younger steep ones, as also seen in (b). Towards the southwest, bedding in the Brèche rouge unit tilts progressively towards the south, suggesting that the structure represents a roll-over anticline. The Turbidites micacées et gypseuses unit south of the Brèche rouge outcrop is pervasively faulted at smaller scale, which probably accommodates extension in the overlying Turbidites et Conglomérats jaunes unit and the development of another roll-over anticline. b) Detail of the Brèche rouge unit, showing horizontal fault, deformed to the left by younger steep faults. c) Stereographic projections (equal area, lower hemisphere) showing orientations of faults and slip directions for the Brèche rouge, Turbidites micacées et gypseuses and Turbidites et Conglomérats jaunes units, with inferred extension directions (grey arrows: early stretching, black arrows: younger stretching). Note that lower profile along western side of the Rambla de Almajalejo represents a mirror image of the actual outcrop. For further explanation see text.

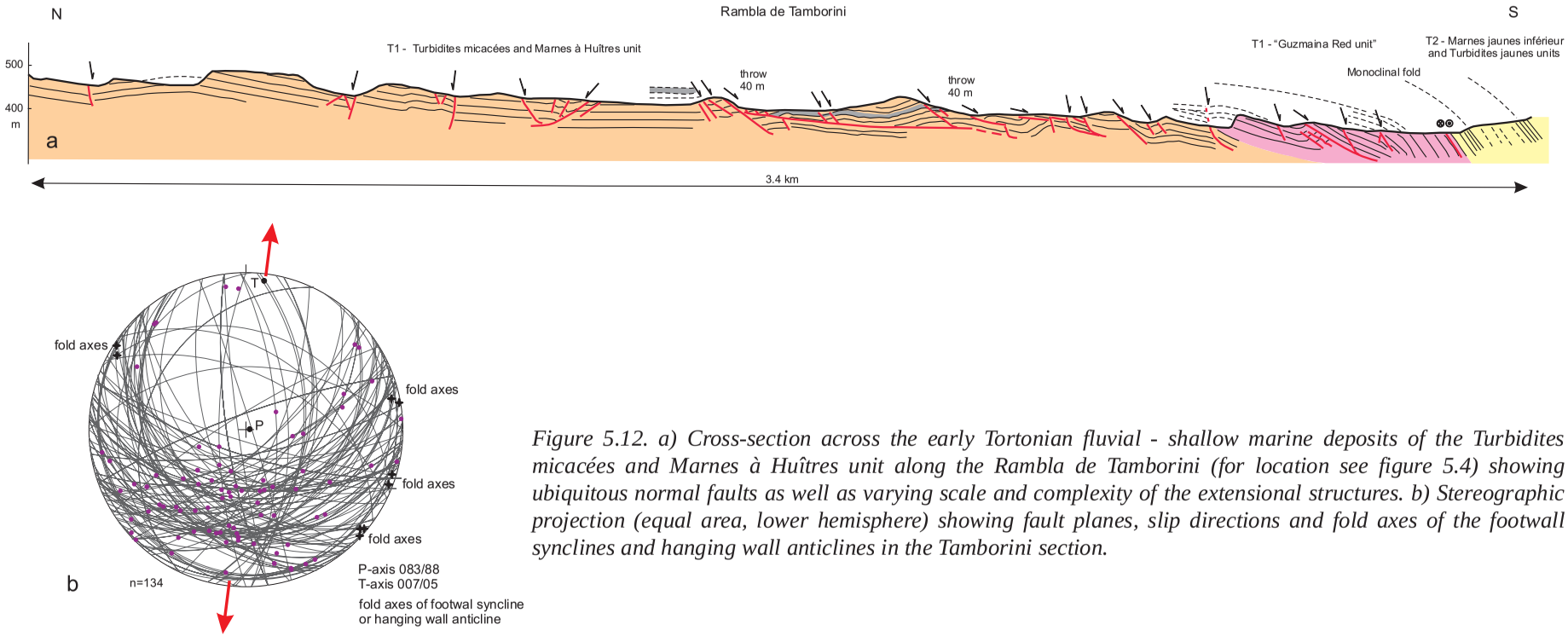

Figure 5.12. a) Cross-section across the early Tortonian fluvial - shallow marine deposits of the Turbidites micacées and Marnes à Huîtres unit along the Rambla de Tamborini (for location see figure 5.4) showing ubiquitous normal faults as well as varying scale and complexity of the extensional structures. b) Stereographic projection (equal area, lower hemisphere) showing fault planes, slip directions and fold axes of the footwall synclines and hanging wall anticlines in the Tamborini section.

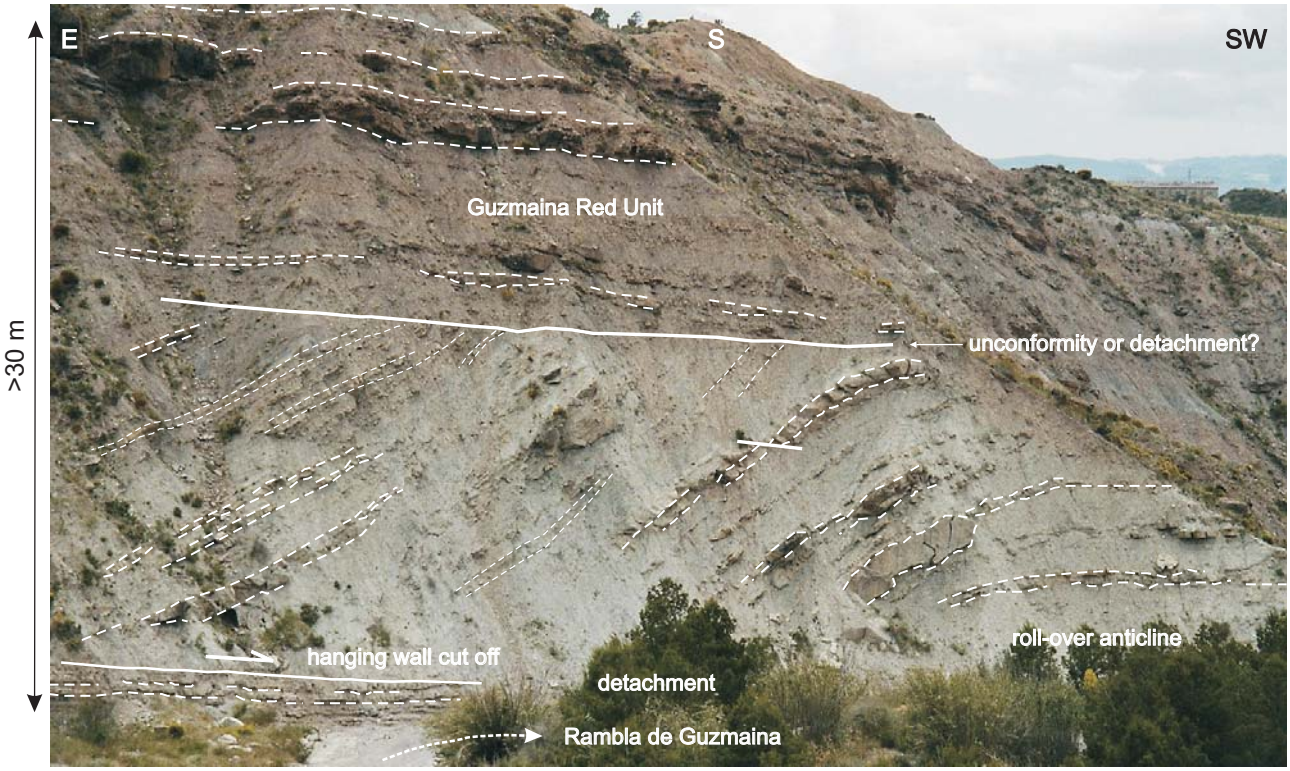

Figure 5.13. Roll-over anticline in the Rambla de Guzmaina (for location see figure 5.4). Beds in the roll-over structure are cut at the base of the cliff by a sub-horizontal detachment. In the middle part of the cliff, the structure is cut by another detachment or possibly an unconformity.

(T1f), and Marnes à Huîtres (T1g) units) exposed in the northern part of the Huercal Overa basin, in the south-western part near Zurgena, in the Puerto Lumbreras basin and in the Almanzora corridor near Purchena (Fig. 5.4) have been pervasively cut and displaced by extensional normal faults. The geometry and complexity of these extensional structures varies from small and large-scale planar normal faults, to complex fault structures comprising ramp-and-flat fault plane geometries accommodated by layer-parallel slip and roll-over anticlines, such as shown in figures 5.12, 5.13 and 5.14.

In a section along the Rambla Tamborini (Figs. 5.4 and 5.12), two groups of normal faults are observed: few steep to vertical N-S trending normal faults, with down-dip to oblique senses of shear and minor (dm to m scale) displacements, and a dominant group of ENE and WNW trending normal faults which in general show large displacements (up to 40 m of throw) and hanging wall movements towards the SE to SW. This dominant group of extensional faults at average suggest N-S to NNE-SSW directed extension. The magnitude of the extension in these fluvial – shallow marine deposits varies from place to place between low values of ~17% ($\beta = 1.17$) up to 90% ($\beta = 1.7$ to 1.9) in the southern part of the section (Fig. 5.12). A complicated extensional structure is seen in an outcrop to the west near the village of Santopetar (Fig. 5.14). Restoration (Fig. 5.14b-c) of this structure, previously studied by Briend (1981), Mora-Gluckstadt (1993) and Augier (2004), reveals several hiatuses in the footwall that provide evidence for syn-sedimentary deformation. The calculated magnitude of extension for this structure is slightly over 70% ($\beta = 1.7$), whilst estimates of the extension on the basis of thickness reduction assuming plane strain yields values up to 90% ($\beta = 1.9$).

Outcrops of the lower Tortonian fluvial to shallow marine sediments near Almajalejo and Zurgena in the southern part of the basin, and near Purchena in the Almanzora Corridor, show in general two set of extensional faults, i.e., a NW trending set pointing to ENE-WSW directed extension, and another group of E-W trending faults indicating NNE-SSW directed extension (Figs. 5.5 l-o). Occasionally, there are clear cross-cutting relationships between the two groups of faults: faults of the second, E-W trending group cut and displace faults that belong to the first, NW trending set.

The upper Tortonian marine deposits (T2) are well exposed in the central and southern part of the

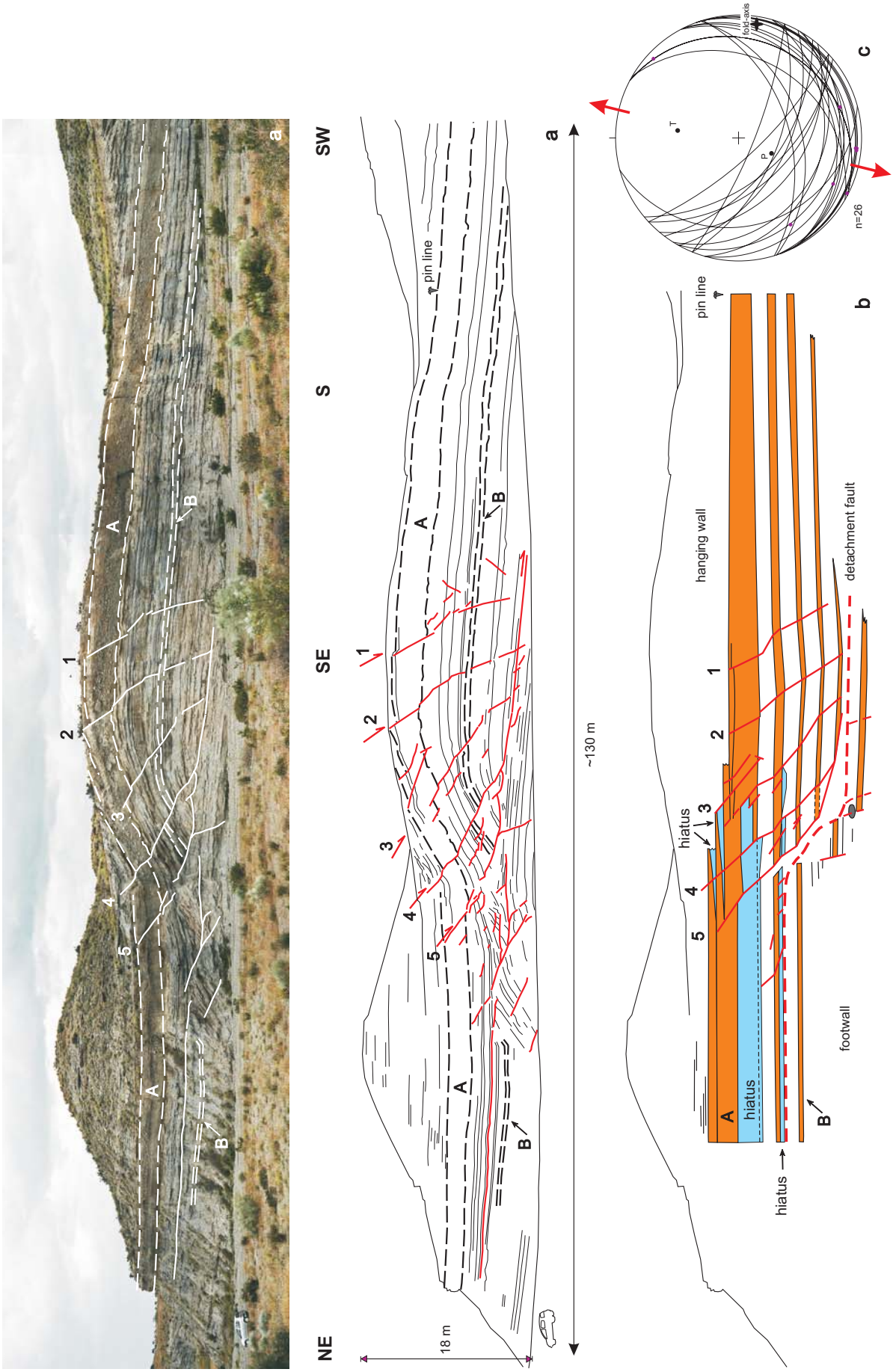
a
SW
S
SE
NE
pin line
A
B
1
2
3
4
5
18 m
~130 m
b
hanging wall
detachment fault
footwall
hiatus
c
fold axis
n=26

Figure 5.14. a) Roll-over anticline in the early Tortonian Turbidites micacées and Marnes à Huîtres unit near the village of Santopetar (for location see figure 5.4). Kinematic indicators on the normal faults point to hanging-wall movement towards the S to SSW. b) Restored section of the roll-over structure showing flat-ramp-flat fault plane geometry of main detachment fault. Hiatuses in footwall and hanging wall suggest syn-sedimentary faulting. Hiatuses in the hanging wall may mark the onset of footwall collapse. c) Stereographic projection (equal area, lower hemisphere) showing orientations of extensional faults in the outcrop. For further details see text.

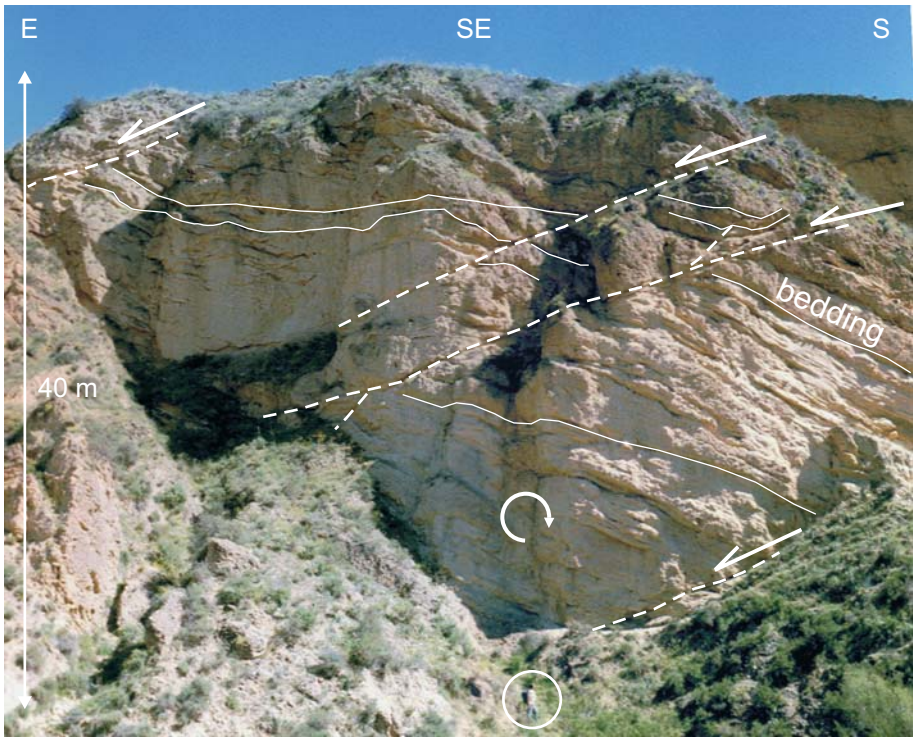

Figure 5.15. Marine deposits of the upper Tortonian Conglomérats jaunes unit in the southern part of the Huercal Overa basin, showing domino-type normal faults. Note geologist for scale. Estimates of the stretching in this outcrop yields values up to 78%.

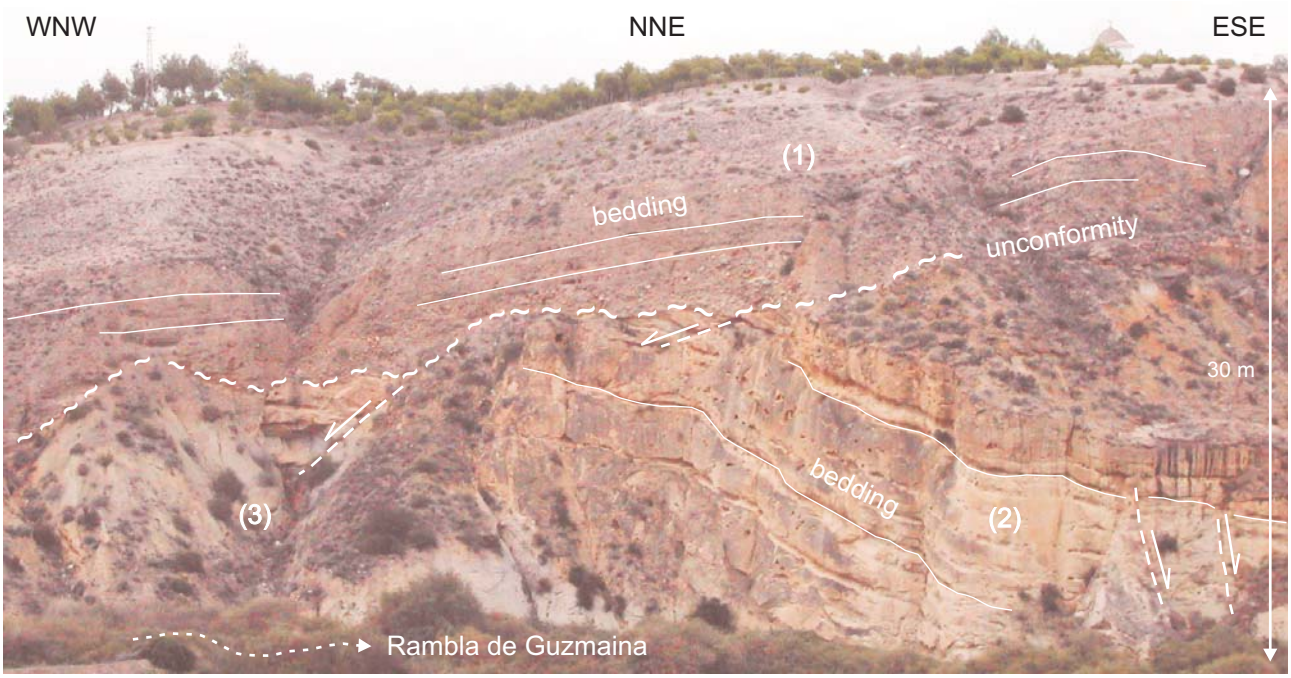

Figure 5.16. Exposure southwest of Huercal Overa showing brown conglomerates (1) of Messinian and/or possibly Pliocene age, which lie unconformably on faulted and tilted marine deposits of the late Tortonian Conglomérats jaunes (2) and Marnes jaunes inférieur (3) units, thus sealing Tortonian extensional normal faults.

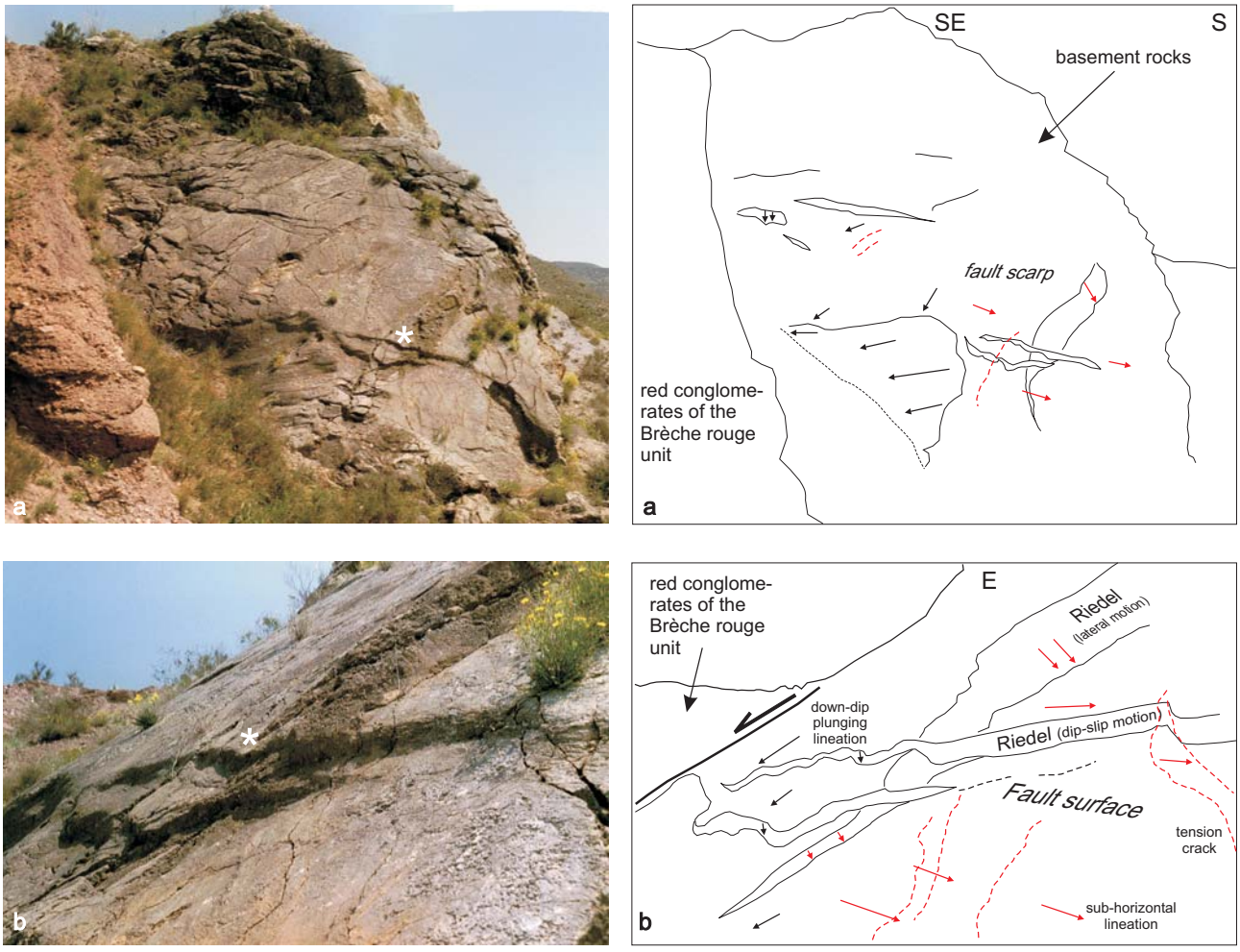

Figure 5.17. a and b) Fault scarp of the basin-bounding Rodrigo fault south of Huercal Overa (for location see figure 5.4) viewed normal (a) and oblique (b) to fault strike. The fault separates lower Tortonian continental basin deposits of the Brèche rouge unit from Alpujarride limestone of the Sierra Almagro. The fault surface contains two groups of structures: one comprising Riedel fractures, tension cracks and down-plunging to oblique lineations related with dip-slip and dextral-oblique slip motions, overprinted by a second group of Riedel fractures, tension cracks and subhorizontal lineations indicating sinistral strike-slip.

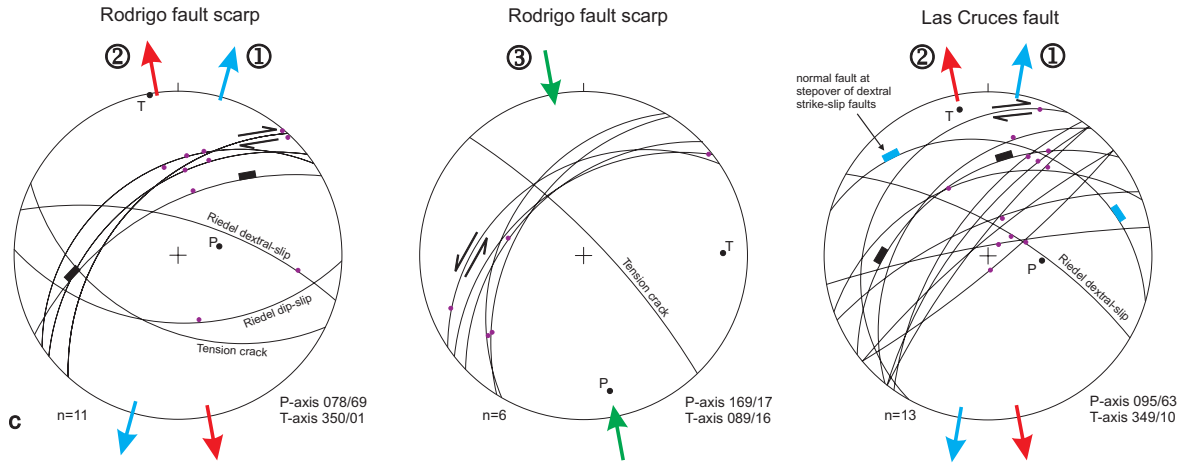

c) Stereographic projections (equal area, lower hemisphere) showing orientations of fault planes and lineations of the Rodrigo fault and of the Las Cruces fault zone south-west of Huercal Overa. Both faults contain structures pointing to dip to oblique slip and occasionally dextral oblique to strike-slip indicating NNE-SSW to NNW-SSE directed extension. The second set of Riedel fractures and tension cracks on the Rodrigo fault surface points to sinistral strike-slip motions indicating NNW-SSE directed compression. Evidence for these later motions is not seen on the Las Cruces fault.

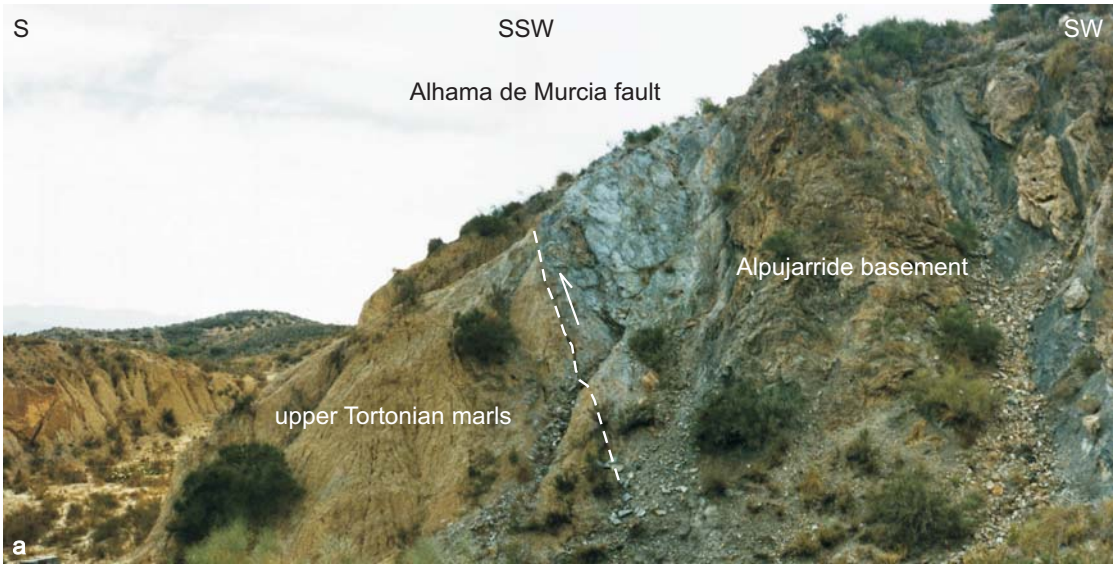
S
SSW
SW
Alhama de Murcia fault
Alpujarride basement
upper Tortonian marls
a


b

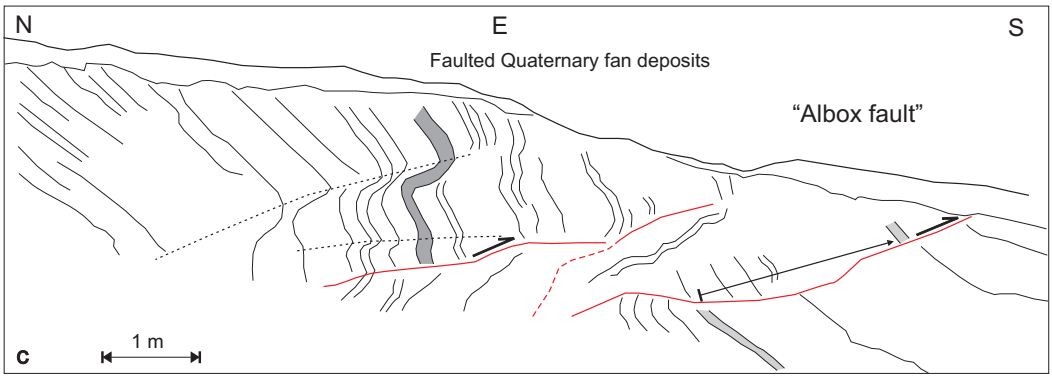
N
E
S
Faulted Quaternary fan deposits
"Albox fault"
1 m
c

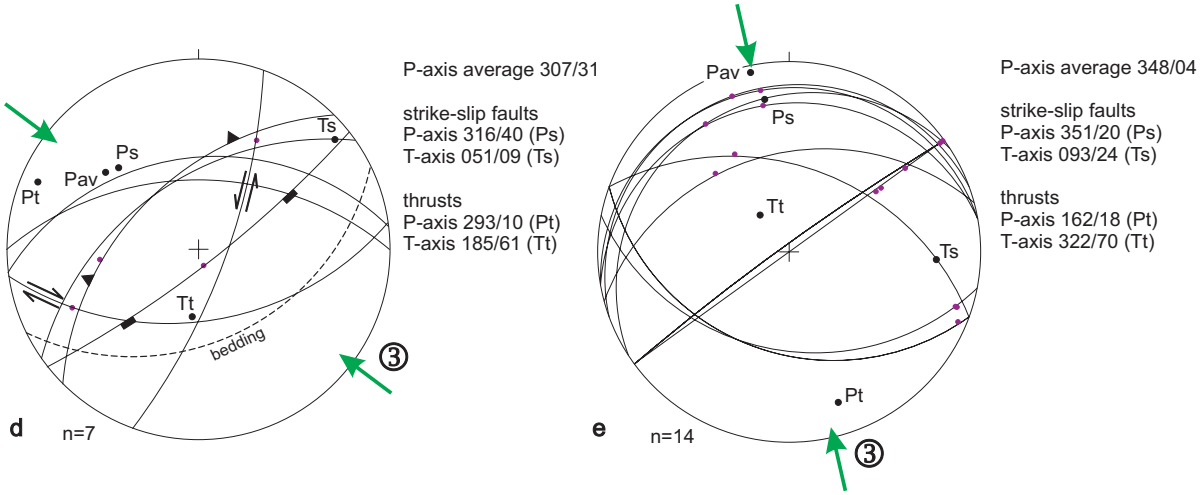
P-axis average 307/31
strike-slip faults
P-axis 316/40 (Ps)
T-axis 051/09 (Ts)
thrusts
P-axis 293/10 (Pt)
T-axis 185/61 (Tt)
Pt
Pav
Ps
Ts
Tt
bedding
③
d
n=7
P-axis average 348/04
strike-slip faults
P-axis 351/20 (Ps)
T-axis 093/24 (Ts)
thrusts
P-axis 162/18 (Pt)
T-axis 322/70 (Tt)
Pav
Ps
Tt
Ts
Pt
③
e
n=14

Huercal Overa basin near Huercal Overa, Almajalejo and Zurgena (Figs. 5.4, 5.11 and 5.15). In the central part of the basin, the pertinent sediments are virtually undeformed. Outcrops of these sediments along the southern margin of the basin, on the other hand, contain dominantly ENE to WNW trending (syn-sedimentary) normal faults and few NNW trending normal faults, indicating NNE-SSW to NW-SE directed extension (Figs. 5.5p-r). The scale and style of faulting varies from small-scale planar faults up to large-scale roll-over structures and listric faults (Fig. 5.11), as well as up to 20 meter wide, rotated "domino" blocks (Fig. 5.15). The direction of hanging wall transport is in general to the north. Again, the magnitude of the extension varies from a minimum of 25% near Almajalejo and Zurgena up to 78% near Huercal Overa (β = 1.25 to 1.78). Sedimentary off-lap with concurrent progressive rotation of the bedding, and a high influx of mass flow deposits in an obviously starved basin suggest that extension in the Huercal Overa basin was associated with tilting of the basin during continuous basement uplift in the ranges.

The upper Tortonian marine sediments, strongly faulted in the southern part of the Huercal Overa basin, are unconformably overlain by Messinian and/or possibly early Pliocene fan conglomerates and marine silts and marls (Figs. 5.4 and 5.16). These sediments thus seal the extensional structures, which places a lower bound to the age of the associated extension. These observations are fully consistent with results of seismic studies of the Alboran Sea equally showing tilted and faulted Tortonian rocks unconformably overlain by essentially undeformed Messinian and Pliocene sediments.

The basin bounding faults along the southern margins of the Huercal Overa basin and Almanzora corridor form part of an ENE to NE trending en-echelon network of NW dipping faults (Fig. 5.4). In the Almanzora corridor these faults clearly show a single set of indicators which point to dextral strike-slip motion (Fig. 5.5v). Near Huercal Overa and Zurgena, however, a complex history of movements has resulted in different sets of overprinting kinematic indicators. The basin bounding faults in these areas occasionally show a vague primary set of indicators suggesting dextral strike-slip, overprinted by a dominant secondary and third set of kinematic indicators (Figs. 5.5s-u and 5.17). The secondary set of indicators point to dip-slip motions associated with approximately NNW-SSE directed extension. The first and secondary sets, i.e. the dextral and dip-slip motions, seem consistent with respectively the ENE-WSW to NE-SW directed extension in the early Tortonian basal continental deposits and the NNE-SSW to NW-SE directed extension in the early Tortonian fluvial – shallow marine and late Tortonian marine deposits. The third set of indicators clearly demonstrates a late-stage sinistral lateral motions indicating N-S to NNW-SSE directed compression.

In the centre of the Huercal Overa basin, where the Alhama de Murcia fault (Fig. 5.18a) passes into the E-ENE trending Albox fault, the Tortonian deposits are folded in a large-scale east-west trending monocline (Figs. 5.4 and 5.12) with a NNW dipping axial plane. This structure seems part of the Albox fault system. To the west, E-W trending steeply tilted Miocene sediments show evidence of layer-parallel reverse and dextral shear senses, consistent with vertical axis rotations at that location (Fig. 5.4). Southeast of the monocline, thick Pliocene and Quaternary alluvial and fluvial sediments have been deposited in the eastern part of the Huercal Overa basin. These sediments are occasionally affected by south directed thrusts (Fig. 5.18b; García-Meléndez *et al.*, 2002 and 2003; Soler *et al.*, 2003; Masana *et al.*, 2005). Like the late lateral motion on faults of the fault-bounded southern side of the basin, these compressional structures suggest NNW-SSE directed shortening. This late-stage compressional deformation is discussed in more detail in chapter 6.

Lorca basin

The Lorca basin is a rectangular basin with a NE trending basin axis (Fig. 5.19). In cross-section, the Lorca basin has a symmetric geometry of a 10 km

Figure 5.18. a) Exposure of the Alhama de Murcia fault northeast of Puerto Lumbreras, carrying Alpujarride rocks of the Sierra de las Estancias towards the SE onto upper Tortonian marls. b and c) Trench exposure of Quaternary fan deposits made and investigated by members of the University of Barcelona in the autumn of 2002 (Trench 3 of Masana et al., 2005). The sediments are tilted, cut and displaced by low-angle south-directed thrusts which form part of the Albox fault. d and e) Stereographic projections (equal area, lower hemisphere) showing orientations of thrusts and strike-slip faults in (d) Miocene - Quaternary sediments and basement rocks in the Alhama de Murcia fault zone near Puerto Lumbreras and (e) Miocene - Quaternary sediments of the Huercal Overa basin along the Albox fault.

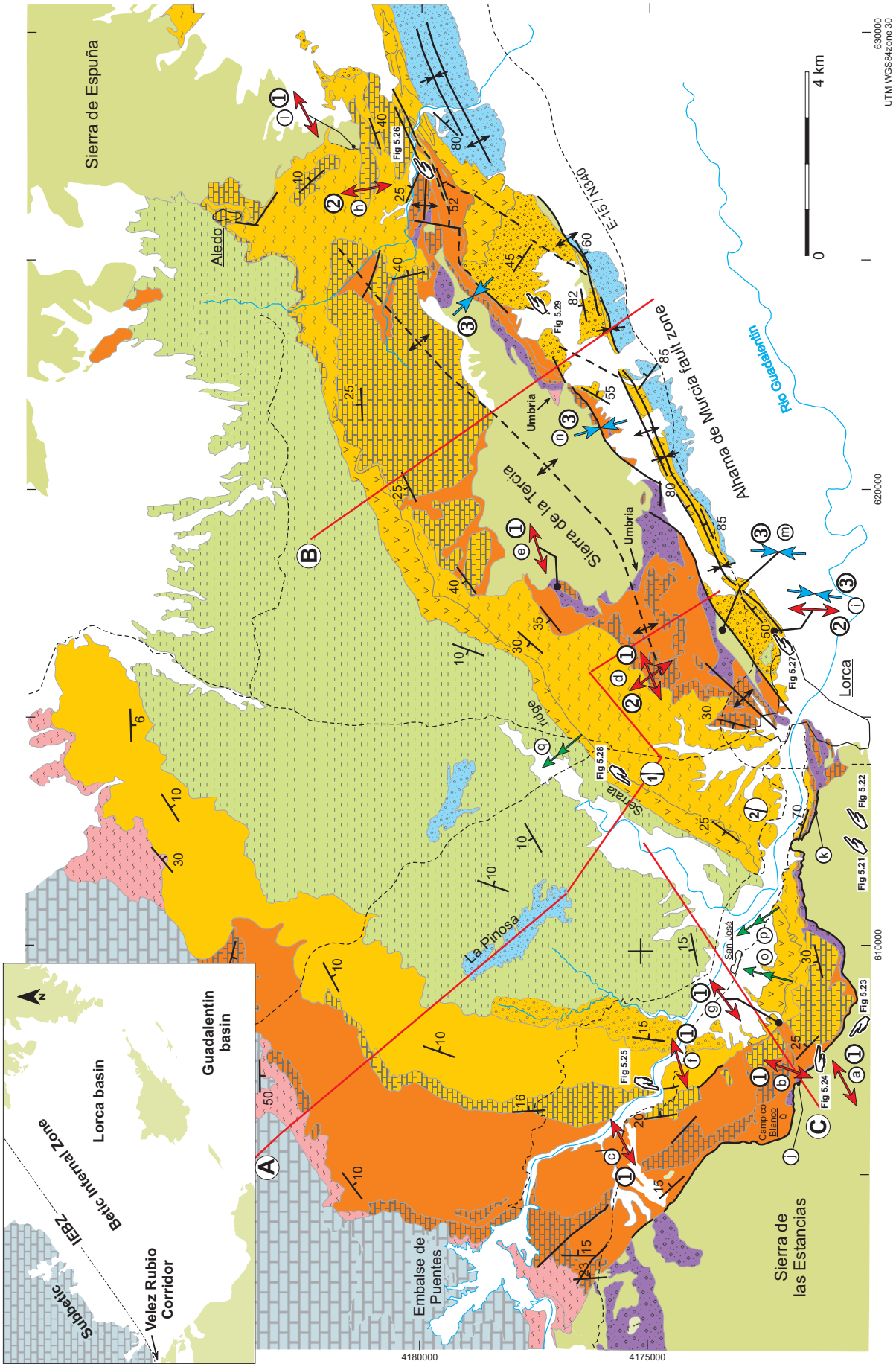
Sierra de Espuña
Aledo
Sierra de la Tercia
Umbria
Alhama de Murcia fault zone
E-15 / N-340
Río Guadalentín
Lorca
Sierra de las Estancias
Embalse de Puentes
La Pinosa
Sierra
Ridge
San José
Campico Blanco
Fig 5.21
Fig 5.22
Fig 5.23
Fig 5.24
Fig 5.25
Fig 5.26
Fig 5.27
Fig 5.28
Fig 5.29
A
B
C
4 km
0
630000
620000
610000
4180000
4175000
UTM WGS84zone 30
Guadalentin basin
Lorca basin
Betic Internal Zone
IEBZ
Subbetic
Velez Rubio Corridor

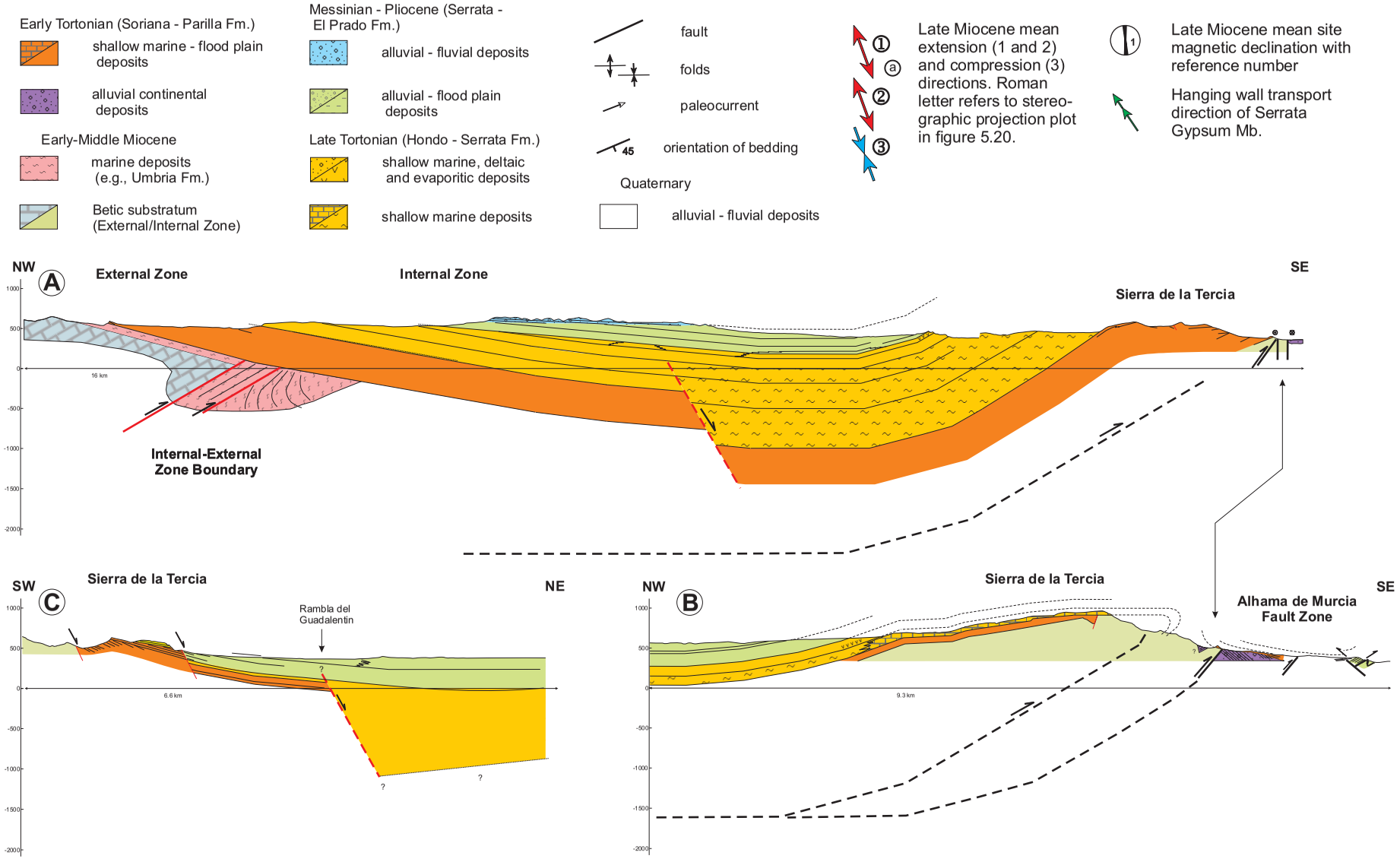

Figure 5.19. Geological map of the Lorca basin, after Kampschuur et al. (1972), Geel (1976), Montenat et al. (1990), Wrobel and Michalzik (1999), Wrobel (2000), and this study. Paleomagnetic data from Dinares-Turell et al. (1997) and Krijgsman et al. (2000).

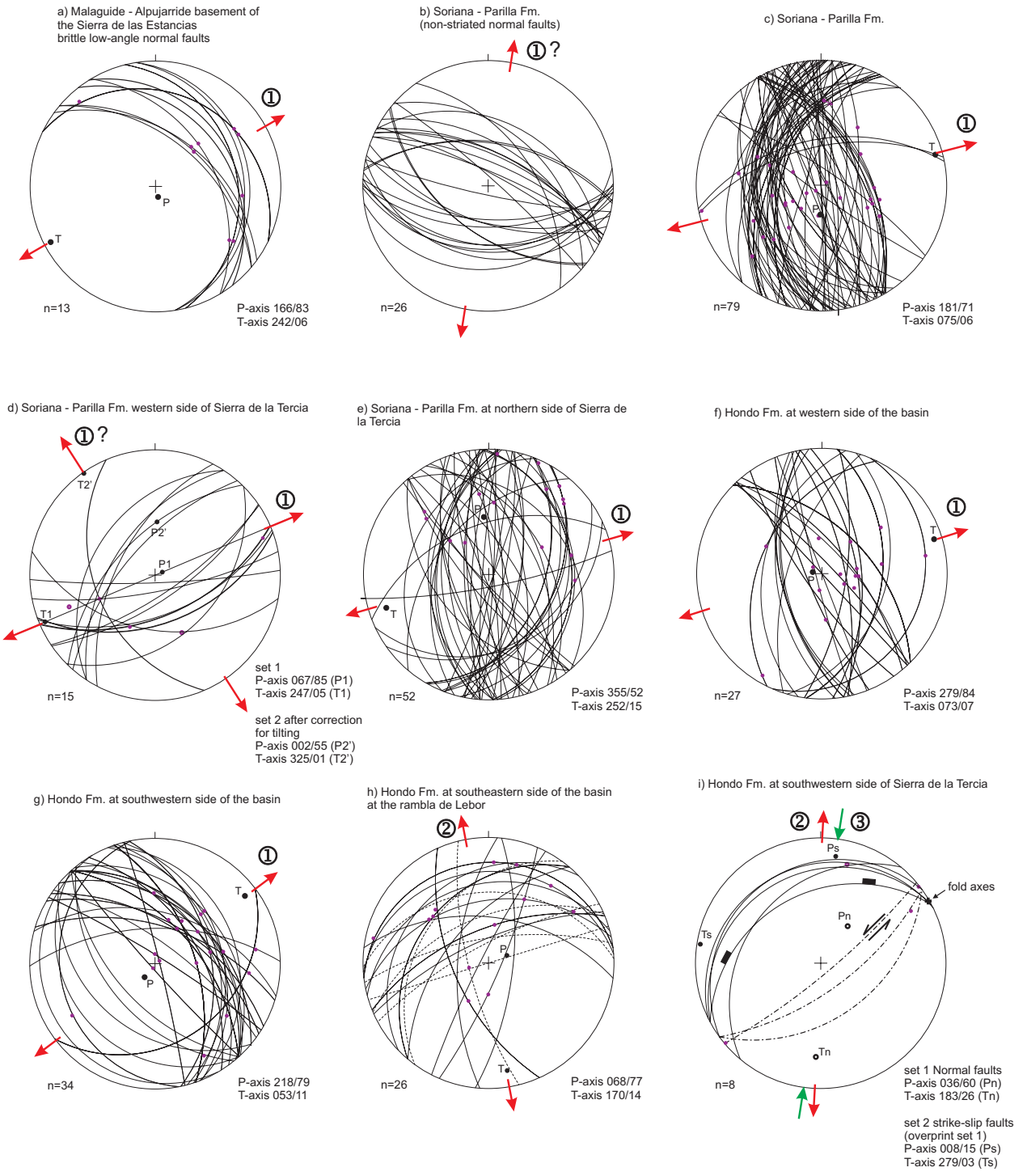

Figure 5.20. Stereographic projections (equal area, lower hemisphere) showing the orientations of the main foliation and stretchings lineations in basement rocks and brittle faults and lineations in basement rocks and basin sediments. Locations of pertinent outcrops are shown in figure 5.19. P- and T-axes represent the mean axes of incremental shortening and extension.

j) basin-bounding fault at western side of basin

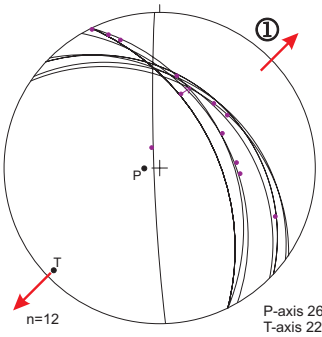

k) basin-bounding fault at southwestern side of basin

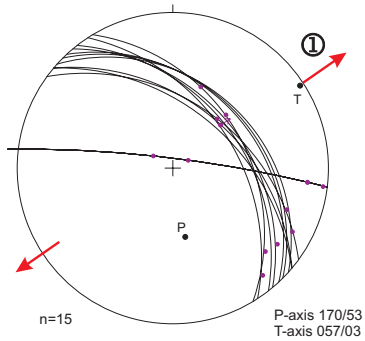

l) basin-bounding fault at eastern side of basin

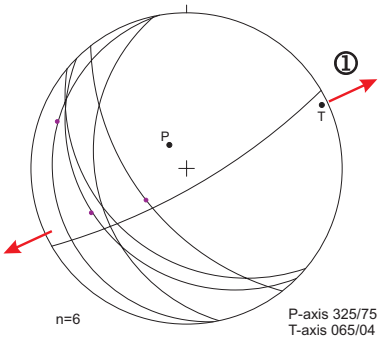

m) Alhama de Murcia fault near Lorca - exposure of gouge zone

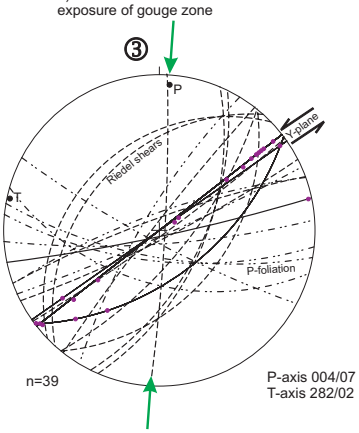

n) Alhama de Murcia fault near Lorca - thrusts at basement - basin contact

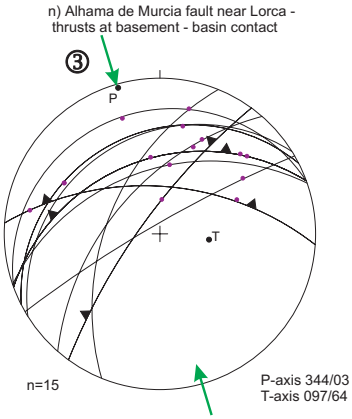

o) Fault planes, bedding parallel detachments and lineations in the Serrata Gypsum Mb. and at the base of the unit

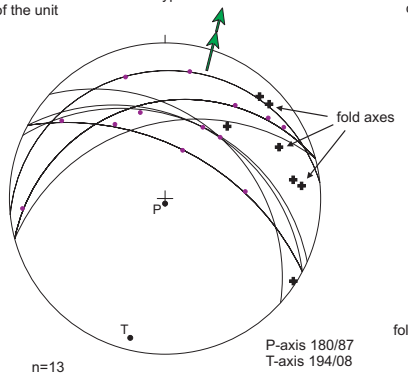

p) Fault planes, bedding parallel detachments and lineations in the Serrata Gypsum Mb. and at the base of the unit

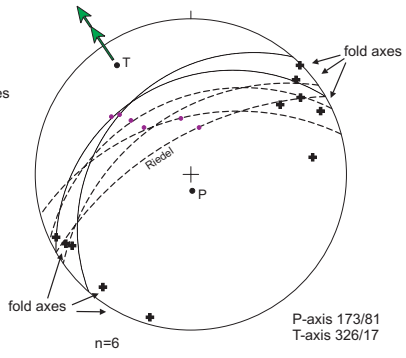

q) Fault planes, bedding parallel detachments and lineations in the Serrata Gypsum Mb. and at the base of the unit

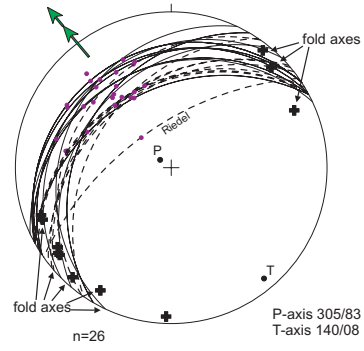

Figure 5.21. Panoramic view of the Lorca basin from the southwest (for location see figure 5.19) showing general northwestward tilt of the upper Miocene Hondo and Serrata formations at the south-eastern side of the basin. Messinian-Pliocene sediments of the El Prado formation exposed around La Pinosa in the north (to the left) lie sub-horizontal or dip gently towards the southeast.

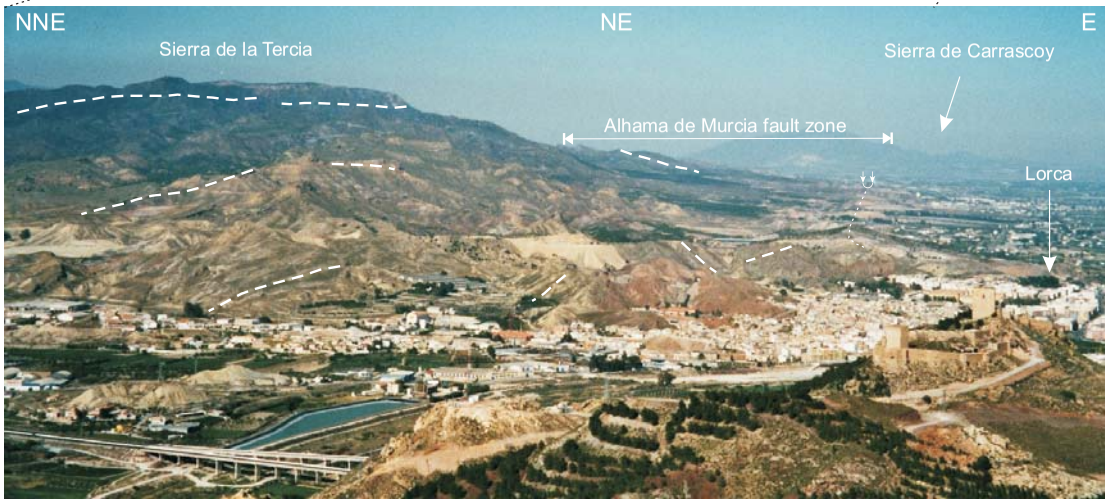

Figure 5.22. Panoramic view of the southern side of the Sierra de la Tercia and Alhama de Murcia fault zone, seen along strike of the Alhama de Murcia fault zone (for location see figure 5.19). The Tortonian sediments of the Soriana, Parilla and Hondo formations in the northwestern part of the Sierra de la Tercia clearly dip shallowly to the northwest. In the Alhama de Murcia fault zone, Miocene sediments in the distance mostly dip to the southeast, whilst Miocene - Pliocene deposits in the foreground show dips towards the northwest and southeast.

scale, open synform (Montenat *et al.*, 1990b; Wrobel and Michalzik, 1999; see Figs. 5.19 and 5.21). The stratigraphically lowermost basin deposits are exposed along the basin margins, and the youngest sediments are seen in the centre of the basin. The basin is dominated by late Miocene to Quaternary sediments, but the basin fill suggests a Tortonian age for the initiation of the basin (chapter 4). The north-eastern part of the Lorca basin is covered by Quaternary alluvial deposits. Along the north-western basin margin, the contact between the Internal and External Zone is defined by the Internal-External Zone Boundary (IEZB, Lonergan *et al.*, 1994). This early Miocene contact is sealed by middle and late Miocene sediments of the Lorca basin (chapter 4). The south-eastern basin margin is characterized by folds and faults that belong to the Alhama de Murcia fault zone (e.g., Montenat *et al.*, 1990b; Martínez-Díaz and Hernández-Enrile, 1992; Fig. 5.22). The south-western and north-eastern margins are dominated by a network of extensional faults (e.g., Montenat *et al.*, 1990b; Wrobel and Michalzik, 1999; Wrobel 2000) or are considered part of, respectively, oblique-dextral and oblique-sinistral fault zones (Guillén Mondéjar *et al.*, 1995). Because of its geometry, and in view of the structure and kinematics of the basins-bounding faults, the Lorca basin is commonly interpreted as a rhomb-graben (pull-apart basin) located at a relay position between two parallel running strike-slip faults (e.g., Montenat *et al.*, 1987; Wrobel, 2000). This interpretation is discussed in detail in chapter 6. Below we focus on (brittle) structures in the basement and in the overlying and adjacent sediments exposed along the south-western and south-eastern basin margins.

The Alpujarride and Malaguide basement rocks of the Sierra de las Estancias forming the south-western margin of the Lorca basin show clear evidence of semi-ductile and brittle extension, as evidenced by spectacular low-angle normal faults (Fig. 5.23). These structures dominantly indicate an ENE-WSW to NE-SW direction of extension. On the basis of the structures in the outcrop shown in figure 5.23, the magnitude of the extension in the Malaguide basement rocks may be as high as 120% ($\beta = 2.2$). The inferred direction of extension is consistent with studies by Lonergan and Platt (1995) and Booth-Rea *et al.* (2002) of ductile-brittle extensional structures at the Malaguide – Alpujarride contact and at different levels in the Malaguide and Alpujarride basement in the Sierra de las Estancias and Sierra de la Tercia. In the basement rocks of the Sierra de la Tercia, Booth-Rea *et al.* (2002) found two groups of low-angle normal faults: an early group with hanging-wall transport directions towards the NW to NNW, and a second group showing hanging wall transport towards the WSW. The second group of extensional structures partially overprints the first group. Fission track cooling ages suggest that extension and exhumation of the Malaguide and Alpujarride basement occurred during the early and middle Miocene (Lonergan and Platt, 1995; Lonergan and Johnson, 1998) and coincided with motions along these ductile-brittle extensional faults. Moreover, the extensional structures in the basement are in general sealed by Serravallian - Tortonian sediments (Booth-Rea *et al.*, 2002).

Exposures of the continental and shallow marine deposits along the south-western part of the basin that make up the base of the basin stratigraphy (Soriana and Parilla Fm., chapter 4) display ubiquitous extensional structures, indicating a NE-SW to ENE-WSW oriented extension direction (Fig. 5.20b-e). The sediments of the Soriana and Parilla formations (Fig. 4.7) are pervasively cut and displaced by faults. Some of these faults have syn-sedimentary characteristics, i.e. they have developed as growth-faults (Fig. 5.24). Outcrops of the sediments of the Umbria and Soriana formations fringing the Sierra de la Tercia show (syn-sedimentary) extensional structures that similarly point to NE-SW to ENE-WNW directed extension (Fig. 5.20d-e). However, some outcrops show two groups of (syn-sedimentary) extensional structures: one group indicating approximately a NW-SE to N-S directed extension, and a dominant second group, superimposed on structures of the first group, pointing to ENE-WSW directed extension. The extension in the sediments in outcrops of the Soriana formation along the south-western side of the Lorca basin and at the north-western side of the Sierra de la Tercia may reach values up to 22 - 29% ($\beta = 1.22 – 1.29$) and 19% ($\beta = 1.19$), respectively.

Like the underlying sediments, outcrops of the stratigraphically higher, fluvial - marine Hondo formation along the south-western part of the Lorca basin show abundant evidence of syn-sedimentary extensional structures, such as shown in figure 5.25. These structures again indicate ENE-WSW to NE-SW directed extension (Fig. 5.20f-g). The sediments of the Hondo formation southeast of Lorca and at the eastern side of the Lorca basin south of Aledo, however, show clear evidence of (syn-sedimentary) NNW-SSE to N-S directed extension (Fig. 5.20h-i). A spectacular outcrop along the Rambla de Lebor shows

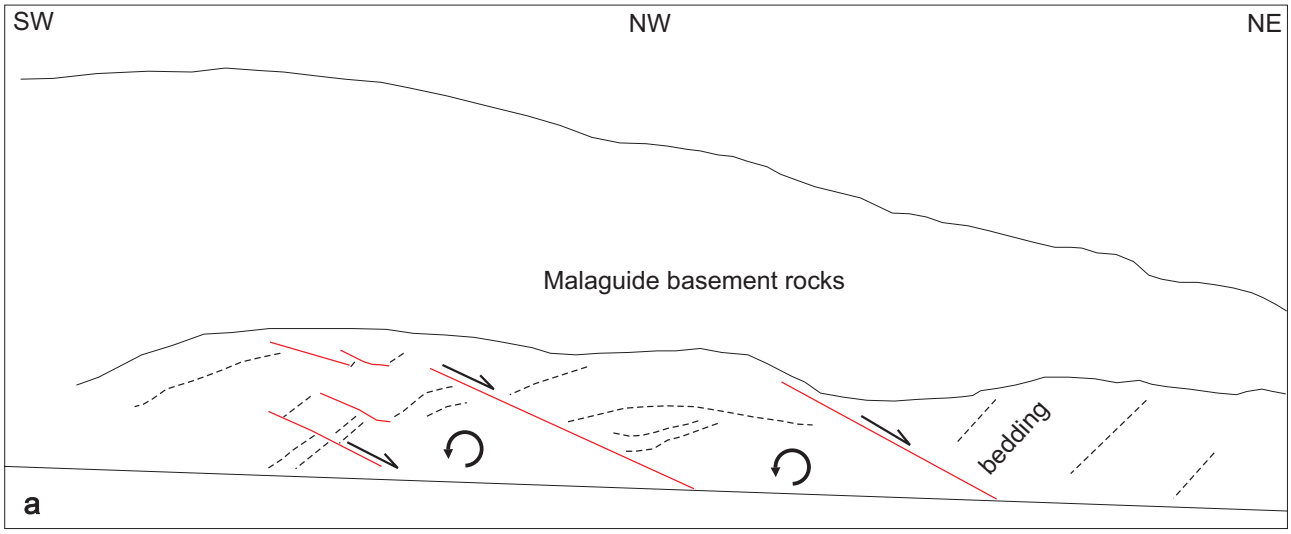

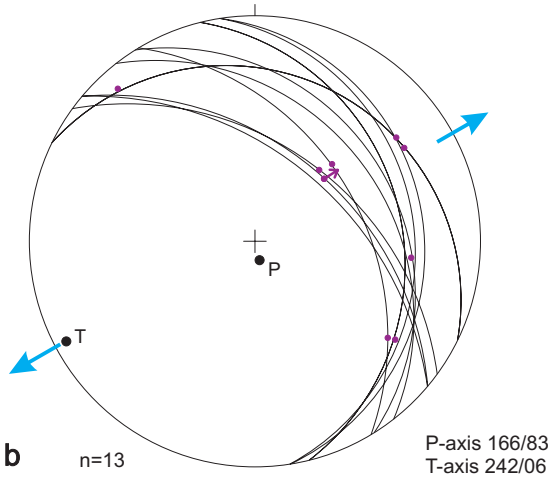

Figure 5.23. a) Outcrop of Malaguide basement rocks in the Sierra de las Estancias at the southwestern side of the Lorca basin (for location see figure 5.19) showing northeast-dipping low-angle normal faults. b) Stereographic projection (equal area, lower hemisphere) showing orientations of faults and slip directions in Malaguide - Alpujarride basement of the Sierra de las Estancias indicating ENE-WSW to NE-SW directed extension.

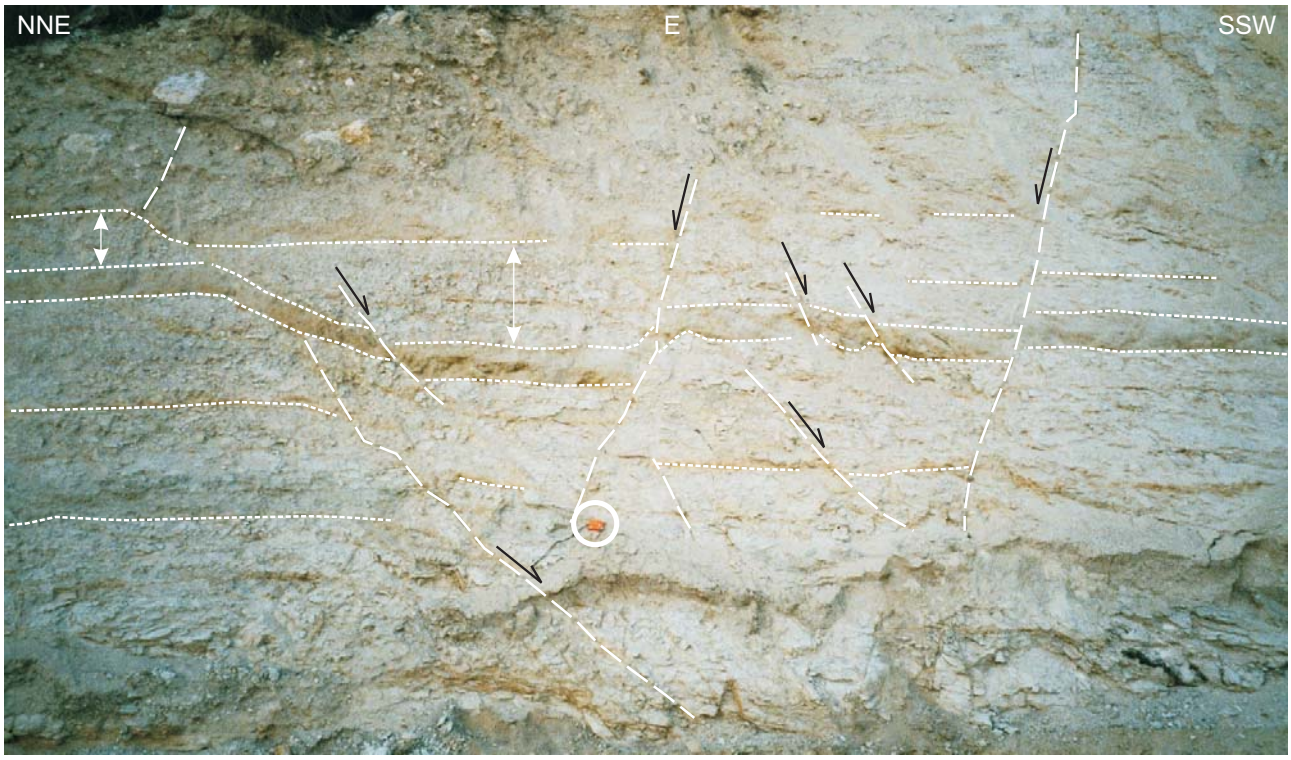

Figure 5.24. Exposure of lower Tortonian shallow marine silts and marls of the Parilla Fm. in the south-western part of the Lorca basin (for location see figure 5.19), deformed by NE and SW dipping extensional normal faults. Differences in thickness of the beds in the foot- and hanging wall suggest syn-sedimentary faulting. Note compass for scale.

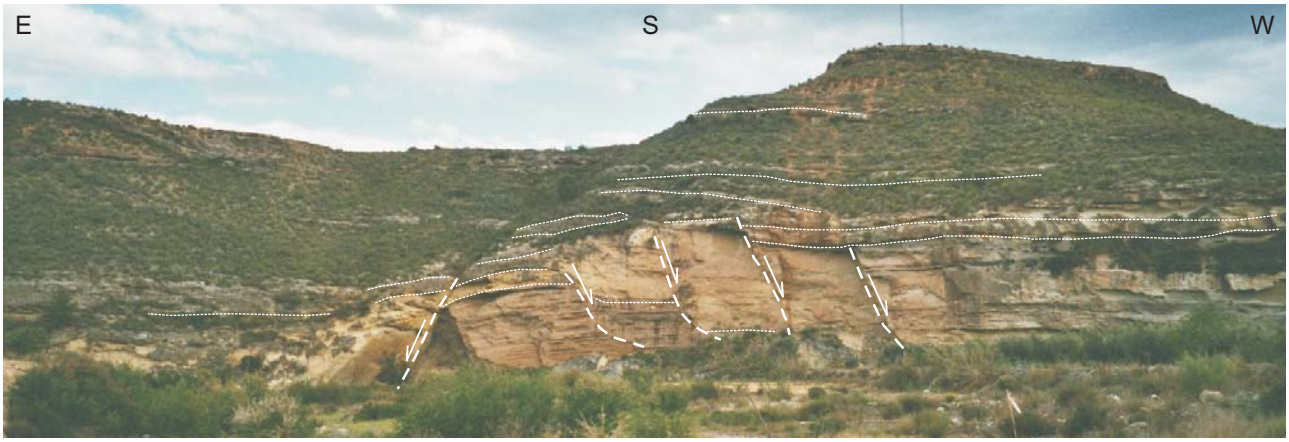

Figure 5.25. Outcrop of upper Tortonian shallow marine silts and marls of the Hondo Fm. in the western part of the Lorca basin (for location see figure 5.19). The outcrop shows E and W-dipping extensional normal faults. Some of the faults are sealed by overlying beds, indicating syn-sedimentary faulting. The extensional faults are associated with ENE-WSW directed extension.

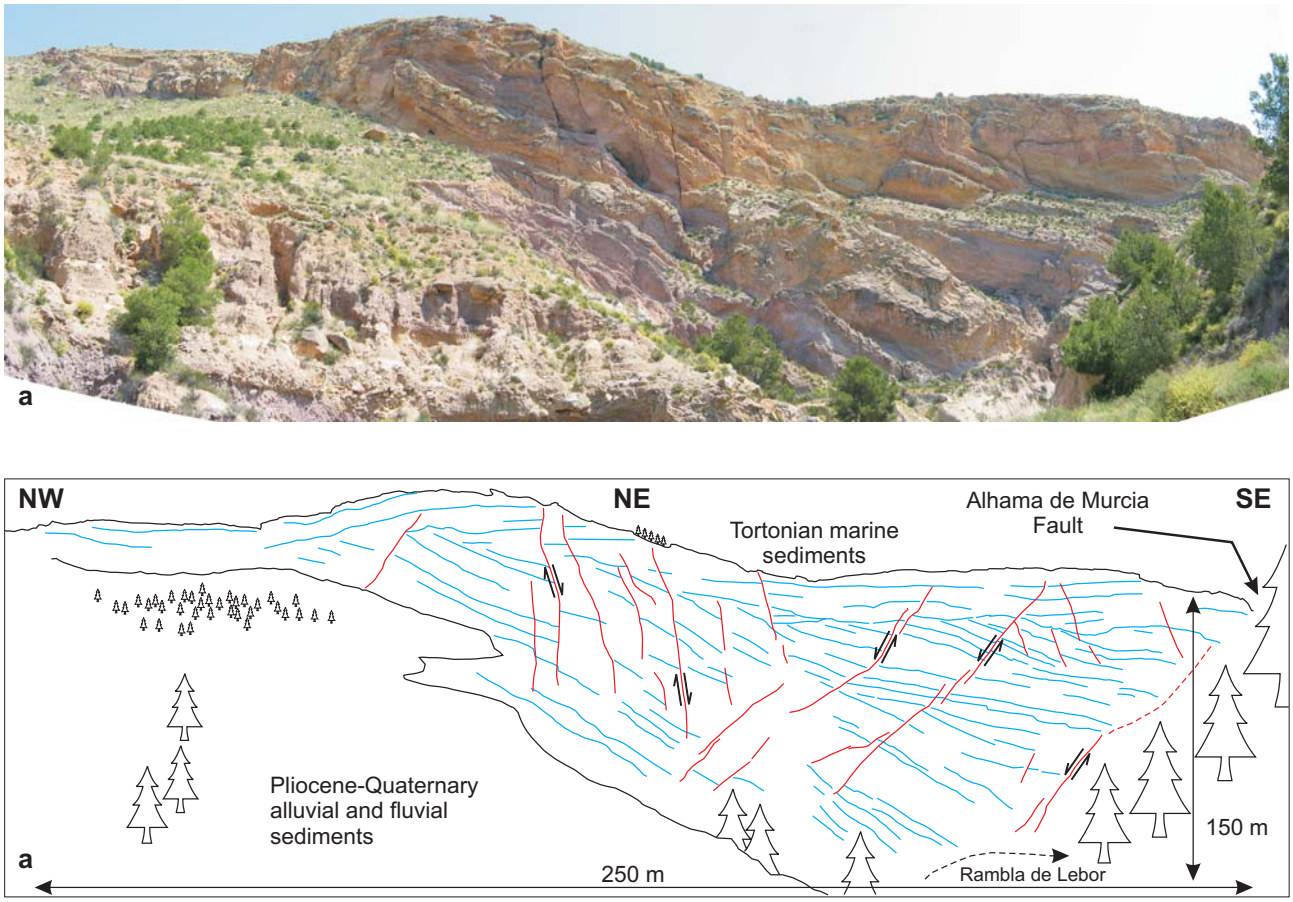

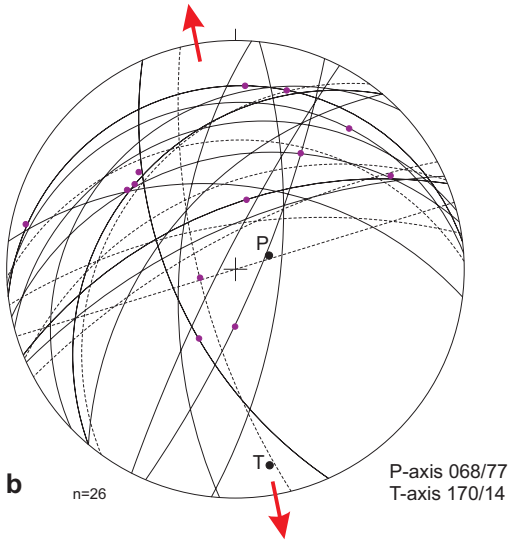

Figure 5.26. a) Cliff exposure along the Rambla de Lebor, southeastern Lorca basin, adjacent to the Alhama de Murcia fault (for location see figure 5.19), showing stratigraphic expansion of Tortonian sediments, in part accommodated by normal faults. Note that some of the faults are sealed by internal unconformities indicating that these faults were active during deposition of the expanding sequence. The structure strongly suggests that during the Tortonian the adjacent Alhama de Murcia fault initiated as a growth fault. b) Stereographic projection (equal area, lower hemisphere) showing orientations of extensional normal faults, Riedel fractures (dashed lines) and slip-vectors of the outcrop shown in (a). Note two sets of faults, i.e., a dominant set of ENE to NE trending faults suggesting N-S extension, and a second set of N-S trending steep faults.

a marked stratigraphic expansion of marine sediments (Fig. 5.26), adjacent to a fault consequently interpreted as a growth fault, i.e., the sediments were deposited during progressive normal faulting. The extension in sediments of the Hondo formation reaches values of up to 47% ($\beta = 1.47$) in the eastern part of the Lorca basin, and smaller values around 7% ($\beta = 1.07$) in the south-western part of the basin.

The basin-bounding faults along the south-western and north-eastern margins of the Lorca basin dominantly show dip-slip kinematics, however, some sets of indicators suggest oblique and lateral motions as well. The geometry of the fault planes and the dominant slip directions indicate an ENE-WSW to NE-SW direction of extension (Fig. 5.20 j-l). These results are consistent with the fault structures and associated extension directions in the early Tortonian continental and marine sediments (Soriana, Parilla and Hondo formations). It is, however, unclear what the amount of displacement along the basin-bounding faults is, and how the extension on these faults and on those in the basin sediments is accommodated in the basement at depth (Fig. 5.19, profile C).

Both in the Lorca basin proper and along the southern margin of the Sierra de la Tercia, the early Tortonian sediments and parts of the basin-bounding faults such as near Aledo are unconformably overlain by the evaporitic and fluvio-deltaic Serrata and fluvial El Prado formations, thereby sealing the early Tortonian extensional structures (see Fig. 5.27). In the western and eastern parts of the Lorca basin, the fluvial sediments of the Serrata and El Prado formations do not show any appreciable deformation. In the Serrata ridge along the north-western side of the Sierra de la Tercia, however, the diatomites and evaporites are clearly deformed showing ubiquitous extensional as well as compressional structures. The diatomites and evaporites of the Serrata ridge are tilted towards the northwest, i.e., orthogonal to the trend of the ridge, at an average dip of around 30° (Fig. 5.28 a). Near the crest of the ridge, the evaporites are intensely stretched through abundant ductile shears and brittle extensional faults (Fig. 5.25 b, c). In places, small-scale shear bands locally interact such as to produce a boudinaged structure. In thin section, the microstructure of the sheared evaporites is marked by bands of elongate gypsum grains (Fig. 5.25 d), sometimes with a distinct lattice preferred orientation indicating genuinely ductile, crystal-plastic flow. The outcrop-scale extensional faults and shears often curve into parallelism with the bedding (Fig. 5.25 b) indicating that the extensional deformation is transferred along layer-parallel evaporite horizons. Towards the north, near the top of the evaporite unit at the north-western side of the Serrata ridge, a complex system occurs of thrusts and folds clearly suggesting compression (Fig. 5.25 e). Kinematic analysis of the extensional structures and of the folds and thrusts indicate that the allied extension and shortening directions are both oriented orthogonal to the Serrata ridge (Fig. 5.20o-q), which strongly suggests that these structures were formed during large-scale slumping. It should be noted that these structures are not syn-sedimentary, but that they clearly developed after deposition of the diatomites and evaporites. In addition, the contact between the evaporites and the underlying diatomites is often marked by a thin but distinct clayey gouge layer, and by slickensides and grooves, and is affected by Riedel-type normal faults indicating movement of the hanging wall evaporites to the NW. In addition, immediately above the contact there are ubiquitous dm to 1m scale folds and small accommodating faults. All of these features clearly show that the contact is a de-

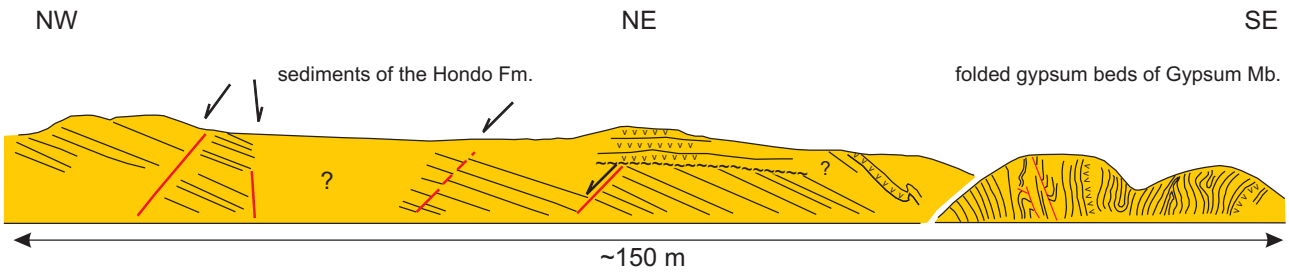

Figure 5.27. Field sketch of upper Tortonian marine sediments of the Hondo Fm. at the southwestern side of the Sierra de la Tercia immediately east of Lorca (for location see figure 5.19), cut and displaced by northwest dipping extensional normal faults, and unconformably overlain by evaporites of the Gypsum Mb. At the south-eastern end of the section, these same evaporites are deformed and isoclinally folded along NE-ENE trending fold axes, indicating NW-SE tot NNW-SSE directed shortening.

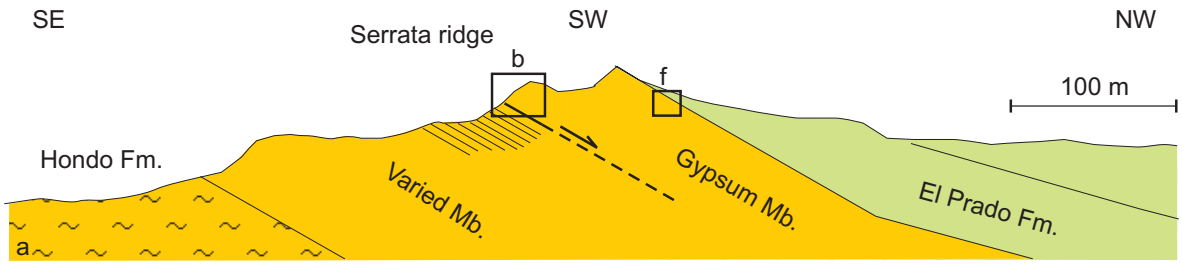
SE
Serrata ridge
SW
NW
b
f
100 m
Hondo Fm.
Varied Mb.
Gypsum Mb.
El Prado Fm.
a


SE
SW
NW
evaporites of Gypsum Mb.
c
marls and diatomites of Varied Mb.
Riedel shear
detachment
b

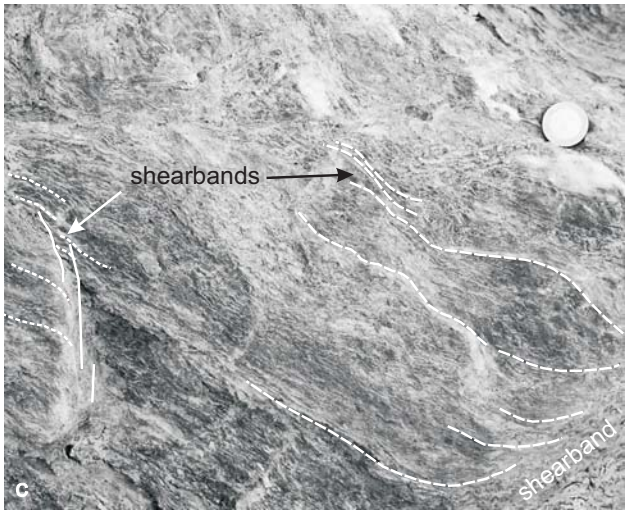
shearbands
shearband
c

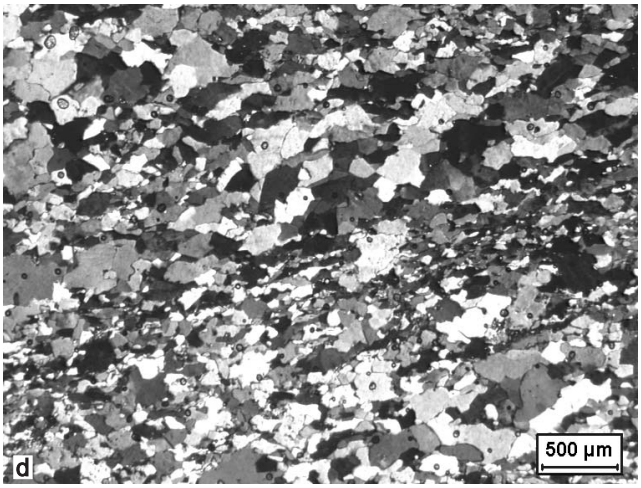
500 µm
d

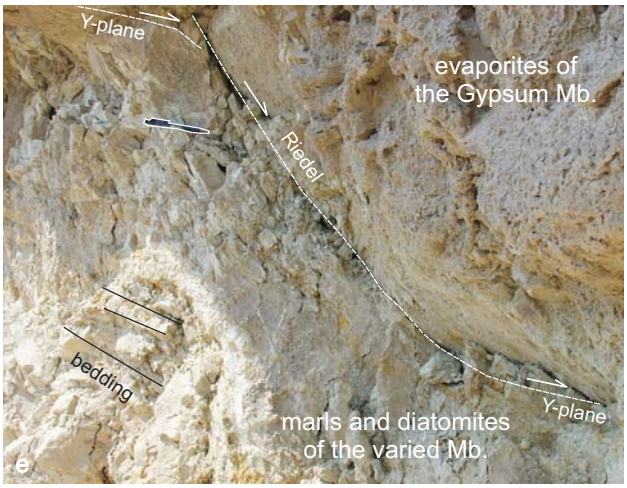
Y-plane
evaporites of the Gypsum Mb.
Riedel
bedding
Y-plane
marls and diatomites of the varied Mb.
e

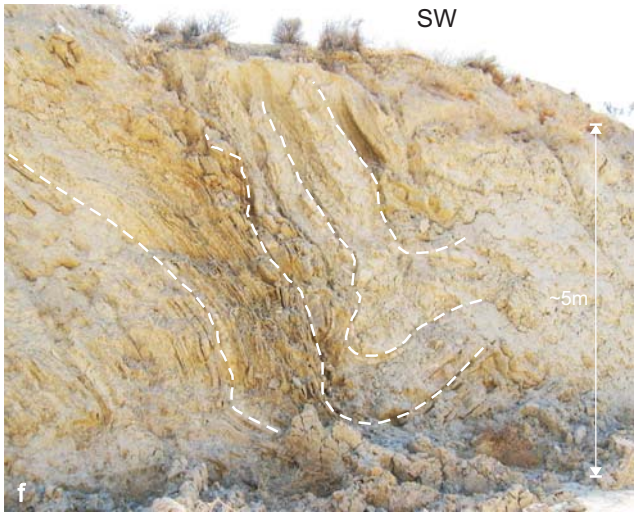
SW
~5m
f

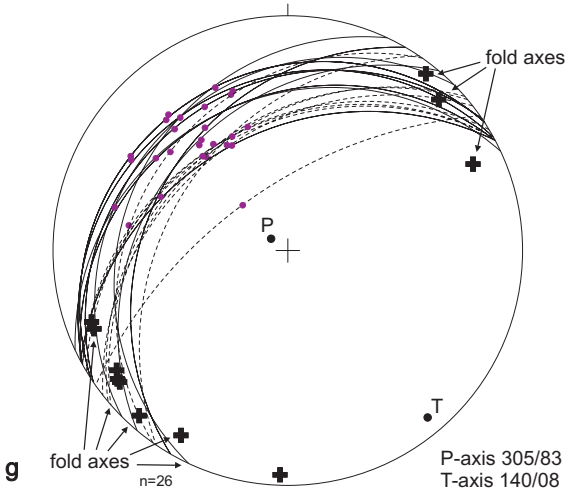
fold axes
P
T
fold axes
n=26
P-axis 305/83
T-axis 140/08
g

formed, rather than an undeformed stratigraphic contact as suggested in earlier studies (e.g., Geel, 1976; Montenat *et al.*, 1990b; Rouchy *et al.*, 1998; Krijgsman *et al.*, 2000). This may have important consequences for the inferred age of the Serrata evaporites recently dated as late Tortonian (Krijgsman *et al.*, 2000). The ubiquitous evidence for intense deformation of the evaporites and for movements along the basal contact suggests that the Serrata evaporite body represents a km-scale slump-like (tectonic) slide. This raises the distinct possibility that the Serrata gypsum has cut down in the direction of transport (i.e., to the NW) into the underlying diatomites, such that un uncertain amount of underlying sediments may have been excised during sliding, entirely similar to the smaller-scale excisions seen in the outcrop of Fig. 5.25b. In view of the absence of any confirmed Tortonian age of the overlying sediments, the possibility therefore exists that the evaporites are essentially Messinian, resting now with a tectonic contact on undoubtedly Tortonian sediments underneath. The cause of the internal deformation and sliding of the evaporites is not unambiguous, but in view of the geometry of the Lorca basin (Figs. 5.19 and 5.21), uplift of the Sierra de la Tercia allied with movements on the Alhama de Murcia fault as discussed below seems the obvious candidate.

The southeastern margin of the Sierra de la Tercia is flanked by a narrow zone of intensely deformed late Miocene sediments, which forms part of the Alhama de Murcia fault zone (Fig. 5.22). The basement-sediment contact forming the sharply defined northern edge of the Alhama de Murcia fault zone is a steep tectonic contact. Kinematic indicators on the pertinent faults suggest transport of the Malaguide and Alpujarride basement towards the south and southeast (Fig. 5.20m-n), placing these basement rocks on top of steeply inclined Tortonian sediments in the footwall. The inferred motion along the basement-sediment contact may vary along strike from sinistral-reverse to reverse. The Tortonian sediments in the footwall form part of a km-scale open footwall syncline (Fig. 5.29), whilst the entire Sierra de la Tercia forms part of a 5 km-scale asymmetric antiformal structure in the hanging wall of the Alhama de Murcia fault system (Fig. 5.19). On outcrop-scale, the Tortonian sediments in the footwall comprising continental, marine and evaporitic deposits of the Soriana, Parilla, Hondo and Serrata formations, are strongly folded and faulted, and some of the normal faults in the Hondo sediments have been reactivated as strike-slip or reverse faults. At the south-western end of the Sierra de la Tercia, sediments belonging to the Soriana and Parilla formations have been faulted by approximately ESE trending, dextral strike-slip faults and NNE trending sinistral faults, which clearly overprint early Tortonian (syn-sedimentary) extensional structures.

The structures and slipvectors on fault planes along different parts of the Alhama de Murcia fault zone suggest a N-S to NW-SE direction of shortening, which is consistent with earlier studies of, e.g., Rutter *et al.* (1986), Silva *et al.* (1992) and Martínez-Díaz *et al.* (2002). These compressional structures must have developed after the deposition of the Miocene sediments, because the extensional structures in the Miocene sediments are either overprinted or reactivated whilst evidence for Miocene syn-sedimentary compressive and strike-slip deformation is clearly lacking. The absence of any Miocene compression and strike-slip deformation is supported by the fact that paleomagnetic sections of the marls and diatomites of the Hondo formation do not show any appreciable rotation of magnetic declination and inclination (Krijgsman *et al.*, 2000; Rouchy *et al.*, 1998; Dinares-Turell *et al.*, 1997).

On the basis of the above data we infer that uplift of the Sierra de la Tercia and Sierra de las Estancias started during the latest Miocene and continued into

Figure 5.28. Structures and fabrics in the evaporates of the Serrata ridge. a) Diagrammatic cross-section across the Serrata ridge (for location see figure 5.19). b) Exposure of the Varied and Gypsum members in abandoned quarry, southeastern side of the Serrata ridge. Marls and diatomites of the Varied Mb. in base of the cliff are relatively undeformed. Basal part of the Gypsum Mb. above detached contact shows 1 m scale folds with NE trending fold axes. Note listric normal faults and shears higher in cliff. Circle: geologist for scale. c) Detail of (b) showing strongly deformed and boudinaged evaporite affected by small-scale shear bands. d) photomicrograph of gypsum rock from (c), showing microstructure dominated by elongate grains suggesting crystal-plastic ductile flow. e) Detail of deformed basal contact of the Gypsum Mb. approximately 500 m southwest of quarry in (b), showing listric normal fault with Riedel fracture orientation displacing faulted (detached) contact (Y-planes). f) Strongly folded gypsum laminae and silt beds near top of the Gypsum Mb., north of the Serrata crest as shown in (a). g) Stereographic projections (equal area, lower hemisphere) showing orientations of fault planes and bedding-parallel detachments (plain greatcircles), Riedel fractures (stippled) and associated lineations (dots). Fold axes shown as crosses. P and T axes refer to extensional structures.

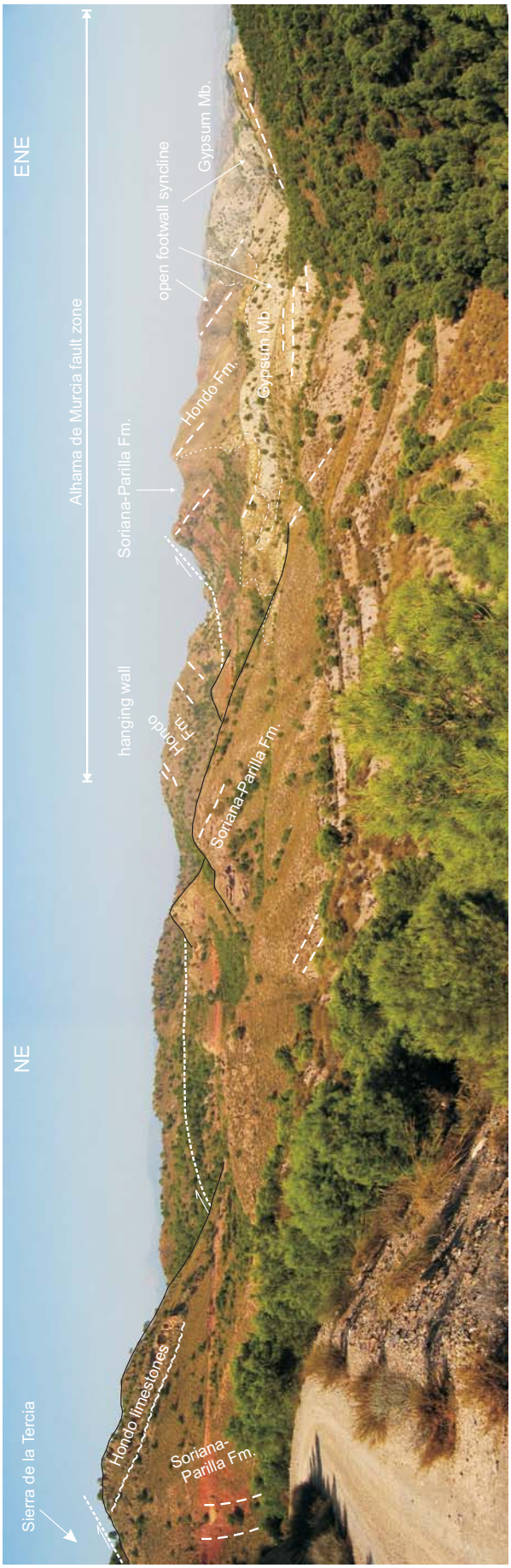

Figure 5.29. Panoramic view of the Alhama de Murcia fault zone at the south-eastern side of the Sierra de la Tercia (for location see figure 5.19) viewed to the northeast, i.e., oblique to the trend of the fault. Tortonian sediments and basement rocks of the Sierra de la Tercia to the north (left) are emplaced on Tortonian sediments in the foot wall that are tilted to the southeast. The contact is a steeply northwest dipping reverse fault, and kinematic analysis suggests hanging wall transport towards the southeast. The sediments in the footwall, which belong to the Soriana, Parilla, Hondo and Serrata formations, are folded into a km-scale open synform with an ENE trending fold axis.

the Quaternary. This uplift may well have produced the slope instability required for downward sliding and slumping of the Serrata evaporites.

Fortuna basin

In map view, the Archena-Mula - Fortuna basin has an elongate shape and a NE trending basin axis. In cross-section, the northern half of the basin shows an up to 7 km wide, open synformal geometry (Poisson and Lukowski, 1990; Fig. 5.30). South of the town of Fortuna and the Sierra Abanilla – Crevillente, however, the sediments dip almost consistently towards the south. The basin is dominated by the marls of the Los Baños formation in the centre and by the continental conglomerates of the Rambla Salada formation in the southeast.

The northern margin of the Archena-Mula - Fortuna basin is defined by the Crevillente fault (e.g., De Smet, 1984; Leblanc and Olivier, 1984; Sanz de Galdeano 1983; see inset of Fig. 5.30), however others have referred to this structures as the North Betic Fault (e.g., Leblanc and Olivier, 1984; Montenat and Ott d'Estevou, 1996). Furthermore, the basin is diagonally transected by the Alhama de Murcia fault zone. It is unclear if and how the Alhama de Murcia fault zone is connected in the eastern part of the basin with the Crevillente fault. In spite of the complexity of the main faults, it is generally believed that the Archena-Mula - Fortuna basin was formed as a strike-slip-generated basin, partly developed as an extensional imbricate fan system or "Queue de cheval" and partly as a pull apart basin or "Sillon sur décrochement" (e.g., Montenat *et al.*, 1987). This aspect is further discussed in chapter 6 below.

Early basin sediments that allow study of the early basin history are exclusively exposed along the basin margins, in particular those north and northeast of Fortuna and Abanilla. In this study we focus on the sediments and structures in this north-eastern part of the Archena-Mula - Fortuna basin (Fig. 5.30) and refer to this area as the Fortuna basin proper.

In the northern and northeastern part of the Fortuna basin, the Miocene sediments overly Mesozoic and early Tertiary rocks of the Betic External Zone exposed along the northern margin of the basin and in the Sierra Abanilla – Crevillente. The rocks of the External Zone comprise a sequence of Triassic evaporites and Jurassic to Paleocene-Eocene limestones, which, in particular in outcrops near Macisvenda and Capres, show clear evidence of folding and thrusting with NE to ENE trending fold axes and north-directed thrusts (Fig. 5.32). These compressive structures point to a NNW-SSE to NW-SE direction of shortening, which is consistent with observations in the External Zone of, e.g., De Ruig *et al.* (1987), Ott d'Estevou *et al.* (1988) and with results of this study presented in chapter 3. The Mesozoic and early Tertiary rocks are unconformably overlain by Tortonian shallow marine and continental deposits. These sediments seal the earlier, pre-Tortonian compressional structures in the External Zone rocks.

Both the Tortonian shallow marine – continental deposits and the underlying Mesozoic and early Tertiary basement rocks have been subject to extension. The pertinent structures are particularly well developed in three areas along the basin margin near Capres, Macisvenda and Abanilla. In the area near Capres, ENE to NNE trending syn-sedimentary normal faults and outcrop scale growth-faults are observed in early Tortonian shallow marine and continental sediments (Brechique, Calcarenitique and Rouge units), as shown in figures 5.31b and 5.33. These extensional faults cut and displace earlier compressive structures, such as thrust planes, in the Mesozoic rocks underneath. In turn, the extensional faults are in part unconformably overlain, hence sealed, by Tortonian reefs and marls of the Los Baños formation (Lukowski and Poisson, 1988; Poisson and Lukowski, 1990; Fig. 5.30). Near Macisvenda and Abanilla, mostly W to NW trending (syn-sedimentary) normal faults developed in the early Tortonian shallow marine and continental deposits of the Calcarenitique and Rouge units as well as in the marine silts and marls of the Los Baños formation. Kinematic analyses of these faults indicate NNE-SSW to NE-SW oriented extension directions (Figs. 5.31c-e). Like in the region of Capres, the silts and marls of the Los Baños formation lie unconformably on tilted and faulted continental conglomerates of the Rouge unit.

Exposures of the basement-basin contact south of the village of Macisvenda shows an excellent example of a genuinely extensional structure (Fig. 5.34). In this area, a 100 m scale south dipping extensional detachment separates strongly tilted Tortonian continental and marine sediments above from the underlying Triassic evaporites and Cretaceous and Paleogene limestones. The displacement along this extensional detachment is estimated at perhaps hundreds of meters and appears to be largely accommodated by the Triassic evaporite horizon (Profile A in Fig. 5.30).

On the basis of drastic and abrupt stratigraphic thickness variations in the Tortonian sediments west

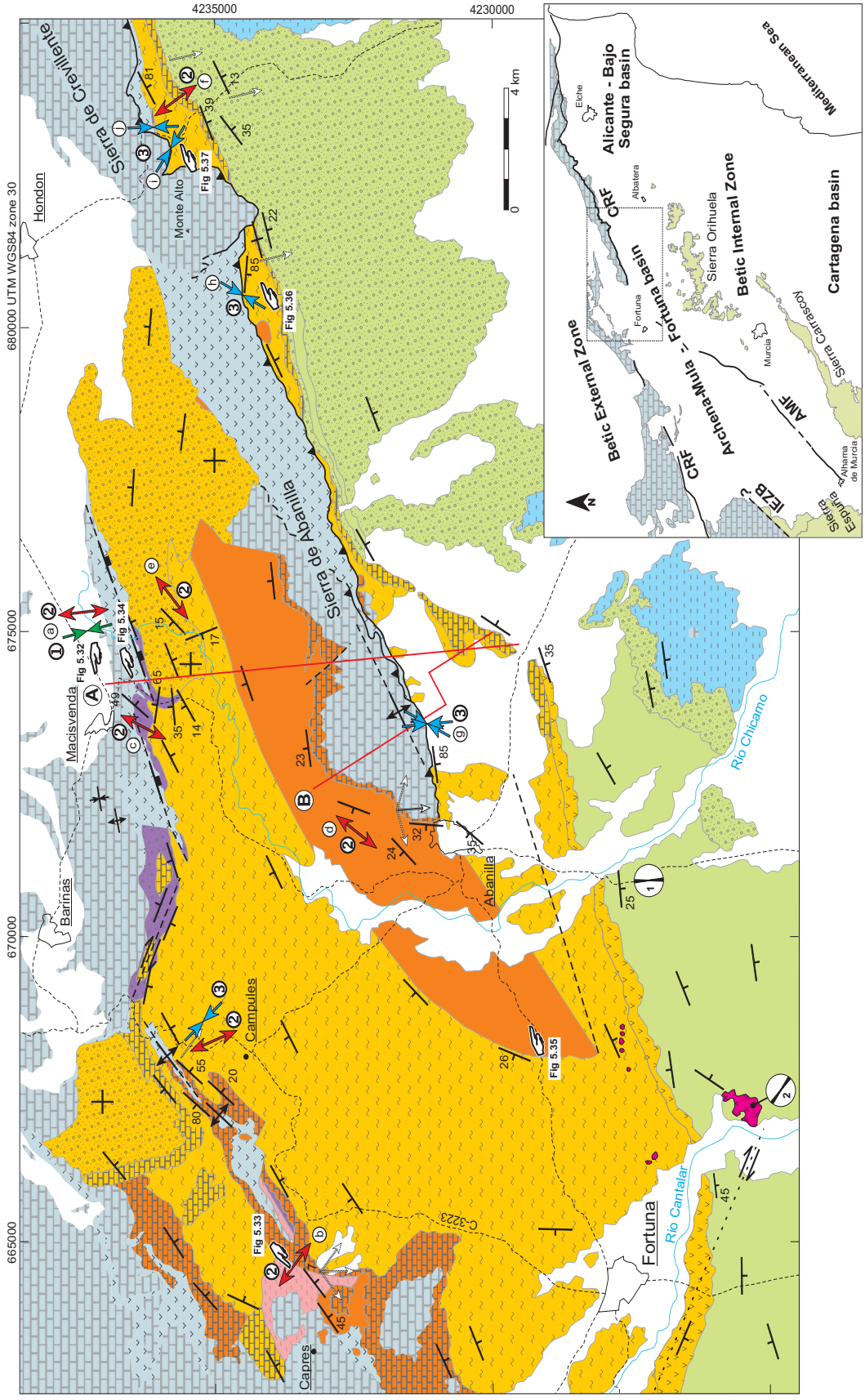
4235000
4230000
680000 UTM WGS84 zone 30
675000
670000
665000
Hondon
Sierra de Crevillente
Monte Alto
Fig 5.37
Fig 5.36
Sierra de Abanilla
Macisvenda
Fig 5.32
Fig 5.34
Barinas
Campules
Capres
Abanilla
Fig 5.35
Fig 5.33
Río Chicamo
Río Cantalar
Fortuna
4 km
0
Mediterranean Sea
Alicante - Bajo Segura basin
Elche
CRF
Albatera
Betic External Zone
Fortuna basin
Fortuna
Betic Internal Zone
Sierra Orihuela
Cartagena basin
Murcia
Sierra Carrascoy
AMF
Archena-Alhama-Mula
CRF
IEZB ?
Sierra Espuña
Alhama de Murcia

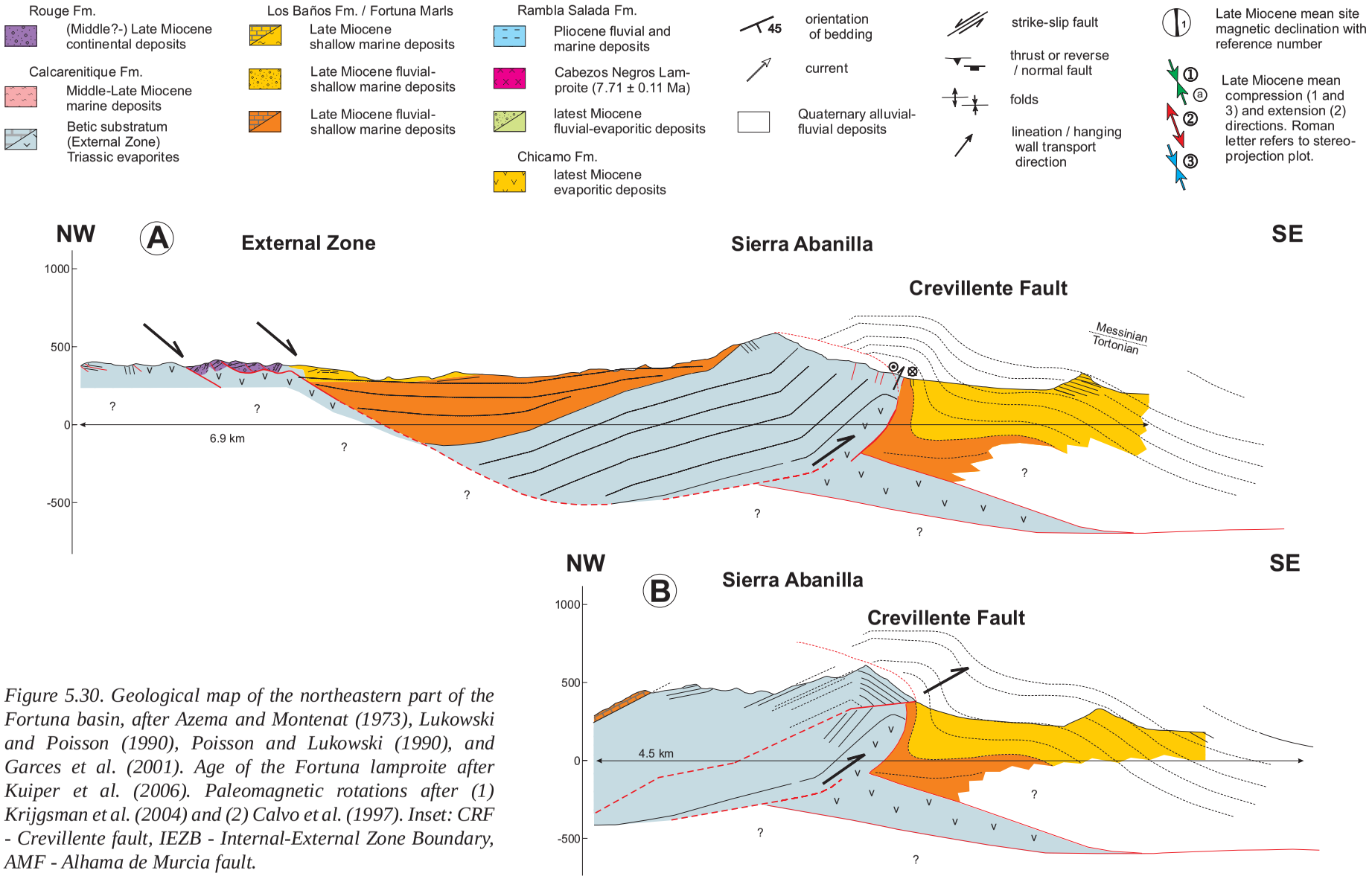

Figure 5.30. Geological map of the northeastern part of the Fortuna basin, after Azema and Montenat (1973), Lukowski and Poisson (1990), Poisson and Lukowski (1990), and Garces et al. (2001). Age of the Fortuna lamproite after Kuiper et al. (2006). Paleomagnetic rotations after (1) Krijgsman et al. (2004) and (2) Calvo et al. (1997). Inset: CRF - Crevillente fault, IEZB - Internal-External Zone Boundary, AMF - Alhama de Murcia fault.

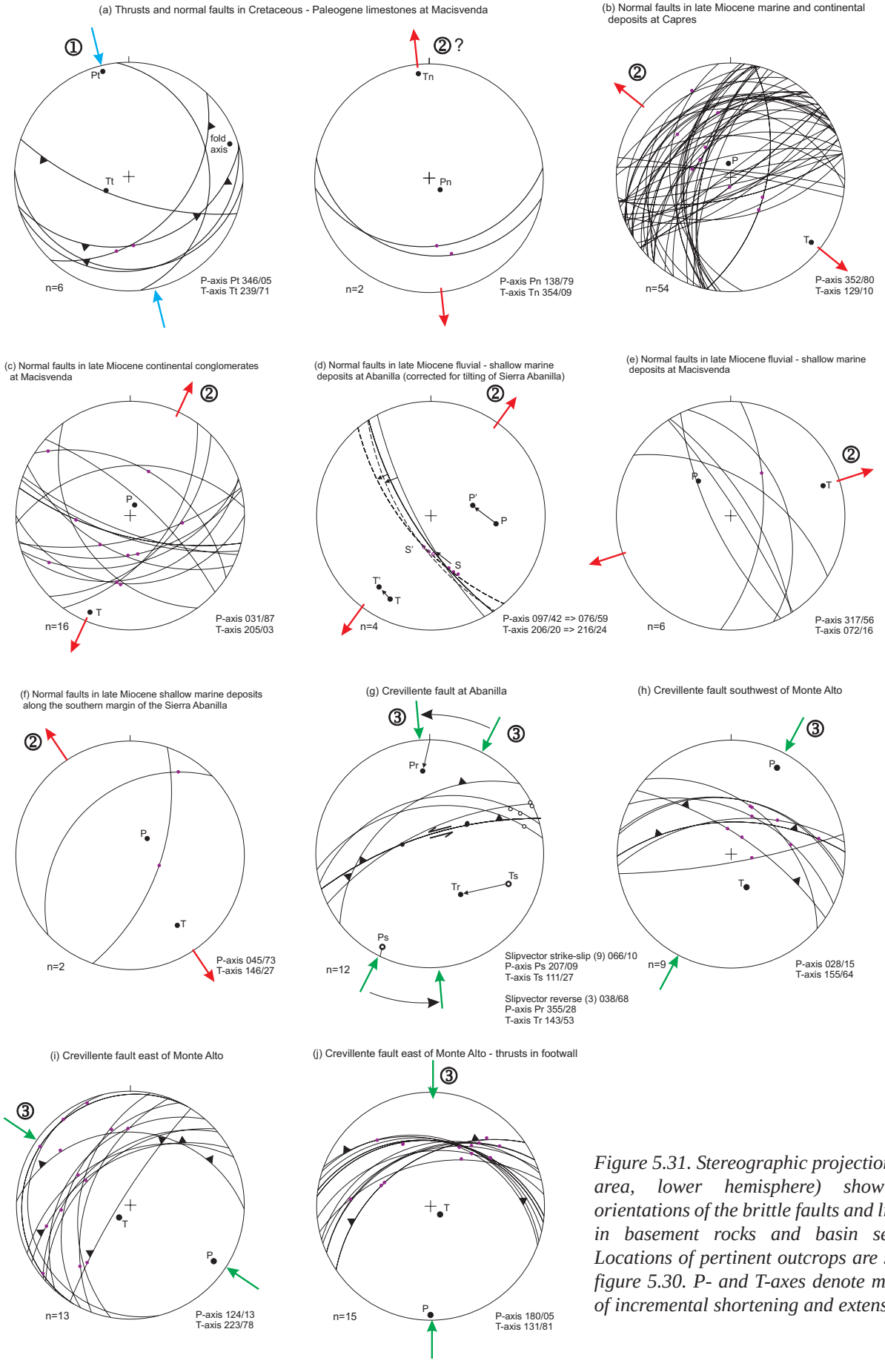

Figure 5.31. Stereographic projections (equal area, lower hemisphere) showing the orientations of the brittle faults and lineations in basement rocks and basin sediments. Locations of pertinent outcrops are shown in figure 5.30. P- and T-axes denote mean axes of incremental shortening and extension.

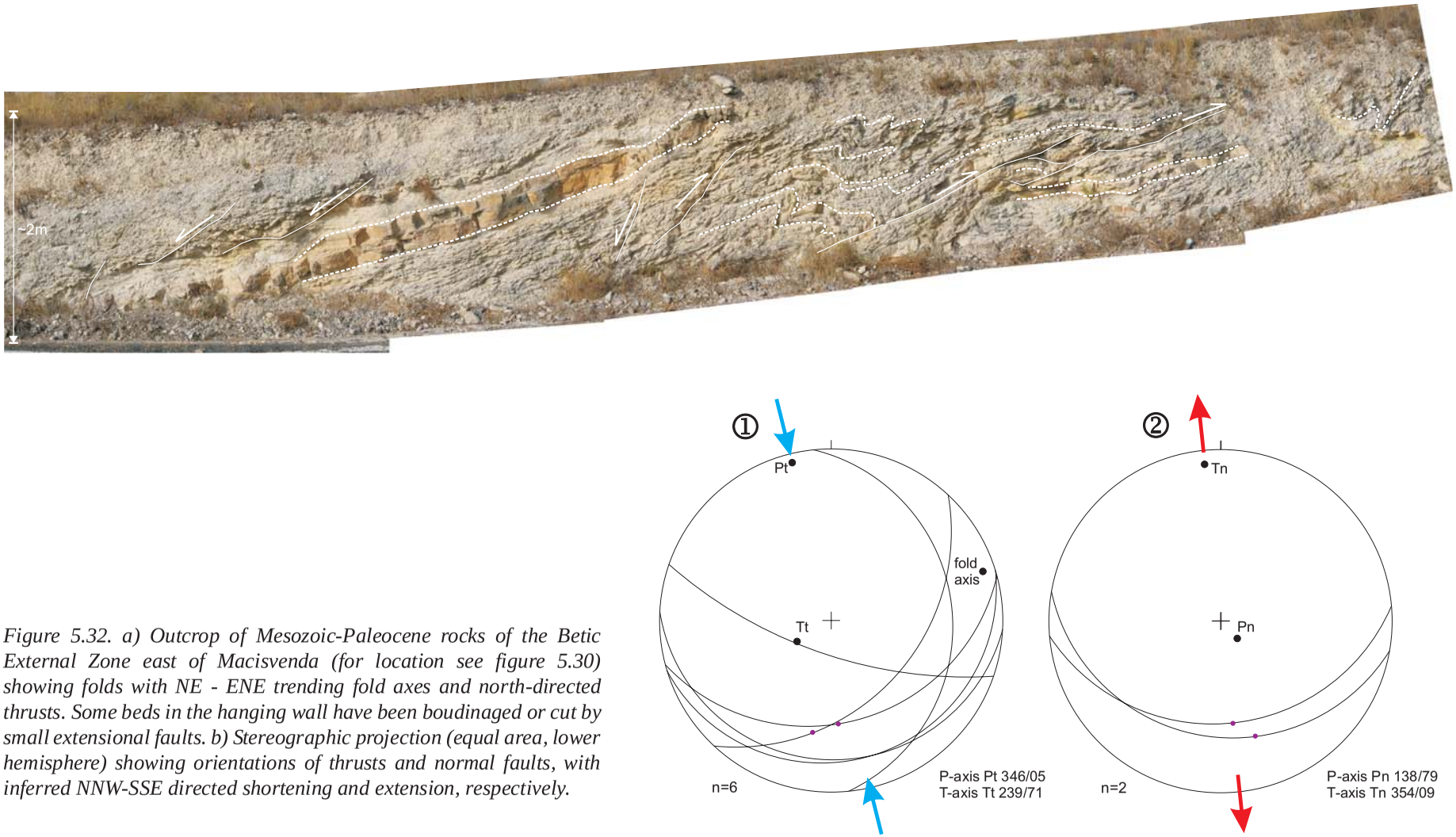

Figure 5.32. a) Outcrop of Mesozoic-Paleocene rocks of the Betic External Zone east of Macisvenda (for location see figure 5.30) showing folds with NE - ENE trending fold axes and north-directed thrusts. Some beds in the hanging wall have been boudinaged or cut by small extensional faults. b) Stereographic projection (equal area, lower hemisphere) showing orientations of thrusts and normal faults, with inferred NNW-SSE directed shortening and extension, respectively.

Figure 5.33. Panoramic view of Tortonian shallow marine and fluvial deposits overlain by reef limestones, northern side of the Fortuna basin near Capres. Road outcrop contains (syn-sedimentary) normal faults indicating NE-SW directed extension. Overlying reef deposits interfinger to the south with the Fortuna marls.

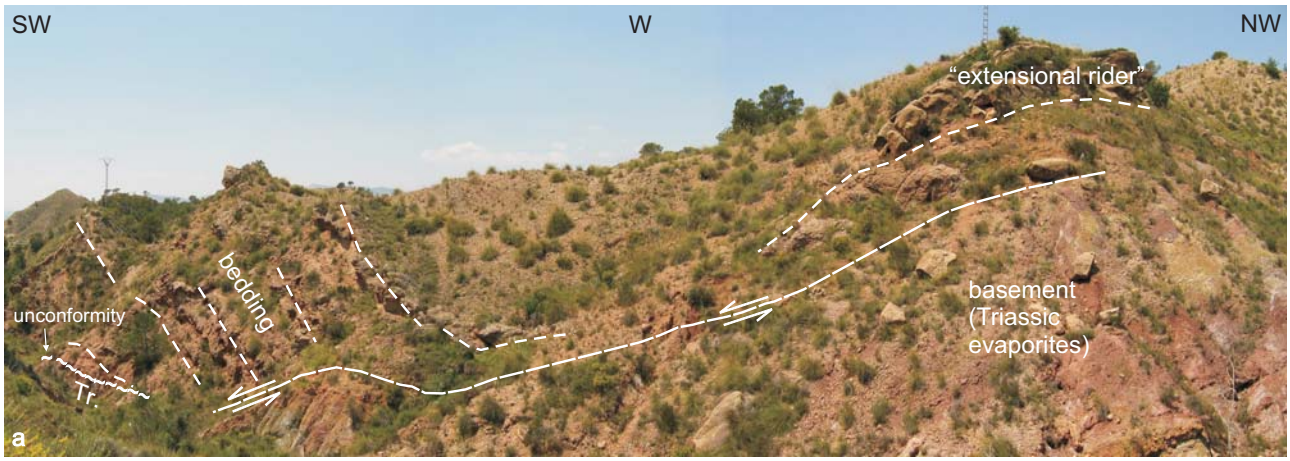

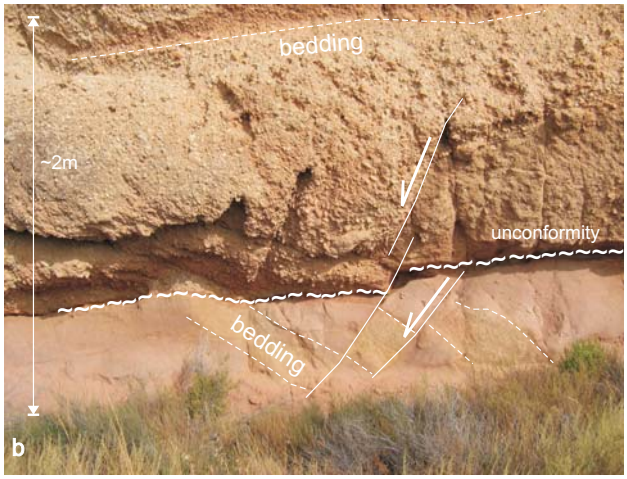

Figure 5.34. Structures along the northern margin of the Fortuna basin. a) Exposure near Macisvenda of red conglomerates and sandstones of the Rouge formation resting unconformably on Triassic evaporites (SW part of the outcrop). The conglomerates and underlying Triassic evaporites have been strongly faulted and tilted, in part accommodated by faults running along and into the evaporites. b) Intraformational unconformity defined by conglomerate seals fault and allied tilted beds in underlying reddish sandstone, and is itself faulted, indicating syn-sedimentary stretching.

of Capres, Poisson and Lukowski (1990) have suggested the presence of a similar extensional structure along the northern basin margin, roughly parallel to the western part of the Crevillente fault.

The extension in the sediments of the Calcarenitique unit at Capres reaches values as high as 78% ($\beta = 1.78$) in the lower parts of the outcrop but decreases upwards in the deposits of the Rouge unit ($\beta = 1.06$). The magnitude of extension in the shallow marine and continental sediments of the Rouge and Los Baños formations in the northeasten part of the Fortuna basin near Macisvenda shows low values of 3 to 20% ($\beta = 1.03$ to 1.20) in the south, but clearly increases towards the basin bounding fault in the north where it may reach values up to 100% ($\beta = 2.0$).

Unfortunately, the marls of the Los Baños formation in the central part of the Fortuna basin are poorly exposed. Along the southern margin of the Sierra Abanilla – Crevillente, however, few NE trending (syn-sedimentary) extensional faults with minor (cm to dm scale) displacements occur in the marine sediments of the uppermost part of the Los Baños formation, pointing to N-S to NW-SE directed extension (Fig. 5.31f). The extensional faults are sealed by the uppermost marine conglomerates and reefs of the Los Baños formation. The evaporites and diatomites of the Chicamo formation and the continental sediments of the Rambla Salada formation, which lie conformable on the sediments of the Los Baños formation, do not contain any extensional structures and appear to seal all earlier extensional structures in the sediments underneath.

In summary, the early Tortonian shallow marine and continental sediments were progressively affected by (syn-sedimentary) extensional normal faults showing ENE to NE trends near Capres and W to NW trends near Macisvenda and Abanilla. As these structures along the northern basin margin are essentially coeval, it is suggested that these variable fault orientations reflect local heterogeneities possibly related to the structure of the underlying basement rather than a progressive rotation of the regional stretching direction through time.

In the northwestern part of the study area, between Capres and Campules, the Triassic evaporites and the overlying Tortonian sediments affected by extensional normal faults are exposed in a km-scale NE trending open antiform (Fig. 5.30). The antiform forms the continuation of structures further southwest that make up the western part of the Crevillente fault or North Betic fault. The antiformal structure terminates against a NW-SE trending deflection of the basement-basin contact. This deflection may be caused by a strike-slip fault but because of poor outcrop this interpretation remains uncertain. In any case, the large-scale fold structure indicates NW-SE directed shortening, that must postdate the extensional structures preserved in the folded sediments.

Along the southern margin of the Sierra de Abanilla and Sierra de Crevillente, Tortonian sediments are steeply tilted towards the southeast and are, in part, tectonically overlain by Mesozoic limestones. This structure delineating the southern margin of the Sierras represents the Crevillente fault proper, and runs from Abanilla towards the northeast (Fig. 5.35). Along strike, the nature of the structure varies from reverse fault to thrust fault (Fig. 5.36), however, there is also local evidence of sinistral strike-slip motion (Fig 5.31g). The trends of the fault planes vary along strike from ENE near Abanilla to more variable orientations around Monte Alto (Fig. 5.31h-j), whilst slip-vectors on the fault planes are variable as well. As a whole, however, the geometry and structure of the Crevillente fault, and the direction of hanging wall transport are consistent with a N-S to NW-SE directed shortening.

Unfortunately, it is unclear if and how the western and eastern segments of the Crevillente fault are connected. The map pattern in fact suggests an 'en echelon' arrangement of the two segments. The large-scale antiform between Capres and Campules and the Crevillente fault at Abanilla both affect the entire (stretched) Tortonian basin stratigraphy which is folded and/or tilted, and the structures may well be contemporaneous in their development. We argue that folding and thrusting initiated not until after the deposition of the Tortonian and perhaps Messinian sediments. This timing is substantiated by two facts: (1) the 7.71±0.11 Ma old volcanic deposits (Kuiper *et al.*, 2006) southeast of Fortuna have rotated anticlockwise after their intrusion (Calvo *et al.*, 1997), and (2) the paleomagnetic sections of the late Tortonian evaporitic unit (7.8-7.6 Ma; Krijgsman *et al.*, 2000) of the Chicamo formation do not show any progressive rotation in the magnetic declination and inclination (Dinarès-Turell *et al.*, 1999; Krijgsman *et al.*, 2000; Garcés *et al.*, 2001), such that the sampled sediment package must have rotated and/or tilted as a whole after sedimentation.

Poisson and Lukowski (1990) have suggested that the Capres-Campules antiform and the development of the Crevillente structure were associated with continued thrusting in the External Zone, contemporane-

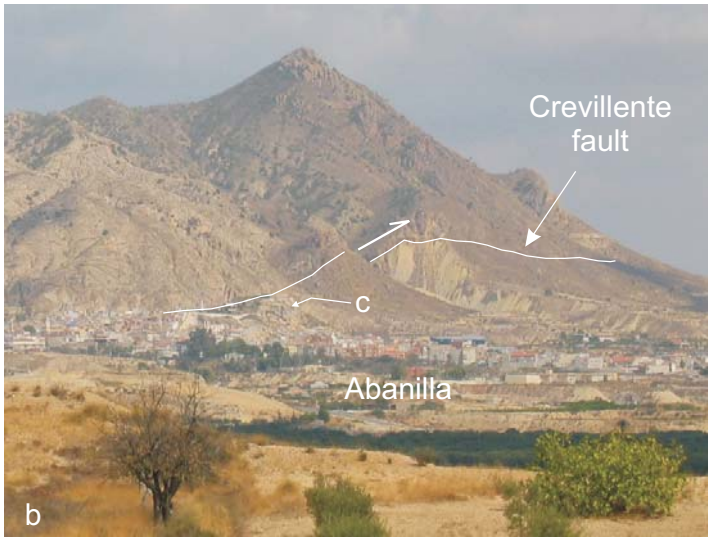

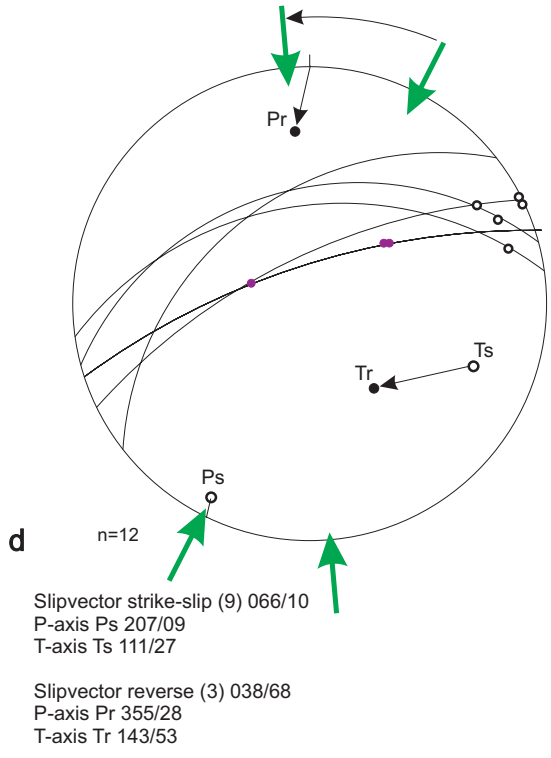

Figure 5.35. Structure of the Crevillente Fault near Abanilla. a) Panoramic view of the Sierra de Abanilla. b) View of the southern side of the Sierra de Abanilla showing Mesozoic limestones of the Betic External Zone thrusted along a NW-dipping fault onto upper Miocene sediments. c) Outcrop at Abanilla of the steep faulted contact between Mesozoic rocks of the Sierra de Abanilla and upper Miocene marls of the Los Baños Formation. d) Stereographic projection (equal area, lower hemisphere) showing orientations of fault planes and slip vectors observed on the Crevillente fault at Abanilla. An early set of sub-horizontal lineations and Riedel fractures is overprinted by a second set of steeply plunging lineations and Riedel fractures. The first set of structures point to sinistral-reverse motion, the second set suggests reverse motions.

ous with extension and sedimentation in the basin during the Tortonian, hence that the Fortuna basin developed in essence as a piggy-back basin. Our structural observations preclude this interpretation, first because several of the extensional structures such as south of Macisvenda can hardly be consistent with an essentially compressive setting, and secondly because deformation along the Crevillente structure is essentially post-Tortonian.

Vertical motions of the basins

Like in earlier studies (e.g., Kenter *et al.*, 1990; Cloetingh *et al.*, 1992; Rodríguez-Fernández et al ., 1999; Garcés *et al.*, 2001; Hanne *et al.*, 2003), tectonic subsidence curves for the Huercal Overa, Lorca and Fortuna basins have been calculated adopting local or "Airy" isostasy. The assumption of local isostasy is clearly an oversimplification. As emphasized by Cloetingh *et al.* (1992) the assumption of local isostasy can be justified by the presence, in the easternmost part of the Betic Cordillera, of thin and weak crust and lithosphere beneath the Miocene basins (Banda and Ansorge, 1980; Cloetingh *et al.*, 1992). However, in this context it is important to note that thrusting of the Internal Zone onto the Iberian margin likely started in the latest Oligocene - early Miocene as evidenced by the development of the IEZB backthrust structure. This structure is sealed by Langhian sediments (chapter 4), which implies that, at the onset of the late Miocene, the Internal Zone crust was well on its way being carried onto thinned Iberian crust. Restoration of the thrust structure in the Prebetics suggests a late Miocene position of the Betic Internal Zone some 50 to 60 km further southeast with respect to the Iberian plate (see also chapter 3). During the late Miocene the Subbetic Zone and the continuously extending Betic Internal Zone became further emplaced onto Iberia.

The above constraints on the setting of the late Miocene basins raise the possibility that the tectonic subsidence of the basins contains a signal of the flexural response of the Iberian plate, albeit that geophysical modelling of the strength of the Iberian plate beneath the Betics suggests a conspicuously low value for the present-day flexural rigidity (van der Beek and Cloetingh, 1992). In addition, Cloetingh *et al.* (1992) and Van der Beek and Cloetingh (1992) conclude that the combined load of the Subbetic and the Betic Zone is insufficient to explain the flexure of the Iberian crust and lithosphere as observed today, i.e. a considerable load is missing. It follows that the tectonic subsidence of the late Miocene basins in the Betic Cordillera may reflect the combined effect of flexural behaviour of the Iberian lithosphere and mechanisms related to ongoing stretching of the crust and lithosphere of the Alboran Domain discussed in chapter 7.

Figure 5.38 shows the mean basement (or total) and tectonic subsidence curves, calculated using the average of minimum and maximum porosity-depth relationships for the different stratigraphic units. The analysis included attempts to correct for eustatic sea level changes and paleobathymetry, but these corrections hardly exert influence on the tectonic subsidence curves. An important factor, though, concerns the details of the stratigraphic column, in particular the stratigraphic thickness of the different units, chosen to represent the basin. In case of the Huercal Overa and Lorca basins, sufficient data (chapter 4) was available to construct a composite stratigraphic column considered representative for the basin as a whole. In the case of the Fortuna basin, our stratigraphic study (chapter 4) has been limited to its north-eastern basin margin, and the stratigraphic column analyzed represents the stratigraphy of the Fortuna basin around Fortuna and Abanilla rather than the Archena-Mula – Fortuna basin as a whole.

From the subsidence curves it is clear that the basins initiated at the onset of the Tortonian, marked by a gradual tectonic subsidence in the Lorca and Fortuna basins, and more rapid tectonic subsidence in the Huercal Overa basin. From respectively 9.5 and 9 Ma, the rate of subsidence in the Fortuna and Lorca basin increased, and continued until ~7.8 Ma, which was followed by a period of uplift during the latest Tortonian and a second episode of subsidence from the latest Tortonian until the late Messinian (~6 and 5.5 Ma, respectively). The Huercal Overa basin, on the other hand, shows continuous subsidence until ~6.5 Ma. Since the late Messinian, the Fortuna, Lorca and Huercal Overa basins all show continuous uplift.

The Huercal Overa basin reached a maximum tectonic subsidence of up to 1500 m, whilst the Lorca and Fortuna basins show lower values of around 900 and less than 500 m, respectively. This latter lower value may be due to the choice of the stratigraphic column analyzed which, in the present case, represents the northern marginal area rather than the entire Archena-Mula – Fortuna basin. The tectonic subsidence curves presented here confirm the main trends of the subsidence curves from previous studies in the

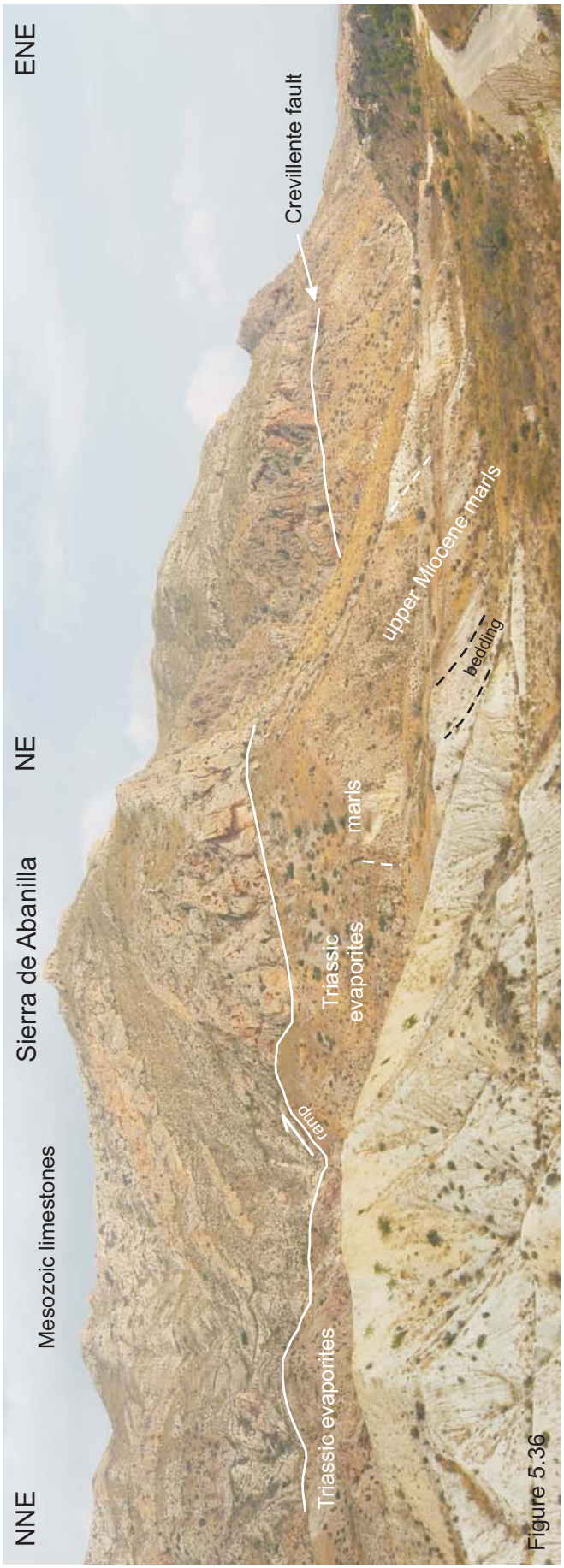

Figure 5.36

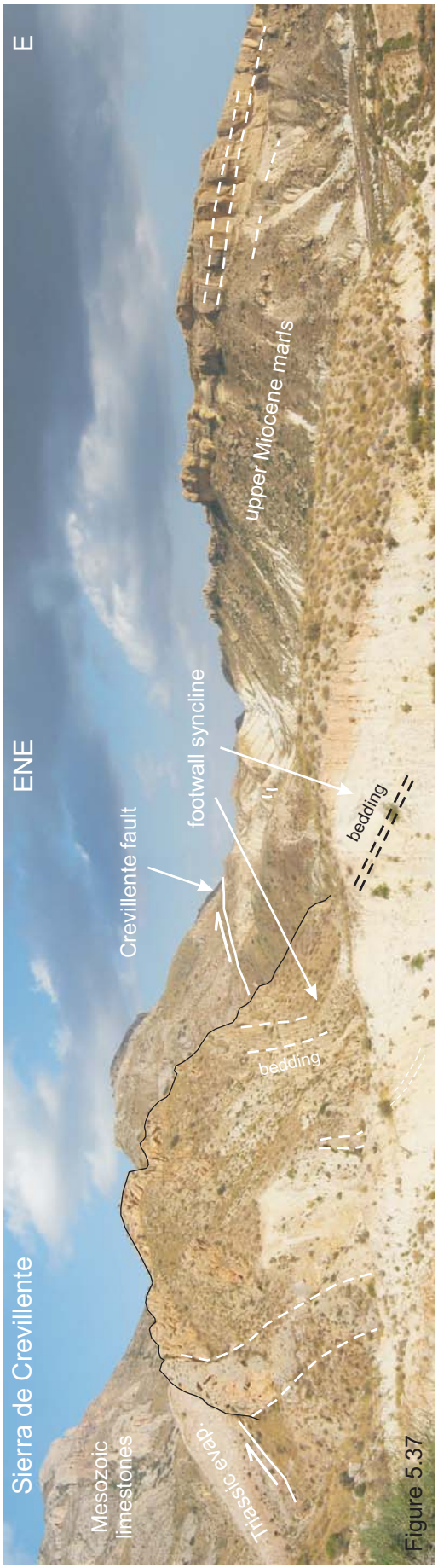

Figure 5.37

Betic basins (e.g., Cloetingh *et al.*, 1992; Rodríguez-Fernández *et al.*, 1999; Garcés *et al.*, 2001; Augier, 2004; see Fig. 5.38). The subsidence curves of these earlier studies, however, show slightly different ages of the 'spikes', i.e., the switches from subsidence to uplift, like for example in tectonic subsidence curves for the Fortuna basin by Cloetingh *et al.* (1992) and Garcés *et al.* (2001). These discrepancies probably result from the use, in these previous studies, of versions of the Neogene time scale that predate the recently improved stratigraphic ages used in this study.

Discussion and conclusions

The large-scale structure of the Huercal Overa basin is that of a half-graben, whilst the Lorca and Fortuna basins show more symmetric geometries. The basins are dominated by a late Miocene to Quaternary basin fill, which points to a late Miocene age of initiation of these basins. However, some of the basins in the Internal Zone preserve relics of the pre-Tortonian stages of basin sedimentation (chapter 4). The pertinent early-middle Miocene sediments now occur as small remnants underneath the latest Serravallian - Tortonian sediments, whilst most of these basins experienced uplift and erosion during the middle Miocene (e.g., Kenter *et al.*, 1990; Sanz de Galdeano and Vera, 1992; Cloetingh *et al.*, 1992; Hanne *et al.*, 2003). The Huercal Overa and Lorca basin, and possibly also the Fortuna basin, may thus have had an earlier history, but most of that history was obliterated during pre-Tortonian uplift and erosion prior to the latest Serravallian - Tortonian subsidence.

The basement beneath the Fortuna and northern part of the Lorca basins is made up of rocks of the External Zone, exposed in the ranges north of the basin. Thrusting and folding of the Mesozoic and Paleogene rocks of the External Zone basement occurred in the early and middle Miocene (Lonergan *et al.*, 1994; Geel and Roep, 1998; chapter 4) and involved N-S to NW-SE directed shortening. The Tortonian sediments unconformably cover and seal the pre-Tortonian compressional structures in the External Zone rocks along the northern margins of the basins.

The basement underlying the Huercal Overa and Lorca basins is largely made up of rocks of the Malaguide and/or Alpujarride Complex of the Internal Zone as exposed in, e.g., the Sierra de las Estancias, Sierra de la Tercia and Sierra Espuña. The structural and metamorphic data from the Alpujarride basement rocks of the Sierra de las Estancias indicate that they became exhumed from synmetamorphic depths of around 12 km to near-surface conditions between 19 and 12 Ma. Exhumation of the basement involved a component of erosion, but also a tectonic component of pervasive ductile to brittle extension and concomitant thinning. This ductile to brittle extension was initially associated with ENE-WSW extension directions, consistent with observations in other Malaguide and Alpujarride rocks in the northern and central parts of the Sierra de las Estancias away from the basins (Lonergan and Platt, 1995; Platzman and Platt, 2004).

Some of the extensional normal fault structures in the basement of the Huercal Overa and Lorca basins were sealed by basal latest Serravallian-Tortonian sediments, others most likely remained active as extension in the basin progressed during sedimentation as evidenced by the syn-sedimentary structures in these basins. The basal deposits contain extensional structures which, like the early set of brittle-ductile extensional structures in the basement rocks, point to an early ENE-WSW to NE-SW direction of extension. We envisage that, at that stage, the basin-bounding faults along the southern margin of the Huercal Overa basin acted as transfer faults. During the Tortonian, in the Huercal Overa and southern part of the Lorca basins the direction of extension must have turned to NNE-SSW to NNW-SSE, as evidenced by the dominant set of E-W trending structures in the late Tortonian sediments and by the second set of mostly brittle extensional structures in the basement rocks and basal conglomerates. In other parts of the Lorca basin the direction of extension remained ENE-WSW,

Figure 5.36. Panoramic view of the Sierra de Abanilla (for location see figure 5.30) showing Mesozoic limestones of the External Zone emplaced on upper Miocene marls as well as on Triassic evaporites. In places, the Crevillente fault dips steeply towards the NNW, but also flattens up-dip, defining a ramp-flat geometry. The Triassic evaporites form part of the footwall and lie structually beneath the upper Miocene sediments. Both the Crevillente fault and faults in the Triassic and Miocene deposits of the footwall contain clear evidence of south directed reverse motion.

Figure 5.37. Panoramic view of the southern flank of the Sierra de Crevillente (for location see figure 5.30). Miocene sediments south of the mountain range dip to the south and gradually steepen towards the mountain range and Crevillente fault, i.e. the sediments delineate an open syncline in the footwall.

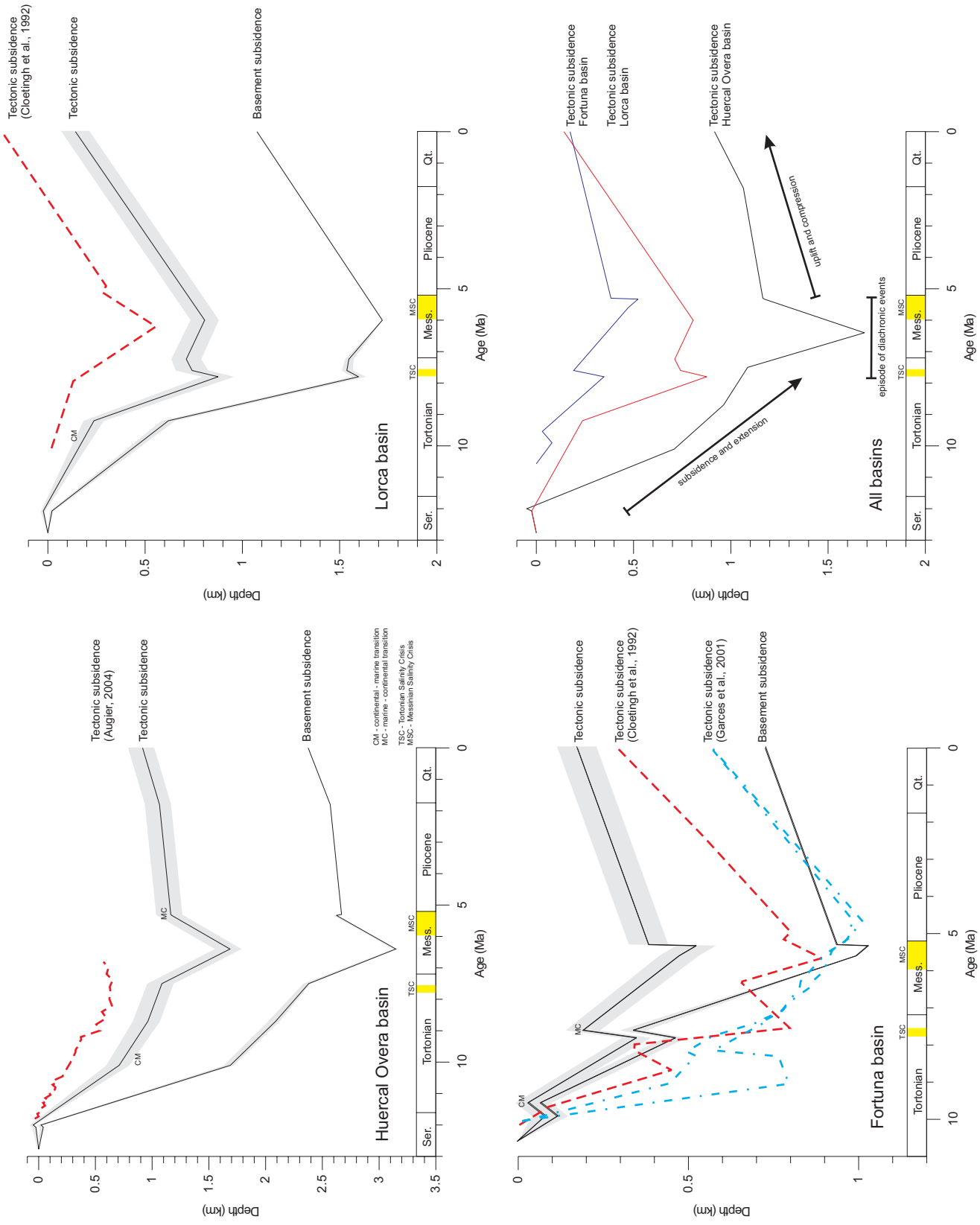
Tectonic subsidence (Cloetingh et al., 1992)
Tectonic subsidence
Basement subsidence
CM
Lorca basin
Depth (km)
Age (Ma)
Ser.
Tortonian
TSC
Mess.
MSC
Pliocene
Qt.
Tectonic subsidence Fortuna basin
Tectonic subsidence Lorca basin
Tectonic subsidence Huercal Overa basin
uplift and compression
subsidence and extension
episode of diachronic events
All basins
Tectonic subsidence (Augier, 2004)
MC
Huercal Overa basin
CM - continental - marine transition
MC - marine - continental transition
TSC - Tortonian Salinity Crisis
MSC - Messinian Salinity Crisis
Tectonic subsidence (Garces et al., 2001)
Fortuna basin

while in the Fortuna basin the direction of extension varied between NW-SE and NNW-SSE near Capres to NE-SW near Macisvenda and Abanilla.

The style of faulting and the magnitude of extension vary over the basins. The style of faulting seems largely related to lithological heterogeneity of the basins sediments. The magnitude of the extension measured in outcrops of faulted sediments shows a range of values in the different stratigraphic units of the basins, but there is no clear increase nor decrease of the stretching values with stratigraphic level. Occasionally, structures in outcrops close to the basin bounding faults show in general high magnitudes of extension, such as e.g. at Macisvenda in the Fortuna basin, at the rambla de Lebor in the Lorca basin (Fig. 5.26) and the southern half of the Huercal Overa basin.

It follows that extension in the basin sediments must in part have been accommodated at depth by ductile to brittle extension of the underlying basement rocks as outlined above, however, it is unclear in how far extension in the basin was accommodated by localized deformation along major detachments deeper in the Betic crust. The frequent occurrence of gypsum blocks and boulders in the basal conglomerates in the southern part of the Huercal Overa basin (chapter 4) may point to tectonic activity along Triassic evaporites of the Alpujarride Complex now exposed in the Sierra Almagro and nearby north-eastern Sierra de los Filabres. On the basis of the present study, however, it is difficult to ascertain if any large-scale detachment like the crustal-scale Betic Movement Zone (Platt and Vissers, 1989; Vissers *et al.*, 1995) actively accommodated for the stretching seen in the Huercal Overa basin. In the Fortuna basin near Macisvenda, on the other hand, extension appears to have been accommodated in particular by the extreme ductility of the underlying Triassic evaporates.

The initial basin subsidence in the early Tortonian coincides with in general NE-SW directed extension, at least in the Lorca and Huercal Overa basins, and a gradual deepening of the basins. The onset of rapid tectonic subsidence in the Tortonian corresponds with a continental-marine facies change and marine transgression which is synchronous in the basins studied (chapter 4), and with a change of the dominant extension direction from roughly NE-SW to N-S.

The rapid subsidence of the marine basins was followed by an initial and relatively short period of uplift which coincides with a second but diachronic transition from marine to continental conditions in the Lorca and Fortuna basins in the late Tortonian. The uplift and deposition of the evaporitic and continental deposits seem to have occurred during a period of relative tectonic "quiescence", i.e. the clearly extensional deformation in the basins had ended. This uplift and associated facies change occurred at an earlier stage in the Fortuna basin in the east and progressed with time via the Lorca basin to the Huercal Overa basin to the southwest (chapter 4).

In a more recent, presumably latest Messinian - early Pliocene to Quaternary stage, the Miocene sediments became folded and faulted, normal faults were reactivated as reverse and strike-slip faults, and the Sierra de la Tercia and Sierra de las Estancias were uplifted due to deformation along the Alhama de Murcia fault zone. This uplift may well have triggered large-scale sliding in the Lorca basin of the Serrata gypsum towards the NW. The folding and reverse and strike-slip motions along the faults relate to N-S to NW-SE directed crustal shortening.

Since the late Messinian, the Huercal Overa, Lorca and Fortuna basins show continuous uplift which more or less coincides with the initiation of compression in the basins and inversion of faults at the basin margins. A similar uplift since the Pliocene has also been documented in other basins in the Betic Cordillera (e.g., Kenter *et al.*, 1990; Cloeting *et al.*, 1992; Rodiguez-Fernández *et al.*, 1999; Garcés *et al.*, 2001), which stresses the regional nature of this event. Note, however, that in earlier studies the onset of uplift and concomitant crustal shortening is inferred to have occurred slightly earlier, i.e., at the Tortonian – Messinian boundary (e.g., Cloeting *et al.*, 1992; Rodiguez-Fernández *et al.*, 1999).

In conclusion, the large scale geometry of the Huercal Overa, Lorca and Fortuna basins, the above extensional structures and analysis of their subsidence history clearly suggests that these basins initially developed as a genuinely extensional basins in the Tortonian and part of the Messinian, and were modified since the latest Miocene – earliest Pliocene by NW-SE directed shortening.

Figure 5.38. Basement and tectonic subsidence curves of the Huercal Overa, Lorca and Fortuna basins, including tectonic subsidence curves of previous studies by Cloetingh et al. (1992), Garces et al. (2001) and Augier (2004). The shaded area marks the error in subsidence limited by the subsidence curves of the minimum and maximum porosity-depth relationships. See text for explanation of the figure.

6

The Alhama de Murcia and Crevillente Faults (Betic Cordillera, SE Spain) and their relationship with Miocene basin development*.

Abstract

The Alhama de Murcia and Crevillente faults in the Betic Cordillera of southeast Spain form part of a network of prominent faults, bounding several of the late Tertiary and Quaternary intermontane basins. Current tectonic interpretations of these basins vary from late-orogenic extensional structures to a pull-apart origin associated with strike-slip movements along these prominent faults. A strike-slip origin of the basins, however, seems at variance both with recent structural studies of the underlying Betic basement and with the overall basin and fault geometry. We have studied the structure and kinematics of the Alhama de Murcia and Crevillente faults as well as the internal structure of the late Miocene basin sediments, to elucidate possible relationships between the prominent faults and the adjacent basins. The structural data lead to the inevitable conclusion that the late Miocene basins developed as genuine extensional basins, presumably associated with the thinning and exhumation of the underlying basement at that time. During the late Miocene, neither the Crevillente fault nor the Alhama de Murcia fault acted as strike-slip faults controlling basin development. Instead, parts of the Alhama de Murcia fault initiated as extensional normal faults, and reactivated as compressional faults during the latest Miocene - early Pliocene in response to continued African-European plate convergence. Both prominent faults presently act as reverse faults with a clear movement sense towards the southeast, which is clearly at variance with the commonly inferred dextral or sinistral strike-slip motions on these faults. We argue that the prominent faults form part of a larger scale zone of post-Messinian shortening made up of SSE and NNW directed reverse faults and NE to ENE trending folds including thrust-related fault-bend folds and fault-propagation folds, transected and displaced by, respectively, WNW and NNE trending, dextral and sinistral strike-slip (tear or transfer) faults.

* In slightly modified form this chapter has been submitted and accepted for publication as: Meijninger, B.M.L., Vissers, R.L.M., *in press*, Miocene extensional basin development in the Betic Cordillera (SE Spain) revealed through analysis of the Alhama de Murcia and Crevillente Faults. Basin Research.

Introduction

The Betic Cordillera of southern Spain, together with the Rif and Tell Mountains in Morocco and Algeria, form the arc-shaped western end of the Alpine orogenic belt (inset of Fig. 6.1), developed since the early Tertiary due to collision of the African and Eurasian plates. The belt can be divided in a non-metamorphic External Zone and a dominantly metamorphic and intensely deformed Internal Zone (Fig. 6.1). The External Zone represents the Mesozoic rifted margin of Iberia (García Hernández *et al.*, 1980; Peper & Cloetingh, 1992), which became folded and thrusted towards the northwest onto the Iberian foreland from possibly the late Oligocene or early Miocene up to the late Miocene (García-Hernández *et al.*, 1980; Banks & Warburton, 1991; Beets & De Ruig, 1992; van der Straaten, 1993; Geel, 1996; Geel & Roep, 1998, 1999; Platt *et al.*, 2003; Guerra *et al.*, 2005). The Internal Zone of the Betic Cordillera has a "Basin and Range" type morphology made up of elongate mountain ranges of mainly metamorphosed Palaeozoic and Mesozoic rocks (e.g., Egeler & Simon, 1969, Platt & Vissers, 1989), which are separated by narrow, elongate basins filled with Neogene to recent continental siliciclastics and marine mixed siliciclastic /carbonate facies, marls and evaporites (e.g., Sanz de Galdeano, 1990; Fig. 6.1).

A notable feature of the south-eastern part of the Betic Cordillera is a NE trending network of prominent major faults with a marked morphological expression, i.e. from NE to SW: the Crevillente fault, the Alhama de Murcia fault, the Palomares fault and the Carboneras fault (Figs. 6.1 and 6.2), which bound several of the late Tertiary (Miocene-Pliocene) and Quaternary basins. Some parts of these faults, i.e. the

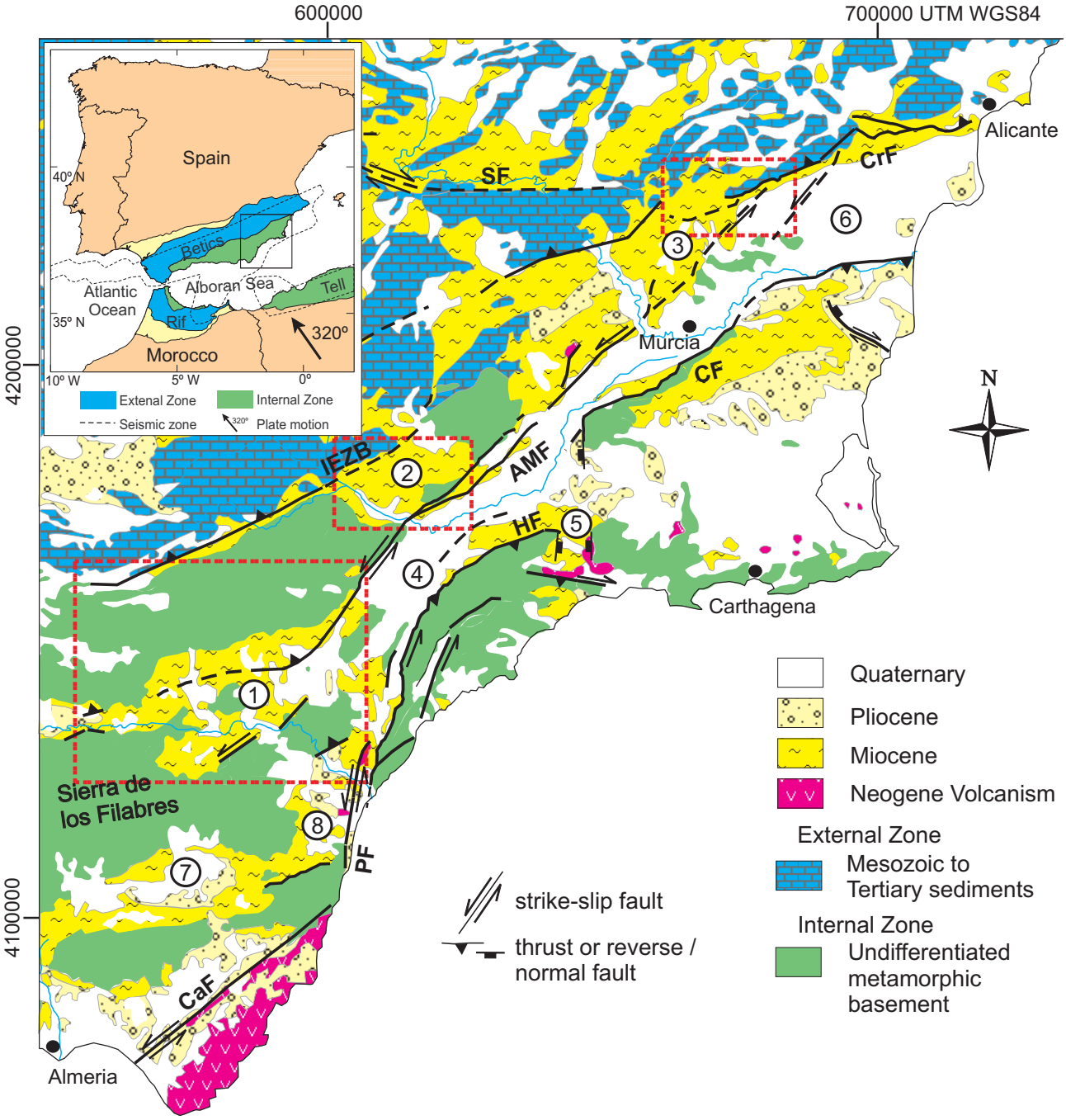

Figure 6.1. Geological map of south-eastern Spain. Numbers: 1) Huercal Overa basin, 2) Lorca basin, 3) Fortuna basin, 4) Guadalentin-Hinojar basin, 5) Mazaron basin, 6) Alicante-Bajo Segura basin, 7) Sorbas-Tabernas basin, 8) Vera basin. Abbreviations: Crf Crevillente fault, CF Carrascoy fault, AMF Alhama de Murcia fault, HF Hinojar Fault, PF Palomares fault, CaF Carboneras fault, SF Socovos fault, IEZB Internal-External Zone Boundary (or North Betic Fault). Modified from Mapa Geologico de la Peninsula Iberica (IGME, 1:1.000.000, 1981), Montenat et al. (1990), de Larouzière et al. (1988) and Gauyau et al. (1977). Seismic zone in inset after Buforn et al. (1988). African-European plate motion vector after DeMets et al. (1994). Frames in Fortuna, Lorca and Huercal Overa basins mark detailed maps of figures 5.4, 5.19 and 5.30, respectively.

Alhama de Murcia, Carboneras and Palomares faults, have been studied in detail and their geometry and kinematics have been documented (e.g., Bousquet & Montenat, 1974; Gauyau *et al.*, 1977; Bousquet, 1979; Rutter *et al.*, 1986; Martínez-Díaz & Hernández Enrile, 1992a; Silva *et al.*, 1992; Keller *et al.*, 1995; Jonk & Biermann (2002), Booth-Rea *et al.*, 2003; Faulkner *et al.*, 2003). Despite these studies, the timing of the initial movements and amounts of displacement on these faults, as well as their relationship with the Neogene basin development, are still a matter of debate.

Several recent studies of the metamorphic rocks from the Internal Zones have provided evidence for rapid exhumation and associated extension of a previously thickened crust (Platt & Vissers, 1989; Jabaloy *et al.*, 1992; Vissers *et al.*, 1995), which started in the late Oligocene – early Miocene and continued well into the Miocene (Monie *et al.*, 1994; Johnson *et al.*, 1997; Lonergan & Johnson, 1998; de Jong, 2003; Platt *et al.*, 2005). Seismic studies of the Granada (Morales *et al.*, 1990; Ruano *et al.*, 2004) and Fortuna-Guadalentin basins (Amores *et al.*, 2001 and 2002), and detailed structural and sedimentological studies, e.g., of the Huercal Overa basin (Mora-Gluckstadt, 1993) demonstrate the existence of late Miocene half graben structures. Seismic surveys in the Alboran Sea have shown similar structures in the Miocene sediments (Comas *et al.*, 1992; Mauffret *et al.*, 1992; Watts *et al.*, 1993). The simultaneous exhumation and thinning of the metamorphic middle to upper crust and the deposition of upper Miocene sediments in an extensional setting suggest a dynamic link: the extensional intermontane basins in fact developed on top of a previously thickened, collapsing or stretching continental crust. In essence, two different models have been proposed to explain the late-orogenic extension in the Internal Zone: removal of a thickened subcontinental lithosphere, either by convection (e.g., Platt & Vissers, 1989) or by lithospheric delamination (e.g., García Dueñas *et al.*, 1992), and subduction roll-back followed by slab-detachment (e.g., Morley, 1993; Lonergan & White, 1997; Spakman & Wortel, 2004). It is emphasized here that the resulting crustal thinning occurred within an overall setting of continuous slow convergence of the African and Eurasian plates.

Montenat *et al.* (1987), Montenat & Ott d'Estevou (1990, 1996 and 1999) and De Larouzière *et al.* (1988), on the other hand, have suggested that the late Miocene intermontane basins, such as the Lorca, Vera, Huercal Overa and Fortuna basins are in fact, respectively, pull-apart, wrench furrow, and compressional and extensional imbricate fan basins (rhomb-graben, "Sillon sur décrochement" and "Queue de cheval" structures at compressional and extensional ends of strike-slip faults), which developed as a result of sinistral movements along the NE trending Alhama de Murcia (Bousquet & Montenat, 1974) and the N trending Palomares (Bousquet *et al.*, 1975) faults, respectively. Both Bousquet and Montenat (1974), Bousquet *et al.* (1975), Gauyau *et al.* (1977), Bousquet (1979), Silva *et al.* (1997), Martínez-Díaz *et al.* (2001), Soler *et al.* (2003) and Masana *et al.* (2004) have shown evidence for intense deformation of Quaternary sediments close to these faults, which demonstrates recent activity of the Alhama de Murcia, Palomares and Carboneras faults. According to, e.g., Bousquet (1979) and Masana *et al.* (2004) such activity may very well be associated with the present-day convergence of the African plate towards Eurasia.

The interpretation, however, of the late Miocene basins as strike-slip controlled pull-apart or compressional basins raises some problems as follows. First, from a structural point of view, many of the late Miocene depocentres such as for example the Huercal Overa, Sorbas, Vera, and Mazaron basins are not located on releasing or restraining bends (Woodcock & Schubert, 1994; Sylvester, 1988) on these faults, as is obvious from comparison of the basin and fault geometries shown in Fig. 6.3.

Secondly, the N-S to NE-SW directed extension implied by extensional normal fault structures in the late Miocene basins as described by, e.g., Balanyá & García-Dueñas (1991), García-Dueñas *et al.*, (1992), Mora-Gluckstadt (1993), Vissers *et al.* (1995), Poisson *et al.* (1999), Augier (2004) and in chapter 5, are in direct conflict with the approximately N-S directed compression that should be associated with a sinistral sense of shear along the Alhama de Murcia and Palomares faults (Figs. 6.3 and 4).

Thirdly, the first-order geometry of the basins at the inferred releasing bends differs from any typical pull-apart basin geometry, and in general the characteristic fault step-over structure (Sylvester, 1988; Dooley & McClay, 1997) seen, e.g., along the San Andreas fault zone, the Dead Sea fault zone or the Abarán basin in the External Zone of the Betics (van der Straaten, 1993), is lacking (Figs. 6.3).

Fourthly, the Lorca basin for example, interpreted as a pull-apart basin by several workers (e.g., Montenat *et al.*, 1990b; Guillén Mondéjar *et al.*, 1995; Krijgsman *et al.* 2000; Vennin *et al.*, 2004), certainly has a rhomboidal shape (Figs. 6.1 and 6.4). Along its

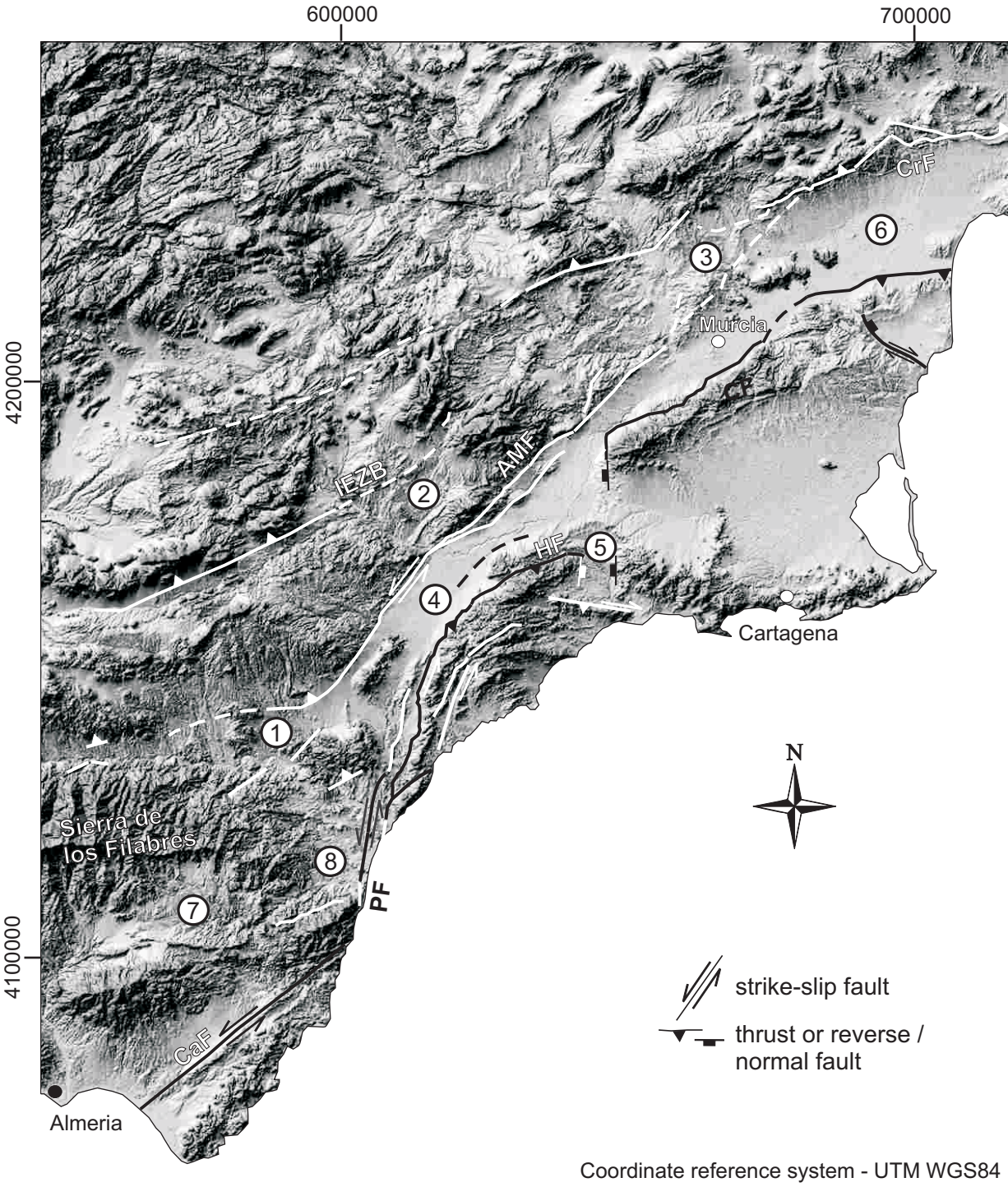

Figure 6.2. Shaded relief model of south-eastern Spain. For numbers and abbreviations see Fig. 6.1.

south-eastern margin, however, the basin is bounded by the Alhama de Murcia fault, which is a continuous fault zone that does not terminate at any of the basin corners (Bousquet, 1979; Silva *et al.*, 1992; Martínez-Díaz & Hernández Enrile, 1992a,b). For the northern margin, De Larouzière *et al.* (1988), Montenat *et al.* (1990b) and Guillén-Mondéjar *et al.* (1995) have suggested that the basin is bound by the NE trending North Betic fault, which they interpret as a sinistral strike-slip fault. On the other hand, according to, e.g., Leblanc & Olivier (1984) and Guillén-Mondéjar *et al.* (1995) the North Betic fault has a dextral sense of shear as opposed to the sinistral movement sense of the Alhama de Murcia fault (Fig. 6.4). Aside the fact that these inferred movement senses are as yet poorly substantiated by structural studies, the opposing

movement senses of the faults at the northern and southern sides of the basin are at variance with the motions expected for a pull-apart fault system. In addition, the inferred North Betic fault (NBF) is virtually continuous with the south directed thrusts of the Internal External Zone Boundary (IEZB; Figs. 6.1 and 6.4), and this structure is unconformably sealed by middle Miocene to Quaternary sediments such that it cannot have played an active role in the development of the Lorca basin during the late Miocene (Lonergan *et al.*, 1994; Geel & Roep, 1998 and 1999).

Finally, a fifth problem concerns recent paleomagnetic data from upper Miocene basin sediments and volcanic deposits suggesting that no rotations occurred during the late Miocene (Krijgsman & Garcés, 2004 and Fig. 6.4) or at least not until after the Tortonian (Calvo *et al.*, 1994 and 1997 and Fig. 6.4), whilst field studies as well as analog and numerical modelling (e.g., Hall, 1981; Ron *et al.*, 1984; Garfunkel and Ron, 1985; Schreurs, 1994; Waldron, 2004) suggest that such rotations are to be expected in sediments deposited in a strike-slip tectonic setting.

Recent structural studies of the major fault systems in SE Spain have so far mainly focussed on the Carboneras (Rutter *et al.*, 1986; Keller *et al.*, 1995; Bell *et al.*, 1997, Scotney *et al.*, 2000; Reicherter & Reiss, 2001; Faulkner *et al.*, 2003) and Palomares faults (Weijermars 1987; Jonk & Biermann, 2002; Booth-Rea *et al.*, 2003). Except for few detailed studies of a small segment of the Alhama de Murcia fault by Rutter *et al.* (1986), Martínez-Díaz & Hernández Enrile (1992a) and Martínez-Díaz (2002), there are virtually no structural data documented from the Crevillente and Alhama de Murcia faults. Aside the allegedly dextral Crevillente fault (e.g., De Smet, 1984), it has been generally accepted that most of the major faults in the SE Betics represent sinistral strike-slip faults, that they are part of a crustal-scale transcurrent shear zone (Montenat *et al.*, 1987; De Larouzière *et al.*, 1988), and that they essentially controlled the development of the late Miocene basins. Alternatively, Vissers *et al.* (1995) and Calvo *et al.* (1997) have suggested that the activity on these faults is essentially latest Miocene to Quaternary, i.e. after most of the Miocene basins had ceased to be active depocentres, and that motion on these faults largely reflects the recent stages of ongoing Africa-Europe convergence.

In this paper we focus on the geometry and kinematics of the prominent faults and on the late Miocene basin fill and basin structure, with the aim to elucidate the relationship between Miocene basin development and the development of the prominent faults. The three basins of interest, the Huercal Overa, Lorca, and Fortuna basins, are situated, respectively, at the end of the Alhama de Murcia fault, alongside the Alhama de Murcia fault and in between the Alhama de Murcia and Crevillente faults. We summarise previous and new data on the basin fill and its structure in each of the three basins, with emphasis on the geometry, kinematics and structural history of the major faults. We conclude that during the Miocene (late Serravallian – late Tortonian) the Huercal Overa, Lorca and Fortuna basins developed as extensional basins, presumably associated with the thinning and exhumation of the underlying basement. During the Tortonian, neither the Crevillente fault nor the Alhama de Murcia fault acted as strike-slip faults controlling basin development. Instead, parts of the Alhama de Murcia fault came into existence as extensional faults, and these were reactivated as oblique contraction faults in the latest Miocene - early Pliocene, in response to the continued African-European plate convergence. Both prominent faults presently act as reverse faults with a clear movement sense towards the southeast, as opposed to the generally assumed dextral or sinistral strike-slip motion. We argue that these reverse faults form part of a larger scale zone of post-Messinian shortening made up of SSE and NNW directed thrusts and NE to ENE trending folds including thrust-related fault-bend folds and fault-propagation folds, displaced by NNE trending sinistral and (mostly outcrop-scale) W to WNW trending dextral strike-slip (tear or transfer) faults, respectively.

In order to determine the sense of shear of faults in the Miocene basins and the kinematics of the prominent Crevillente and Alhama de Murcia faults we have studied both structures on fault planes (such as tensile fractures, Riedel fractures, striations) and shear structures in fault gouges (Riedel, P, Y, R_2 and X shears and striations on these shear planes) as described by e.g., Logan *et al.* (1979), Rutter *et al.* (1986), Gamond (1987), Hancock (1987), Petit (1987), Means (1987), Sylvester (1988), and Woodcock & Schubert (1994).

Basin stratigraphy

The Miocene and Pliocene stratigraphy of the Fortuna, Lorca and Huercal Overa basins and the geometry of the Lorca and Huercal Overa basins in particular have been thoroughly studied and documented (Geel, 1976; Briend, 1981; Briend *et al.*, 1990;

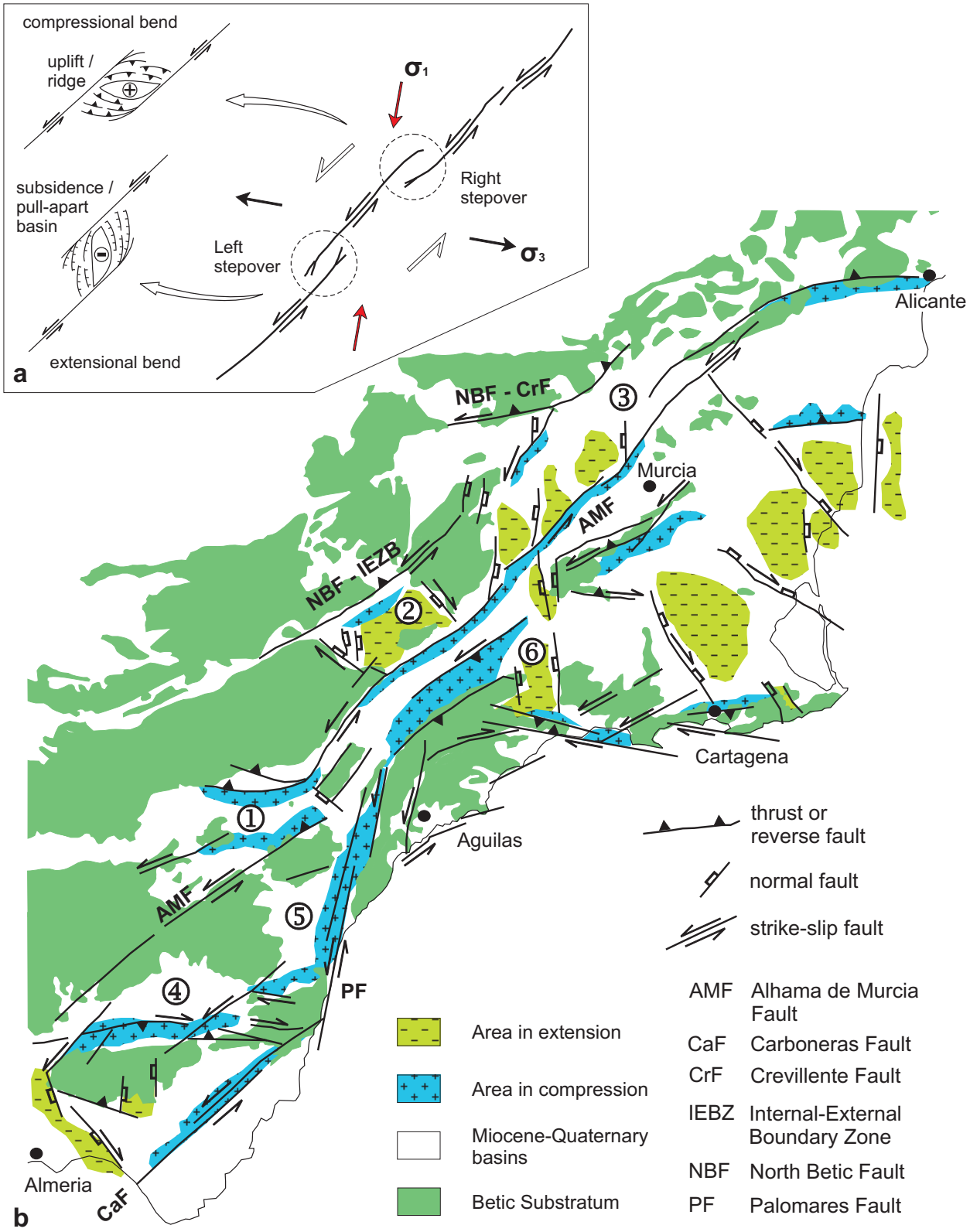

Figure 6.3. a) Sketch map illustrating how regional sinistral shear, shown for an orientation similar to the Alhama de Murcia fault, can be distributed along fault segments that are not coplanar. Slip is relayed from one segment to another at a stepover. At a restraining stepover, compression and thrusting occur, resulting in a ridge. At a releasing stepover, extension and subsidence occur, resulting in a pull-apart basin. Maximum and minimum principal stress axes are shown consistent with Andersonian faulting. b) Tectonic map of south-eastern Spain, after Montenat et al. (1987). Numbers: 1) Huercal Overa basin, 2) Lorca basin, 3) Fortuna basin, 4) Sorbas basin, 5) Vera basin, 6) Hinojar - Mazaron basin.

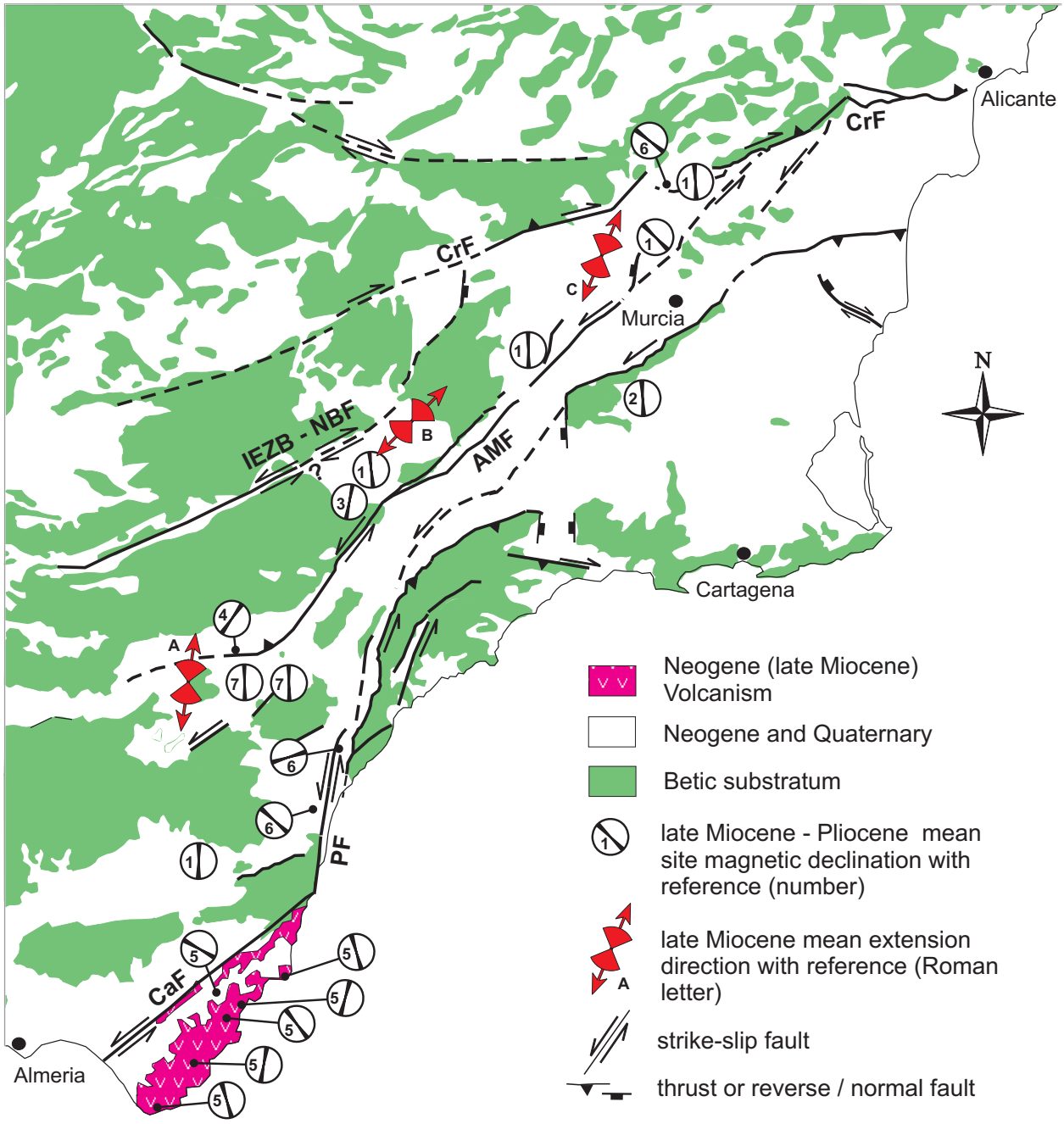

Figure 6.4. Tectonic map of south-eastern Spain showing average Miocene extension directions and paleomagnetic rotations. NBF North Betic Fault, for other abbreviations see Fig. 6.1. Miocene extension directions are derived from tectonic structures in Miocene basin sediments (this study) and from literature; (A) Mora-Gluckstadt (1993), Augier (2004) and this study (chapter 5), (B) Booth-Rea et al. (2002) and this study (chapter 5), and (C) Poisson and Lukowski (1990) and this study (chapter 5). Paleomagnetic rotations from (1) Krijgsman et al. (2004), (2) Krijgsman et al. (in press), (3) Dinares-Turell et al. (1997), (4) Mora-Gluckstadt (1993), (5) Calvo et al. (1994), (6) Calvo et al. (1997) and (7) Meijninger et al. (in prep.).

Montenat *et al.*, 1990b; Lukowski & Poisson, 1990; Poisson & Lukowski, 1990; Mora-Gluckstadt, 1993; Geel & Roep, 1998; Rouchy *et al.*, 1998; Geel & Roep, 1999; Wrobel & Michalzik, 1999; Krijgsman *et al.*, 2000; Wrobel, 2000; Vennin *et al.*, 2004; Augier, 2004; chapter 4). In map view, the Fortuna, Lorca and Huercal Overa basins have a rhomboidal shape with an ENE trending basin axis (overview in Fig. 6.1, details in Figs. 5.4, 5.19 and 5.30). In cross-section, the Fortuna and Lorca basins have a symmetric geometry of a 10 km scale, very open synform (Montenat *et al.*, 1990b; Poisson & Lukowski, 1990; Wrobel & Michalzik, 1999). The Huercal Overa basin, however, shows a clearly asymmetric (half-graben) geometry with mostly south-dipping strata. The Fortuna basin is fault-bounded at its northern and southern sides (Lukowski & Poisson, 1990). The Huercal Overa and Lorca basins are fault-bounded at their southern sides, whilst at their northern margins the Miocene sediments lie unconformably on basement rocks of, respectively, the Internal and the External Zone (Briend 1981; Mora-Gluckstadt, 1993; Geel, 1976).

Within the basins studied here, early Miocene sediments are only exposed along the northern margin of the Lorca basin, which have been deposited prior to the development of the Lorca basin (Geel & Roep, 1998 and 1999). These deposits include Aquitanian and Burdigalian marine sediments that are cut by a low-angle, south directed thrust of the IEZB and are tectonically overlain by Mesozoic limestones of the External Zone (Lonergan *et al.*, 1994).

The lower Miocene sediments and the basement rocks of the External and the Internal Zone along the northern Lorca basin margin are unconformably overlapped by middle Miocene (upper Langhian and Serravallian) marine sediments deposited in a prograding delta system (Geel & Roep, 1999). Stratigraphically upwards, these sediments pass into a thick series of continental alluvial fan and playa/sabkha deposits. As compared to the lower Miocene sediments, the detritus of these continental deposits is markedly polymict and includes material derived from both the External and the Internal Zone. The precise age of the continental deposits is unknown, but part of the metamorphic detritus in the Lorca and Huercal Overa basins clearly originates from the Sierra de los Filabres in the Internal Zone (Fig. 6.1). According to Johnson *et al.* (1997) the greenschist facies metamorphic rocks of the Sierra de Los Filabres cooled to near-surface temperatures during the mid-Serravallian (12±1 Ma), which is consistent with a late Serravallian to early Tortonian age for the continental sediments containing this Filabride detritus.

Both lower-middle Miocene sediments and Internal-External Zone basement rocks are unconformably overlain by Tortonian transgressive marine sediments. Along the margins of the basins, prograding reefs and submarine fans interfinger with marine pelagic marls and turbidites in the central parts of the basins (Geel, 1976; Briend, 1981; Briend *et al.*, 1990; Lukowski & Poisson, 1990; Vennin *et al.*, 2004).

In the Fortuna and Lorca basins the upper Tortonian marine sediments change stratigraphically upwards into a regressive sequence of mixed continental alluvial and lacustrine/shallow marine diatomite-evaporitic deposits of late Tortonian to early Pliocene age (Lukowski & Poisson, 1990, Poisson & Lukowski, 1990; Rouchy *et al.*, 1998; Krijgsman *et al.*, 2000; Garcés *et al.*, 2001). In the Huercal Overa basin, marine conditions persisted well into the early Messinian, and were followed by a rapid shallowing (Briend, 1981; Briend *et al.*, 1990). Uppermost Miocene - Pliocene continental alluvial and shallow marine deposits partly cover and fill a late Miocene paleorelief (Briend, 1981; Briend *et al.*, 1990; García-Meléndez *et al.*, 2003).

Both Miocene and Pliocene sediments are covered by Quaternary continental alluvial fans and travertine deposits and have been subsequently incised by Quaternary rivers (Briend, 1981; Briend *et al.*, 1990; Stokes & Mather, 2003).

Basin structure and geometry and kinematics of the prominent faults

Middle and upper Miocene sediments unconformably overlie lower Miocene deposits and thus seal lower Miocene compressional structures (Lonergan *et al.*, 1994). The upper Serravallian to upper Tortonian sediments of the Fortuna, Lorca and Huercal Overa basins contain clear evidence for syn-sedimentary extensional tectonics in the form of a variety of structures at outcrop as well as at larger scales, including large-scale roll-overs and growth-fault structures (chapter 5). The extensional structures in the upper Serravallian to upper Tortonian basin sediments, as well as the fault-bounded southern side of the Huercal Overa basin show sets of dip-slip shear indicators (Fig. 5.17). Moreover, in the eastern part of the Lorca basin in the Rambla de Lebor, a marked stratigraphic expansion of Tortonian sediments, in part accommodated by normal faults, occurs towards the Alhama de Murcia fault (Fig. 5.26). The

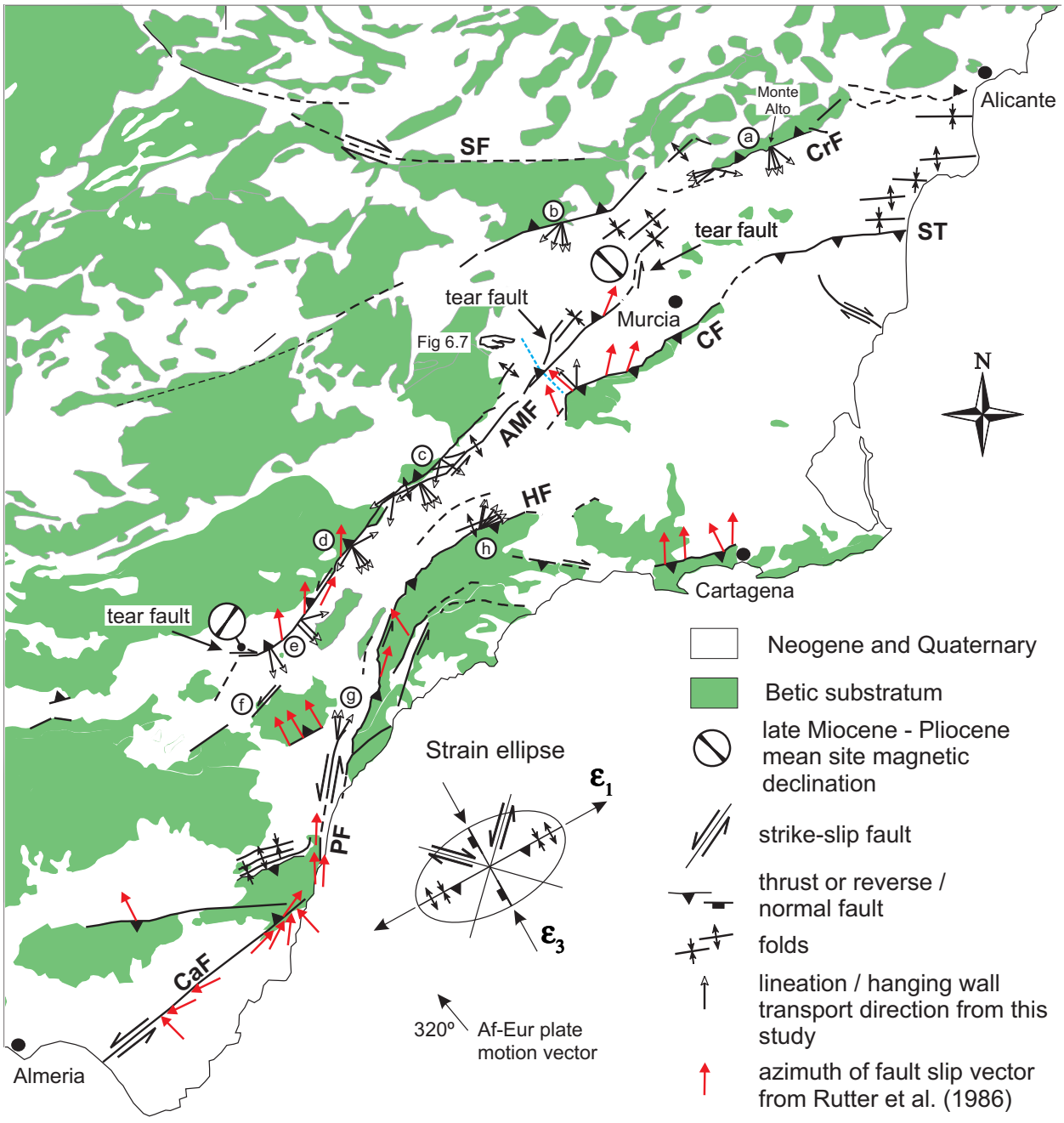

Figure 6.5. Tectonic map of south-eastern Spain. For abbreviations see Fig. 6.1. Slip vectors shown represent either group average or single measurements, based on striations on fault surfaces and shear planes in fault gouges or movement directions determined from Riedel shear and P-foliation geometries in fault gouges. Roman letters refer to stereographic projection plots of fault measurements shown in Fig. 6.6. Paleomagnetic rotations from Krijgsman et al. (2004) and Mora-Gluckstadt (1993). Strain ellipse based on structural data and on fault-plane solutions from Jimenez-Munt et al. (2001), Stich et al. (2003) and Buforn et al. (2004). African-European plate motion vector from DeMets et al. (1994).

orientations of the extensional structures in the Miocene basins vary, but lineations and shear senses are in general consistent with a NNE to ENE extension direction (Figs. 5.4, 5.19 and 5.30). The faulted upper Miocene sediments are unconformably overlain by uppermost Miocene and Pliocene sediments, which poses a lower bound to the age of the extensional deformation.

In the surrounding basement rocks of both the Internal and External Zones, earlier (ductile) deformational structures are overprinted by brittle extensional structures. Like the extensional structures

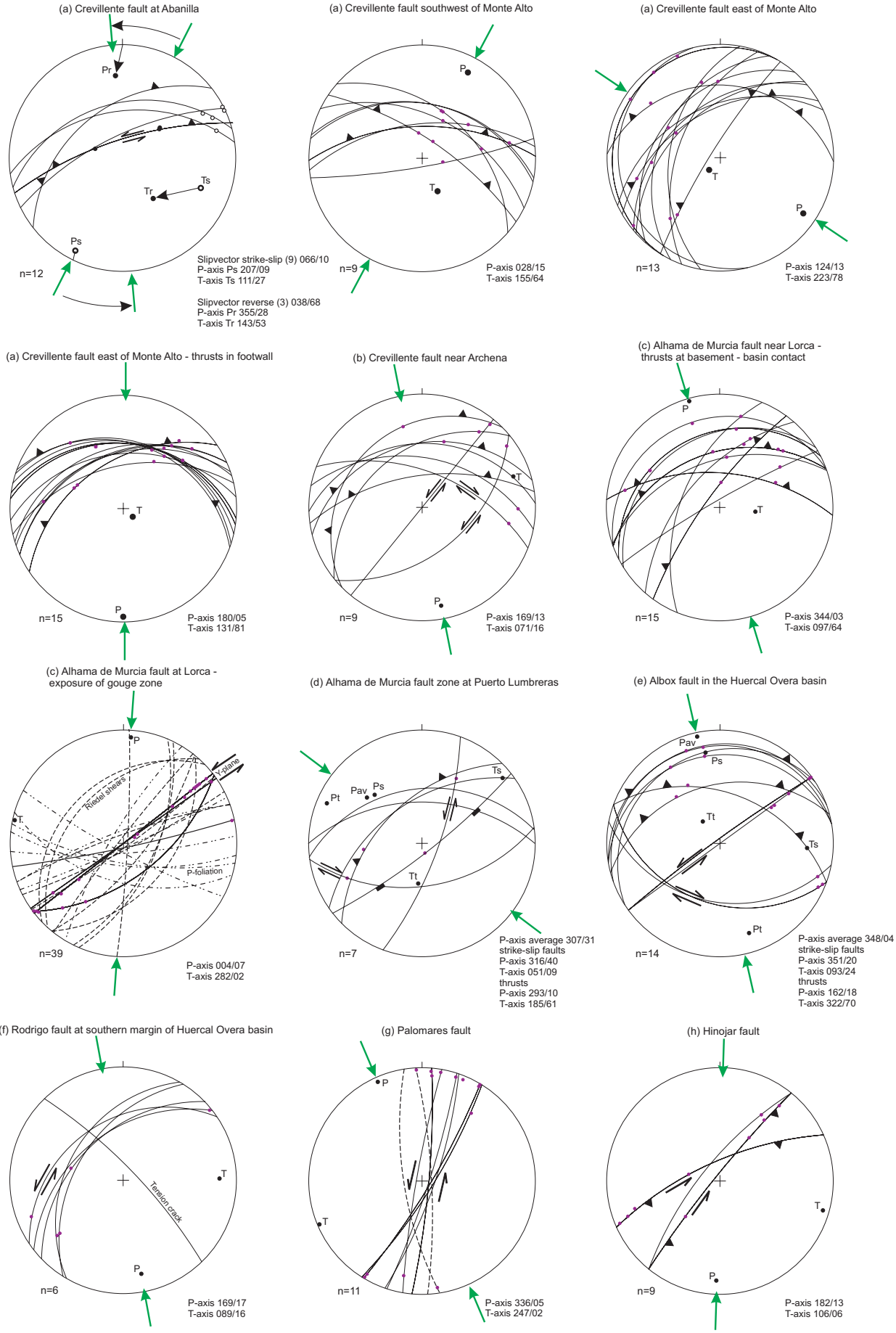
(a) Crevillente fault at Abanilla
Pr
Tr
Ts
Ps
n=12
Slipvector strike-slip (9) 066/10
P-axis Ps 207/09
T-axis Ts 111/27
Slipvector reverse (3) 038/68
P-axis Pr 355/28
T-axis Tr 143/53
(a) Crevillente fault southwest of Monte Alto
P
T
n=9
P-axis 028/15
T-axis 155/64
(a) Crevillente fault east of Monte Alto
T
P
n=13
P-axis 124/13
T-axis 223/78
(a) Crevillente fault east of Monte Alto - thrusts in footwall
T
P
n=15
P-axis 180/05
T-axis 131/81
(b) Crevillente fault near Archena
T
P
n=9
P-axis 169/13
T-axis 071/16
(c) Alhama de Murcia fault near Lorca - thrusts at basement - basin contact
P
T
n=15
P-axis 344/03
T-axis 097/64
(c) Alhama de Murcia fault at Lorca - exposure of gouge zone
P
R
Y-plane
Riedel shears
T
P-foliation
n=39
P-axis 004/07
T-axis 282/02
(d) Alhama de Murcia fault zone at Puerto Lumbreras
Pt
Pav
Ps
Ts
Tt
n=7
P-axis average 307/31
strike-slip faults
P-axis 316/40
T-axis 051/09
thrusts
P-axis 293/10
T-axis 185/61
(e) Albox fault in the Huercal Overa basin
Pav
Ps
Tt
Ts
Pt
n=14
P-axis average 348/04
strike-slip faults
P-axis 351/20
T-axis 093/24
thrusts
P-axis 162/18
T-axis 322/70
(f) Rodrigo fault at southern margin of Huercal Overa basin
T
Tension crack
P
n=6
P-axis 169/17
T-axis 089/16
(g) Palomares fault
P
T
n=11
P-axis 336/05
T-axis 247/02
(h) Hinojar fault
T
P
n=9
P-axis 182/13
T-axis 106/06

in the upper Miocene sediments, these latter brittle structures are consistent with an approximately ENE to NE or NE to NNE directed extension (Mora-Gluckstadt, 1993; García-Dueñas *et al.*, 1992; Vissers *et al.*, 1995; Booth-Rea *et al.*, (2002); Platzman & Platt, 2004; Augier, 2004; chapter 5).

As opposed to these extensional structures, the geometry and kinematics of the morphologically prominent faults bounding the Fortuna, Lorca and Guadalentin-Hinojar basins indicate that they are in fact thrusts or reverse faults (Fig. 6.5). Lineations on fault surfaces as well as shear senses in fault gouges associated with these prominent faults systematically indicate hanging wall transport directions towards the S to SE (Crevillente and Alhama de Murcia faults; Fig. 6.6a-e) or the N (Hinojar fault; Fig. 6.6h), which is largely consistent with observations of, e.g., Rutter *et al.* (1986), also shown in Fig. 6.5. Segments of the Alhama de Murcia and Crevillente faults, for example, accommodate a southward movement of the hanging-wall basement of respectively the Sierra de la Tercia and the Sierra de Crevillente on steeply north-dipping reverse faults (Fig. 5.29 and 5.35). Along the northern sides of these ENE trending ranges, upper Miocene sediments lie unconformably on the basement rocks but are now tilted to the north. Upper Miocene sediments in the footwall are steeply tilted to the south and are folded along a NE to ENE trending fold axis associated with an ENE trending footwall syncline. The (syn-sedimentary) extensional structures in the upper Miocene sediments are tilted and folded or, in the footwall, have been reactivated as reverse faults. Balanced cross-sections of the essentially asymmetric antiformal Sierra de la Tercia and Sierra Crevillente suggest that their main structure is in fact thrust-related: a fault propagation fold in case of the Sierra de la Tercia and a fault-bend fold in case of the Sierra de Crevillente. We estimate that these thrust-related fold structures accommodated at least 1600 m of shortening in the Sierra de la Tercia, and at least 1000 m shortening in the Sierra de Crevillente.

In the Fortuna basin, and between the city of Murcia and the Lorca basin, the Alhama de Murcia and Crevillente faults are in fact fault zones that consist of a series of en-echelon stepping or parallel running thrusts and folds (see also Bousquet and Montenat, 1974; Gauyau *et al.*, 1977; Bousquet, 1979; Silva *et al.*, 1992; Martínez-Díaz & Hernández Enrile, 1992a,b; Amores *et al.*, 2001 and 2002). These compressional structures are discontinuous along strike, and the shortening is transferred via small and large-scale NNE trending sinistral and mainly small-scale WNW trending dextral strike-slip faults that act as tear or transfer faults (Sylvester, 1988). These latter faults notably show slip vectors that deviate from the transport direction on the main fault (Fig. 6.5). Aside these outcrop data, a seismic profile across the Fortuna basin and the Alhama de Murcia fault southwest of Murcia (Amores *et al.*, 2001; Fig 6.7) clearly shows a series of NW-dipping reverse faults that mark the position of the Alhama de Murcia fault zone. This seismic profile shows three other important aspects of the Alhama de Murcia fault zone, i.e., (1) a listric geometry of the faults of this fault zone, (2) a conspicuous thickening of middle and late Miocene sediments in the hanging wall towards the fault zone, and (3) intraformational unconformities, all indicating that the Alhama de Murcia fault initially acted as an extensional structure, i.e., as a growth fault.

Along the southern margin of the Lorca basin and along the Sierra de las Estancias, the Alhama de Murcia fault is a morphologically sharp, NE trending linear structure (Bousquet & Montenat, 1974; Fig. 6.2) associated with the contact of basement and Quaternary basin sediments, and defined by a steep NW dipping fault (Figs. 6.6c-d and 5.18). Kinematic indicators consistently indicate a sinistral reverse movement on this fault. Scarce outcrops of steeply tilted Miocene sediments of the footwall, oriented parallel to the main fault, reveal both layer-parallel reverse and sinistral shear senses and are cut and displaced by NNE trending sinistral and WNW trending dextral strike-slip faults.

The Huercal Overa basin straddles the south-western end of the Alhama de Murcia fault (Figs. 6.1 and 6.2), where the fault passes into a ENE to E trending morphological structure in the central part of the basin, which is considered part of the Albox fault (Masana *et al.*, 2005; Figs. 5.12 and 6.6e). Here, upper Miocene sediments are folded in a 100 meter scale monocline with a NNW dipping axial plane. To the west, E-W trending steeply tilted Miocene sediments reveal layer-parallel reverse and dextral shear senses. Southeast of the monoclinic fold, thick Pliocene and

Figure 6.6. Stereographic projections (equal area, lower hemisphere) of faults and lineations in outcrops, and in particular at the basin-basement contacts, along the Crevillente, Alhama de Murcia, Palomares and Hinojar fault zones. For locations see Fig. 6.5. P- and T-axes denote the principal axes of incremental shortening and extension inferred from fault plane orientation, lineations on the fault plane and slip direction, following Marrett and Allmendinger (1990).

Quaternary sediments have been deposited in the eastern part of the Huercal Overa basin. These sediments are occasionally affected by south directed thrusts (García-Meléndez *et al.*, 2002 & 2003; Soler *et al.*, 2003, Masana *et al.*, 2005; Fig. 5.18). Importantly, dip-slip shear sense markers on exposed fault surfaces of the fault-bounded southern side of the Huercal Overa basin are clearly overprinted by kinematic indicators pointing to a sinistral strike-slip motion (Figs. 5.17 and 6.6f).

Segments of the Palomares fault on the eastern margin of the Vera basin are vertical, N to NNE trending sinistral strike-slip faults, as evidenced by kinematic data illustrated in Fig. 6.6g (see also Booth-Rea *et al*. 2003 and 2004). The Palomares fault passes into the NE to E trending Hinojar fault along the southern margin of the Guadalentin-Hinojar basin (Fig. 6.6h).

Discussion

In this study we question current interpretations of the Miocene basins in SE Spain as strike-slip controlled pull-apart or compressional basins. As outlined above, such interpretations are faced with problems regarding the overall geometry of the basins and adjacent bounding faults, as well as with conflicting structural data.

The largely syn-sedimentary extensional structures in the upper Miocene basin sediments are either unconformably sealed by uppermost Miocene to Pliocene sediments, or they have been reactivated since as reverse faults. This interpretation is strongly supported by seismic profiles both onshore (Amores *et al.*, 2001 and 2002; Fig. 6.7) and offshore (Watts *et al.*, 1993; Bourgois *et al.*, 1992; Comas *et al.*, 1992; Woodside & Maldonado, 1992). Evidence of deformed Quaternary sediments close to the Alhama de Murcia and Palomares faults (Bousquet and Montenat, 1974; Bousquet *et al.*, 1975; Gauyau *et al.*, 1977; Bousquet, 1979; Silva *et al.*, 1997; Martínez-Díaz *et al.*, 2001; Soler *et al.*, 2003; Masana *et al.*, 2004; Fig. 5.18) demonstrate recent activity of these faults.

Our structural data indicate that the basins discussed here developed their rhomboidal geometry from the late Serravallian to the late Tortonian in response to approximately N to NE directed extension. This stage of Miocene basin development thus represents a precursor stage to the present-day "Basin and Range" type morphology of the region. We emphasize that the average N to NE oriented extension direction, inferred from extensional faults in the basins and in the underlying basement, is entirely inconsistent with sinistral motion on main faults such as the Alhama de Murcia fault. Consequently, and in view of the various other problems surrounding pull-apart or imbricate fan interpretations of the late Miocene basins as outlined above, we suggest that these basins developed as genuinely extensional basins (half-grabens) until the latest Miocene, a process presumably associated with thinning and exhumation of the underlying basement prior to inversion of both basins and faults.

This raises the question in how far prominent faults such as the Alhama de Murcia and Crevillente faults, or their precursors, played a role in late Miocene basin development. As outlined above, the Alhama de Murcia and Crevillente faults in fact define a fault zone (deformation zone) running from Alicante towards the Huercal Overa basin (Fig. 6.5). This deformation zone embraces a number of discontinuous, ENE to NE trending morphologically prominent reverse faults and thrusts, which bound the northern and/or southern margins of the Miocene-Quaternary basins, as well as folds (mainly in the Fortuna and Alicante basins) and thrust-related folds (Huercal Overa basin, Sierra de la Tercia and Sierra de Crevillente). Similar structures have been observed on seismic profiles onshore and offshore Alicante (Alfaro *et al.*, 2002a,b: the Bajo Segura fault) and the Alboran Sea (Comas *et al.*, 1992). Segments of the Alhama de Murcia and Crevillente faults unequivocally reveal a reverse sense of movement on ENE trending, steeply NNW-dipping faults, accommodating hanging wall movements to the S to SE (Fig. 6.6). These compressional structures are clearly discontinuous along strike, and the associated shortening is transferred via small and large-scale NNE-trending sinistral, and mostly small-scale WNW-trending dextral strike-slip faults (tear or transfer faults). The NNE-trending sinistral Palomares fault is the clearest and largest-scale example of such a transfer fault, as already suggested by Booth-Rea *et al.* (2003). The Palomares fault connects the compressive structures along the southern margin of the Vera basin and/or the Carboneras fault zone with the Hinojar fault at the southern margin of the Guadalentin-Hinojar basin. The existence of such transfer faults is also supported by counter clockwise and clockwise paleomagnetic rotations in the Fortuna (Krijgsman & Garcés, 2004) and Huercal Overa basins (Mora-Gluckstadt, 1993), respectively (Fig. 6.5).

An important notion to be emphasized here con-

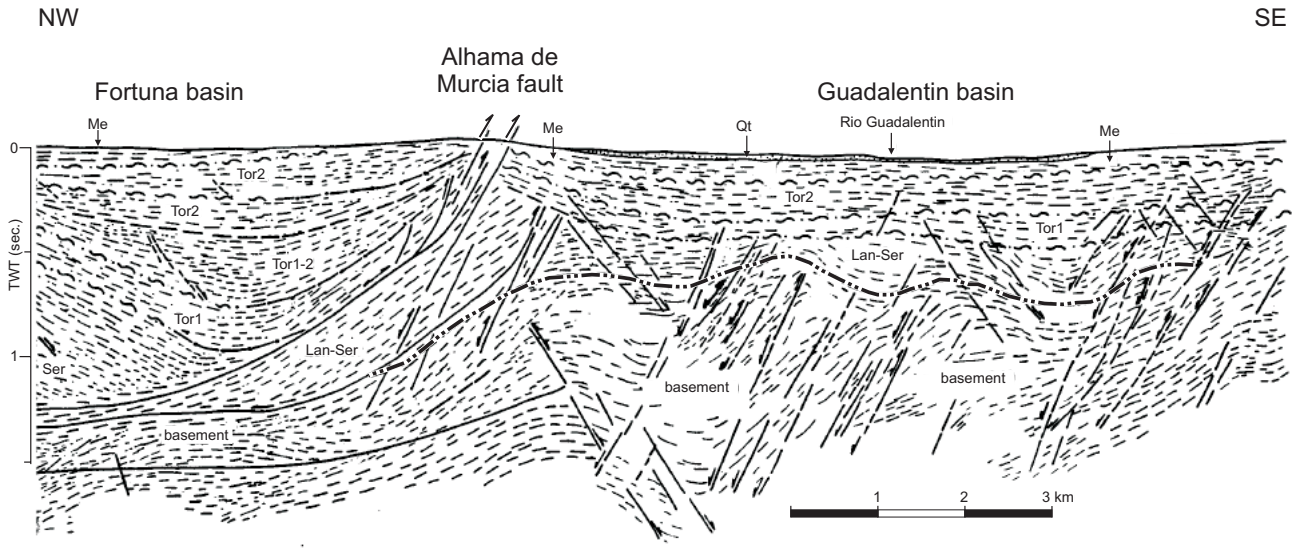

Figure 6.7. Seismic profile across the Fortuna basin, the Alhama de Murcia fault zone and Guadalentin basin. Modified from Amores et al. (2001). For location see Fig. 6.5. Abbreviations: Lan-Ser – Langhian-Serravallian deposits; Tor1, Tor2 – lower and upper Tortonian sediments; Me – Messinian sediments; Qt – Quaternary sediments.

cerns the age of the structure. The Huercal Overa, Guadalentin-Hinojar, Fortuna and Alicante basins form a large ENE to NE trending synclinal depocentre of Plio-Quaternary age, bound by compressive structures along its northern and southern margins (Fig. 6.5). This depocentre was syn-tectonically and progressively filled with Pliocene and Quaternary sediments as demonstrated by Briend (1981), Briend *et al.* (1990), Alfaro *et al.* (2002a,b) and García-Meléndez *et al.* (2002, 2003). The activity of the strike-slip tear/transfer faults started not earlier than the latest Miocene - early Pliocene as substantiated with paleomagnetic data (Calvo *et al.*, 1994 and 1997; Krijgsman & Garcés, 2004), although Booth-Rea *et al.* (2003) suggest a latest Tortonian age for the initial activity of the Palomares fault. In other words, the Alhama de Murcia, Crevillente and Palomares faults clearly form part of a compression zone that initiated at the end of the Miocene or onset of the early Pliocene.

It follows that there are in essence two problems arising from the structural data. First, the late Miocene motions on extensional faults in and adjacent to the late Miocene sediments are inconsistent with sinistral strike–slip on the main faults. Secondly, the geometry and kinematics of most of these main faults are consistent with NNW-SSE directed shortening rather than genuine strike-slip, albeit that the Alhama de Murcia Fault certainly has a component of sinistral strike-slip motion. But more importantly, these main faults became active (or reactivated) in the latest Miocene or early Pliocene, hence motions on these faults postdate late Miocene basin development.

Our inference, that the main faults in fact represent a zone of shortening rather than a strike slip corridor, is consistent with independent observations. First, earthquakes are clearly abundant and distributed over the south-eastern part of the Betic Cordillera (Buforn *et al.*, 1995; Sanz de Galdeano *et al.*, 1995; López Casado *et al.*, 2001; Stich *et al.*, 2003; Buforn *et al.*, 2004; Masana *et al.*, 2004), but the characteristic marked localisation of earthquake epicentres along strike-slip faults, such as seen, e.g., along the North Anatolian fault in northern Turkey or the Dead Sea fault in the Middle East, is lacking, albeit that this localisation along these main faults clearly concerns the large-magnitude earthquakes. Moreover, the absence of earthquakes in the eastern offshore as well as the lack of any strike-slip related submarine morphological structures suggests the absence of any continuation of the Crevillente fault as a strike-slip structure offshore Alicante. Secondly, the orientations and kinematics of the ENE trending thrusts, reverse faults, folds and thrust related faults, and the NNE trending sinistral and WNW trending dextral strike-slip faults are remarkably consistent with a N to NW direction of compression (Giménez *et al.*, 2000; Figs. 6.5 and 6.6), which is supported by fault-plane solutions of recent earthquakes (Buforn *et al.*, 1995; López Casado *et al.*, 2001; Stich *et al.*, 2003; Buforn *et al.*, 2004; Masana *et al.*, 2004) showing a NW to NNW trending compression axis and allied orthogonal extension. This suggests that the present-day, as well as Pliocene to Quaternary, crustal deformations in the Betic

Cordillera are mainly driven by the NW directed convergence of Africa-Eurasian plates (Dewey *et al.*, 1989, DeMets *et al.*, 1994; Mazzoli & Helman, 1994; Jimenez-Munt *et al.*, 2001; Stich *et al.*, 2003).

All available data indicate that the prominent faults such as the Alhama de Murcia fault did not act as sinistral strike-slip faults during the late Miocene, and that their latest Miocene to Quaternary motion was reverse, in places with a sinistral component of motion. An important remaining question, however, concerns the possible role of these faults during the late Miocene. In this context we emphasize the marked stratigraphic expansion of the late Miocene strata seen in the Lebor section near the NE termination of the Sierra de la Tercia as well as in the seismic profile across the Fortuna basin (Figs. 5.26 and 6.7), clearly suggesting that during sedimentation the Alhama de Murcia Fault acted as a growth fault, hence a normal fault. Likewise, the moderately dipping main bounding fault of the Huercal Overa basin separating the basin sediments from the Sierra Almagro to the south (Fig. 5.17) clearly shows a multiple slip history, with early dip-slip, normal fault displacements overprinted by younger kinematic indicators pointing to sinistral strike-slip motion.

On the basis of these data we conclude that the prominent faults may have been active during late Miocene basin development, however, that they did not act as strike-slip faults but principally as normal faults accommodating N to NE directed extension. The basins were thus not generated as strike-slip controlled pull-apart or compressional basins but as truly extensional structures. Many of the prominent faults, commonly referred to as strike-slip faults may indeed have a strike-slip component but are dominated by a reverse component related to latest Miocene to Quaternary shortening. The Palomares fault, however, acted as a transfer fault and is probably one of the very few indisputable strike-slip faults.

Conclusions

We conclude that the late Miocene basins are truly extensional basins developed on an extending underlying crust and lithosphere. This notion is clearly at variance with prevailing interpretations of these basins in the south-eastern Betic Cordillera as pull-apart or compressional basins related to alleged strike-slip motions on the Alhama de Murcia and Crevillente faults. The syn-sedimentary extensional fault structures seen in the late Serravallian to late Tortonian sediments as well as in the underlying basement of the Internal Zone point to approximately NE directed extension, which is in conflict with N-S directed compression necessarily associated with a sinistral sense of shear on the Alhama de Murcia fault. In fact, during the late Serravallian to the late Tortonian, neither the Crevillente fault nor the Alhama de Murcia fault acted as strike-slip faults controlling basin development. Instead, parts of the Alhama de Murcia fault zone initiated as extensional faults, and these were reactivated as oblique contraction faults in the early Pliocene, presumably in response to continued African-European plate convergence. Our structural data indicate that both prominent faults are at present reverse faults, with a clear movement sense of their hanging walls towards the southeast, i.e., they show movement senses that clearly differ from the commonly quoted dextral (Crevillente fault) or sinistral (Alhama de Murcia fault) strike-slip motion. These reverse faults form part of a larger scale zone of post-Messinian shortening, made up of SSE and NNW directed thrusts and NE to ENE trending folds including thrust-related fault-bend folds and fault-propagation folds, displaced by WNW and NNE trending dextral and sinistral strike-slip (tear or transfer) faults, respectively.

7

Synthesis

Introduction

The geometric, kinematic and age data obtained in this study of the south Spanish Neogene basins invite to evaluate the development of these basins in a large-scale geodynamic context. As outlined in the foregoing, the structural and kinematic data from the basins and adjacent basin-bounding faults clearly preclude interpretations of the basins as being the result of progressive deformation in a crustal-scale transcurrent shear zone as suggested by Montenat *et al.* (1987), Montenat and Ott d'Estevou (1990, 1996 and 1999) and De Larouziere *et al.* (1988). Instead, the evidence presented in chapters 5 and 6 indicates that the pertinent large-scale fault network includes reactivated (normal) faults as well as younger faults that in essence post-date the onset of late Miocene basin development. The question therefore remains how the development of the Miocene basins in the Betic Internal Zone can be understood in terms of a large-scale process involving late-orogenic extension in a region dominated by slow, but continuous, plate convergence.

Below we first summarize the main characteristics of the Betic-Rif-Tell orogenic arc and Alboran domain. We then proceed to shortly review current hypotheses concerning the geodynamics of the western Mediterranean and their predicted consequences. Model predictions and comparison with key geological observations form the basis for differentiation between the contending hypotheses. This is followed by a tectonic history of the Alboran region from a basin geology perspective, and a discussion of main geological aspects and their geodynamic significance.

First-order aspects of the Alboran system

Main characteristics

The Betic-Rif-Tell orogenic arc of south-western Europe (Fig. 7.1) shows the following characteristics (e.g., Platt and Vissers, 1989; Comas *et al.*, 1999). The arc is defined by the Pre- and Subbetic rocks of southern Spain, the External Rif in Morocco and the Tell Mountains of north-western Algeria, representing the remnants of the Iberian and African Mesozoic-Cenozoic passive margins, strongly deformed since the latest Oligocene into an *arc-shaped fold-and-thrust belt*. Tectonic transport occurred towards the NW in the eastern Betics, towards the W in the western Betics, towards the WSW and SW in the Rif and towards the S to SSE in the Tell Mountains (e.g., Frizon de Lamotte *et al.*, 2000, Platt *et al.*, 2003 and references therein), i.e., roughly orthogonal to the main trend of the arc. The *internal part of the arc* comprises the Internal or Betic Zone of southern Spain and the Internal Rif in northern Morocco. The pertinent rocks are largely metamorphic, with evidence for Mesozoic to early Tertiary high-pressure low temperature metamorphism suggesting a stage of crustal thickening, pervasively overprinted since the latest Oligocene by ductile and brittle extensional deformation, in part localized along major low-angle detachments that separate higher grade rocks below from low-grade rocks above (e.g., Vissers *et al.*, 1995). The onset of extension was accompanied by the emplacement, into the collisional edifice, of solid bodies of lherzolite at up to asthenospheric temperature, whilst at several localities evidence is found for intermediate to low pressure, high temperature metamorphism of early Miocene age. The eastern Internal Zone of the Betics in particular has a pronounced Basin-and-Range type morphology of elongate mountain ranges of mostly metamorphic rocks flanked by Neogene intramontane basins. The *Alboran basin in the centre of the system* is marked by thin continental crust (13-20 km) including metamorphic rocks entirely similar to those exposed onland in the Internal Zones, a mostly E-W trending horst and graben morphology, and scattered Neogene mafic, intermediate and silicic volcanism. Since the middle Miocene, the basin underwent between 2 and 4 km of subsidence. At first inspection, the arc seems roughly symmetric, but the Internal Zone rocks are unevenly distributed, with virtually no onland exposure east of the Internal Rif.

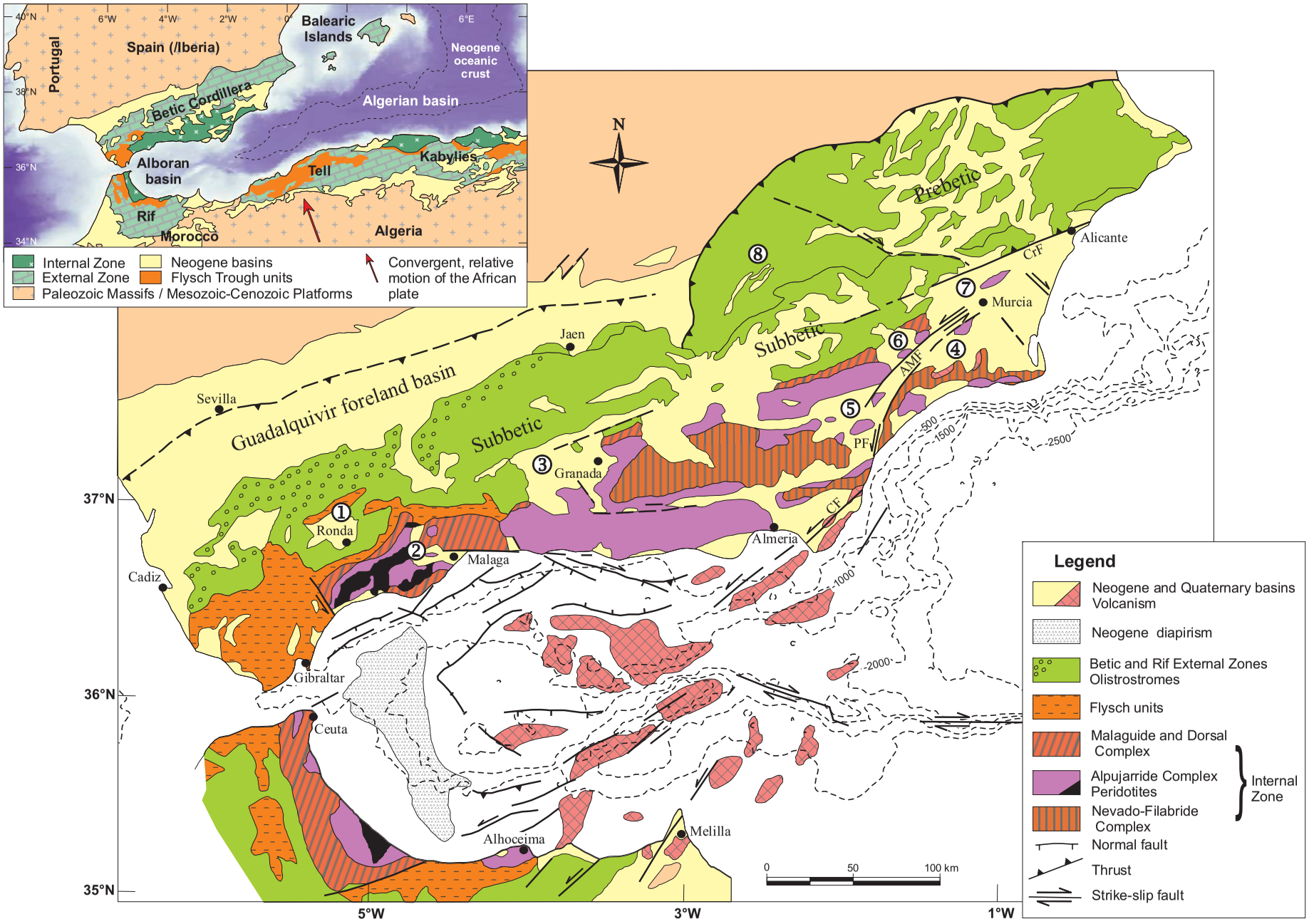
Balearic Islands
Spain (Iberia)
Portugal
Neogene oceanic crust
Algerian basin
Betic Cordillera
Alboran basin
Tell
Kabylies
Rif
Morocco
Algeria
Internal Zone
External Zone
Paleozoic Massifs / Mesozoic-Cenozoic Platforms
Neogene basins
Flysch Trough units
Convergent, relative motion of the African plate
N
Prebetic
Subbetic
Guadalquivir foreland basin
Sevilla
Jaen
Granada
Murcia
Alicante
Almeria
Malaga
Ronda
Cadiz
Gibraltar
Ceuta
Alhoceima
Melilla
CrF
AMF
PF
CF
-500
-1000
-1500
-2000
-2500
37°N
36°N
35°N
5°W
3°W
1°W
0
50
100 km
Legend
Neogene and Quaternary basins Volcanism
Neogene diapirism
Betic and Rif External Zones Olistrostromes
Flysch units
Malaguide and Dorsal Complex
Alpujarride Complex Peridotites
Nevado-Filabride Complex
Internal Zone
Normal fault
Thrust
Strike-slip fault

First-order kinematics

Paleogeographic and tectonic reconstructions of the Alboran region place the Alboran domain and Betic and Rif Internal Zones near the Oligocene Balearic margin (e.g., Sanz de Galdeano, 1990; Lonergan and White, 1997; Geel and Roep, 1998; Rosenbaum *et al.*, 2002a; Meulenkamp and Sissingh, 2003). These reconstructions have been based primarily on striking similarities of the geology of the Betic, Rif and Kabylie Internal Zones, in particular of the Malaguide rocks and the Oligocene – early Miocene sediments, with parts of Calabria, Sicily and Sardinia. The reconstructions imply that the Betic – Alboran – Rif system was transported at least 400 km and possibly as much as 900 km towards the west to its present location (e.g., Sanz de Galdeano, 1990; Lonergan and White, 1997; Spakman and Wortel, 2004). A palinspastic reconstruction using restored sections of the Betic and Rif fold and thrust belt (Platt *et al.*, 2003) places the Internal Zone of the system at least 250 km but possibly 400 km back to the east, which substantiates significant westward transport of the Internal Zones as envisaged in the reconstructions.

External boundary conditions

Analysis of the Africa-Eurasia (Iberia) plate convergence history based on plate motion reconstruction models outlined in chapter 2, and comparison of these results with geological data leads to the following three main conclusions. First, Africa-Iberia plate convergence slowed down and possibly came to a halt during the Neogene in the same period in which the western Mediterranean region began to develop through opening of the Algerian basin and the westward migration of the Betic-Alboran-Rif Internal Zone. Secondly, there is a marked discrepancy between the magnitude of Africa-Iberia plate convergence since the late Oligocene - early Miocene and the amount of shortening documented in the external parts of the Betic-Rif-Alboran system: 150 km up to possibly more than 400 km of shortening in the External Betics and Rif is not accounted for in the plate motion reconstruction models. It follows that the excess shortening must in some way be compensated by extension known to have taken place in the internal parts of the system during the late Oligocene and early Miocene. Thirdly, since the late Miocene the Alboran region is dominated by NW directed Africa-Iberia plate convergence.

Geodynamic models for late-orogenic extension in the Alboran Domain

The complicated history and allied geometry and kinematics of the orogen developed along the Africa-Eurasia plate boundary has been subject of debate and controversy leading to numerous and occasionally contradictory models, including, e.g., an upwelling mantle diapir (van Bemmelen, 1969; Loomis, 1975; Weijermars *et al.*, 1985), and the westward motion of an Alboran microplate (Andrieux *et al.*, 1971). More recently, two competing classes of lithosphere-scale dynamic models have been proposed to explain the Neogene geology of the Betic Rif arc and Alboran Sea: removal of a thickened subcontinental lithosphere, either by (1a) convection (Platt and Vissers, 1989; Houseman, 1996; Fig. 1.2a) or by (1b) lithospheric delamination, leading to extensional collapse of previously thickened crust (e.g., García Dueñas *et al.*, 1992; Docherty and Banda, 1995; Seber *et al.*, 1996; Calvert *et al.*, 2000; Fig. 1.2a), and (2) subduction roll-back followed by slab-detachment (e.g., Morley, 1993; Zeck, 1996; Lonergan and White, 1997; Spakman and Wortel, 2004; Fig. 1.2b). As discussed below, these models predict Neogene extension in the Internal Zone and the coeval development of the Miocene basins, including the Alboran basin, as respectively “collapse basins” or back-arc basins. They can also account for the fact that Neogene extension and thinning of the Internal Betic and Alboran crust were largely coeval with outwardly directed thrusting in the surrounding fold-and-thrust belt, while Africa and Europe converged slowly, hence that extension must have been driven within the system.

Models for late-orogenic extension

The models which can largely explain the late-orogenic extension and the formation of the Alboran basin can be summarised as follows:

(1a) Extension was the result of convective removal in the latest Oligocene of the relatively cold, hence gravitationally unstable lithospheric root of a pre-Miocene collision zone developed in response to

Figure 7.1. Geological map of the Alboran region modified after Sanz de Galdeano et al. (1995). CrF - Crevillente fault, AMF - Alhama de Murcia fault, PF - Palomares fault, CF - Carboneras fault. (1) Ronda basin, (2) Guadalhorce Corridor, (3) Granada basin, (4) Guadalentin-Hinojar basin (5) Huercal Overa basin, (6) Lorca basin, (7) Fortuna basin, (8) Pontones - Santiago de la Espada basin.

Africa-Eurasian plate convergence (Platt and Vissers, 1989; Houseman, 1996). The removed lithospheric part of the root was replaced by hot asthenosphere, resulting in surface uplift of the relatively buoyant and thickened crust and increase of the gravitational potential energy of the remainder lithospheric column, driving (radial) extensional collapse followed by subsidence of the Betic-Alboran crust.

(1b) Extension was a consequence of delamination (or "peeling") of the lithosphere from beneath the Alboran-Betic crust (e.g., García Dueñas *et al.*, 1992; Docherty and Banda, 1995; Seber *et al.*, 1996; Tandon *et al.*, 1998; Calvert *et al.*, 2000). This mechanism, initially proposed by Bird (1978), can be expected to have a similar but more pronounced effect in that in this model removal of the lithospheric mantle occurs at the crust-mantle boundary. In the case of the Alboran region, geological data including seismic profiles and borehole data as well as geophysical data led several authors to suggest a westward migrating delamination process (e.g., García Dueñas *et al.*, 1992; Seber *et al.*, 1996; Calvert *et al.*, 2000), whilst others (e.g., Docherty and Banda 1995; Tandon *et al.*, 1998) have suggested (south)eastward delamination.

(2) Extension was the result of roll-back of a slab of passively subducting oceanic lithosphere. Forces at the retreating subduction zone are transmitted to the overriding plate resulting in back-arc extension. In the case of the western Mediterranean it is suggested that subduction of oceanic crust and lithosphere of the Alp-Tethys ocean initiated in the latest Oligocene near the Balearic Islands and Sardinia to the east. Roll-back of the slab during the Miocene, accommodated by slab detachment and lithosphere tearing along the Balearic margin and African plate boundary, is thought to have occurred to the west-southwest towards the present position of the Betic-Rif arc (e.g., Lonergan and White, 1997; Spakman and Wortel, 2004).

Both mantle delamination and subduction roll-back have received particular attention in the last few years, in view of recent tomography results, surface velocity data (GPS) and seismic surveys west of Gibraltar as follows. Seismic tomography studies of the Alboran region (Blanco and Spakman, 1993; Calvert *et al.*, 2000; Gutscher *et al.*, 2002; Spakman and Wortel, 2004) have provided clear evidence for an east-dipping velocity anomaly beneath Gibraltar and the western Alboran Sea, which turns beneath the Betic Cordillera to an ENE strike and a dip to the southeast. This velocity anomaly is interpreted as a slab of relatively cold subducted oceanic lithosphere and thinned continental crust and lithosphere that belonged to the Alp-Tethys (or Ligurian) ocean and pertinent continental margins. According to Spakman and Wortel (2004), the dimensions of this Betic – Alboran slab (200 km wide by 700-800 km long) agree well with the size and geometry of the western part of the Alp-Tethys (or Ligurian) Ocean in many of the tectonic reconstructions of the Western Mediterranean region (e.g., Rosenbaum *et al.*, 2002a). In addition, tomographic images suggest that below the eastern and central part of the Betic Cordillera the Betic – Alboran slab may have been detached.

Recent studies of surface displacements, derived from global positioning (GPS) surveys, show that the western part of the Alboran region (Gibraltar and part of the Rif) moves towards the west and southwest (~3-4 mm/yr) relative to respectively Iberia and Africa, (Fadil *et al.*, 2006; Fernandes *et al.*, 2006), which is interpreted in terms of a combination of African – Eurasian plate convergence and ongoing westward delamination or roll-back in the western part of the Alboran region. Moreover, seismic surveys offshore in the Gulf of Cadiz and west of Gibraltar show clear evidence of Miocene to recent westward thrusting in the accretionary wedge (Maldonado *et al.*, 1999; Gutscher *et al.*, 2002; Medialdea *et al.*, 2004), which confirms the westward motion of the western part of the Alboran region.

Predicted consequences of the models

Each of the large-scale geodynamic models outlined above explains the tectonics of the western Mediterranean in terms of transient changes in the upper mantle structure of the African-Eurasian convergence zone that seem impossible to test directly. The models each involve a switch from early Tertiary crustal thickening to late-orogenic extension in the late Oligocene – early Miocene and are, at least qualitatively, capable of explaining the overall geometry of the arc, the exhumation of early high pressure rocks in an extensional setting, the development of a large marine basin, and the coeval development of a peripheral fold-and-thrust belt. The models, however, also lead to diverse predicted consequences with regard to, e.g., vertical motions, thermal structure of the lithosphere and the nature and distribution of Neogene volcanism that can be compared with geological and geophysical observations. These aspects, discussed in detail by, e.g., Comas *et al.* (1999) can be summarized as follows.

Convective removal of part of the lithosphere and complete delamination of the lithospheric mantle

along the crust-mantle boundary have many similarities in their predicted consequences for vertical uplift, thermal state of the lithosphere and magmatism, but the effects are more extreme for the case of delamination. Both mechanisms lead to significant surface uplift which, depending on initial thickness and composition of the lithosphere may be as high as 3000 m for the case of delamination, and to heating of the crust and high-temperature metamorphism. Again, heating of the crust can be expected to be more extreme in the case of delamination where it should inevitably lead to widespread crustal melting, possibly enhanced by the ascent of basaltic melts due to decompression melting of the underlying asthenosphere. Roll-back models on the other hand are expected to show much similarity with passive stretching models in which the thermal structure results essentially from stretching unless there is a significant heat input from magmatism. Depending on crustal thickness at the onset of extension, the allied vertical motion is likely to be mainly subsidence, although local uplift may occur in the footwalls of major faults. Coeval magmatism should have a clear subduction signature.

Comparison with model predictions: the Alboran system

Evaluation of the above models on the basis of their predicted thermal and magmatic consequences clearly lies beyond the scope of the present study, and for these aspects the reader is necessarily referred to other workers (e.g., Platt *et al.*, 1998 and 2003; Comas et al, 1999; Turner *et al.*, 1999; Duggen *et al.*, 2004). It is noted, however, that analysis of the Neogene magmatism has as yet led to conflicting conclusions, in that the geochemistry of the magmatic rocks has been considered as being best explained by convective removal by Turner *et al.* (1999) whilst these same magmatic rocks are interpreted by Duggen *et al.* (2004) as being exclusively consistent with a slab roll-back scenario. The early Miocene high-temperature metamorphism, however, seems difficult to explain without the heat input expected from convective removal or delamination (e.g., Comas *et al.*, 1999; Platt *et al.*, 2003), albeit noted that the heat input expected from complete delamination of the lithospheric mantle would probably lead to a much higher degree of crustal melting than observed in the rocks of the Internal Zone.

From a basin geology perspective, the predicted vertical motions clearly provide a basis to discriminate between the above models. A crucial observation in this respect concerns the nature of the early and middle Miocene sediments of the Alboran basin and the onland basins of the Internal Zone. The marked uplift of a collisional ridge in response to either convective removal or delamination in the latest Oligocene should by necessity lead to widespread continental conditions, whilst the early and middle Miocene sediments are almost exclusively marine (see, e.g, Sanz de Galdeano and Vera, 1992; Rodríguez-Fernández et al, 1999; chapter 4). In addition, the late Miocene diachronic marine to continental transition in the eastern Betic basins identified in this study (chapter 4) seems fully consistent with the progressive westward tearing of an underlying slab as interpreted in recent mantle tomography. In view of these basin stratigraphy data, taking the tomography results into account suggesting a coherent east and southeast-dipping slab beneath the Alboran region, and noting the asymmetric distribution of the Internal Zones conveniently explained by slab tearing along the north African margin, we favour to view the history of the late Miocene basins outlined below in a roll-back scenario as envisaged by Lonergan and White (1997) and Spakman and Wortel (2004).

Tectonic history of the Neogene basins

Betic External Zone

Shortening in the External Zone probably initiated in the late Oligocene – early Miocene, close to the Internal – External Zone boundary. The onset of thrusting thus marks the collision of the Betic-Alboran crust with the thinned Iberian continental crust of the External (Subbetic) Zone. Thrusting in the External Zone was mainly directed to the NW and WNW. During the Miocene, the growing fold and thrust belt progressively migrated outward towards the peripheral parts of the External Zone (e.g., Platt *et al.*, 2003; see also chapter 3). Most of the shortening in the External Zone as well as the observed clockwise rotations about vertical axes occurred during the early and middle Miocene (e.g., Allerton *et al.*, 1993; Lonergan and White, 1997; Platt *et al.*, 2003; Krijgsman and Garcés, 2004; Osete *et al.*, 2004; Platzman and Platt, 2004). As shown in chapter 2, African – Eurasian plate convergence during the early and middle Miocene was slow or possibly came to a halt, and the amount of convergence by itself cannot account for the shortening seen in the Betic and Rif External Zones: at least 150 up to possibly 400 km of shortening cannot be explained by African – Eurasian plate convergence.

However, simultaneous with the opening of the oceanic Algerian basin during the early and middle Miocene, the Alboran Domain shows evidence of large-scale east-west directed extension and associated cooling and exhumation of metamorphic rocks of the Internal Zone (e.g., Comas *et al.*, 1999). We therefore envisage that extension and concomitant westward migration of the Internal Zone together with the opening of the Algerian basin are directly related to the excess shortening documented in the External Zones of the system. The early Miocene compressional structures at the Internal - External Zone Boundary are sealed by middle-late Miocene sediments.

Prior to late Miocene folding and thrusting in the peripheral part of the External Zone, a large marine basin made up the northern connection between the Atlantic Ocean and the Mediterranean (the North Betic Strait). Abrupt subsidence of this basin and its development into a genuine foredeep basin during the middle Miocene most likely occurred in response to the forward migrating load, exerted on the Iberian plate by the growing and migrating thrust system. Shallowing of the basin in the late Miocene was immediately followed by the onset of folding and NW directed thrusting in the western Prebetics. The structures addressed in chapter 3 clearly show that the Miocene basins in the Prebetics developed in a compressive setting. Progressive thrusting led to segmentation of the North Betic Strait into smaller basins, gradual incorporation in the growing and migrating Betic fold and thrust belt, and closure of the northern Atlantic-Mediterranean connection in the late Tortonian – early Messinian. Since the Tortonian, the Prebetics have accommodated 50-60 km of NW directed shortening, whilst the Neogene basin sediments have experienced up to 1500 m of uplift.

Internal Zone and Alboran Sea

The bulk of the extension and crustal thinning in the Internal Zone and Alboran crust occurred (intermittently) during the early and middle Miocene (e.g., Docherty and Banda, 1992; Watts *et al.*, 1993; Rodríguez-Fernández *et al.*, 1999; Hanne *et al.*, 2003). This resulted in a weakened and thinned Betic-Alboran crust and a rapid tectonic subsidence of different parts of the Alboran basin. In total, up to 7 km of predominantly (deep) marine, Miocene to recent sediments have been deposited in the Alboran basin. Albeit that the trends and geometries of the extensional structures in the basement and Miocene basins of the Internal Zone and Alboran Sea floor are diverse and complex, there is general consensus that the dominant early-middle Miocene structures reflect E-W to NE-SW directed extension (e.g., Platt and Vissers, 1989; García-Dueñas *et al.*, 1992; Jabaloy *et al.*, 1992; Mauffret *et al.*, 1992; Mauffret *et al.*, 2004). Paleomagnetic declinations, however, of early Miocene mafic dikes in the Malaguide Complex in the western and eastern parts of the Betics point to large clockwise rotations (50° up to 134°; Platzman *et al.*, 2000; Platzman and Platt, 2004) during the early and middle Miocene, indicating that extension in the Internal Zone during this period was in places also NNE-SSW directed (Platzman and Platt, 2004).

Whilst extension at the end of the middle Miocene continued, and the Alboran basin continued to subside (albeit at a slower rate, e.g., Watts *et al.*, 1993; Rodríguez-Fernández *et al.*, 1999; Hanne *et al.*, 2003), the basins of the Betic Internal Zone experienced large-scale uplift and widespread erosion (Sanz de Galdeano, 1990). A new geometry of extensional basins started to develop in the late Serravallian – early Tortonian. A notable aspect of these new, intramontane basins is that the majority of these basins are located in the eastern part of the Betic Cordillera. The intramontane basins, in particular the Huercal Overa and Sorbas – Tabernas basins, were initially filled with large amounts of coarse-clastic continental deposits. These sudden continental conditions seem to have coincided with a marked eustatic sea level drop. The fault structures in the intramontane basins clearly show that the basins initially developed as genuinely extensional basins, probably associated with the thinning and exhumation of the underlying basement at that time (chapter 5). The initiation of the intramontane basins may have occurred synchronically, however, accurate age constraints on the pertinent sediments are lacking. The (syn-sedimentary) extensional structures in the early Tortonian continental basin sediments and in the surrounding basement generally indicate ENE-WSW to NE-SW directed extension and a gradual basin subsidence.

During the early Tortonian, the continental basins gradually changed into marine basins. In the Huercal Overa and Lorca basins, a clear basin-wide dominance of marine conditions does not occur until approximately 10 Ma, which probably also holds for the Guadix-Baza, Fortuna and Murcia-Cartagena basins. In the Vera and Sorbas-Tabernas basins, however, marine transgression seems to have occurred earlier. This marine transgression coincides with a eustatic sea level rise, however, the observed basin subsidence can only in part be explained by a changing sea level,

because the lower to upper Tortonian deposits in the Huercal Overa and parts of the Lorca and Fortuna basins show evidence of (syn-sedimentary) faulting pointing to NNE-SSW to NW-SE directed extension and a concomitant sudden increase in basin subsidence, which call for a tectonic explanation. Note again that this extension is coeval with ongoing late Tortonian thrusting in the External (Prebetic) Zone

From approximately 7.8 Ma (late Tortonian) till the late Messinian, the eastern Betic basins show a diachronic change, from marine to continental conditions, which progressively migrated towards the southwest (Fig. 4.12). In the Fortuna basin, the transition is marked by the deposition of late Tortonian diatomites and evaporites (referred to as the Tortonian Salinity Crisis, Krijgsman *et al.*, 2000), which coincides with cessation of the dominantly extensional deformation in the basin and a short period of abrupt basin uplift. The Lorca basin shows progressive shallowing during the latest Tortonian, but the precise age of the marine to continental transition remains unclear because of localized deformation affecting the contact between the diatomites and overlying evaporites (chapter 5). In contrast, the Huercal Overa basin as well as the Vera and Sorbas-Tabernas basins to the southwest show clear evidence for continued, relatively open marine conditions and basin subsidence during the late Tortonian and early Messinian (Fig. 4.12).

During the Messinian, the Lorca and Fortuna basins continued to act as slowly subsiding, continental depocenters whilst in the Huercal Overa and Vera basins most of the Messinian is absent. From the late Messinian onwards these basins experienced rapid uplift. The Sorbas and Tabernas basins, on the other hand, remained marine basins until the late Messinian (5.60-5.54 Ma; Krijgsman *et al.*, 2001), when massive evaporites mark the onset of a marine-continental transition. This transition coincides with a drastic late Messinian (~5.5 Ma) eustatic sea level drop. The Miocene basins (e.g., Ronda and Quadalquivir basins) and corridors (e.g., Guadalhorce corridor) in the western part of the Betics are the last areas from which the marine waters receded during the latest Miocene and Pliocene (e.g., Serrano Lozano, 1980; Soria *et al.*, 1999; Martín *et al.*, 2001) most likely due to a combination of uplift and eustatic sea level fall.

The late Miocene to recent history of the offshore Alboran basin seems to be somewhat variable, i.e., in some parts of the Alboran basin extension continued during the late Miocene whilst in other parts extension had ceased (e.g., Bourgois *et al.*, 1992; Comas *et al.*, 1992; Tandon *et al.*, 1998; Hanne *et al.*, 2003). Subsidence curves in general show decreasing subsidence of the basins from the late Miocene to recent (e.g., Docherty and Banda, 1992; Watts *et al.*, 1993; Rodriquez-Fernández *et al.*, 1999). The Messinian of the Alboran basin is marked by a distinct unconformity indicating that the basin emerged due to the sea level drop associated with the Messinian Salinity Crisis (e.g., Comas *et al.*, 1992; Rodriquez-Fernández *et al.*, 1999).

From the Pliocene onward, the Betic basins show uplift (e.g., Cloetingh *et al.*, 1992; Rodriquez-Fernández *et al.*, 1999; Braga *et al.*, 2003; Martín *et al.*, 2003; Sanz de Galdeano and Alfaro, 2004) and receive continental, alluvial and fluvial sediments. However, some basins such as the Huercal Overa Vera, and Fortuna basins may have experienced a short marine incursion in the earliest Pliocene, which consequently may have coincided with a Pliocene eustatic sea level rise, and was shortly followed by again continental conditions. The Alboran basin, on the other hand, was re-flooded in the Pliocene and has since remained a marine basin.

During the latest Miocene to Pliocene, there is a marked change in the Internal Zone and Alboran domain from an overall extensional tectonic setting to roughly NW-SE directed shortening. Onland, the Alhama de Murcia and Crevillente faults initiated or reactivated during the late Messinian – early Pliocene as contractional faults with a clear movement sense towards the southeast. These prominent faults form part of a larger-scale zone of post-Messinian shortening made up of SSE and NNW directed reverse faults and NE to ENE trending folds, transected and displaced by respectively WNW and NNE trending, dextral and sinistral strike-slip (tear or transfer) faults (chapter 6). In the Alboran basin, Miocene sediments are folded, strike-slip faults developed, and some of the Miocene extensional faults became inversed (e.g., Campos *et al.*, 1992; Comas *et al.*, 1992, Alfaro *et al.*, 2002). The data seem to indicate that during the latest Miocene the extensional domain in the internal part of the arc became progressively smaller, and that crustal shortening started to dominate. The trends of the compressional structures and the directions of the slip-vectors on the pertinent strike-slip and reverse faults, as well as fault plane solutions of the abundant earthquakes in the Internal Zone and Alboran basin (e.g., Buforn *et al.*, 1988, 1995 and 2004; Stich *et al.*, 2003) point to NW-SE directed shortening, presumably in response to continued NW-SE directed African-European plate convergence.

Discussion and conclusions

An important aspect in the discussion of the intramontane basins and their large-scale geodynamic context concerns the position of the basins during the late Miocene. Reconstructions of the Alboran region at the onset of the late Miocene place the Alboran basin and the Betic and Rif Internal Zones close to their current position (e.g., Sanz de Galdeano, 1990; Lonergan and White, 1997; Geel and Roep, 1998; Rosenbaum *et al.*, 2002a; Meulenkamp and Sissingh, 2003; Spakman and Wortel, 2004). This interpretation is supported by the fact that extension in the Alboran domain largely ceased in the late Tortonian. The large clockwise rotations about vertical axes in the Betic External and Internal Zones (Lonergan and White, 1997; Platt *et al.*, 2003 and references therein) occurred during the early and middle Miocene, whilst late Miocene sediments in the basins show no evidence for late Miocene rotations about vertical axes (Krijgsman and Garcés, 2004). Furthermore, since the Tortonian (~10 Ma), approximately 50 to 60 km of NW-directed shortening has been accommodated in the western Prebetics which, in view of the cessation of extension in the Internal Zone and Alboran domain since the latest Miocene, is most likely related to ongoing African-Eurasian plate convergence. The above implies first that the motions of the Betic crust were NW-directed with respect to the Iberian plate, and secondly that at the onset of the late Miocene the Internal Zone with its developing intramontane basins was located 50 to 60 km southeast of its present position, i.e., south of what is currently considered as the "edge" of the Iberian plate.

Geodynamic setting in the late Micoene

We assume that by the late Miocene, slab roll-back and concomitant E-W extension and westward migration of the Alboran domain had proceeded to a stage that the retreating suture formed an arc-shaped structure close to the present position of the Betic Rif arc. The inferred upper mantle structure envisaged for the Tortonian is shown in Figure 7.2. The Tortonian position of the retreating slab and overlying Betic-Alboran domain largely explains the cessation of extension in large parts of the Alboran basin, whilst NNE-SSW to NW-SE directed extension, i.e., approximately orthogonal to the arc, continued to affect the Betic Internal Zone and northern and western parts of the Alboran basin.

The Internal Zone, as opposed to the Alboran basin, shows uplift and erosion at the end of the middle Miocene, removing most of the early-middle Miocene sediments prior to the initiation of the late Miocene intramontane basins. It is emphasized again, that the peripheral parts of the Internal Zone already collided with the Subbetic crust in the early Miocene and that, at the onset of the late Miocene, the Internal Zone crust was well on its way being carried onto thinned Iberian crust. We suggest that the Betic crust, while extension continued, became further emplaced onto the Iberian plate during the late Serravallian – early Tortonian. The intramontane basins thus started as emerged continental extensional basins, whilst a roughly coeval eustatic sea level drop enhanced the transition from previously marine to continental conditions. The intramontane basins initially show evidence for ENE-WSW to NE-SW directed extension during the Tortonian, however, in the Fortuna basin, the southern part of the Lorca basin and the Huercal Overa basin the direction of extension changed towards NNE-SSW to NW-SE. This rotation of the extension direction coincides with a marine transgression and a rapid basin subsidence. The marine transgression can only in part be accounted for by a eustatic sea level rise, i.e., the subsidence is clearly related to a lithospheric process. In view of the inferred position of the eastern Betics above the progressively retreating slab, also supported by geophysical models of the strength of the Iberian crust and lithosphere beneath the Betics indicating a missing load (Cloetingh *et al.*, 1992; Van der Beek and Cloetingh, 1992), the observed change towards a NNE-SSW to NW-SE oriented extension direction and the rapid subsidence of the basins may result from arc-normal pull (e.g., Meijer and Wortel, 1996; ten Veen and Meijer, 1998), due to the slab attached to the Iberian plate beneath the Betics.

Late Miocene slab-detachment

An aspect of particular importance in the above context is the inference made from recent mantle tomography (Spakman and Wortel, 2004) that the slab underneath the eastern Betics has been detached along a southwestward propagating tear (Fig. 7.2). Such a lateral propagation of slab detachment may be accompanied by a conspicuous signal of vertical motions in the overriding lithosphere, including first a marked subsidence followed by uplift whilst the tear propagates further along strike (Wortel and Spakman, 2000). The marked change from continental to full-marine conditions in the Fortuna, Lorca and Huercal Overa basins (Fig. 4.12), and the associated marked tectonic subsidence (Fig. 5.38) may thus reflect the

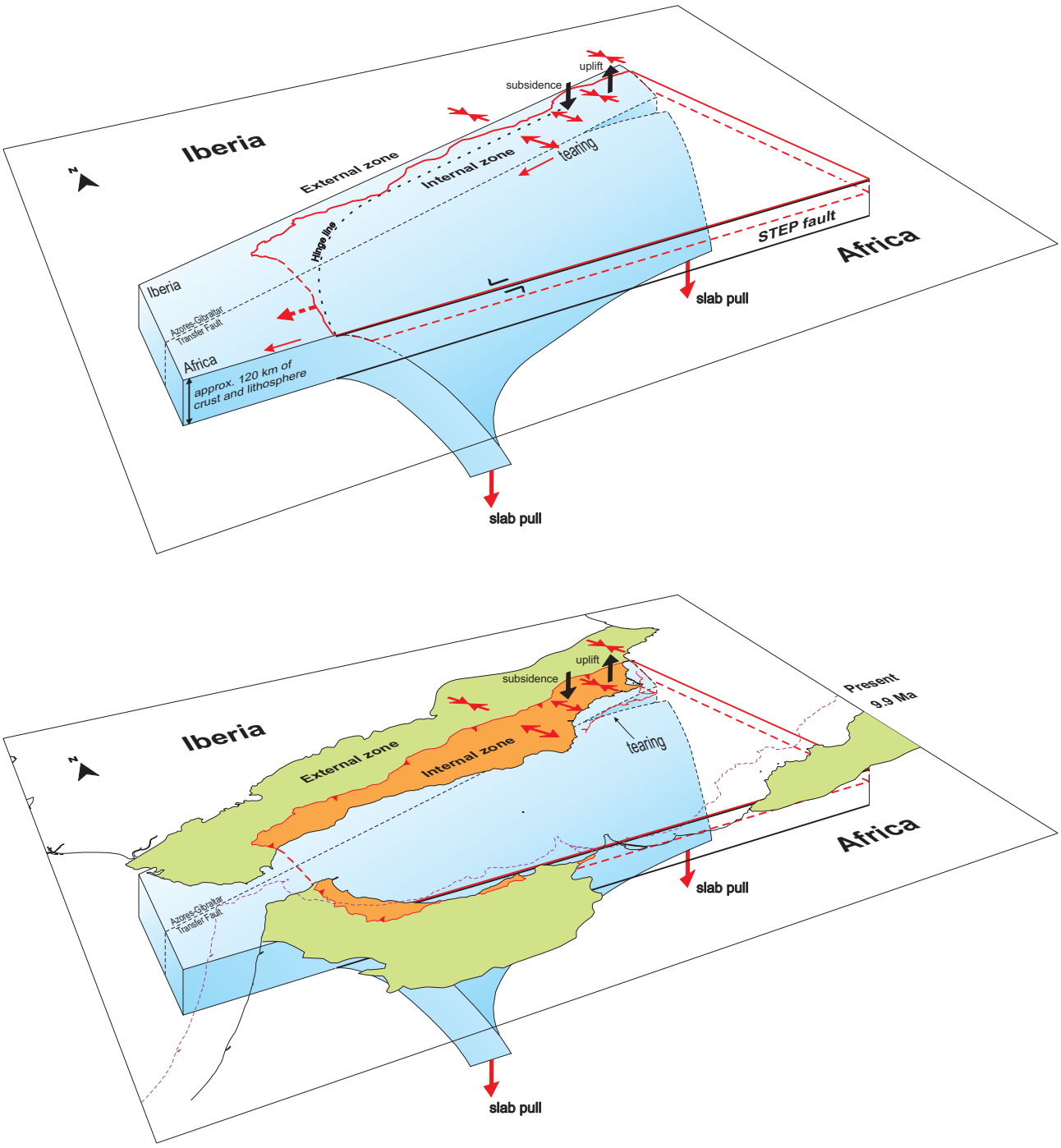

Figure 7.2. Inferred lithosphere-scale geometry of the Betic-Alboran system in the late Tortonian. Subduction trench terminates at a transfer or STEP fault (Govers and Wortel, 2005), which runs roughly parallel to the African margin. See text for explanation.

early stages of detachment of the slab underneath the basins in question. The available age data are, unfortunately, not diagnostic to reveal any diachrony in the continental-marine transition, expected for the case of lateral propagation of slab detachment, although the spikes marking maximum tectonic subsidence may indicate that the process occurred later in the Huercal Overa basin than in the Fortuna and Lorca basins. The observed diachronic marine to continental transition, on the other hand, ranging from late Tortonian in the easterly Fortuna basin to the early Messinian in the Huercal Overa basin and late Messinian in the Sorbas basin further southwest, lends clear support to southwest-directed propagation of slab detachment beneath the Betics. A similar process has been observed and modelled in other parts of the Mediterranean region (Meijer and Wortel, 1996, Van der Meulen *et al.*, 2000). The strong (and local) response of the overriding plate on lithospheric processes such as slab-pull and slab-detachment can be explained by the fact the Betic and Alboran crust and lithosphere have been extremely stretched and thinned during the Miocene, resulting in a weakened crust (low elastic strength) underlain at that stage by hot asthenosphere at shallow depth (R. Govers and M.J.R. Wortel, pers. comm.).

The diachronic transition from marine to continental conditions roughly coincides with cessation of extension, the onset of late Messinian – Pliocene uplift, inversion of the basins and basin bounding folds, and folding of the Miocene basin deposits. The continuous uplift since the late Messinian - Pliocene may in part be a result of flexural rebound of the Iberian plate after detachment of the slab. The development of the latest Miocene to recent compressional structures seems directly related to ongoing African-Eurasian plate convergence, since subduction zone rollback and slab detachment no longer control the dynamics of the Internal Zone and eastern part of the Alboran basin.

In conclusion, the late Miocene intramontane basins in the eastern part of the Betics developed as genuinely extensional basins in the later stages of a late Oligocene - Miocene lithospheric process. Both geological and geophysical data suggest westward subduction-zone rollback as the mechanism driving extension in the Betics and Alboran basin. The tectonic history of the intramontane basins is consistent with progressive, southwestward directed detachment of a east-northeast trending slab underneatch the Betics. A tantalizing problem, however, remains the early Miocene emplacement of the upper mantle peridotites in the crustal nappe stack of the Internal Zone, and the early Miocene low pressure, high temperature event documented in Alpujarride basement rocks of the Internal Zone and Alboran sea floor. In view of the early Miocene ages, these features should in some way be related to the hitherto poorly documented initiation of the rollback process in late Oligocene times.

References

Alfaro, P., Andreu, J. M., Delgado, J., Estévez, A., Soria, J.-M. & Teixido, T. (2002a) Quaternary deformation of the Bajo Segura blind fault (eastern Betic Cordillera, Spain) revealed by high-resolution reflection profiling. *Geological Magazine*, **139**, 331-341.

Alfaro, P., Delgado, J., Estévez, A., Soria, J.-M. & Yebenes, A. (2002b) Onshore and offshore compressional tectonics in the eastern Betic Cordillera. *Marine Geology*, **186**, 337-349.

Allen, P. A. & Allen, J. R. (2005) *Basin Analysis: Principles and Applications*. Blackwell Publishing.

Allerton, S., Lonergan, L., Platt, J. P., Platzman, E. S. & McClelland, E. (1993) Palaeomagnetic rotations in the eastern Betic Cordillera. *Earth and Planetary Science Letters*, **119**, 225-241.

Amores, R., Hernández-Enrile, J. L. & Martínez-Díaz, J. J. (2001) Sobre los factores relacionados con la evaluación de la peligrosidad sísmica en la región de Murcia. *2o Congreso Iberoamericano de Ingeniería Sísmica*, Madrid, Spain, Asociación Española de Ingeniería Sísmica.

Amores Lahidalga, R., Hernández-Enrile, J. L. & Martínez-Díaz, J. J. (2002) Estudio gravimetrico previo aplicado a la identificación de fallas ocultas como fuentes sismogenéticas en la Depresión del Guadalentin (Región de Murcia). *Geogaceta*, **32**, 307-310.

Andeweg, B. (2002) Cenozoic tectonic evolution of the Iberian peninsula: causes and effects of changing stress fields. Unpublished Thesis, Vrije Universiteit, Amsterdam, 178 pages.

Andrieux, J., Fontbote, J.-M. & Mattauer, M. (1971) Sur un modele explicatif de l'Arc de Gibraltar. *Earth and Planetary Science Letters*, **12**, 191-198.

Arboleya, M. L., Teixell, A., Charroud, M. & Julivert, M. (2004) A structural transect through the High and Middle Atlas of Morocco. *Journal of African Earth Sciences*, **39**, 319-327.

Argus, D. F., Gordon, R. G., De Mets, C. & Stein, S. (1989) Closure of the Africa-Eurasia-North America plate motion circuit and tectonics of the Gloria Fault. *Journal of Geophysical Research*, **94**, 5585-5602.

Augier, R. (2004) Evolution Tardi-Orogenique des Cordilleres Betiques (Espagne): Apports d'une etude integree. Unpublished Thesis, Universite Pierre et Marie Curie, Paris, 400 pages.

Azañón, J. M. & Goffé, B. (1997) Ferro- and magnesiocarpholite assemblages as record of high-P, low-T metamorphism in the central Alpujarrides, Betic Cordillera (SE Spain). *European Journal of Mineralogy*, **9**, 1035-1051.

Azema, J. & Montenat, C. (1973) Fortuna (892). *Mapa Geologico de España* (1:50.000), Instituto Geologico y Minero de España, Madrid.

Balanyá, J. C. & García-Dueñas, V. (1991) Fallas normales de bajo angulo a gran escala en las Beticas occidentales. *Geogaceta*, **9**, 30-32.

Banda, E. & Ansorge, J. (1980) Crustal structure under the central and eastern part of the Betic Cordillera. *Geophysical Journal of the Royal Astronomical Society*, **63**, 515-532.

Banda, E., Udías, A., Mueller, S., Mezcua, J., Boloix, M., Gallart, J. & Aparicio, A. (1983) Crustal structure beneath Spain from seismic sounding experiments. *Physics of the Earth and Planetary Interiors*, **31**, 277-280.

Banks, C. J. & Warburton, J. (1991) Mid-crustal detachment in the Betic system of southeast Spain. *Tectonophysics*, **191**, 275-289.

Beauchamp, W., Allmendinger, R. W., Barazangi, M., Demnati, A., El Alji, M. & Dahmani, M. (1999) Inversion tectonics and the evolution of the High Atlas Mountains, Morocco, based on a geological-geophysical transect. *Tectonics*, **18**, 163-184.

Beaumont, C., Munoz, J. A., Hamilton, J. & Fullsack, P. (2000) Factors controlling the Alpine evolution of the central Pyrenees inferred from a comparison of observations and geodynamical models. *Journal of Geophysical Research*, **105**, 8121-8145.

Beets, C. J. & De Ruig, M. J. (1992) 87Sr/86Sr dating of coralline algal limestones and its implications for the tectono-stratigraphic evolution of the eastern Prebetic (Spain). *Sedimentary Geology*, **78**, 233-250.

Bell, J. W., Amelung, F. & King, G. C. P. (1997) Pre-

liminary Late Quaternary slip history of the Carboneras fault, southeastern Spain. *Journal of Geodynamics*, **24**, 51-66.

Bessis, F. (1986) Some remarks on the study of subsidence of sedimentary basins; Application to the Gulf of Lions margin (Western Mediterranean). *Marine and Petroleum Geology*, **3**, 37-63.

Biddle, K. T. & Christie-Blick, N. (1985) Glossary - Strike-slip deformation, basin formation, and sedimentation. *Society of Economic Paleontologists and Mineralogists Special Publication*, **37**, 375-386.

Bird, P. (1978) Initiation of intracontinental subduction in the Himalaya. *Journal of Geophysical Research*, **83**, 4975-4987.

Blanco, M. J. & Spakman, W. (1993) The P-wave velocity structure of the mantle below the Iberian Peninsula: evidence for subducted lithosphere below southern Spain. *Tectonophysics*, **221**, 13-34.

Blankenship, C. L. (1992) Structure and paleogeography of the External Betic Cordillera, southern Spain. *Marine and Petroleum Geology*, **9**, 256-264.

Bond, G. C. & Kominz, M. A. (1984) Construction of tectonic subsidence curves for the early Paleozoic miogeocline, southern Canadian Rocky Mountains: Implications for subsidence mechanisms, age of breakup and crustal thinning. *Geological Society of America Bulletin*, **95**, 155-173.

Booth-Rea, G., Azañón, J. M. & García-Dueñas, V. (2003) Uppermost Tortonian to Quaternary depocentre migration related with segmentation of the strike-slip Palomares Fault Zone, Vera Basin (SE Spain). *C. R. Geoscience*, **335**, 751-761.

Booth-Rea, G., Azañón, J. M., Azor, A. & García-Dueñas, V. (2004) Influence of strike-slip fault segmentation on drainage evolution and topography. A case study: the Palomares Fault Zone (southeastern Betics, Spain). *Journal of Structural Geology*, **26**, 1615-1632.

Booth-Rea, G., García-Dueñas, V. & Miguel Azañón, J. (2002) Extensional attenuation of the Malaguide and Alpujarride thrust sheets in a segment of the Aboran basin folded during the Tortonian (Lorca area, Eastern Betics). *Comptes Rendus Geoscience*, **334**, 557-563.

Bourgois, J., Mauffret, A., Ammar, A. & Demnati, A. (1992) Multichannel seismic data imaging of inversion tectonics of the Alboran Ridge (Western Mediterranean Sea). *Geo-Marine Letters*, **12**, 117-122.

Bousquet, J.-C. (1979) Quaternary strike-slip faults in southeastern Spain. *Tectonophysics*, **52**, 277-286.

Bousquet, J.-C., Dumas, B. & Montenat, C. (1975) Le Décrochement de Palomares: Décrochement Quaternaire senestre du bassin de Vera. (Cordillères bétiques orientales. Espagne). *Cuadernos de Geologia, Universidad de Granada*, **6**, 113-119.

Bousquet, J.-C. & Montenat, C. (1974) Présence de décrochements NE-SW plio-quaternaires, dans les Cordillères bétiques orientales (Espagne). Extension et signification générale. *Comptes Rendus Hebdomadaires des Seances de l'Academie des Sciences, Serie D: Sciences Naturelles*, **278**, 2617-2620.

Braga, J. C., Martín, J. M. & Quesada, C. (2003) Patterns and average rates of late Neogene-Recent uplift of the Betic Cordillera, SE Spain. *Geomorphology*, **50**, 3-26.

Brede, R., Hauptmann, M. & Hernig, H. G. (1992) Plate tectonics and intracratonic mountain ranges in Morocco - The Mesozoic-Cenozoic development of the central High Atlas and the Middle Atlas. *International Journal of Earth Sciences*, **81**, 127-141.

Briend, M. (1981) Evolution morpho-tectonique du basin Neogene de Huercal Overa (cordillères bétiques orientales - espagne). *Documents et Travaux de l'Institut Geologique Albert de Lapparent (IGAL)*, **4**, 208.

Briend, M., Montenat, C. & Ott d'Estevou, P. (1990) Le Bassin de Huercal Overa. *Documents et Travaux de l'Institut Geologique Albert de Lapparent (IGAL)*, **12-13**, 239-259.

Buforn, E., Bezzeghoud, M., Udías, A. & Pro, C. (2004) Seismic sources on the Iberia-African plate boundary and their tectonic implication. *Pure and Applied Geophysics*, **161**, 623-646.

Buforn, E., Sanz de Galdeano, C. & Udías, A. (1995) Seismotectonics of the Ibero-Maghrebian Region. *Tectonophysics*, **248**, 247-261.

Buforn, E., Udías, A. & Colombas, M. A. (1988) Seismicity, source mechanisms and tectonics of the Azores - Gibraltar plate boundary. *Tectonophysics*, **152**, 89-118.

Bulnes, M. & Poblet, J. (1999) Estimating the detachment depth in cross sections involving detachment folds. *Geological Magazine*, **136**, 395-412.

Butler, R. W. H. (1982) The terminology of structures in thrust belts. *Journal of Structural Geology*, **4**, 239-245.

Butler, R. W. H. (1987) Thrust sequences. *Journal of the Geological Society of London*, **144**, 619-634.

Calvert, A., Sandvol, E., Seber, D., Barazangi, M., Roecker, S., Mourabit, T., Vidal, F., Alguacil, G. & Jarbour, N. (2000) Geodynamic evolution of the lithosphere and upper mantle beneath the Alboran region of the western Mediterranean: Constraints from travel time tomography. *Journal of Geophysical Research*, **105**, 10871-10898.

Calvo, J. P., Elizaga, E., López Martín, N., Robles, F. & Usera, J. (1978) El Mioceno superior continental del Prebetico Externo: Evolucion del Estrecho Nordbetico. *Boletin Geologico y Minero*, **89**, 407-426.

Calvo, M., Osete, M. L. & Vegas, R. (1994) Palaeomagnetic rotations in opposite senses in southeastern Spain. *Geophysical Research Letters*, **21**, 761-764.

Calvo, M., Vegas, R. & Osete, M. L. (1997) Palaeomagnetic results from Upper Miocene and Pliocene rocks from the Internal Zone of the eastern Betic Cordilleras (southern Spain). *Tectonophysics*, **277**, 271-283.

Campos, J., Maldonado, A. & Campillo, A. C. (1992) Post-Messinian evolutional patterns of the central Alboran Sea. *Geo-Marine Letters*, **12**, 173-178.

Cande, S. C. & Kent, D. V. (1995) Revised calibration of the geomagnetic polarity timescale forate Cretaceous and Cenozoic. *Journal of Geophysical Research*, **100**, 6093-6095.

Carminati, E., Wortel, M. J. R., Meijer, P. T. & Sabadini, R. (1998a) The two-stage opening of the western-central Mediterranean basins: a forward modeling test to a new evolutionary model. *Earth and Planetary Science Letters*, **160**, 667-679.

Carminati, E., Wortel, M. J. R., Spakman, W. & Sabadini, R. (1998b) The role of slab detachment processes in the opening of the western-central Mediterranean basins: some geological and geophysical evidence. *Earth and Planetary Science Letters*, **160**, 651-665.

Chalouan, A. & Michard, A. (2004) The Alpine Rif Belt (Morocco): A case of mountain building in a subduction-subduction-transform fault triple junction. *Pure and Applied Geophysics*, **161**, 489-519.

Chang, T., Stock, J. M. & Molnar, P. (1990) The rotation group in plate tectonics and the representation of uncertainties of plate reconstructions. *Geophysical Journal International*, **101**, 649-661.

Chase, C. G. (1978) Plate kinematics: The Americas, East Africa and the rest of the world. *Earth and Planetary Science Letters*, **37**, 355-368.

Cloetingh, S., Beek, A. v. d., Rees, D. v., Roep, T. B., Biermann, C. & Stephenson, R. A. (1992) Flexural interaction and the dynamics of Neogene extensional basin formation in the Alboran-Betic region. *Geo-Marine Letters*, **12**, 66-75.

Cohen, C. R. (1980) Plate tectonic model for the Oligo-Miocene evolution of the Western Mediterranean. *Tectonophysics*, **68**, 283-311.

Comas, M. C., García-Dueñas, V. & Jurado, M. J. (1992) Neogene tectonic evolution of the Alboran Sea from MCS data. *Geo-Marine Letters*, **12**, 157-164.

Comas, M. C., Platt, J. P., Soto, J. I. & Watts, A. B. (1999). The origin and tectonic history of the Alboran basin: insights from Leg 161 results. In: *Proceedings of the Ocean Drilling Program, Scientific Results* (Ed. by R. Zahn, M. C. Comas & A. Klaus), **161**, 555-580.

Coward, M. P. (1983) Thrust tectonics, thin skinned or thick skinned, and the continuation of thrusts to deep in the crust. *Journal of Structural Geology*, **5**, 113-123.

Cox, A. & Hart, R. B. (2002) *Plate Tectonics: How it works*. Blackwell Publishing.

Crespo-Blanc, A. & Campos, J. (2001) Structure and kinematics of the South Iberian paleomargin and its relationship with the Flysch Trough units; extensional tectonics within the Gibraltar Arc fold-and-thrust belt (western Betics). *Journal of Structural Geology*, **23**, 1615-1630.

Dabrio, C. J. & Polo, M. D. (1988). Late Neogene fan deltas and associated coral reefs in the Almanzora Basin, Almeria Province, southeastern Spain. In: *Fan deltas: Sedimentary and tectonic settings* (Ed. by W. Nemec & R. J. Steel), 354-367. Balckie and Son.

Dabrio, C. J. (1970) Bosquejo estratigrafico de la region de el Tranco Pontones-Santiago de la Espada (zona Prebetica, provincia de Jaen). *Cuadernos de Geologia, Universidad de Granada*, **1**, 141-148.

Dabrio, C. J. (1972) Santiago de la Espada (908). *Mapa de Geologico de Espana* (1:50.000), Instituto Geologico y Minero de Espana, Madrid.

Dabrio, C. J., Fernández, J. & Polo, M. D. (1971) La Formacion de Santiago de la Espada. (Mioceno, SE de la provincia de Jaen). *Cuadernos de Geologia, Universidad de Granada*, **2**, 31-40.

Dahlen, F. A. (1990) Critical Taper model of fold-and-thrust belts and accretionary wedges. *Annual Review of Earth Planetary Sciences*, **18**, 55-99.

Dahlstrom, C. D. A. (1969) Balanced cross sections. *Canadian Journal of Earth Sciences*, **6**, 743-757.

Davis, D., Suppe, J. & Dahlen, F. A. (1983) Mechanics of fold and thrust belts and accretionary wedges.

Journal of Geophysical Research, **88**, 1153-1172.

Davison, I. (1986) Listric normal fault profiles: calculation using bed-length balance and fault displacement. *Journal of Structural Geology*, **8**, 209-210.

de Booy, T. & Egeler, C. G. (1961) The occurrence of Betic of Malaga in the Sierras de Almagro, Cabrera and Alhamilla (SE Spain). *Geologie en Mijnbouw*, **6**, 209-218.

de Jong, K. (1991) Tectono-metamorphic studies and radiometric dating in the Betic Cordilleras (SE Spain) - with implications fot the dynamics of extension and compression in the western Mediterranean area. Unpublished Thesis, Vrije Universiteit, Amsterdam, 204 pages.

de Jong, K. (2003) Very fast exhumation of high-pressure metamorphic rocks with excess 40Ar and inherited 87Sr, Betic Cordilleras, southern Spain. *Lithos*, **70**, 91-110.

de Larouzière, F. D., Bolze, J., Bordet, P., Hernández, J., Montenat, C. & Ott d'Estevou, P. (1988) The Betic segment of the lithospheric Trans-Alboran shear zone during the Late Miocene. *Tectonophysics*, **152**, 41-52.

de Roever, W. P. & Nijhuis, H. J. (1964) Plurifacial alpine metamorphism in the eastern Betic Cordilleras (SE Spain) with special reference to the genesis of glaucophane. *Geologische Rundschau*, **53**, 324-336.

de Ruig, M. J., Mier, R. M. & Stel, H. (1987) Interference of compressional and wrenching tectonics in the Alicante region, SE Spain. *Geologie en Mijnbouw*, **66**, 201-212.

de Smet, M. E. M. (1984) Wrenching in the External Zone of the Betic Cordilleras, southern Spain. *Tectonophysics*, **107**, 57-79.

de Vries, W. C. P. & Zwaan, K. B. (1967) Alpujarride successions in the central Sierra de las Estancias, Province of Almeria, SE Spain. *Proceedings of the Koninklijke Nederlandse Akademie van Wetenschappen*, **70**, 443-453.

DeMets, C., Gordon, R. G., Argus, D. F. & Stein, S. (1994) Effect of recent revisions to the geomagnetic reversal time scale on estimates of current plate motions. *Geophysical Research Letters*, **21**, 2191-2194.

Dercourt, J., Zonenshain, L. P., Ricou, L. E., Kazmin, V. G., Le Pichon, X., Knipper, A. L., Grandjacquet, C., Sbortshikov, I. M., Geyssant, J., Lepvrier, C., Pechersky, D. H., Boulin, J., Sibuet, J. C., Savostin, L. A., Sorokhtin, O., Westphal, M., Bazhenov, M. L., Lauer, J. P. & Biju-Duval, B. (1986) Geological evolution of the Tethys belt from the Atlantic to the Pamirs since the Lias. *Tectonophysics*, **123**, 241-315.

Dewey, J. F., Helman, M. L., Turco, E., Hutton, D. H. W. & Knott, S. D. 1989. Kinematics of the western Mediterranean. In: *Alpine Tectonics* (edited by Coward, M. P., Dietrich, D. & Park, R. G.). *Geological Society Special Publication* **45**, 265-283.

Dinares-Turell, J., Orti, F., Playa, E. & Rosell, L. (1999) Palaeomagnetic chronology of the evaporitic sedimentation in the Neogene Fortuna Basin (SE Spain); early restriction preceding the "Messinian salinity crisis". *Palaeogeography, Palaeoclimatology, Palaeoecology*, **154**, 161-178.

Dinares-Turell, J., Sprovieri, R., Caruso, A., Di Stefano, E., Gomis-Coll, E., Pueyo, J. J., Rouchy, J. M. & Taberner, C. (1997) Preliminary integrated magnetostratigraphic and biostratigraphic correlation in the Miocene Lorca basin (Murcia, SE Spain). *Acta Geologica Hispanica*, **32**, 161-170.

Docherty, C. & Banda, E. (1995) Evidence for the eastward mirgration of the Alboran Sea based on regional subsidence analysis; a case for basin formation by delamination of the subcrustal lithosphere? *Tectonics*, **14**, 804-818.

Docherty, J. I. C. & Banda, E. (1992) A note on the subsidence history of the northern margin of the Alboran Basin. *Geo-Marine Letters*, **12**, 82-87.

Dooley, T. & McClay, K. R. (1997) Analog modelling of pull-apart basins. *American Association of Petroleum Geologists Bulletin*, **81**, 1804-1826.

Dubelaar, C. W. (1980) Geologie van het Centrale deel van het bekken van Albox. Unpublished Thesis, University of Amsterdam, pages.

Duggen, S., Hoernle, K., Bogaard, P. v. d., Rupke, L. & Morgan, J. P. (2003) Deep roots of the Messinian salinity crisis. *Nature*, **422**, 602-606.

Dula, W. F. (1991) Geometric models of listric normal faults and rollover folds. *American Association of Petroleum Geologists Bulletin*, **75**, 1609-1625.

Egeler, C. G. & Simon, O. J. (1969) Orogenic evolution of the Betic Zone (Betic Cordilleras, Spain), with emphasis on the nappe structures. *Geologie en Mijnbouw*, **48**, 296-305.

Elliot, D. (1983) The construction of balanced cross-sections. *Journal of Structural Geology*, **5**, 101.

Fadil, A., Vernant, P., McClusky, S., Reilinger, R., Gomez, F., Ben Sari, D., Mourabit, T., Feigl, K. & Barazangi, M. (2006) Active tectonics of the western Mediterranean: Geodetic evidence for rollback of a delaminated subcontinental lithospheric slab beneath the Rif Mountains, Morocco. *Geology*, **34**, 529-532.

Faulkner, D. R., Lewis, A. C. & Rutter, E. H. (2003) On the internal structure and mechanics of large strike-slip fault zones: field observations of the Carboneras fault in southeastern Spain. *Tectonophysics*, **367**, 235-251.

Fernandes, R. M. S. (2004) Present-day kinematics at the Azores-Gibraltar plate boundary as derived from GPS observations. Unpublished Thesis, Technical University of Delft, 202 pages.

Fernandes, R. M. S., Miranda, J. M., Meijninger, B. M. L., Bos, M. S., Noomen, R., Bastos, L., Ambrosius, B. A. C. & Riva, R. E. M. (2006) Surface velocity field of the Ibero-Maghrebian segment of the Eurasia-Nubia plate boundary. *Geophysical Journal International*, in press.

Fisher, N. I., Lewis, T. & Embleton, B. J. J. (1987) *Statistical analysis of spherical data*. Cambridge University Press, Cambridge, United Kingdom.

Frizon de Lamotte, D., Andrieux, J. & Guezou, J.-C. (1991) Cinematique des chevauchements neogens dans l'Arc betico-rifian: discussion sur les modeles geodynamiques. *Bulletin de la Societe Geologique de France*, **162**, 611-626.

Frizon de Lamotte, D., Saint Bezar, B., Bracene, R. & Mercier, E. (2000) The two main steps of the Atlas building and geodynamics of the western Mediterranean. *Tectonics*, **19**, 740-761.

Gamond, J. F. (1987) Bridge structures as sense of displacement criteria in brittle fault zones. *Journal of Structural Geology*, **9**, 609-620.

Garcés, M., Krijgsman, W. & Agustí, J. (1998) Chronology of the late Turolian deposits of the Fortuna basin (SE Spain): implications for the Messinian evolution of the eastern Betics. *Earth and Planetary Science Letters*, **163**, 69-81.

Garcés, M., Krijgsman, W. & Agustí, J. (2001) Chronostratigraphic framework and evolution of the Fortuna basin (Eastern Betics) since the Late Miocene. *Basin Research*, **13**, 199-216.

García-Dueñas, V., Balanyá, J. C. & Martínez-Martínez, J. M. (1992) Miocene extensional detachments in the outcropping basement of the northern Alboran basin (Betics) and their tectonic implications. *Geo-Marine Letters*, **12**, 88-95.

Govers, R. & Wortel, M. J. R. (2005) Lithosphere tearing at STEP faults: Response to edges of subduction zones. *Earth and Planetary Science Letters*, in press.

García-Hernández, M., López-Garrido, A. C., Rivas, P., Sanz de Galdeano, C. & Vera, J. A. (1980) Mesozoic palaeogeographic evolution of the External zones of the Betic Cordillera. *Geologie en Mijnbouw*, **59**, 155-168.

García-Meléndez, E., Ferrer-Julia, M., Goy, J. L. & Zazo, C. (2002) Reconstruccion morfoestructural mediante modelos de elevacion digital en un SIG del fondo de la cuenca sedimentaria de la Cubeta del Saltador (Cordilleras Beticas Orientales). *Geogaceta*, **32**, 203-206.

García-Meléndez, E., Goy, J. L. & Zazo, C. (2003) Neotectonics and Plio-Quaternary landscape development within the eastern Huercal-Overa Basin (Betic Cordilleras, southeast Spain). *Geomorphology*, **50**, 111-133.

García-Veigas, J., Orti, F., Rosell, L. & Ingles, M. (1994) Caracterizacion petrologica y geoquimica de la Unidad Salina messiniense de la cuence de Lorca (sondeos S4 y S5). *Geogaceta*, **15**, 78-81.

García-Veigas, J., Orti, F., Rosell, L., Ayora, C., Rouchy, J. M. & Lugli, S. (1995) The Messinian salt of the Mediterranean: geochemical study of the salt from the Central Sicily Basin and comparison with the Lorca Basin (Spain). *Bulletin de la Societe Geologique de France*, **166**, 699-710.

Garfunkel, Z. & Ron, H. (1985) Block rotation and deformation by strike-slip faults; 2, The properties of a type of macroscopic discontinuous deformation. *Journal of Geophysical Research*, **B 90**, 8589-8602.

Gauyau, F., Bayer, R., Bousquet, J.-C., Lachaud, J.-C., Lesquer, A. & Montenat, C. (1977) Le prolongement de l'accident d'Alhama de Murcia entre Murcia et Alicante (Espagne meridionale). *Bull. Soc. geol. France*, **7**, 623-629.

Geel, T. & Roep, T. B. (1998) Oligocene to middle Miocene basin development in the Eastern Betic Cordilleras, SE Spain (Velez Rubio Corridor - Espuña): reflections of West Mediterranean plate-tectonic reorganisations. *Basin Research*, **10**, 325-343.

Geel, T. & Roep, T. B. (1999) Oligocene to Middle Miocene basin development in the Velez Rubio Corridor - Espuña (Internal-External Zone boundary; Eastern Betic Cordilleras, SE Spain). *Geologie en Mijnbouw*, **77**, 39-61.

Geel, T. (1996) Paleogene to Early Miocene sedimentary history of the Sierra Espuña Espuña (Malaguide complex, Internal Zone of the Betic Cordilleras, SE Spain), Evidence for extra-Malaguide (Sardinian?) Provenance of Oligocene conglomerates: paleogeographic implications. *Estudios Geologicos*, **52**, 211-230.

Geel, T. 1976. Messinian gypsiferous deposits of the Lorca basin (Province of Murcia, SE Spain). In:

Messinian evaporites in the Mediterranean (edited by Catalano, R., Ruggieri, G. & Sprovieri, R.). *Memorie della Societa Geologica Italiana* **16**, 369-384.

Geel, T., Roep, T. B., ten Kate, W. & Smit, J. (1992) Early-Middle Miocene stratigraphic turning points in the Alicante region (SE Spain); reflections of Western Mediterranean plate-tectonic reorganizations. *Sedimentary Geology*, **75**, 223-239.

Gimenez, J., Surinach, E. & Goula, X. (2000) Quantification of vertical movements in the eastern Betics (Spain) by comparing levelling data. *Tectonophysics*, **317**, 237-258.

Gomez, F., Beauchamp, W. & Barazangi, M. (2000) Role of the Atlas Mountains (northwest Africa) within the African-Eurasian plate-boundary zone. *Geology*, **28**, 775-778.

Gordon, R. G. (1998) The plate tectonic approximation: Plate nonrigidity, diffuse plate boundaries, and global plate reconstructions. *Annual Review of Earth Planetary Sciences*, **26**, 615-624.

Gradstein, F. M., Agterberg, F. P., Ogg, J. G., Hardenbol, J., van Veen, P., Thierry, J. & Huang, Z. (1994) A Mesozoic time scale. *Journal of Geophysical Research*, **99**, 24051-24074.

Groshong, R. H. (2002) *3-D Structural Geology: A practical guide to surface and subsurface map interpretation*. Springer-Verlag.

Gueguen, E., Doglioni, C. & Fernández, M. (1998) On the post-25 Ma geodynamic evolution of the western Mediterranean. *Tectonophysics*, **298**, 259-269.

Guerra, F., Martín-Martín, M., Perrone, V. & Tramontana, M. (2005) Tectono-sedimentary evolution of the southern branch of the western Tethys (Maghrebian Flysch Basin and Lucanian Ocean): consequences for Western Mediterranean geodynamics. *Terra Nova*, **17**, 358-367.

Guerra-Merchán, A. & Serrano, F. (1993) Tectosedimentary setting and chronostratigraphy of the Neogene reefs in the Almanzora corridor (Betic Cordillera, Spain). *Geobios*, **26**, 57-67.

Guillén Mondéjar, F., Rodríguez Estrella, T., Arana, R. & López Aguayo, F. (1995) Historia geológica de la cuenca de Lorca (Murcia): influencia de la tectónica en la sedimentación. *Geogaceta*, **18**, 30-33.

Gutscher, M. A., Malod, J., Rehault, J.-P., Contruci, I., Klingelhoefer, F., Mendes-Victor, L. & Spakman, W. (2002) Evidence for active subduction beneath Gibraltar. *Geological Society of America*, **30**, 1071-1074.

Hall, C. A. (1981) San Luis Obispo Transform Fault and middle Miocene rotation of the Western Transverse Ranges, California. *Journal of Geophysical Research*, **86**, 1015-1031.

Hancock, P. L. & Barka, A. A. (1987) Kinematic indicators on active normal faults in western Turkey. *Journal of Structural Geology*, **9**, 573-584.

Hanne, D., White, N. & Lonergan, L. (2003) Subsidence analyses from the Betic Cordillera, southeast Spain. *Basin Research*, **15**, 1-21.

Haq, B. U., Hardenbol, J. & Vail, P. R. (1988). Mesozoic and Cenozoic chronostratigraphy and cycles of sea-level change. In: *Sea-level changes; An integrated approach* (Ed. by C. K. Wilgus, B. S. Hastings, C. A. Ross, H. W. Posamentier, J. Van Wagoner & C. G. S. C. Kendall), *Society of Economic Paleontologists and Mineralogists (SPEM)Special Publications*, **42**, 72-108.

Hardenbol, J., Thierry, J., Farley, M., Jacquin, T., de Graciansky, P. C. & Vail, P. R. (1998). Mesozoic and Cenozoic sequence chronostratigraphic chart. In: *Mesozoic and Cenozic sequence stratigraphy of European Basins* (Ed. by P. C. de Graciansky, J. Hardenbol, T. Jacquin & P. R. Vail), *SEPM Special Publication*, **60**.

Hellinger, S. J. (1981) The uncertainties of finite rotations in Plate Tectonics. *Journal of Geophysical Research*, **86**, 9312-9318.

Hermes, J. J. 1978. The stratigraphy of the Subbetic and southern Prebetic of the Velez Rubio-Caravaca area and its bearing on transcurrent faulting in the Betic Cordilleras of Southern Spain. In: *Proceedings of the KNAW* **81, series B: palaeontology, geology, physics chemistry**.

Hodgson, D. M., Platt, J. P. & Pickering, K. T. Coarse-grained delta devlopment in responce to abrupt basement reorganisation during the Serravallian to early Tortonian in the Eastern Betic Cordillera, Spain. *Basin Research*, in review.

Homza, T. X. & Wallace, W. K. (1995) Geometric and kinematic models for detachment folds with fixed and variable detachment depths. *Journal of Structural Geology*, **17**, 575-588.

Hossack, J. R. (1979) The use of balanced cross-sections in the calculation of orogenic contraction: A review. *Journal of the Geological Society of London*, **136**, 705-711.

Houseman, G. (1996) From mountains to basin. *Nature*, **379**, 771-772.

Huestis, S. P. & Acton, G. D. (1997) On the construction of geomagnetic timescales from non-prejudicial treatment of magentic anomaly data from mul-

tiple ridges. *Geophys. Journal International*, **129**, 176-182.

Jabaloy, A., Galindo-Zaldívar, J. & González-Lodeiro, F. (1992) The Mecina extensional system: Its relation with the post-Aquitanian piggyback basins and the paleostresses evolution (Betic Cordilleras, Spain). *Geo-Marine Letters*, **12**, 96-103.

Jerez Mir, F. & Abril Hurtado, J. (1979) Yetas de Abajo (888). *Mapa de Geologico de Espana* (1:50.000), Instituto Geologico y Minero de Espana, Madrid.

Jerez Mir, L., Jerez Mir, F. & García-Monzon, G. (1972) Mula (912). *Mapa Geologico de Espana* (1:50.000), Instituto Geologico y Minero de Espana, Madrid.

Jimenez-Munt, I., Fernández, M., Torné, M. & Bird, P. (2001) The transition from linear to diffuse boundary in the Azores-Gibraltar region: results from a thin-sheet model. *Earth and Planetary Science Letters*, **192**, 175-189.

Johnson, C., Harbury, N. & Hurford, A. J. (1997) The role of extension in the Miocene denudetion denudation of the Nevado-Filabride Complex, Betic Cordillera (SE Spain). *Tectonics*, **16**, 189-204.

Jolivet, L. & Faccenna, C. (2000) Mediterranean extension and the Africa-Eurasia collision. *Tectonics*, **19**, 1095-1106.

Jonk, R. & Biermann, C. (2002) Deformation in Neogene sediments of the Sorbas and Vera basins (SE Spain): constraints on simple-shear deformation and rigid body rotation along major strike-slip faults. *Journal of Structural Geology*, **24**, 963-977.

Jurdy, D. M. & Stefanick, M. (1987) Errors in plate rotations as described by covariance matrices and their combination in reconstructions. *Journal of Geophysical Research*, **92**, 6310-6318.

Kampschuur, W., Langenberg, C. V., Rondeel, H. E., Espejo, J. A., Crespo, A. & Fignatelli, R. (1972) Lorca (953). *Mapa de Geologico de España* (1:50.000), Instituto Geologico y Minero de España, Madrid.

Keller, J. V. A., Hall, S. H., Dart, C. J. & McClay, K. R. (1995) The geometry and evolution of a transpressional strike-slip system: the Carboneras fault, SE Spain. *Journal of the Geological Society of London*, **152**, 339-351.

Kenter, J. A. M., Reymer, J. J. G. & Van der Straaten, H. C. (1990) Facies patterns and subsidence history of the Jumilla-Cieza region (southeastern Spain. *Sedimentary Geology*, **67**, 263-280.

Kirkwood, B. H., Royer, J.-Y., Chang, T. C. & Gordon, R. G. (1999) Statistical tools for estimating and combining finite rotations and their uncertainties. *Geophysical Journal International*, **137**, 408-428.

Krijgsman, W. & Garcés, M. (2004) Palaeomagnetic constraints on the geodynamic evolution of the Gibraltar Arc. *Terra Nova*, **16**, 281-287.

Krijgsman, W., Fortuin, A. R., Hilgen, F. J. & Sierro, F. J. (2001) Astrochronology for the Messinian Sorbas basin (SE Spain) and orbital (precessional) forcing for evaporite cyclicity. *Sedimentary Geology*, **140**, 43-60.

Krijgsman, W., Garcés, M., Agustí, J., Raffi, I., Taberner, C. & Zachariasse, W. J. (2000) The 'Tortonian salinity crisis' of the eastern Betics (Spain). *Earth and Planetary Science Letters*, **181**, 497-511.

Krijgsman, W., Leewis, M. E., Garcés, M., Kouwenhoven, T. J., Kuiper, K. & Sierro, F. J. (2006) Tectonic control for evaporite formation in the Eastern Betics. *Sedimentary Geology*.

Kuiper, K., Krijgsman, W., Garcés, M. & Wijbrans, J. R. (2006) Revised isotopic (40Ar/39Ar) age for the lamproite volcano of Cabezos Negros, Fortuna Basin (Eastern Betics, SE Spain). *Palaeogeography, Palaeoclimatology, Palaeoecology*, in press.

Leblanc, D. & Olivier, P. (1984) Role of strike-slip faults in the Betic-Rifian orogeny. *Tectonophysics*, **101**, 345-355.

Logan, J. M., Friedman, M., Higgs, N., Dengo, C. & Shimamoto, T. (1979). Experimental studies of simulated gouge and their application to studies of natural fault zones. In: *Proceedings of Conference VIII; Analysis of actual fault zones in bedrock.* (Ed. by R. C. Speed, R. V. Sharp & J. F. Evernden), *Open-File Report*, 305-343. U.S Geological Survey.

Loiseau, J., Ott d'Estevou, P. & Montenat, C. (1990) Le secteur d'Archena - Mula. *Documents et Travaux de l'Institut Geologique Albert de Lapparent (IGAL)*, **12-13**, 287-301.

Lonergan, L. & Johnson, C. (1998) Reconstructing orogenic exhumation histories using synorogenic detritial zircons and apatites: an example from the Betic Cordillera, SE Spain. *Basin Research*, **10**, 353-364.

Lonergan, L. & Platt, J. P. (1995) The Malaguide-Alpujarride boundary: a major extensional contact in the Internal Zone of the eastern Betic Cordillera, SE Spain. *Journal of Structural Geology*, **17**, 1655-1671.

Lonergan, L. & White, N. (1997) Origin of the Betic-

Rif mountain belt. *Tectonics*, **16**, 504-522.

Lonergan, L., Platt, J. P. & Gallagher, L. (1994) The Internal-External Zone Boundary in the eastern Betic Cordillera, SE Spain. *Journal of Structural Geology*, **16**, 175-188.

Loomis, T. P. (1975) Tertiary mantle diapirism, orogeny and plate tectonics east of the Strait of Gibraltar. *American Journal of Science*, **275**, 1-30.

López Casado, C., Sanz de Galdeano, C., Molina Palacios, S. & Henares Romero, J. (2001) The structure of the Alboran Sea: an interpretation from seismological and geological data. *Tectonophysics*, **338**, 79-95.

Lourens, L. J., Hilgen, F. J., Laskar, J., Shackleton, N. J. & Wilson, D. (2004). The Neogene period. In: *A Geologic Time Scale 2004* (Ed. by F. Gradstein, J. Ogg & A. Smith), Cambridge University Press, Cambridge, in press.

Luján, M., Balanyá, J. C. & Crespo-Blanc, A. (2000) Contractional and extensional tectonics in Flysch and Penibetic units (Gibraltar Arc, SW Spain): new constraints on emplacement mechanisms. *Comptes Rendus de l'Academie des Sciences, Serie II. Sciences de la Terre et des Planetes*, **330**, 631-638.

Lukowski, P. & Poisson, A. M. (1988). The Tortonian-Messinian synsedimentary tectonic in the Fortuna basin (Betic Cordilleras, Murcia, Spain. In: *Symposium on the geology of the Pyrenees and Betics* (Ed. by J. A. Munoz, C. Sanz de Galdeano & P. Santanach), 31. Barcelona.

Lukowski, P. & Poisson, A. M. (1990) Le bassin de Fortuna. *Documents et Travaux de l'Institut Geologique Albert de Lapparent (IGAL)*, **12-13**, 303-311.

Madialdea, T., Vegas, R., Somoza, L., Vazquez, J. T., Maldonado, A., Diaz-del-Rio, V., Maestro, A., Cordoba, D. & Fernández-Puga, M. C. (2004) Structure and evolution of the "Olistostrome"complex of the Gibraltar Arc in the Gulf of Cadiz (eastern Central Atlantic): evidence from two long seismic cross-sections. *Marine Geology*, **209**, 173-198.

Maldonado, A., Somoza, L. & Pallares, L. (1999) The Betic orogen and the Iberian-African boundary in the Gulf of Cadiz: geological evolution (central North Atlantic). *Marine Geology*, **155**, 9-43.

Marrett, R. & Allmendinger, R. W. (1990) Kinematic analysis of fault-slip data. *Journal of Structural Geology*, **12**, 973-986.

Martín, J. M., Braga, J. C. & Betzler, C. (2001) The Messinian Guadalhorce corridor: the last northern, Atlantic-Mediterranean gateway. *Terra Nova*, **13**, 418-424.

Martín, J. M., Braga, J. C. & Betzler, C. (2003) Late Neogene-Recent uplift of the Cabo de Gata volcanic province, Almeria, SE Spain. *Geomorphology*, **50**, 27-42.

Martínez del Olmo, W. & Nunez Galiana, A. (1973) Villacarrillo (907). *Mapa Geologico de Espana* (1:50.000), Instituto Geologico y Minero de Espana, Madrid.

Martínez-Díaz, J. J. & Hernández-Enrile, J. L. (1992a) Tectónica reciente y rasgos sismotectónicos en el sector Lorca-Totana de la falla de Alhama de Murcia. *Estudios Geologicos*, **48**, 153-162.

Martínez-Díaz, J. J. & Hernández Enrile, J. L. (1992b) Fracturación y control tectosedimentario neógeno en el borde sureste de la Cuenca de Lorca. *Boletín Geológico y Minero*, **103**, 3-15.

Martínez-Díaz, J. J. & Hernández-Enrile, J. L. (2001) Using travertine deformations to characterize paleoseismic activity along an active oblique-slip fault: the Alhama de Murcia fault (Betic Cordillera, Spain). *Acta Geologica Hispanica*, **36**, 297-313.

Martínez-Díaz, J. J. (2002) Stress field variation related to fault interaction in a reverse oblique-slip fault: the Alhama de Murcia fault, Betic Cordillera, Spain. *Tectonophysics*, **356**, 291-305.

Martín-Suarez, E., Freudenthal, M. & Civis, J. (2001) Rodent palaeoecology of the Continental Upper Miocene of Crevillente (Alicante, SE Spain). *Palaeogeography, Palaeoclimatology, Palaeoecology*, **165**, 349-356.

Masana, E., Martínez-Díaz, J. J., Hernández Enrile, J. L. & Santanach, P. (2004) The Alhama de Murcia fault (SE Spain), a seismogenic fault in a diffuse plate boundary: Seismotectonic implications for the Ibero-Magrebian region. *Journal of Geophysical Research*, **109**, B01301.

Masana, E., Pallas, R., Perea, H., Ortuno, M., Martínez-Díaz, J. J., García-Meléndez, E. & Santanach, P. (2005) Large Holocene morphogenic earthquakes along the Albox fault, Betic Cordilleras, Spain. *Journal of Geodynamics*, **40**, 119-133.

Mauffret, A., Frizon de Lamotte, D., Lallemant, S., Gorini, C. & Maillard, A. (2004) E-W opening of the Algerian basin (Western Mediterranean). *Terra Nova*, **16**, 257-264.

Mauffret, A., Maldonado, A. & Campillo, A. C. (1992) Tectonic framework of the eastern Alboran

and the western Algerian basins, western Mediterranean. *Geo-Marine Letters*, **12**, 104-110.

Mazzoli, S. & Helman, M. L. (1994) Neogene patterns of relative plate motion for Africa-Europe: some implications for recent central Mediterranean tectonics. *Geologische Rundschau*, **83**, 464-468.

Means, W. D. (1987) A newly recognized type of slickenside striation. *Journal of Structural Geology*, **9**, 585-590.

Meijer, P. T. & Wortel, M. J. R. (1996) Temporal variation in the stress field of the Aegean region. *Geophysical Research Letters*, **23**, 439-442.

Meulenkamp, J. E. & Sissingh, W. (2003) Tertiary palaeogeography and tectonostratigraphic evolution of the Northern and Southern Peri-Tethys platforms and the intermediate domains of the African-Eurasian convergent plate boundary zone. *Palaeogeography, Palaeoclimatology, Palaeoecology*, **196**, 209-228.

Minster, J. B. & Jordan, T. H. (1978) Present-day plate motions. *Journal of Geophysical Research*, **83**, 5331-5354.

Mitra, S. (2002) Structural models of faulted detachment folds. *AAPG Bullentin*, **86**, 1673-1694.

Molnar, P. & Stock, J. M. (1985) A method for bounding uncertainties in combined plate reconstructions. *Journal of Geophysical Research*, **90**, 12537-12544.

Monié, P., Galindo Zaldívar, J., González-Lodeiro, F., Goffe, B. & Jabaloy, A. (1991) 40Ar/39Ar geochronology of Alpine tectonism in the Betic Cordilleras (southern Spain). *Journal of the Geological Society of London*, **148**, 289-297.

Monie, P., Torres Roldán, R. L. & García Casco, A. (1994) Cooling and exhumation of the western Betic Cordilleras, $^{40}Ar/^{39}Ar$ thermochronological constraints on a collapsed terrane. *Tectonophysics*, **238**, 353-379.

Montenat, C. & Ott d'Estevou, P. (1990) Eastern Betic Neogene basins - A review. *Documents et Travaux de l'Institut Geologique Albert de Lapparent (IGAL)*, **12-13**, 9-15.

Montenat, C. & Ott d'Estevou, P. (1996). Late Neogene basins evolving in the Eastern Betic transcurrent fault zone: an illustrated review. In: *Tertiary basins of Spain, the stratigraphic record of crustal kinematics* (Ed. by P. F. Friend & C. J. Dabrio), *World and regional geology*, **6**, 372-386. Cambridge University Press.

Montenat, C. & Ott d'Estevou, P. (1999) The diversity of Late Neogene sedimentary basins generated by wrench faulting in the Eastern Betic Cordillera, SE Spain. *Journal of Petroleum Geology*, **22**, 61-80.

Montenat, C. (1973) Les formations néogènes et quaternaires du levant espagnol (province d'Alicante et de Murcie). Unpublished Thesis, Universite de Paris Sud, Paris, 1170 pages.

Montenat, C., Ott d'Estevou, P. & Aelllen de la Chapelle, M. (1990a) Les series Neogenes entre Lorca et Huercal Overa. *Documents et Travaux de l'Institut Geologique Albert de Lapparent (IGAL)*, **12-13**, 281-286.

Montenat, C., Ott d'Estevou, P. & Delort, T. (1990b) Le Bassin de Lorca. *Documents et Travaux de l'Institut Geologique Albert de Lapparent (IGAL)*, **12-13**, 261-280.

Montenat, C., Ott d'Estevou, P. & Masse, P. (1987) Tectonic-sedimentary characters of the Betic Neogene basins evolving in a crustal transcurrent shear zone (SE Spain). *Bull. Centr. Rech. Expl. Prod. Elf Aquitaine*, **11**, 1-22.

Montenat, C., Ott d'Estevou, P. & Pierson D'Autrey, L. (1996). Miocene basins of the eastern Prebetic Zone: some tectonosedimentary aspects. In: *Tertiary basins of Spain, the stratigraphic record of crustal kinematics* (Ed. by P. F. Friend & C. J. Dabrio), *World and regional geology*, **6**, 346-352. Cambridge University Press.

Mora-Gluckstadt, M. (1993) Tectonic and sedimentary analysis of the Huercal Overa region, South East Spain, Betic Cordillera. Unpublished Thesis, University of Oxford, 300 pages.

Morales, J., Vidal, F., de Miguel, F., Alguacil, G., Posadas, A. M., Ibáñez, J. M., Guzmán, A. & Guirao, J. M. (1990) Basement structure of the Granada basin, Betic Cordilleras, Southern Spain. *Tectonophysics*, **177**, 337-348.

Morley, C. K. (1993) Discussion of origins of hinterland basins to the Rif-Betic Cordillera and Carpathians. *Tectonophysics*, **226**, 359-376.

Müller, D. W. & Hsü, K. J. (1987) Event stratigraphy and paleoceanography in the Fortuna basin (southeast Spain): a scenario for the Messinian salinity crisis. *Paleoceanography*, **2**, 679—696.

Müller, P. D. & Roest, W. R. (1992) Fracture Zones in the North Atlantic from Combined Geosat and Seasat Data. *Journal of Geophysical Research*, **97**, 3337-3350.

Orti, F., García-Veigas, J., Rosell, L., Rouchy, J. M., Ingles, M., Gimeno, D., Kasprzyk, A. & Playa, E. (1993) Correlacion litostratigrafica de las evaporitas messinienses en las cuencas de Lorca y Fortuna. *Geogaceta*, **14**, 98-101.

Osete, M. L., Villalain, J. J., Palencia, A., Osete, C., Sandoval, J. & García-Duenas, V. (2004) New palaeomagnetic data from the Betic Cordillera: Constraints on the timing and the geographical distribution of the tectonic rotations in southern Spain. *Pure and Applied Geophysics*, **161**, 701-722.

Ott d'Estevou, P., Montenat, C., Ladure, F. & Pierson D'Autrey, L. (1988) Evolution tectono-sedimentaire du domaine prebetique oriental (Espagne) au Miocene. *Comptes Rendus de l'Academie des Sciences, Serie II. Sciences de la Terre et des Planetes*, **307**, 789-796.

Passchier, C. W. & Trouw, R. A. J. (1998) *Microtectonics*. Springer-Verlag, Berlin.

Peper, T. & Cloetingh, S. (1992) Lithosphere dynamics and tectono-stratigraphic evolution of the Mesozoic Betic rifted margin (southeastern Spain). *Tectonophysics*, **203**, 345-361.

Perrier, R. & Quiblier, J. (1974) Thickness changes in sedimentary layers during compaction history; methods for evaluation. *American Association of Petroleum Geologists Bulletin*, **58**, 507-520.

Petit, J. P. (1987) Criteria for the sense of movement on fault surfaces in brittle rocks. *Journal of Structural Geology*, **9**, 597-608.

Pignatelli García, R., Espejo Molina, J. A. & Crespo Zamorano, A. (1972) Elche (893). *Mapa Geologico de Espana* (1:50.000), Instituto Geologico y Minero de Espana, Madrid.

Platt, J. P. & Leggett, J. K. (1986) Stratal extension in thrust footwalls, Makran Accretionary prism: Implications for thrust tectonics. *AAPG Bullentin*, **70**, 191-203.

Platt, J. P. & Vissers, R. L. M. (1989) Extensional collapse of thickened continental lithosphere: A working hypothesis for the Alboran Sea and Gibraltar arc. *Geology*, **17**, 540-543.

Platt, J. P. & Whitehouse, M. J. (1999) Early Miocene high-temperature metamorphism and rapid exhumation in the Betic Cordillera (Spain): evidence from U-Pb zircon ages. *Earth and Planetary Science Letters*, **171**, 591-605.

Platt, J. P. (1986) Dynamics of orogenic wedges and the uplift of high-pressure metamorphic rocks. *Geological Society of America Bulletin*, **97**, 1037-1053.

Platt, J. P., Allerton, S., Kirker, A., Mandeville, C., Mayfield, A., Platzman, E. S. & Rimi, A. (2003) The ultimate arc: Differential displacement, oroclinal bending, and vertical axis rotation in the External Betic-Rif arc. *Tectonics*, **22**, 29.

Platt, J. P., Kelley, S. P., Carter, A. & Orozco, M. (2005) Timing of tectonic events in the Alpujarride Complex, Betic Cordillera, southern Spain. *Journal of the Geological Society of London*, **162**, 1-12.

Platt, J. P., Soto, J. I., Whitehouse, M. J., Huford, A. J. & Kelly, S. P. (1998) Thermal evolution, rate of exhumation, and tectonic significance of metamorphic rocks from the floor of the Alboran extensional basin, western Mediterranean. *Tectonics*, **17**, 671-689.

Platzman, E. S. & Platt, J. P. (2004) Kinematics of a twisted core complex: a paleomagnetic and structural investigation of the Sierra de las Estancias (Betic Cordillera, southern Spain). *Tectonics*, **23**.

Platzman, E. S., Platt, J. P., Kelley, S. P. & Allerton, S. (2000) Large clockwise rotations in an extensional allochton, Alboran Domain (southern Spain). *Journal of Geological Society, London*, **157**, 1187-1197.

Playa, E., Dinares-Turell, J., Orti, F., Gomis, E. & Rosell, L. (1999) Datacion magnetoestratigrafica de las evaporitas de la cuenca neogena de Fortuna (Murcia). *Geogaceta*, **25**, 163-166.

Playa, E., Orti, F. & Rosell, L. (2000) Marine to non-marine sedimentation in the upper Miocene evaporites of the Eastern Betics, SE Spain; sedimentological and geochemical evidence. *Sedimentary Geology*, **133**, 135-166.

Poblet, J. & Bulnes, M. (2005) Fault-slip, bed-length and area variations in experimental rollover anticlines over litric normal faults: influence in extension and depth to detachment estimations. *Tectonophysics*, **396**, 97-117.

Poisson, A. M. & Lukowski, P. (1990) The Fortuna basin: a piggyback basin in the Eastern Betic Cordilleras (SE Spain). *Annales Tectonicae*, **4**, 52-67.

Poisson, A. M., Morel, J. L., Andrieux, J., Coulon, M., Wernli, R. & Guernet, C. (1999) The origin and development of Neogene basins in the SE Betic Cordillera (SE Spain): a case study of the Tabernas-Sorbas and Huercal Overa Basins. *Journal of Petroleum Geology*, **22**, 97-114.

Priem, H. N. A., Hebeda, E. H., Boelrijk, N. A. I. M., Verdurmen, T. E. A. & Oen, I. S. (1979) Isotopic dating of the emplacement of the ultramafic masses in the Serrania de Ronda, southern Spain. *Contributions to Mineralogy and Petrology*, **61**, 103-109.

Raffi, L., Mozzato, C., Fornaciari, E., Hilgen, F. J. & Rio, D. (2003) Late Miocene calcareous nannofossil biostratigraphy and astrobiochronology for the Mediterranean region. *Micro-*

paleontology, **49**, 1-26.

Reicherter, K. R. & Reiss, S. (2001) The Carboneras Fault Zone (southeastern Spain) revisited with Ground Penetrating Radar - Quarternary structural styles from high-resolution images. *Netherlands Journal of Geosciences / Geologie en Mijnbouw*, **80**, 129-138.

Reicherter, K. R. (2001) Paleoseismic advances in the Granada basin (Betic Cordilleras, southern Spain). *Acta Geologica Hispanica*, **36**, 267-281.

Reicherter, K. R., Pletsch, T., Kuhnt, W., Manthey, J., Homeier, G., Wiedmann, J. & Thurow, J. (1994) Mid-Cretaceous paleogeography and paleoceanography of the Betic Seaway (Betic Cordillera, Spain). *Palaeogeography, Palaeoclimatology, Palaeoecology*, **107**, 1-33.

Rodríguez-Fernández, J. & Sanz de Galdeano, C. (1992) Onshore Neogene stratigraphy in the north of the Alboran Sea (Betic Internal Zones): Paleogeographic implications. *Geo-Marine Letters*, **12**, 123-128.

Rodríguez-Fernández, J., Comas, M. C., Soria, J.-M., Martín-Perez, J. A. & Soto, J. I. (1999). The sedimentary record of the Alboran basin: an attempt at sedimentary sequence correlation and subsidence analysis. In: *Proceedings of the Ocean Drilling Program, Scientific Results* (Ed. by R. Zahn, M. C. Comas & A. Klaus), **161**, 69-76.

Roest, W. R. & Srivastava, S. P. (1991) Kinematics of the plate boundaries between Eurasia, Iberia, and Africa in the North Atlantic from the late Cretaceous to the present. *Geology*, **19**, 613-616.

Ron, H., Freund, R., Garfunkel, Z. & Nur, A. (1984) Block rotation by strike-slip faulting; structural and paleomagnetic evidence. *Journal of Geophysical Research*, **B 89**, 6256-6270.

Rosenbaum, G., Lister, G. S. & Duboz, C. (2002a) Reconstruction of the tectonic evolution of the western Mediterranean since the Oligocene. *Journal of the Virtual Explorer*, **8**, 107-126.

Rosenbaum, G., Lister, G. S. & Duboz, C. (2002b) Relative motions of Africa, Iberia and Europe during Alpine orogeny. *Tectonophysics*, **359**, 117-129.

Rouchy, J. M., Taberner, C., Blanc-Valleron, M.-M., Sprovieri, R., Russell, M., Pierre, C., Stefano, E. D., Pueyo, J. J., Caruso, A., Dinares-Turell, J., Gomis-Coll, E., Wolff, G. A., Cespuflio, G., Ditchfield, P., Pestrea, S., Combourieu-Nebout, N., Santisteban, C. & Grimalt, J. O. (1998) Sedimentary and diagenetic markers of the restriction in a marine basin: the Lorca basin (SE Spain) during the Messinian. *Sedimentary Geology*, **121**, 23-55.

Royden, L. H. (1993) Evolution of retreating subduction boundaries formed during continental collision. *Tectonics*, **12**, 629-638.

Ruano, P., Galindo Zaldívar, J. & Jabaloy, A. (2004) Recent tectonic structures in a transect of the Central Betic Cordillera. *Pure and Applied Geophysics*, **161**, 541-563.

Rutter, E. H., Maddock, R. H., Hall, S. H. & White, S. H. (1986). Comparative microstructures of natural and experimentally produced clay-bearing fault gouges. In: *International structure of fault zones* (Ed. by Y. Wang-Chi), *Pure and Applied Geophysics*, **124**, 3-30.

Saadallah, A. & Caby, R. (1996) Alpine extensional detachment tectonics in the Grande Kabylie metamorphic core complex of the Maghrebides (northern Algeria). *Tectonophysics*, **267**, 257-273.

Sabat, F., Munoz, J. A. & Santanach, P. (1988) Transversal and oblique structures at the Serres de Llevant thrust belt (Mallorca Island). *Geologische Rundschau*, **77**, 529-538.

Sanz de Galdeano, C. & Alfaro, P. (2004) Tectonic significance of the present relief of the Betic Cordillera. *Geomorphology*, **63**, 175-190.

Sanz de Galdeano, C., López Casado, C., Delgado, J. & Peinado, M. A. (1995) Shallow seismicity and active faults in the Betic Cordillera. A preliminary approach to seismic sources associated with specific faults. *Tectonophysics*, **248**, 293-302.

Sanz de Galdeano, C. & Vera, J. A. (1992) Stratigraphic record and paleogeographical context of the Neogene basins in the Betic Cordillera, Spain. *Basin Research*, **4**, 21-36.

Sanz de Galdeano, C. (1983) Los accidents y fractures principales de las Cordilleras Beticas. *Estudios Geologica*, **39**, 157-165.

Sanz de Galdeano, C. (1990) Geologic evolution of the Betic Cordilleras in Western Mediterranean, Miocene to the present. *Tectonophysics*, **172**, 107-119.

Schreurs, G. (1994) Experiments on strike-slip faulting and block rotation. *Geology*, **22**, 567-570.

Sclater, J. G. & Christie, P. A. F. (1980) Continental stratching: An explanation of the post-Mid-Cretaceous subsidence of the Central North Sea Basin. *Journal of Geophysical Research*, **85**, 3711-3739.

Scotney, P., Burgess, R. & Rutter, E. H. (2000) 40Ar/39Ar age of the Cabo the Gata volcanic series and displacements on the Carboneras fault zone, SE Spain. *Journal of the Geological Society of London*, **157**, 1003-1008.

Seber, D., Barazangi, M., Ibenbrahim, A. & Demnati,

A. (1996) Geophysical evidence for lithospheric delamination beneath the Alboran Sea and the Rif-Betic mountains. *Nature*, **379**, 785-790.

Serrano Lozano, F. (1980) Los materiales del Mioceno de la cuenca de Ronda (Malaga). *Estudios Geologicos*, **36**, 231-236.

Silva, P. G., Goy, D. L. & Zazo, C. (1992) Características estructurales y geométricas de la falla de desgarre de Lorca-Alhama. *Geogaceta*, **12**, 7-10.

Silva, P. G., Goy, J. L., Zazo, C., Lario, J. & Bardají, T. (1997) Paleoseismic indications along 'aseismic' fault segments in the Guadalentin depression (SE Spain). *Journal of Geodynamics*, **24**, 105-115.

Simon, O. J., Martín García, L. & Gomez Prieto, J. A. (1978) Cantoria (995). *Mapa Geologico de Espana* (1:50.000), Instituto Geologico y Minero de Espana, Madrid.

Soler, R., Masana, E. & Santanach, P. (2003) Evidencias geomorfológicas y estructurales del levantamiento tectónico reciente debido al movimiento inverso de la terminacion sudoccidental de la falla de Alhama de Murcia (Cordillera Betica Oriental). *Revista de la Sociedad Geológica de España*, **16**, 123-134.

Soria, J. M., Fernández, J. & Viseras, C. (1999) Late Miocene stratigraphy and paleogeographic evolution of the intramontane Guadix Basin (Central Betic Cordillera, Spain): implications for an Atlantic-Mediterranean connection. *Palaeogeography, Palaeoclimatology, Palaeoecology*, **151**, 255-266.

Spakman, W. & Wortel, M. J. R. (2004). A tomographic view on Western Mediterranean Geodynamics. In: *The TRANSMED Atlas: The Mediterranean Region from Crust to Mantle* (Ed. by W. Cavazza, F. Roure, W. Spakman, G. M. Stamplfli & P. A. Ziegler), pp. 31-52. Springer Verlag, Berlin.

Srivastava, S. P. & Tapscott, C. R. (1986). Plate kinematics of the North Atlantic. In: *The western North Atlantic Region* (Ed. by P. R. Vogt & B. E. Tucholke), *The Geology of North America*, **M**, 379-404. The Geological Society of North America.

Srivastava, S. P., Roest, W. R., Kovacs, L. C., Oakey, G., Levesque, S., Verhoef, J. & Macnab, R. (1990a) Motion of Iberia since the Late Jurassic: Results from detailed aeromagnetic measurements in the Newfoundland basin. *Tecontophysics*, **184**, 229-260.

Srivastava, S. P., Schouten, H., Roest, W. R., Klitgord, K. D., Kovacs, L. C., Verhoef, J. & Macnab, R. (1990b) Iberian plate kinematics: a jumping plate boundary between Eurasia and Africa. *Nature*, **344**, 756-759.

Steckler, M. S. & Watts, A. B. (1978) Subsidence of the Atlantic-type continental margin off New York. *Earth and Planetary Science Letters*, **41**, 1-13.

Steffahn, J. & Michalzik, D. (2000) Foraminiferal paleoecology and biostratigraphy in the pre- and post-evaporitic late Miocene (Messinian) of the Lorca Basin, SE Spain. *Neues Jahrbuch für Geologie und Paläontologie. Abhandlungen*, **217**, 267-288.

Stich, D., Ammon, C. J. & Morales, J. (2003) Moment tensor solutions for small and moderate earthquakes in the Ibero-Maghreb region. *Journal of Geophysical Research*, **108**.

Stock, J. M. & Molnar, P. (1983) Some geometrical aspects of uncertainties in combined plate reconstructions. *Geology*, **11**, 697-701.

Stokes, M. & Mather, A. E. (2003) Tectonic origin and evolution of a transverse drainage: the Rio Almanzora, Betic Cordillera, Southeast Spain. *Geomorphology*, **50**, 59-81.

Suppe, J. (1983) Geometry and kinematics of fault-bend folding. *American Journal of Science*, **283**, 684-721.

Sylvester, A. G. (1988) Strike-slip faults. *Geological Society of America Bulletin*, **100**, 1666-1703.

Tandon, K., Lorenzo, J. M. & La Linde Rubio, J. d. (1998) Timing of rifting in the Alboran Sea basin - correlation of borehole (ODP Leg 161 and Andalucia A-1) to seismic reflection data: implications for basin formation. *Marine Geology*, **144**, 275-294.

Teixell, A., Arboleya, M. L. & Julivert, M. (2003) Tectonic shortening and topography in the central High Atlas. *Tectonics*, **22**, 13 pages.

ten Veen, J. H. & Meijer, P. T. (1998) Late Miocene to recent tectonic evolution of Crete (Greece): geological observations and model analysis. *Tectonophysics*, **298**, 191-208.

Thompson, G. A. 1960. Problem of late Ceonozoic structure of the Basin Ranges. In: *Proceedings of the 21st International Geological Congress* **18**, Copenhagen, 62-68.

Torné, M. & Banda, E. (1992) Crustal thinning from the Betic Cordillera to the Alboran Sea. *Geo-Marine Letters*, **12**, 76-81.

Turner, S. P., Platt, J. P., George, R. M. M., Kelley, S. P., Pearson, D. G. & Nowell, G. M. (1999) Magmatism associated with orogenic collapse of the Betic-Alboran Domain, SE Spain. *Journal of*

Petrology, **40**, 1011-1036.

van Bemmelen, R. W. (1969) Origin of the western Mediterranean Sea. *Geologie en Mijnbouw*, **26**, 13-52.

van der Beek, P. A. & Cloetingh, S. (1992) Lithospheric flexure and the tectonic evolution of the Betic Cordilleras (SE Spain). *Tectonophysics*, **203**, 325-344.

van der Meulen, M. J., Buiter, S. J. H., Meulenkamp, J. E. & Wortel, M. J. R. (2000) An early Pliocene uplift of the central Apenninic foredeep and its geodynamical significance. *Tectonics*, **19**, 300-313.

van der Straaten, H. C. (1993) Neogene strike-slip faulting in southeastern Spain; the deformation of the pull-apart basin of Abaran. *Geologie en Mijnbouw*, **71**, 205-225.

van der Wal, D. & Vissers, R. L. M. (1993) Uplift and emplacement of upper mantle rocks in the western Mediterranean. *Geology*, **21**, 1119-1122.

van Hinsbergen, D. J. J., Kouwenhoven, T. J. & van der Zwaan, G. J. (2005) Paleobathymetry in the backstripping procedure: Correction for oxygenation effects on depth estimates. *Palaeogeography, Palaeoclimatology, Palaeoecology*, **221**, 245-265.

van Hinte, J. E. (1978) Geohistory analyis - Application of Micropaleotology in Exploration Geology. *American Association of Petroleum Geologists Bulletin*, **62**, 201-222.

Veeken, P. C. H. (1983) Stratigraphy of the Neogene-Quaternary Pulpi Basin, provinces Murcia and Almeria (SE Spain). *Geologie en Mijnbouw*, **62**, 255-265.

Vennin, E., Rouchy, J. M., Chaix, C., Blanc-Valleron, M.-M., Caruso, A. & Rommevau, V. (2004) Paleoecology constraints on reef-coral morphologies in the Tortonian-early Messinian of the Lorca basin, SE Spain. *Palaeogeography, Palaeoclimatology, Palaeoecology*, **213**, 163-185.

Vissers, R. L. M. (1975) Geologie van het oostelijk Albox bekken rond en ten noorden van Huércal-Overa (Almería, SE Spanje). Unpublished Thesis, Univeristy of Amsterdam, pages.

Vissers, R. L. M., Platt, J. P. & Wal, D. v. d. (1995) Late Orogenic extension of the Betic Cordillera and the Alboran Domain: A lithospheric view. *Tectonics*, **14**, 786-803.

Voermans, F. M., Simon, O. J., Martín García, L. & Gómez Prieto, J. A. (1972) Huercal Overa (996). *Mapa de Geologico de Espana* (1:50.000), Instituto Geologico y Minero de Espana, Madrid.

Völk, H. R. & Rondeel, H. E. (1964) Zur Gliederung des Jungtertiars im Becken von Vera, Sudostspanien. *Geologie en Mijnbouw*, **43**, 310-315.

Völk, H. R. (1964) Zur Geologie und Stratigraphie des Neogenbeckens von Vera, sudost-Spanien. Unpublished Thesis, Universiteit van Amsterdam, 164 pages.

Waldron, J. W. F. (2004) Anatomy and evolution of a pull-apart basin, Stellarton, Nova Scotia. *Geological Society of America Bulletin*, **116**, 109-127.

Watts, A. B. (1992) The effective elastic thickness of the lithosphere and the evolution of foreland basins. *Basin Research*, **4**, 169-178.

Watts, A. B., Platt, J. P. & Buhl, P. (1993) Tectonic evolution of the Alboran Sea Basin. *Basin Research*, **5**, 153-177.

Weijermars, R. (1987) The Palomares brittle-ductile Shear Zone of southern Spain. *Journal of Structural Geology*, **9**, 139-157.

Weijermars, R., Roep, T. B., Eeckhout, B. v. d., Postma, G. & Kleverlaan, K. (1985) Uplift history of a Betic fold nappe inferred from Neogene-Quaternary sedimentation and tectonics (in the Sierra Alhamilla and Almeria, Sorbas and Tabernas Basins of the Betic Cordilleras, SE Spain). *Geologie en Mijnbouw*, **64**, 397-411.

Wernicke, B. & Burchfiel, B. C. (1982) Modes of extensional tectonics. *Journal of Structural Geology*, **4**, 105-115.

White, N. J., Jackson, J. A. & McKenzie, D. P. (1986) The relationship between the geometry of normal faults and that of the sedimentary layers in their hanging walls. *Journal of Structural Geology*, **8**, 897-909.

Williams, G. & Vann, I. (1987) The geometry of listric normal faults and deformation in their hanging walls. *Journal of Structural Geology*, **9**, 789-795.

Woodcock, N. H. & Schubert, C. (1994) Continental strike-slip tectonics. In: *Continental Deformation* (Ed. by P. L. Hancock), pp. 251-263. Pergamon Press.

Woodside, J. M. & Maldonado, A. (1992) Styles of compressional neotectonics in the eastern Alboran Sea. *Geo-Marine Letters*, **12**, 111-116.

Wortel, M. J. R. & Spakman, W. (2000) Subduction and slab detachment in the Mediterranean-Carpathian region. *Science*, **290**, 1910-1917.

Wrobel, F. & Michalzik, D. (1999) Facies successions in the pre-evaporitic Late Miocene of the Lorca Basin, SE Spain. *Sedimentary Geology*, **127**, 171-191.

Wrobel, F. (2000) Das Lorca-Becken (Obermiozan, SE Spanien) - Faziesinterpretation, Sequenzstratigraphie, Beckenanalyse. Unpublished Thesis, Universitat Hannover, 143 pages.

References

Zeck, H. P. (1996) Betic-Rif orogeny: subduction of Mesozoic Tethys lithosphere under eastward drifting Iberia, slab detachment shortly before 22 Ma, and subsequently uplift and extensional tectonics. *Tectonophysics*, **254**, 1-16.

Zwart, H. J. (1962) On the determination of polymetamorphic mineral associations, and its application to Bosost area (Central Pyrenees). *Geologische Rundschau*, **52**, 38-65.

Samenvatting in het Nederlands (Summary in Dutch)

Halverwege de vorige eeuw heeft binnen de aardwetenschappen een ware revolutie plaatsgevonden met de intrede van het concept van de plaattektoniek, welke heeft geleid tot een beter inzicht in de ontwikkeling van gebergten. Een gebergte wordt nu gezien als het gevolg van de botsing van twee naar elkaar toe bewegende platen of schollen, waarbij een van de twee platen onder de andere schuift. Dit proces wordt subductie genoemd. Van de onderschuivende (subducerende) plaat wordt over het algemeen het bovenste deel afgeschraapt en opgenomen in de overschuivende plaat. De rest van de onderschuivende plaat duikt de mantel van de aarde in.

Met de botsing van twee platen vormt zich over het algemeen een verdikking van de korst (een gebergte) in het gebied waar de twee platen elkaar treffen (de collisie zone). Het zo ontstane gebergte is een topografisch hoog gebied, met daaronder een zogenaamde wortel welke in de diepere mantel van de aarde steekt, hetgeen in principe te vergelijken is met een ijsberg. Een gebergte is in essentie een instabiel systeem, omdat de zwaartekracht tegen de vorming van een topografie inwerkt. Zolang de platen naar elkaar toe bewegen wordt het gebergte verder op- en uitgebouwd, maar zodra de spanningen (druk) tussen de platen verminderen of zelfs wegvallen, omdat bijvoorbeeld de platen niet langer naar elkaar toe bewegen of hun relatieve bewegingsrichting veranderd is, kan een gebergte uiteen zakken of zelfs uit elkaar getrokken worden.

Vanaf ongeveer 120 miljoen jaar geleden (in de tijdsperiode van het Krijt) heeft zich een brede gebergtegordel ontwikkeld welke zich uitstrekte van het westelijke deel van het Middellandse Zee gebied (de Pyreneeën, de Betische Cordillera, de Atlas, de Alpen) naar het oosten (de Karpaten, de Helleniden, de Tauriden) tot aan de Himalaya. Dit Alpiene gebergte ontwikkelde zich als gevolg van de botsing van de Afrikaanse en Indische platen met de Euraziatische plaat, waarbij de tussenliggende Tethys Oceaan gesloten werd. De op- en uitbouw (orogenese) van deze gebergtegordel, met als meest opvallende gebergten de Alpen en de Himalaya, gaat nog steeds door als gevolg van de continu naderende beweging van de Afrikaanse en Euraziatische platen. Op een aantal plaatsen echter, zoals bijvoorbeeld in het westelijke Middellandse Zee gebied, is dit gebergte uiteen gezakt (laat-orogene extensie). Het uiteen zakken van dit deel van het gebergte begon ongeveer 20 miljoen jaar geleden (begin van de tijdsperiode van het Mioceen), maar dit proces stopte aan het einde van het Mioceen (~10 miljoen jaar geleden) of in het Plioceen (~5 miljoen jaar geleden).

Op dit moment is het meest westelijke deel van het Middellandse Zee gebied gekenmerkt door een hoefijzervormige gebergteketen welke bestaat uit de Betische Cordillera in het zuiden van Spanje, het Rif gebergte in Marokko en het Tell-Kabylies gebergte in Algerije en Tunesië. Deze gebergteketen omsluit het meest westelijke deel van de Middellandse Zee, ook aangeduid als de Alboran Zee. De binnenzijde van deze hoefijzervormige gebergteketen en de bodem van de Alboran Zee vormen samen de Interne Zone van de keten. Deze Interne Zone bestaat uit metamorfe gesteenten welke zich oorspronkelijk op grote diepte bevonden en door het uiteenzakken en uit elkaar trekken van het oude gebergte aan de oppervlakte zijn gekomen (exhumatie). De buitenzijde van de keten (de Externe Zone) bestaat uit op elkaar gestapelde restanten (sedimenten) van de Tethys oceaanbodem, welke nu verdwenen is. Deze restanten zien we nu in een sterk vervormde zone die in de geologie een plooings- en overschuivingszone genoemd wordt. Een belangrijk aspect van dit gedeelte van het gebergte is, dat het onstaan van deze plooings- en overschuivingszone gelijktijdig plaatsvond met het uiteenzakken van de Interne Zone, het opengaan van de Alboran Zee en de westelijke Middellandse Zee, en met de vorming van de hoefijzer geometrie van de huidige Betische, Rif, Tell en Kabylies gebergteketen.

Met het uiteenzakken van het gebergte zijn domeinen in de aardkorst opengetrokken welke vervolgens werden gevuld met sediment. Zulke domeinen worden in de geologie sedimentaire bekkens genoemd. De grootste bekkens worden gevormd

door de huidige westelijke Middellandse en Alboran Zee, maar een aantal relatief kleine bekkens bevindt zich nu op land met name in de Betische Cordillera van zuid Spanje. De bekkens zijn voor het merendeel gevuld met afbraak produkten (erosie materialen) afkomstig van het omringende uiteenzakkende gebergte, en de sedimenten in de bekkens hebben het uiteenzakken van dit gebergte als het ware gedocumenteerd.

Een opvallend en ogenschijnlijk contrasterend gegeven is dat het uiteenzakken van het oorspronkelijke gebergte gebeurde terwijl de Euraziatische en Afrikaanse platen naar elkaar toe bleven bewegen. In de afgelopen decennia zijn een aantal scenario's ontwikkeld welke de gebeurtenissen, zoals boven beschreven, kunnen verklaren. Eén scenario wijt de geologische ontwikkeling in het westelijke Middellandse Zee gebied toe aan het loskomen van de wortel van het oor-spronkelijke gebergte en het wegzinken van deze wortel in de diepere mantel. Omdat de topografie van het gebergte niet meer in evenwicht is met de wortel van het gebergte, zakt het gebergte onder de invloed van zwaartekracht in elkaar en spreidt vervolgens uit elkaar. Een tweede scenario schrijft het uiteenzakken van het oorspronkelijke gebergte en de vorming van het huidige westelijke Middellandse Zee gebied toe aan het terugwaarts migreren (terugrollen) van de subductie zone waar de Afrikaanse plaat onder de Euraziatische plaat schuift. Doordat bijvoorbeeld de convergentiesnelheid tussen de Afrikaanse en Euraziatische platen afneemt wordt het effect van de zwaartekracht op de subducerende Afrikaanse plaat groter, waardoor deze steiler naar beneden gaat duiken en de subductie zone zich terug gaat trekken, met als gevolg dat de overschuivende Euraziatsche plaat uit elkaar wordt getrokken. Deze scenario's worden in **hoofdstuk 1** in enig detail uiteengezet.

Deze studie richt zich op een specifiek deel van het westelijk Middellandse zeegebied, namelijk het oostelijke deel van de Betische Cordillera in het zuiden van Spanje, en de in dit gebied gevormde sedimentaire bekkens. Dit gebied wordt gecompliceerd door een netwerk van breuken met horizontale verplaatsing langs verticale breukvlakken ("strike-slip" breuken). Er wordt over het algemeen aangenomen dat deze strike-slip breuken een belangrijke rol hebben gespeeld in de ontwikkeling van met name het oostelijke deel van de Betische Cordillera en de vorming van de bekkens in dit gebied, een hypothese die in deze studie grondig wordt onderzocht.

Omdat de ontwikkeling van het westelijk Middellandse Zee gebied gecompliceerd wordt door de simultane werking van processen binnen het systeem (zoals het uiteenzakken van het gebergte) en door processen werkend van buitenaf op het systeem (zoals plaatbewegingen tussen Afrika en Europa) wordt als eerste gekeken naar de processen werkend van buitenaf op het systeem, teneinde te bepalen in welke mate deze van invloed zijn geweest op de geologische ontwikkeling binnen het systeem. In **hoofdstuk 2** wordt dit gedaan door in detail te kijken naar veranderingen in de richting en snelheid van de relatieve plaat bewegingen tussen Afrika en Europa voor het westelijke Middellandse Zee gebied in de afgelopen 33 miljoen jaar, en deze te vergelijken met het ontstaan van vervormingsstructuren in de plooing- en overschuivingszone (Externe Zone) van de Betische Cordillera, het Rif gebergte en de Tell-Kabylies gebergten. Er kan geconcludeerd worden dat het oorspronkelijke gebergte in het westelijke Middellandse Zee gebied uiteen begon te zakken op het zelfde moment (ongeveer 20 miljoen jaar geleden) dat de snelheid en richting van de Afrikaanse plaat ten opzichte van Europa drastisch veranderde. Een tweede conclusie is dat de ontwikkeling van de deformatie structuren in de Externe Zone voor een deel het gevolg kan zijn van de convergerende beweging tussen de Afrikaanse en Euraziatische platen, maar voor een deel ook het gevolg moet zijn geweest van processen werkend binnen het systeem.

In **hoofdstuk 3** worden twee bekkens in de Betische plooings- en overschuivingszone (Externe Zone) bestudeerd. In deze bekkens zijn rekstructuren ontwikkeld welke contrasteren met het duidelijk samendrukkende (compressie) karakter van de plooings- en overschuivingszone. Het blijkt dat de ontwikkeling van deze rekstucturen inherent is aan de ontwikkeling van compressieve structuren in de plooings- en overschuivingszone, en los staat van de laat-orogene extensie in de Interne Zone op slechts enkele tientallen kilometers ten zuiden hiervan. Een tweede belangrijke observatie is, dat terwijl de Interne Zone van de Betische Cordillera uiteen zakte, deze op de zuidelijke rand van het Spaanse continent schoof en zo een van de bestaande verbindingen tussen de Atlantische Oceaan en de Middellandse Zee afsloot.

In de navolgende hoofdstukken (4, 5 en 6) ligt de focus op de bekkens in het zuidoostelijke deel van de

Betische Cordillera (de Interne Zone). De sedimenten in deze bekkens hebben zoals gezegd het uiteen zakken en spreiden van de fragmenten van het oorspronkelijke gebergte zowel als bewegingen langs de grote "strike-slip" breuken gedocumenteerd. Studie van deformatie structuren (breuken) in de sedimenten en het bepalen van het tijdstip waarop deformatie van de sedimenten en gesteenten gebeurde verschaft inzicht in de ontwikkeling van de bekkens door de tijd, maar ook in de ontwikkeling van het omringende gebergte en de onderliggende aardkorst, hetgeen een sleutel vormt tot de plaattektonische processen die daar mogelijk aan ten grondslag liggen.

Als eerste wordt de sedimentaire opeenvolging (de stratigrafie) van een aantal bekkens beschreven en met elkaar vergeleken (**hoofdstuk 4**). Dit is van belang in verband met de vraag of het ontstaan van een gegeven bekken en de daarop volgende gebeurtenissen in dat bekken (bijvoorbeeld veranderingen in het leef milieu) gelijktijdig (synchroon) of niet gelijktijdig (diachroon) met een soortgelijke verandering in een naast gelegen bekken plaatsvond. Het tijdstip van ontstaan van een bekken of een gebeurtenis in een bekken kan onder meer bepaald worden aan de hand van fossielen in de sedimenten. Met name microscopisch kleine fossielen (foraminiferen) in mariene sedimenten zijn geschikt om te dateren, maar ook om af te leiden wat de levensomstandigheden waren en om te bepalen of het een diep of ondiep milieu was. De reconstructie van de diepte van een bekken door de tijd geeft de mogelijkheid om verticale bewegingen in een bekken te reconstrueren. Voor het onderzoek zijn deels bestaande datasets (ouderdommen van sedimenten) gebruikt, waar nodig en mogelijk uitgebreid en verbeterd aan de hand van nieuw verzameld en bestudeerd gesteentemateriaal. Een belangrijke conclusie in dit hoofdstuk is dat de onderzochte bekkens in het oostelijke deel van de Betische Cordillera gelijktijdig (synchroon) ontstonden en zich in het vroegere deel van hun geschiedenis (de tijdsperiode van het Tortoon) ontwikkelden tot mariene bekkens. Een daarop volgende grote ommezwaai in het leef milieu in het latere deel van de geschiedenis (de tijdsperiode van het laatste deel van het Tortoon en het Messinien) ging gepaard met omhoog komen en verlanding van de bekkens. Dit gebeurde echter niet gelijktijdig in de verschillende bekkens, maar verliep diachroon van de meer noordoostelijke naar de meer zuidwestelijk gelegen bekkens. Dit diachroon omhoog komen en verlanden van de bekkens in de Betische Cordillera kan niet gerelateerd worden aan bijvoorbeeld een zeespiegel verandering, maar moet het gevolg zijn geweest van een tektonisch proces.

In **hoofdstuk 5** worden de deformatie structuren in de sedimenten van de verschillende bekkens en in de metamorfe gesteenten van de omringende gebergten beschreven met het doel de tektonische geschiedenis van het bekken maar ook van de omringende Betische Cordillera zo veel mogelijk te ontrafelen. Het type deformatie structuren (rek- of compressie breuken) geeft informatie over het tektonische regime (verkorting of rek en de bijbehorende richtingen) tijdens de ontwikkeling van deze structuren. De mate en aard van de waargenomen verplaatsingen langs de breukvlakken geeft daarbij informatie over de horizontale bewegingen in de aardkorst. In combinatie met de ouderdommen van de sedimenten kan zelfs de duur van een deformatie fase bepaald worden. Samen met de diepte reconstructie van een bekken geven de deformatie structuren een volledig beeld van de verticale en horizontale bewegingen van een bekken, welke direct gekoppeld zijn aan bewegingen in de onderliggende aardkorst en dus inzicht kunnen geven in de grootschalige (plaat-) tektonische processen. De deformatiestructuren in de bekkens wijzen er duidelijk op dat de bekkens echte extensie bekkens zijn. De structuren in de oudste bekkensedimenten wijzen erop dat het ontstaan van de bekkens het gevolg was van ruwweg noordoost-zuidwest gerichte rek in de Betische korst, gelijktijdig met het aan het oppervlak komen (exhumatie) van de metamorfe gesteenten in het omringende gebergte. De structuren in de jongere bekkensedimenten wijzen erop dat de rekrichting door de tijd heen veranderde naar een meer noord-zuid georiënteerde rekrichting hetgeen gepaard ging met een snelle verdieping van de bekkens. Daarop volgde de diachrone ontwikkeling in het oostelijke deel van de Betische Cordillera zoals beschreven in hoofdstuk 4 waarbij de bekkens verlandden terwijl zij omhoog kwamen. Deze diachrone gebeurtenis lijkt niet gepaard te gaan met belangrijke bewegingen langs breuken. Pas in een relatief recent stadium lijken de sedimenten als gevolg van een jong compressief tektonisch regime opnieuw gedeformeerd te worden, waarbij oude breuken zijn gereactiveerd.

In **hoofdstuk 6** wordt de relatie tussen bekkenontwikkeling en bewegingen langs een aantal van de grote breuken in het oostelijke deel van de Betische

Cordillera nader onderzocht. De hoofdconclusie van dit hoofdstuk is dat het ontstaan van de sedimentaire bekkens in het onderzochte gebied niet het gevolg was van strike-slip activiteit langs deze grote breuken, maar dat deze breuken deels jong en deels gereactiveerde structuren zijn, samenhangend met de meest recente geschiedenis van de Betische Cordillera onder invloed van een compressief tektonisch regime, waarschijnlijk als gevolg van de convergerende plaatbeweging tussen Afrika en Europa.

In het laatste hoofdstuk (**hoofdstuk 7**) worden een aantal eerste-orde aspecten van het gebied rondom de Alboran Zee samengevat en vergeleken met voorspellingen van de eerder genoemde modellen (hoofdstuk 1). Vanuit het perspectief van de laatorogene bekken ontwikkeling in het oostelijke deel van de Betische Cordillera wordt de keuze gemaakt voor het westwaarts terugrollen van een subductie zone als een plausibele verklaring voor de geologische geschiedenis van het gehele systeem. Het onstaan van de bekkens en het vroegere deel van hun ontwikkeling kan in verband worden gebracht met het gewicht van de onderduikende plaat en het effect hiervan op de overschuivende Interne Zone van de Betische Cordillera. De markante diachrone gebeurtenis in de latere geschiedenis van de bekkens kan verklaard worden met het van noordoost naar zuidwest losscheuren en wegzinken van de subducerende plaat in de mantel onder de Betische Cordillera, waardoor het effect van het gewicht op de overschuivende plaat wegvalt. De reactivatie van breuken en de jonge vervorming van sedimenten gedurende de recentste geschiedenis van de Betische Cordillera wordt hier toegeschreven aan de voortgaande convergerende plaatbeweging van Afrika en Eurazië, een proces dat blijkens veelvuldige lichte aardbevingen tot op heden voortduurt.

Dankwoord - Acknowledgements

Na ruim vier jaar zwoegen en zweten kan ik dan eindelijk zeggen dat de klus geklaard is. Met ontzettend veel plezier en grote inzet heb ik aan dit project gewerkt en ik heb hiervan bijzonder veel geleerd. Ik zal in de komende jaren nog vaak terug denken aan de mensen en de leuke dingen van deze tijd. Veel van deze mensen hebben, direct dan wel indirect, aan dit resultaat bij gedragen en ik zou hen graag willen bedanken.

Als allereerste wil ik natuurlijk Reinoud Vissers, mijn promotor, bedanken voor de mogelijkheid om dit onderzoek te kunnen doen. Hij heeft mij in de afgelopen vier jaar in het veld en op het instituut een hoop geleerd en hij heeft mij veel gestimuleerd om over de verschillende geologische en geofysische aspecten van dit onderzoek na te denken. Dit laatste gebeurde met name ‘s avonds op het terras onder het genot van een groot glas bier na een dag hard ploeteren in het veld in het zuiden van Spanje. Bedankt, Reinoud! Je hebt inderdaad mijn horizon weten te verleggen van de Kennemer Duinen naar de Betische Cordillera in Zuid Spanje. En net als jij kijk ik ook reikhalzend uit naar de eerste commentaren op ons artikel (Hoofdstuk 6).

Daarna wil ik graag Paul Meijer bedanken voor de grote bijgedrage die hij geleverd heeft aan de opzet, ideeën en discussies voor hoofdstuk 2. Daarnaast wist Paul altijd wat tijd voor mij vrij te maken wanneer ik weer eens zijn kamer binnen kwam stormen met vragen over allerlei geofysische problemen welke hij vervolgens kalm en geduldig beantwoordde. Paul, bedankt! Ik heb ook zeker met groot plezier met jou en Ildiko en de andere leden van de OPCOM samengewerkt in het organiseren van lezingen, cursussen en excursies.

Verder hebben de mensen van de vakgroep Stratigrafie en Paleontologie, zoals Bert van der Zwaan, Jan-Willem Zachariasse, Frits Hilgen, Tanja Kouwenhoven, Luc Lourens, geholpen met mijn onderzoek door het beantwoorden van mijn vragen over foraminiferen of het dateren van mijn monsters uit Zuid Spanje. Ik wil hen hartelijk bedanken hiervoor en dan met name Jan-Willem die na het slaken van een diepe zucht en met een zekere wanhoop vanwege de matige preservatie van de forams, menig maal monsters voor mij heeft bekeken en gedateerd. Agata, I would like to thank you for your effort in trying to date the samples I sent you. Douwe, jou wil ik graag bedanken voor je hulp met de P-B ratio analyses van de monsters. Marianne en Hayfaa, hoewel het veldwerk in het zuiden van Spanje goed verliep, vielen de resultaten op het eerste gezicht wat tegen, maar met een beetje hulp van Wout, waren deze data toch nog prima te gebruiken. Klaudia, bedankt voor het dateren van de vulkanische as. Jouw werk, en dat van Douwe, Agata, Wout, Marianne en Hayfaa komt in een artikel. Ik beloof jullie, het artikel komt eraan!

Otto Stiekema en Gerrit van ’t Veld wil ik bedanken voor het prepareren van de monsters en het maken van dunne doorsneden van de gesteenten. En Maarten Zeylmans van Emmichoven en Tom van Hinte van de GIS afdeling, bedankt voor jullie hulp met het scannen en printen van de kaarten en satelliet beelden. Zonder jullie hulp zouden de figuren in het proefschrift nooit zo goed zijn geworden. En de mensen van de Geomedia dienst, en met name Margot, hartelijk bedankt voor jullie hulp met de vormgeving van het proefschrift. Verder wil ik de mensen van de bibliotheek bedanken, en met name Jan, voor hun hulp in de afgelopen jaren met het zoeken en aanvragen van artikelen in vakbladen en boeken in bibliotheken in alle uithoeken van Europa.

Armelle, jou en je collega’s van Midland Valley wil ik graag bedanken voor het mogen gebruiken van het computer programma 2D-Move. Dit programma was bijzonder nuttig voor met name hoofdstuk 2 en het heeft me een hoop handwerk bespaard. Bedankt!

Further, I would like to thank de members of the reading committee, John Platt, Laurent Jolivet, Rinus Wortel and Johan Meulenkamp for careful reading and evaluation of the thesis. Vooral Johan wil ik graag bedanken, omdat hij het was die in eerste instantie Reinoud en mij aan elkaar heeft voorgesteld en toen hij mee was met ons laatste veldwerk in de Betische Cordillera was hij het die mij op nog een aantal problemen wees, die we vervolgens samen vakkundig

onder de loep hebben genomen. Johan, hartelijk bedankt!

Wim Spakman, Rob Govers, en Rinus Wortel, jullie wil ik bedanken voor de discussies die we hadden, vaak tijdens de lunch, over modelleringen of geofysische aspecten in de geologie. Jullie hebben mij geleerd de situatie rondom de Alboran Zee vanuit een geofysisch oogpunt te bekijken. Bedankt hiervoor!

Rui, it was really nice working with you on the present-day motions in the Alboran region. You really helped me to understand the present-day tectonics of that region as well as the people from Delft.

Wim Sissingh, met jou was het altijd een plezier te discussiëren over de geologie van Zuid Spanje en je wist mij altijd te vertellen waar en in welke artikelen of boeken ik bepaalde informatie kon vinden. Bedankt hiervoor!

Uiteraard mag ik de secretaresses, Magda en Ildiko niet vergeten. Jullie hebben mij regelmatig geholpen met allerlei organisatorische en bureaucratische rompslomp, zoals het boeken van vluchten en hotels en het reserveren van auto's. Dank jullie wel! Mijn collega's op de vakgroep, Martyn, Gill, Herman, Stan, Kim, Hugo, Dolors, Siska en Laurie, wil ik bedanken voor jullie interesse in mijn werk, voor jullie hulp met vertalen of corrigeren (Frans, Spaans en Engels) of om er te zijn voor een gezellig gesprek. En speciaal Martyn en Gill wil ik bedanken. Sinds jullie een moestuin onderhouden, hebben jullie ervoor gezorgd dat ik mijn dagelijkse twee ons groente binnenkreeg. En natuurlijk wil ik Dirk, mijn kamergenoot, bedanken. Ruim vier jaar geleden hebben we samen de deur van onze kamer op het instituut open gedaan, en hebben we van af dat moment heel wat meegemaakt en heel wat lol gehad. En nu hebben we gelijktijdig ons proefschrift afgerond. Je bent een prima collega en een geweldige vriend, en ik ga je zeker missen nu jij naar Japan gaat.

Ik heb in de afgelopen jaren de aio's en collega's van de andere vakgroepen, Hans, Chris, Colin, Saskia, Tony, Gert, Andre, Arthur, Suzanne, Reinier, Emilia, Thomas, Joost, Paul Mason, Hemmo, Maisha, Nicoline, Robbert, Christine, Boudewijn 't Hart en vele studenten, zoals Floor, Jelmer, Willem-Jan, Agnes en Esther, heel goed leren kennen. Het was altijd gezellig met jullie een biertje te drinken na de vrijdagmiddag solidrock seminar of na het veldwerk. Bedankt voor jullie interesse en steun.

Daarnaast wil ik mijn vrienden Stefan, Marc, Jolanda, Aarnoud, Wilfried, Robert, Silja, Phil, Mark, Vincent en mijn buurvrouw Monique bedanken. Jullie hebben mij gelukkig met grote regelmaat achter mijn computer vandaan getrokken om een biertje te gaan drinken, een filmpje te pakken, een fietstochtje te maken of een reisje naar de Eiffel, Italië, Lands-end of Londen te maken. And Phil, thanks for being my climbing-buddy. Climbing really kept my mind of things.

En als laatste natuurlijk wil ik graag mijn ouders, mijn broer Wouter, mijn zus Astrid en haar vriend Kees bedanken voor alle steun, liefde, interesse en vooral geduld. Vooral mijn broer heeft mij de nodige handige tips gegeven, omdat hij het van pad van promotie onderzoek al had afgelegd. Bedankt Wouter! En bedankt dat jullie altijd voor mij klaar stonden en bedankt voor jullie vertrouwen in mij.

Dan rest mij slechts met de volgende wijze woorden af te sluiten: "Wat er ook gebeurt, altijd blijven lachen", of zoals mijn oma altijd zei: "Houd de zonzijde".

Curriculum Vitae

12 July 1978	Born in Brielle, the Netherlands
1990-1996	Secondary school, Maerlant College, Brielle, the Netherlands
1996-2001	Study of Geology, Utrecht University, the Netherlands
2001-2002	Junior Geologist at Fugro Robertson, Leiden, the Netherlands
2002-2006	PhD Student in the Structural Geology and Tectonics department, Faculty of Geosciences, Utrecht University, the Netherlands

VMSG Excursion to the Alps, September 2005.